NASA TECHNICAL NOTE

NASA TN D-4557

c. 1

NASA TN D-4557

INVESTIGATION OF A NEARLY ISENTROPIC MIXED-COMPRESSION AXISYMMETRIC INLET SYSTEM AT MACH NUMBERS 0.6 TO 3.2

by Donald B. Smeltzer and Norman E. Sorensen

Ames Research Center
Moffett Field, Calif.

NATIONAL AERONAUTICS AND SPACE ADMINISTRATION • WASHINGTON, D. C. • MAY 1968

INVESTIGATION OF A NEARLY ISENTROPIC MIXED-COMPRESSION AXISYMMETRIC INLET SYSTEM AT MACH NUMBERS 0.6 TO 3.2

By Donald B. Smeltzer and Norman E. Sorensen

Ames Research Center
Moffett Field, Calif.

NATIONAL AERONAUTICS AND SPACE ADMINISTRATION

For sale by the Clearinghouse for Federal Scientific and Technical Information
Springfield, Virginia 22151 – CFSTI price $3.00

INVESTIGATION OF A NEARLY ISENTROPIC MIXED-COMPRESSION AXISYMMETRIC INLET SYSTEM AT MACH NUMBERS 0.6 TO 3.2

By Donald B. Smeltzer and Norman E. Sorensen

Ames Research Center

SUMMARY

A 20-inch capture diameter model of a mixed-compression axisymmetric inlet system has been designed and tested. The inlet system was 1.4 capture diameters long measured from the cowl lip to the engine face. The design Mach number was 3.0, and off-design performance was obtained by translation of the cowl. Vortex generators were employed just downstream of the throat to reduce the total-pressure distortion at the engine face. The main test objective was to determine experimentally the major inlet parameters of bleed mass-flow ratio, total-pressure recovery, and total-pressure distortion at the engine face. Tests were conducted over the Mach number range 0.6 to 3.2 at angles of attack from 0° to 8° and at a tunnel total pressure of 15 psia which corresponded to a Reynolds number of about 2×10^{6} per foot at Mach number 3.0.

The supersonic diffuser of the inlet was designed with the aid of a computer program which employs the method of characteristics. The subsonic diffuser was designed to have a linear variation of Mach number from the end of the throat to the engine face. Results indicated a level of performance at Mach number 3.0 of 90 to 93 percent total-pressure recovery at the engine face with a bleed mass-flow ratio of 7.5 to 12 percent and a total-pressure distortion level of about 10 percent. The off-design performance was generally better than at Mach number 3.0. Other results obtained at Mach number 3.0 indicated that the inlet would remain started at 2° to 3° angle of attack without a change in geometry if the maximum pressure recovery at 0° were degraded about 2 to 3 percent. The transonic results for Mach numbers from 0.6 to 1.3 included experimentally measured additive drag as well as the internal performance.

INTRODUCTION

Results of several investigations of mixed-compression axisymmetric inlet systems designed for optimum performance at Mach number 3.0 and capable of off-design performance by translation of the cowl are presented in references 1 to 3. Analysis of these results and further theoretical studies indicated the potential for achieving higher levels of performance over the Mach number range from 0 to 3.0 than were reported for these inlet systems. These studies revealed that the supersonic diffuser could be re-designed to allow a potential improvement in pressure recovery of about 3.5 percent at Mach 3.0.

The length of this re-designed diffuser would be about the same as the length of those of reference 3. Also, there were indications that the use of vortex generators to reduce total-pressure distortion at the engine face station would permit the length of the subsonic diffuser to be reduced without a large attendant loss in performance. It, therefore, seemed reasonable to expect that a shorter inlet system could be designed that would perform as well as those discussed in references 1 to 3, or better.

The purpose of this investigation was to design a large-scale model of an inlet system according to the findings discussed above and to measure its performance in wind-tunnel tests. The model was tested at Mach numbers from 0.6 to 3.2 and at angles of attack from 0° to 8°. For all the tests, the wind-tunnel total pressure was constant at the value corresponding to a Reynolds number of about 2×10^{6} per foot at Mach number 3.0. Quantities deduced from the measurements were total-pressure recovery, bleed mass-flow ratio, total-pressure distortion at the engine face station, sensitivity to unstarting caused by changes in the angle of attack, and transonic additive drag.

SYMBOLS

A_c	capture area
A_{min}	minimum duct area normal to the average local flow
A_x	local duct area normal to the inlet centerline
b	span of vortex generators
C_{D_a}	additive drag coefficient based on A_c
D	capture diameter
h	local height
M	Mach number
m	mass flow
p	static pressure
p_p	pitot pressure
p_t	total pressure
Δp_{t_2}	total-pressure distortion parameter, $\dfrac{p_{t_{2_{max}}} - p_{t_{2_{min}}}}{\bar{p}_{t_2}}$
$\dfrac{r}{R}$	ratio of cowl or centerbody radius to capture radius

$\frac{x}{R}$ ratio of axial distance measured from the tip of the centerbody to capture radius

$\left(\frac{x}{R}\right)_c$ ratio of axial distance measured from the cowl lip to capture radius

$\frac{\Delta x}{R}, \left(\frac{\Delta x}{R}\right)_c$ incremental $\frac{x}{R}, \left(\frac{x}{R}\right)_c$

$\left(\frac{x}{R}\right)_{lip}$ ratio of the axial distance from the tip of the centerbody to the cowl lip divided by the capture radius

α inlet angle of attack, deg

α_u angle of attack for incipient unstart, deg

Subscripts

∞ free stream

o inlet lip (theoretical)

i inlet lip (measured)

l local

1 throat

2 engine face

bl bleed

Superscript

$-$ average value

NOTE: The letters A, B, and C on the plotted and tabulated data refer to progressively restricted bleed exit settings, A being the maximum flow condition and C the most restricted.

MODEL AND INSTRUMENTATION

The model is shown in figure 1 installed in one of the supersonic wind tunnels. Detailed sketches of the model and instrumentation are presented in figure 2. It is evident from figure 2(a) that off-design operation of the model is achieved by translating the inlet cowl while off-design operation of the inlet in flight would be achieved by translating the inlet centerbody. It was found that model construction could be simplified without altering off-design internal area distributions by designing the cowl rather than the centerbody to be movable. Also shown is a translating sleeve and a fixed plug near the rear of the model. These were used to control the terminal shock-wave position. The outer shell of the model was attached to four hollow struts mounted on the centerbody sting support. The struts provided both support for the cowl and ducting for the centerbody bleed airflow to the free stream. Further details of the design and test instrumentation are presented in the following sections.

Design Considerations

This inlet was designed according to principles similar to those used in the design of the inlets discussed in references 1-3. High total-pressure recovery, low bleed-mass-flow ratio, and low total-pressure distortion at the engine face over the entire Mach number range from 0 to 3.0 were prime considerations, along with the requirement for low cowl drag and low transonic additive drag. The inlet coordinates are presented in table I. Also, they are presented graphically in figure 3 along with the internal area distributions for the various cowl lip positions tested. The important aspects of the design are discussed in the following paragraphs.

Supersonic diffuser.- This portion of the inlet was designed with the aid of the computer program described in reference 4 which employs the method of characteristics. The selected contours yielded nearly isentropic compression with an average theoretical total-pressure recovery of 0.993 at the inlet throat. The 0° initial internal cowl angle allowed a low external cowl angle satisfying the requirement for low cowl drag. A 10° half-angle cone was used for the initial part of the centerbody, $x/R = 0$ to 1.502. Between $x/R = 1.502$ and 3.502 a linear rate of change of surface angle with distance was used so that the total turning of the surface was 15° at station $x/R = 3.502$. With these initial contours the remaining internal contours of the cowl and centerbody were adjusted and "tested" using the computer program until the desired conditions were attained at the throat. These conditions were a uniform Mach number distribution of about 1.2 with essentially parallel flow and a total-pressure recovery above 0.990. Another constraint imposed on the design was that the pressure rise across a shock wave reflection on the centerbody or cowl could not exceed the value for incipient boundary layer separation as defined in reference 5. The capture mass flow at Mach number 1.0 was 39.1 percent. If desired, the capture mass flow in the transonic range could be increased through the use of a contracting centerbody. The design resulted in a cowl translation distance of about 0.7 capture diameter for withdrawing the cowl to the station of maximum centerbody diameter. No boundary-layer compensation was included in the design of the supersonic diffuser since previous experience (ref. 3) indicated that with the boundary-layer removal system none would be required. Local static pressure and Mach number distributions calculated by the method of characteristics computer program are presented in figure 4 for the design Mach number.

Subsonic diffuser.- The subsonic diffuser design was based upon the study reported in reference 3. The Mach number at the beginning of the subsonic diffuser was obtained from the calculations made for the supersonic diffuser (fig. 4). The location and area of the engine-face station were fixed. In the throat region ($x/R = 4.022$ to 4.252) the centerbody and cowl surfaces were frustums of cones which diverged from one another with a 2° included angle, the inner cowl surface being a straight-line continuation of the surface at the end of the supersonic diffuser. This provided a low and constant divergence of the duct area in the throat region for a range of cowl translation distance. These considerations caused the minimum throat area to be located at about $x/R = 4.0$. Area and continuity relationships were used to design the remainder of the subsonic diffuser from the aft end of the throat to the engine-face station ($x/R = 4.252$ to 5.352) to yield a linear Mach number variation. This variation was maintained for a range of cowl translation distances. As in the case of the supersonic diffuser no boundary-layer compensation was included. The resulting inlet was 1.4 capture diameters long measured from the cowl lip to the engine-face station.

Boundary-layer bleed system.- Control of the boundary layer to prevent flow separations caused by shock-wave impingements on the boundary layer in an adverse pressure gradient is of critical importance. Control in the present case was accomplished by removal of part of the boundary-layer flow through porous bleed zones. The model had four bleed zones as indicated in figure 2. Each had separate and remotely controlled exits to regulate each bleed flow from zero to maximum flow. Separation of the bleed air exit ducting on both the cowl and the centerbody prevented recirculation of the flow from the higher to the lower pressure regions. To insure choked flow at the bleed exits during the supersonic tests, exit fairings were used to maintain low back pressures. Cowl bleed zone I was located just upstream of the first shock-wave impingement shown in figure 4. Bleed zone II was located just upstream of the second shock-wave impingement on the centerbody. These locations were selected on the basis of the results of tests reported in reference 6. In these areas 0.125-inch-diameter holes were drilled to provide a uniform porosity of 41.5 percent. The bleed zones in the throat region (III and IV) were drilled with a similar pattern, but with every other row of holes eliminated. This resulted in an overall porosity of 20.8 percent. The bleed pattern in each zone could be altered by filling the holes with a plastic resin material. Figure 2(b) shows the pattern selected for investigation throughout the Mach number range.

Vortex generators.- Vortex generators were used to reduce the total-pressure distortion at the engine face station thereby permitting the length of the subsonic diffuser to be minimized. They were installed just aft of the throat region. Forty generators were mounted on the centerbody and 54 on the cowl. Vortex generator details are shown in figure 2. They were designed according to procedures discussed in reference 7.

Instrumentation

Conventional but rather detailed instrumentation was provided. Six 6-tube total-pressure rakes were provided at the engine-face station. The

Tube spacing shown in the sketch in table II was used to obtain area weighted total pressure measurements. Measurements from the static-pressure rakes near the main duct exit (fig. 2(a)) were used in conjunction with the choked main duct exit area and the duct area at the rake station to calculate the main duct mass flow. The rakes were located to give an area-weighted average pressure. Static-pressure orifices were located in single opposing rows along the top internal surfaces of the cowl and centerbody. They extended to the end of the subsonic diffuser. Boundary-layer rakes were located as shown in figure 2(b). Measurements from a 9-tube pitot-pressure rake located at the beginning of the throat were used to evaluate the performance of the supersonic diffuser. Bleed-flow rate measurements in the centerbody boundary-layer removal ducts were made with 4-tube total-pressure rakes, each with a single static-pressure tube. Three of these rakes were mounted in the outer duct and four in the inner duct. The known choked areas and the static pressure measured in the bleed plenum chambers of the cowl were used to evaluate the bleed mass flow through the two zones on the cowl surface. Pressures were also measured in the centerbody bleed plenum chambers. For the transonic tests four rakes were installed at the point of maximum centerbody diameter to measure the total and static pressure at this station. Five total-pressure tubes and two static-pressure tubes were included on each rake. Both static- and total-pressure tubes were located to give area-weighted average pressures. The measurements from these rakes were used to calculate the inlet mass flow and the total momentum change from the free stream to the rake measurement station. These measurements, the pressure distribution on the centerbody, and a friction drag term were used to calculate the additive drag by the mathematical procedure of reference 8.

TEST PROCEDURE

The investigation was conducted in the 8- by 7-foot, 9- by 7-foot, and 11- by 11-foot test sections of the Ames Aeronautics Division Wind Tunnels and covered the Mach number range from 0.6 to 3.2. Data were obtained at angles of attack of 0°, 2°, 5°, and 8°.

Various patterns of boundary-layer bleed holes were tested at Mach number 3.0 in an attempt to achieve high total-pressure recovery, low total-pressure distortion at the engine face, and low bleed mass flow. For the selected bleed pattern shown in figure 2(b) the contraction ratio that produced the best performance was determined. Three levels of bleed mass flow were obtained with 3 different bleed-exit settings. These correspond to bleed-exit settings A, B, and C referred to on the plotted data. Exit setting A represented the maximum bleed mass flow that could be removed for the selected boundary-layer-bleed hole pattern. Exit settings B and C represented progressively more reduced bleed mass flow. Data were obtained at all angles of attack and at off-design Mach numbers for these bleed-exit settings and the selected bleed pattern. No attempt was made to improve angle of attack or off-design performance by alteration of the boundary-layer-bleed hole pattern or the bleed-exit settings. At angles of attack and off-design Mach numbers, data were recorded only for contraction ratios near the maximum (lowest throat Mach number) for which the inlet would remain started.

PRECISION OF DATA

The following table presents the estimated uncertainties of the primary parameters.

Parameter	Uncertainty
p_t/p_{t_∞}	±0.005
m_{bl}/m_∞	±0.005
α	±0.1°
p/p_∞	±0.2
M_∞	±0.05
m_2/m_∞	±0.020, α=0° and 2°

At angles of attack of 5° and 8°, mass-flow ratio may be in error by the order of ±0.050 or more. The uncertainties in all the parameters except m_2/m_∞ and m_{bl}/m_∞ have been well established by many wind-tunnel tests. The bleed mass-flow ratio, m_{bl}/m_∞, was determined from measurements of the change in the main duct flow with bleed-exit settings. The assumption was made that changes in the main duct mass flow could be measured more precisely than its absolute value. This method for determining bleed mass-flow ratio is more fully described in reference 3. The main duct mass-flow ratio, m_2/m_∞, was determined by comparison of the measured results with the difference of the mass flow known to be entering the inlet and the bleed mass flow.

RESULTS AND DISCUSSION

Detailed analysis of the data is not made in this report. The most important results already have been published in reference 2, and a thorough discussion of the results of the first three inlets of the series is presented in reference 3. The following, therefore, will be confined to a brief discussion of the pertinent results. Some of the significant trends of the data are noted, however, to aid in the understanding of the results.

Results of the investigation are tabulated in table II and plotted in figures 5 to 33. Table III is an index to the plotted data. Bleed mass-flow ratio is used as a parameter for much of the plotted data rather than the more conventional mass-flow ratio at the engine face. This is done because bleed mass flow is believed to be the more reliable quantity as was noted in the discussion of precision of data. At 0° angle of attack, mass flow at the engine face can be obtained by subtracting bleed mass flow from the theoretical mass flow shown in figure 5. These mass flows were obtained from a subprogram of reference 4 in which streamlines from the bow shock wave to the inlet lip radius were calculated. Variables are cowl lip position and free-stream Mach number. The curves on this figure are applicable only at 0° angle of attack. Inlet contraction ratio as a function of cowl lip position is shown in figure 6. The symbols indicate the contraction ratios where data at 0° angle of attack were obtained. At Mach number 3.0, maximum pressure recovery occurred at the indicated contraction ratio. The contraction ratio at Mach number 3.2 was not changed from that at Mach number 3.0 and was therefore not optimum but represented an overspeed condition.

Supersonic Performance

Maximum design performance, exit setting B.- Shown in figure 7 are the maximum pressure recoveries with associated bleed mass-flow ratios and total-pressure distortions at the engine face obtained for various positions of the cowl lip. The maximum pressure recovery was obtained at other than maximum contraction ratio. With the cowl lip at the position for maximum pressure recovery, data were obtained for three levels of bleed mass-flow ratio, and those maximum points are shown in figure 8. Total-pressure distortion at the engine face is virtually unaffected over the range of bleed mass-flow ratios investigated.

Supercritical performance, $M_{\infty} = 3.20 - 1.55$, $\alpha = 0^{\circ}$.- Performance in the supercritical range for the Mach number 3.0 maximum pressure recovery points of figure 7 is shown in figure 9. The maximum pressure recovery represents the point where the terminal shock wave system was near its most upstream position for which the inlet would remain started. Any further forward movement reduced the recovery or unstarted the inlet. As the terminal shock system was moved downstream from the throat (by increasing the main duct exit area), the pressure recovery at the engine face decreased due to the increased losses through the shock system resulting from the higher terminal shock wave Mach numbers. Concomitantly, the bleed flow decreased as a result of movement of the terminal shock system with respect to the porous bleed areas and the decrease in internal duct pressure. When the terminal shock system was downstream of the porous bleed area, further downstream movement did not change the bleed flow and the pressure recovery dropped abruptly. Only small changes in distortion occurred when the terminal shock system was moved within the confines of the porous bleed area but a rapid rise in distortion occurred as the terminal shock system was withdrawn downstream of the porous bleed area. The peculiarity of the shape of the curves of pressure recovery and distortion for the lowest contraction ratio tested, $(x/R)_{lip} = 2.658$, probably was caused by the considerable displacement of the bleed areas from the proper design position.

Performance in the supercritical operating range for Mach numbers 3.2 to 1.55 is shown in figure 10. Total-pressure recovery and total-pressure distortion at the engine face are plotted for three ranges of bleed mass-flow ratio, each curve corresponding to fixed bleed-exit area settings. The Mach number 3.2 data were obtained with the Mach number 3.0 geometry and therefore represent an overspeed condition. The contraction ratio used at other off-design Mach numbers was near the maximum for which the inlet remained started. Figure 10 includes data obtained with the inlet unstarted. These points are separated from the supercritical data by dashed lines. Tabulated pressure recoveries and mass-flow ratios are included in table II for the conditions represented by the half-filled symbols.

Off-design maximum performance, $M_\infty = 3.20 - 1.55$, $\alpha = 0^\circ$.- The maximum pressure recovery points from figure 10 are summarized in figure 11. The low-pressure recovery and high distortion at Mach number 2.9 probably result from poor boundary-layer control on the centerbody side of the flow passage. The low performance at this Mach number might be avoided by relocating the centerbody bleed areas.

Supercritical performance at angle of attack, $M_\infty = 3.00 - 1.75$.- Performance in the supercritical operating range for the Mach numbers investigated is shown in figure 12. Total-pressure recovery and total-pressure distortion for bleed-exit setting B are shown. Mass-flow ratio at the engine face as measured by the main duct instrumentation is used as a parameter to facilitate inlet-engine matching studies at angle of attack. However, the mass-flow ratio at 5° and 8° may be in error by ±0.050 or more. Data at these angles of attack should, therefore, be treated as qualitative. Points shown with the inlet unstarted (figs. 12(e) and (f)) are separated from the supercritical data by dashed lines.

Maximum performance at angle of attack, $M_\infty = 3.00 - 1.55$.- Figure 13 shows the variation with Mach number of the maximum total-pressure recovery and corresponding total-pressure distortion for several angles of attack. Data for the three fixed bleed-exit settings are presented. The half-filled symbols indicate points where more data are available in table II.

Total-pressure profiles at the engine face, $M_\infty = 3.20 - 1.55$, $\alpha = 0^\circ$.- Total-pressure profiles from each of the six equally spaced rakes shown in the sketch of table II are presented in figure 14. The data presented are for the maximum pressure recovery points in figure 11. Additional data are tabulated in table II.

Bleed mass-flow details, $M_\infty = 3.20 - 1.55$, $\alpha = 0^\circ$.- Bleed mass-flow ratio through each of the four individual bleed zones is presented in figure 15. Summations of these individual bleed zone mass flows were shown in figure 10.

Bleed plenum chamber pressure recoveries, $M_\infty = 3.20 - 1.55$, $\alpha = 0^\circ$.- Total-pressure recoveries within the individual bleed plenum chambers are shown in figure 16. They are the total-pressure recoveries associated with the bleed mass-flow ratios of figure 15. Data for the three bleed exit settings are shown. All the plenum pressures were measured by the static pressure orifices in the bleed plenum chambers shown in figure 2(b). Since the flow velocity was small, these orifices were assumed to measure total pressure. The maximum pressure recovery points from figure 16 are summarized in figure 17 as a function of free-stream Mach number.

Boundary-layer and throat flow profiles, $M_\infty = 3.00 - 2.50$, $\alpha = 0^\circ$.- Figure 18 shows pitot pressure profiles at different stations along the inlet.

The profiles presented are for the contraction ratios giving maximum pressure recovery with bleed-exit setting B. A total-pressure profile at the engine-face station is shown for Mach number 3.0. Mixing induced by the vortex generators appears to have removed all semblance of a boundary layer. This profile was obtained by bending the tubes nearest the centerbody surface to the heights indicated by the profile. No profiles were obtained for Mach numbers below 2.5.

Static-pressure distributions, $M_\infty = 3.20 - 1.55$, $\alpha = 0^{\circ}$.- Figures 19 through 27 present surface static-pressure distributions for both the cowl and centerbody for the Mach number range investigated. The pressure distributions are for the conditions corresponding to those for the half-filled symbols of figure 10 for bleed-exit setting B. The inlet geometry at each Mach number is indicated schematically on each of the figures.

Effect of unstarting the inlet, $M_\infty = 3.0 - 1.55$, $\alpha = 0^{\circ}$.- Figures 28 through 30 show results obtained when the inlet is unstarted. Figure 28 shows the changes in total-pressure recovery, total-pressure distortion at the engine face, and bleed mass-flow ratio. Figures 29 and 30 show changes in the individual bleed zone mass flows and plenum pressure recoveries, respectively. The unfilled symbols are maximum pressure recovery points obtained from figures 10, 15, and 16. At Mach number 1.75 and below the inlet could be restarted without alteration of the inlet geometry.

Sensitivity to angle of attack, $M_\infty = 3.00$.- Figure 31 shows the effect of supercritical inlet operation on the angle of attack that the inlet will tolerate without unstarting. The curves show the supercritical performance data at 0° angle of attack from figure 10(b). To aid in the understanding of these curves the following explanation of the curve for bleed-exit setting A is made. With the inlet operating initially at 0° angle of attack and maximum pressure recovery, the angle of attack can be changed to about 0.5° without unstarting the inlet as shown on the curve. If the total-pressure recovery at 0° angle of attack is reduced about 1 percent by withdrawing the terminal shock wave system downstream, the angle of attack can be changed to about 1.1° before the inlet unstarts. If the total-pressure recovery is decreased further, the angle of attack can be increased from 0° to a limiting value of 2.9° without unstarting the inlet. At this point reducing the total-pressure recovery further will not alter the angle of attack that the inlet will tolerate without unstarting. Similar results were obtained for bleed-exit settings B and C except that the limiting angle of attack was 2.75°.

Transonic Performance

Performance, $M_\infty = 0.6 - 1.3$, $\alpha = 0^{\circ}$.- Figure 32 presents total-pressure recovery, total-pressure distortion at the engine face, and additive drag for the transonic Mach number range. The data presented are for the bleed exits fixed in the open position. No attempt was made to determine the mass flow passing through the bleed zones. The most retracted cowl lip position was $(x/R)_{lip} = 3.952$, which coincided with the station of the maximum centerbody diameter. Data are presented for two other lip positions forward of this station. Some data were obtained with the bleed exits closed but they are not presented herein since they generally showed lower values of total-pressure recovery and higher values of distortion at the engine face.

Performance at angle of attack, $M_\infty = 0.6 - 1.0$.- Engine-face total-pressure recovery and total-pressure distortion are presented in figure 33. Results are shown for angles of attack from 0° to 8°. The 0° data are the filled symbols of figure 32 and the data for nonzero angle of attack were obtained by pitching the model with the 0° geometry settings. No attempt was made to measure additive drag with the inlet at nonzero angle of attack.

Ames Research Center
National Aeronautics and Space Administration
Moffett Field, Calif., Jan. 19, 1968
720-03-01-01-00-21

REFERENCES

1. Sorensen, Norman E.; and Smeltzer, Donald B.: Study and Development of an Axisymmetric Supersonic Inlet. Presented at AIAA Propulsion Joint Specialist Conference, Colorado Springs, Colorado, June 14-17, 1965.

2. Sorensen, Norman E.; Anderson, Warren E.; Wong, Norman D.; and Smeltzer, Donald B.: Performance Summary of a Two-Dimensional and an Axisymmetric Supersonic Inlet System. NASA TM X-1302, 1966.

3. Sorensen, Norman E.; and Smeltzer, Donald B.: Investigation of a Large-Scale Mixed Compression Axisymmetric Inlet System Capable of High Performance at Mach Number 0.6 to 3.0. NASA TM X-1507, 1968.

4. Sorensen, Virginia L.: Computer Program for Calculating Flow Fields in Supersonic Inlets. NASA TN D-2897, 1965.

5. Kuehn, Donald M.: Experimental Investigation of the Pressure Rise Required for the Incipient Separation of Turbulent Boundary Layers in Two-Dimensional Supersonic Flow. NASA MEMO 1-21-59A, 1959.

6. Strike, W. T.; and Rippy, J.: Influence of Suction on the Interaction of an Oblique Shock With a Turbulent Boundary Layer at Mach Number 3. AEDC-TN-61-129, October 1961.

7. Taylor, H. D.: Summary Report on Vortex Generators. UAC Research Department Report R-05280-9, March 7, 1950.

8. Sibulkin, Merwin: Theoretical and Experimental Investigation of Additive Drag. NACA Rep. 1187, 1954.

TABLE I.- INLET COORDINATES

CENTERBODY

$\frac{x}{R}$	$\frac{r}{R}$
0	0
Straight taper	
1.502	.265
1.600	.282
1.800	.320
2.000	.359
2.200	.400
2.400	.442
2.600	.487
2.800	.534
3.000	.582
3.200	.632
3.400	.684
3.500	.710
3.550	.723
3.575	.729
3.600	.735
3.625	.740
3.650	.746
3.675	.751
3.700	.756
3.725	.760
3.750	.764
3.775	.768
3.800	.771

$\frac{x}{R}$	$\frac{r}{R}$
3.825	.774
3.850	.776
3.875	.778
3.900	.779
3.925	.780
3.952	.7802
3.975	.780
4.000	.778
4.022	.776
Straight taper	
4.252	.738
4.300	.730
4.400	.709
4.500	.688
4.600	.666
4.700	.643
4.800	.616
4.900	.585
5.000	.545
5.100	.498
5.150	.471
5.200	.442
5.250	.420
5.300	.405
5.352	.400

Straight line

COWL

$\left(\frac{x}{R}\right)_c$	$\frac{r}{R}$
0	1.000
Straight line	
.2745	1.000
.350	1.000
.450	.999
.550	.997
.650	.995
.750	.991
.850	.986
.950	.976
1.050	.970
1.152	.960
Straight taper	
2.5245	.791
2.575	.787
2.625	.787
2.675	.793
2.725	.808
2.775	.820
2.8245	.825 ← Engine-face rakes

Straight line

TABLE II.- ENGINE-FACE PRESSURE RECOVERY DATA, p_{t_2}/p_{t_∞}

The following include total pressure recoveries from the individual tubes mounted at the engine face. Other quantities of interest are also included. The sketch below shows location of each tube.

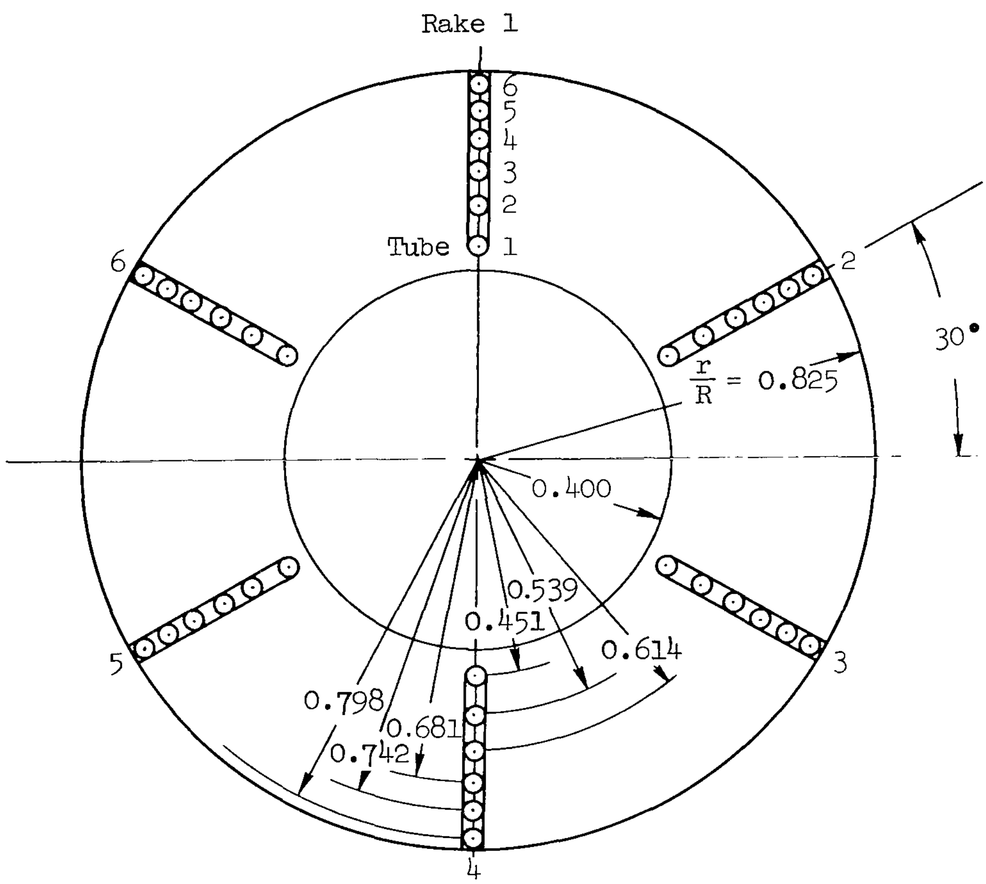

Engine-face pressure tube location looking downstream

TABLE II.- ENGINE-FACE PRESSURE RECOVERY DATA, p_{t_2}/p_{t_∞} - Continued

M_∞ = 3.20 α = 0.0° m_o/m_∞ = 1.000 Exit setting = A

$\bar{p}_{t_2}/p_{t_\infty}$ = 0.799 m_{bl}/m_∞ = 0.085 Δp_{t_2} = 0.147 p_2/p_∞ = 36.7

RAKE NO.	TUBE NO. 1	2	3	4	5	6	RAKE NO.	TUBE NO. 1	2	3	4	5	6
1	0.804	0.788	0.773	0.743	0.734	0.736	2	0.852	0.836	0.842	0.833	0.772	0.747
3	0.830	0.838	0.779	0.832	0.807	0.753	4	0.796	0.783	0.769	0.772	0.751	0.742
5	0.840	0.840	0.837	0.834	0.823	0.771	6	0.850	0.829	0.832	0.837	0.802	0.756

M_∞ = 3.20 α = 0.0° m_o/m_∞ = 1.000 Exit setting = A

$\bar{p}_{t_2}/p_{t_\infty}$ = 0.780 m_{bl}/m_∞ = 0.078 Δp_{t_2} = 0.156 p_2/p_∞ = 36.0

RAKE NO.	TUBE NO. 1	2	3	4	5	6	RAKE NO.	TUBE NO. 1	2	3	4	5	6
1	0.791	0.743	0.726	0.724	0.717	0.719	2	0.819	0.805	0.816	0.806	0.763	0.733
3	0.816	0.824	0.766	0.817	0.788	0.743	4	0.774	0.770	0.764	0.750	0.733	0.728
5	0.821	0.822	0.827	0.807	0.806	0.759	6	0.839	0.816	0.818	0.814	0.774	0.732

M_∞ = 3.20 α = 0.0° m_o/m_∞ = 1.000 Exit setting = A

$\bar{p}_{t_2}/p_{t_\infty}$ = 0.764 m_{bl}/m_∞ = 0.068 Δp_{t_2} = 0.172 p_2/p_∞ = 35.8

RAKE NO.	TUBE NO. 1	2	3	4	5	6	RAKE NO.	TUBE NO. 1	2	3	4	5	6
1	0.746	0.766	0.796	0.820	0.814	0.760	2	0.793	0.812	0.798	0.766	0.726	0.704
3	0.782	0.789	0.702	0.799	0.779	0.735	4	0.740	0.716	0.699	0.691	0.688	0.694
5	0.808	0.806	0.816	0.787	0.767	0.730	6	0.745	0.759	0.780	0.809	0.800	0.760

M_∞ = 3.20 α = 0.0° m_o/m_∞ = 1.000 Exit setting = B

$\bar{p}_{t_2}/p_{t_\infty}$ = 0.816 m_{bl}/m_∞ = 0.098 Δp_{t_2} = 0.170 p_2/p_∞ = 38.9

RAKE NO.	TUBE NO. 1	2	3	4	5	6	RAKE NO.	TUBE NO. 1	2	3	4	5	6
1	0.752	0.768	0.807	0.829	0.851	0.888	2	0.755	0.775	0.799	0.820	0.846	0.882
3	0.751	0.759	0.826	0.834	0.862	0.889	4	0.753	0.781	0.821	0.854	0.863	0.886
5	0.753	0.767	0.792	0.819	0.843	0.867	6	0.756	0.779	0.801	0.818	0.841	0.881

TABLE II.- ENGINE-FACE PRESSURE RECOVERY DATA, p_{t_2}/p_{t_∞} - Continued

M_∞ = 3.20 α = 0.0° m_o/m_∞ = 1.000 Exit setting = B

$\bar{p}_{t_2}/p_{t_\infty}$ = 0.797 m_{bl}/m_∞ = 0.077 Δp_{t_2} = 0.134 p_2/p_∞ = 36.2

RAKE NO.	TUBE NO. 1	2	3	4	5	6	RAKE NO.	TUBE NO. 1	2	3	4	5	6
1	0.799	0.769	0.792	0.828	0.827	0.790	2	0.786	0.813	0.831	0.826	0.829	0.819
3	0.776	0.804	0.845	0.826	0.811	0.788	4	0.750	0.806	0.799	0.809	0.804	0.778
5	0.739	0.745	0.761	0.769	0.785	0.801	6	0.755	0.784	0.797	0.807	0.819	0.834

M_∞ = 3.20 α = 0.0° m_o/m_∞ = 1.000 Exit setting = B

$\bar{p}_{t_2}/p_{t_\infty}$ = 0.766 m_{bl}/m_∞ = 0.062 Δp_{t_2} = 0.176 p_2/p_∞ = 36.0

RAKE NO.	TUBE NO. 1	2	3	4	5	6	RAKE NO.	TUBE NO. 1	2	3	4	5	6
1	0.738	0.756	0.795	0.828	0.825	0.776	2	0.805	0.822	0.809	0.763	0.720	0.704
3	0.789	0.806	0.703	0.798	0.785	0.743	4	0.740	0.708	0.697	0.694	0.693	0.693
5	0.806	0.808	0.818	0.786	0.765	0.725	6	0.763	0.772	0.792	0.807	0.796	0.753

M_∞ = 3.20 α = 0.0° m_o/m_∞ = 1.000 Exit setting = C

$\bar{p}_{t_2}/p_{t_\infty}$ = 0.796 m_{bl}/m_∞ = 0.073 Δp_{t_2} = 0.193 p_2/p_∞ = 37.5

RAKE NO.	TUBE NO. 1	2	3	4	5	6	RAKE NO.	TUBE NO. 1	2	3	4	5	6
1	0.721	0.737	0.790	0.827	0.839	0.856	2	0.728	0.734	0.756	0.803	0.833	0.864
3	0.731	0.749	0.800	0.821	0.845	0.866	4	0.726	0.756	0.802	0.843	0.841	0.852
5	0.722	0.742	0.780	0.798	0.830	0.862	6	0.731	0.762	0.790	0.817	0.842	0.875

M_∞ = 3.20 α = 0.0° m_o/m_∞ = 1.000 Exit setting = C

$\bar{p}_{t_2}/p_{t_\infty}$ = 0.772 m_{bl}/m_∞ = 0.058 Δp_{t_2} = 0.176 p_2/p_∞ = 36.6

RAKE NO.	TUBE NO. 1	2	3	4	5	6	RAKE NO.	TUBE NO. 1	2	3	4	5	6
1	0.734	0.755	0.782	0.819	0.833	0.806	2	0.765	0.799	0.822	0.809	0.787	0.742
3	0.783	0.790	0.704	0.788	0.774	0.738	4	0.754	0.717	0.702	0.698	0.697	0.699
5	0.823	0.818	0.825	0.791	0.768	0.727	6	0.757	0.776	0.797	0.817	0.812	0.787

TABLE II.- ENGINE-FACE PRESSURE RECOVERY DATA, p_{t_2}/p_{t_∞} - Continued

M_∞ = 3.00 α = 0.0° m_o/m_∞ = 0.997 Exit setting = A

$\bar{p}_{t_2}/p_{t_\infty}$ = 0.934 m_{bl}/m_∞ = 0.123 Δp_{t_2} = 0.098 p_2/p_∞ = 32.1

RAKE NO.	TUBE NO. 1	2	3	4	5	6	RAKE NO.	TUBE NO. 1	2	3	4	5	6
1	0.886	0.928	0.912	0.946	0.950	0.929	2	0.878	0.943	0.949	0.952	0.948	0.959
3	0.895	0.925	0.970	0.942	0.940	0.940	4	0.914	0.951	0.969	0.939	0.934	0.903
5	0.919	0.922	0.926	0.959	0.961	0.943	6	0.906	0.924	0.902	0.952	0.960	0.928

M_∞ = 3.00 α = 0.0° m_o/m_∞ = 0.997 Exit setting = A

$\bar{p}_{t_2}/p_{t_\infty}$ = 0.913 m_{bl}/m_∞ = 0.103 Δp_{t_2} = 0.090 p_2/p_∞ = 31.3

RAKE NO.	TUBE NO. 1	2	3	4	5	6	RAKE NO.	TUBE NO. 1	2	3	4	5	6
1	0.864	0.894	0.884	0.924	0.924	0.930	2	0.863	0.923	0.916	0.927	0.928	0.937
3	0.882	0.910	0.945	0.924	0.921	0.924	4	0.907	0.927	0.944	0.921	0.914	0.919
5	0.881	0.897	0.898	0.935	0.926	0.941	6	0.889	0.895	0.878	0.927	0.926	0.936

M_∞ = 3.00 α = 0.0° m_o/m_∞ = 0.997 Exit setting = A

$\bar{p}_{t_2}/p_{t_\infty}$ = 0.880 m_{bl}/m_∞ = 0.085 Δp_{t_2} = 0.100 p_2/p_∞ = 29.7

RAKE NO.	TUBE NO. 1	2	3	4	5	6	RAKE NO.	TUBE NO. 1	2	3	4	5	6
1	0.831	0.832	0.863	0.886	0.891	0.910	2	0.874	0.864	0.870	0.876	0.875	0.893
3	0.897	0.884	0.919	0.877	0.880	0.887	4	0.877	0.893	0.919	0.889	0.885	0.911
5	0.862	0.859	0.872	0.897	0.896	0.889	6	0.865	0.838	0.845	0.893	0.905	0.885

M_∞ = 3.00 α = 0.0° m_o/m_∞ = 0.997 Exit setting = B

$\bar{p}_{t_2}/p_{t_\infty}$ = 0.920 m_{bl}/m_∞ = 0.108 Δp_{t_2} = 0.106 p_2/p_∞ = 31.5

RAKE NO.	TUBE NO. 1	2	3	4	5	6	RAKE NO.	TUBE NO. 1	2	3	4	5	6
1	0.881	0.899	0.897	0.939	0.939	0.935	2	0.856	0.929	0.915	0.943	0.939	0.947
3	0.891	0.926	0.954	0.939	0.935	0.925	4	0.897	0.930	0.951	0.937	0.926	0.917
5	0.869	0.892	0.893	0.945	0.935	0.918	6	0.872	0.922	0.893	0.941	0.944	0.933

TABLE II.- ENGINE-FACE PRESSURE RECOVERY DATA, p_{t_2}/p_{t_∞} - Continued

M_∞ = 3.00 α = 0.0° m_o/m_∞ = 0.997   Exit setting = B

$\bar{p}_{t_2}/p_{t_\infty}$ = 0.922 m_{bl}/m_∞ = 0.097 Δp_{t_2} = 0.096 p_2/p_∞ = 31.5

RAKE NO.	TUBE NO. 1	2	3	4	5	6	RAKE NO.	TUBE NO. 1	2	3	4	5	6
1	0.870	0.894	0.895	0.936	0.937	0.934	2	0.869	0.933	0.917	0.942	0.934	0.953
3	0.903	0.923	0.957	0.935	0.934	0.930	4	0.889	0.930	0.955	0.941	0.928	0.927
5	0.879	0.903	0.902	0.948	0.948	0.937	6	0.877	0.906	0.888	0.944	0.950	0.929

M_∞ = 3.00 α = 0.0° m_o/m_∞ = 0.977   Exit setting = B

$\bar{p}_{t_2}/p_{t_\infty}$ = 0.909 m_{bl}/m_∞ = 0.088 Δp_{t_2} = 0.097 p_2/p_∞ = 30.9

RAKE NO.	TUBE NO. 1	2	3	4	5	6	RAKE NO.	TUBE NO. 1	2	3	4	5	6
1	0.858	0.881	0.876	0.923	0.925	0.933	2	0.878	0.917	0.896	0.924	0.918	0.923
3	0.915	0.910	0.946	0.921	0.919	0.904	4	0.888	0.918	0.942	0.926	0.914	0.933
5	0.872	0.888	0.883	0.933	0.931	0.925	6	0.873	0.886	0.869	0.926	0.932	0.921

M_∞ = 3.00 α = 0.0° m_o/m_∞ = 0.997   Exit setting = B

$\bar{p}_{t_2}/p_{t_\infty}$ = 0.872 m_{bl}/m_∞ = 0.076 Δp_{t_2} = 0.137 p_2/p_∞ = 29.6

RAKE NO.	TUBE NO. 1	2	3	4	5	6	RAKE NO.	TUBE NO. 1	2	3	4	5	6
1	0.824	0.817	0.825	0.873	0.877	0.936	2	0.844	0.849	0.838	0.875	0.878	0.922
3	0.862	0.867	0.903	0.889	0.885	0.919	4	0.864	0.874	0.901	0.883	0.876	0.934
5	0.852	0.838	0.844	0.881	0.889	0.910	6	0.852	0.824	0.820	0.873	0.891	0.913

M_∞ = 3.00 α = 0.0° m_o/m_∞ = 0.997   Exit setting = C

$\bar{p}_{t_2}/p_{t_\infty}$ = 0.901 m_{bl}/m_∞ = 0.084 Δp_{t_2} = 0.131 p_2/p_∞ = ---

RAKE NO.	TUBE NO. 1	2	3	4	5	6	RAKE NO.	TUBE NO. 1	2	3	4	5	6
1	0.853	0.879	0.879	0.921	0.920	0.929	2	0.824	0.907	0.875	0.918	0.912	0.935
3	0.889	0.913	0.940	0.924	0.911	0.909	4	0.870	0.914	0.942	0.924	0.910	0.912
5	0.844	0.879	0.874	0.926	0.914	0.892	6	0.847	0.901	0.870	0.925	0.923	0.914

TABLE II.- ENGINE-FACE PRESSURE RECOVERY DATA, p_{t_2}/p_{t_∞} - Continued

M_∞ = 3.00 α = 0.0° m_o/m_∞ = 0.997 Exit setting = C

$\bar{p}_{t_2}/p_{t_\infty}$ = 0.903 m_{bl}/m_∞ = 0.075 Δp_{t_2} = 0.108 p_2/p_∞ = 30.6

RAKE NO.	TUBE NO. 1	2	3	4	5	6	RAKE NO.	TUBE NO. 1	2	3	4	5	6
1	0.849	0.865	0.873	0.917	0.918	0.932	2	0.864	0.906	0.890	0.914	0.909	0.922
3	0.907	0.912	0.946	0.911	0.906	0.903	4	0.889	0.913	0.943	0.919	0.909	0.924
5	0.863	0.882	0.876	0.927	0.923	0.922	6	0.862	0.874	0.861	0.921	0.928	0.909

M_∞ = 3.00 α = 0.0° m_o/m_∞ = 0.997 Exit setting = C

$\bar{p}_{t_2}/p_{t_\infty}$ = 0.879 m_{bl}/m_∞ = 0.068 Δp_{t_2} = 0.126 p_2/p_∞ = 29.6

RAKE NO.	TUBE NO. 1	2	3	4	5	6	RAKE NO.	TUBE NO. 1	2	3	4	5	6
1	0.830	0.822	0.835	0.878	0.886	0.932	2	0.857	0.862	0.851	0.877	0.876	0.933
3	0.887	0.878	0.913	0.887	0.885	0.917	4	0.874	0.884	0.909	0.892	0.887	0.932
5	0.838	0.854	0.849	0.898	0.895	0.911	6	0.854	0.835	0.827	0.889	0.898	0.912

M_∞ = 2.90 α = 0.0° m_o/m_∞ = 0.977 Exit setting = A

$\bar{p}_{t_2}/p_{t_\infty}$ = 0.903 m_{bl}/m_∞ = 0.121 Δp_{t_2} = 0.170 p_2/p_∞ = 27.0

RAKE NO.	TUBE NO. 1	2	3	4	5	6	RAKE NO.	TUBE NO. 1	2	3	4	5	6
1	0.822	0.849	0.854	0.881	0.945	0.967	2	0.858	0.909	0.888	0.942	0.934	0.951
3	0.852	0.922	0.867	0.945	0.936	0.953	4	0.813	0.864	0.870	0.899	0.922	0.944
5	0.824	0.924	0.918	0.942	0.942	0.947	6	0.825	0.887	0.875	0.927	0.946	0.950

M_∞ = 2.90 α = 0.0° m_o/m_∞ = 0.977 Exit setting = A

$\bar{p}_{t_2}/p_{t_\infty}$ = 0.892 m_{bl}/m_∞ = 0.108 Δp_{t_2} = 0.182 p_2/p_∞ = 26.6

RAKE NO.	TUBE NO. 1	2	3	4	5	6	RAKE NO.	TUBE NO. 1	2	3	4	5	6
1	0.809	0.833	0.833	0.869	0.938	0.959	2	0.867	0.885	0.870	0.927	0.931	0.952
3	0.870	0.896	0.854	0.941	0.930	0.950	4	0.797	0.845	0.851	0.900	0.919	0.940
5	0.809	0.901	0.899	0.934	0.946	0.944	6	0.813	0.866	0.854	0.908	0.943	0.948

TABLE II.- ENGINE-FACE PRESSURE RECOVERY DATA, p_{t_2}/p_{t_∞} - Continued

M_∞ = 2.90 α = 0.0° m_0/m_∞ = 0.977 Exit setting = A

$\bar{p}_{t_2}/p_{t_\infty}$ = 0.864 m_{bl}/m_∞ = 0.090 Δp_{t_2} = 0.192 p_2/p_∞ = 25.5

RAKE NO.	TUBE NO. 1	2	3	4	5	6	RAKE NO.	TUBE NO. 1	2	3	4	5	6
1	0.775	0.800	0.795	0.844	0.927	0.937	2	0.816	0.834	0.833	0.898	0.895	0.929
3	0.855	0.861	0.821	0.911	0.899	0.915	4	0.771	0.822	0.830	0.899	0.899	0.917
5	0.773	0.859	0.859	0.900	0.934	0.924	6	0.797	0.819	0.815	0.889	0.928	0.926

M_∞ = 2.90 α = 0.0° m_0/m_∞ = 0.977 Exit setting = B

$\bar{p}_{t_2}/p_{t_\infty}$ = 0.889 m_{bl}/m_∞ = 0.120 Δp_{t_2} = 0.097 p_2/p_∞ = 26.0

RAKE NO.	TUBE NO. 1	2	3	4	5	6	RAKE NO.	TUBE NO. 1	2	3	4	5	6
1	0.905	0.891	0.896	0.883	0.873	0.882	2	0.892	0.895	0.899	0.877	0.878	0.879
3	0.904	0.915	0.907	0.885	0.883	0.878	4	0.926	0.899	0.900	0.858	0.862	0.839
5	0.919	0.895	0.909	0.877	0.884	0.860	6	0.919	0.890	0.902	0.887	0.882	0.860

M_∞ = 2.90 α = 0.0° m_0/m_∞ = 0.977 Exit setting = B

$\bar{p}_{t_2}/p_{t_\infty}$ = 0.899 m_{bl}/m_∞ = 0.104 Δp_{t_2} = 0.182 p_2/p_∞ = 26.7

RAKE NO.	TUBE NO. 1	2	3	4	5	6	RAKE NO.	TUBE NO. 1	2	3	4	5	6
1	0.811	0.847	0.847	0.874	0.944	0.966	2	0.843	0.904	0.883	0.934	0.934	0.953
3	0.836	0.914	0.872	0.947	0.930	0.949	4	0.803	0.871	0.864	0.919	0.926	0.946
5	0.818	0.909	0.906	0.939	0.939	0.940	6	0.841	0.871	0.863	0.922	0.938	0.949

M_∞ = 2.90 α = 0.0° m_0/m_∞ = 0.977 Exit setting = B

$\bar{p}_{t_2}/p_{t_\infty}$ = 0.869 m_{bl}/m_∞ = 0.085 Δp_{t_2} = 0.197 p_2/p_∞ = 25.8

RAKE NO.	TUBE NO. 1	2	3	4	5	6	RAKE NO.	TUBE NO. 1	2	3	4	5	6
1	0.778	0.807	0.805	0.838	0.928	0.942	2	0.829	0.851	0.839	0.909	0.907	0.938
3	0.812	0.864	0.828	0.920	0.906	0.926	4	0.771	0.836	0.824	0.891	0.898	0.927
5	0.780	0.864	0.863	0.912	0.931	0.933	6	0.799	0.846	0.828	0.884	0.931	0.940

TABLE II.- ENGINE-FACE PRESSURE RECOVERY DATA, p_{t_2}/p_{t_∞} - Continued

M_∞ = 2.90 α = 0.0° m_o/m_∞ = 0.977 Exit setting = C

$\bar{p}_{t_2}/p_{t_\infty}$ = 0.879 m_{bl}/m_∞ = 0.101 Δp_{t_2} = 0.141 p_2/p_∞ = 25.5

RAKE NO.	TUBE NO. 1	2	3	4	5	6	RAKE NO.	TUBE NO. 1	2	3	4	5	6
1	0.901	0.876	0.892	0.866	0.860	0.864	2	0.904	0.886	0.893	0.861	0.860	0.863
3	0.910	0.908	0.896	0.872	0.872	0.872	4	0.927	0.894	0.893	0.836	0.848	0.803
5	0.919	0.887	0.904	0.873	0.874	0.848	6	0.918	0.881	0.901	0.876	0.874	0.835

M_∞ = 2.90 α = 0.0° m_o/m_∞ = 0.977 Exit setting = C

$\bar{p}_{t_2}/p_{t_\infty}$ = 0.894 m_{bl}/m_∞ = 0.087 Δp_{t_2} = 0.164 p_2/p_∞ = 26.3

RAKE NO.	TUBE NO. 1	2	3	4	5	6	RAKE NO.	TUBE NO. 1	2	3	4	5	6
1	0.805	0.857	0.838	0.912	0.929	0.951	2	0.852	0.896	0.872	0.925	0.913	0.932
3	0.835	0.913	0.922	0.934	0.908	0.926	4	0.811	0.909	0.899	0.929	0.901	0.919
5	0.811	0.890	0.871	0.930	0.909	0.908	6	0.864	0.882	0.861	0.931	0.908	0.920

M_∞ = 2.90 α = 0.0° m_o/m_∞ = 0.977 Exit setting = C

$\bar{p}_{t_2}/p_{t_\infty}$ = 0.866 m_{bl}/m_∞ = 0.072 Δp_{t_2} = 0.207 p_2/p_∞ = 25.5

RAKE NO.	TUBE NO. 1	2	3	4	5	6	RAKE NO.	TUBE NO. 1	2	3	4	5	6
1	0.773	0.811	0.805	0.856	0.911	0.945	2	0.840	0.850	0.839	0.899	0.889	0.927
3	0.860	0.875	0.833	0.913	0.894	0.907	4	0.767	0.839	0.830	0.892	0.883	0.921
5	0.766	0.848	0.863	0.893	0.926	0.931	6	0.787	0.828	0.818	0.873	0.927	0.943

M_∞ = 2.75 α = 0.0° m_o/m_∞ = 0.955 Exit setting = A

$\bar{p}_{t_2}/p_{t_\infty}$ = 0.953 m_{bl}/m_∞ = 0.137 Δp_{t_2} = 0.088 p_2/p_∞ = 21.8

RAKE NO.	TUBE NO. 1	2	3	4	5	6	RAKE NO.	TUBE NO. 1	2	3	4	5	6
1	0.939	0.940	0.952	0.960	0.963	0.900	2	0.929	0.959	0.964	0.977	0.981	0.935
3	0.947	0.950	0.984	0.971	0.970	0.901	4	0.965	0.968	0.982	0.963	0.969	0.921
5	0.925	0.944	0.938	0.983	0.981	0.940	6	0.968	0.947	0.937	0.975	0.975	0.910

TABLE II.- ENGINE-FACE PRESSURE RECOVERY DATA, p_{t_2}/p_{t_∞} - Continued

M_∞ = 2.75 α = 0.0° m_o/m_∞ = 0.955 Exit setting = A

$\bar{p}_{t_2}/p_{t_\infty}$ = 0.935 m_{bl}/m_∞ = 0.118 Δp_{t_2} = 0.086 p_2/p_∞ = 21.3

RAKE NO.	TUBE NO. 1	2	3	4	5	6	RAKE NO.	TUBE NO. 1	2	3	4	5	6
1	0.919	0.918	0.924	0.943	0.942	0.904	2	0.920	0.928	0.938	0.947	0.937	0.922
3	0.964	0.943	0.962	0.939	0.934	0.915	4	0.969	0.948	0.961	0.937	0.945	0.898
5	0.927	0.921	0.933	0.968	0.965	0.895	6	0.954	0.921	0.914	0.951	0.955	0.888

M_∞ = 2.75 α = 0.0° m_o/m_∞ = 0.955 Exit setting = A

$\bar{p}_{t_2}/p_{t_\infty}$ = 0.876 m_{bl}/m_∞ = 0.105 Δp_{t_2} = 0.124 p_2/p_∞ = 19.8

RAKE NO.	TUBE NO. 1	2	3	4	5	6	RAKE NO.	TUBE NO. 1	2	3	4	5	6
1	0.864	0.854	0.831	0.851	0.852	0.914	2	0.883	0.875	0.867	0.842	0.851	0.905
3	0.924	0.889	0.895	0.847	0.854	0.889	4	0.940	0.890	0.899	0.847	0.854	0.900
5	0.921	0.857	0.864	0.870	0.874	0.923	6	0.899	0.831	0.837	0.855	0.868	0.906

M_∞ = 2.75 α = 0.0° m_o/m_∞ = 0.955 Exit setting = B

$\bar{p}_{t_2}/p_{t_\infty}$ = 0.950 m_{bl}/m_∞ = 0.123 Δp_{t_2} = 0.094 p_2/p_∞ = 21.6

RAKE NO.	TUBE NO. 1	2	3	4	5	6	RAKE NO.	TUBE NO. 1	2	3	4	5	6
1	0.934	0.936	0.945	0.963	0.963	0.906	2	0.907	0.953	0.945	0.976	0.979	0.942
3	0.953	0.946	0.984	0.969	0.968	0.918	4	0.957	0.964	0.982	0.959	0.964	0.905
5	0.924	0.936	0.939	0.984	0.982	0.937	6	0.963	0.940	0.936	0.973	0.974	0.895

M_∞ = 2.75 α = 0.0° m_o/m_∞ = 0.955 Exit setting = B

$\bar{p}_{t_2}/p_{t_\infty}$ = 0.934 m_{bl}/m_∞ = 0.108 Δp_{t_2} = 0.087 p_2/p_∞ = 21.1

RAKE NO.	TUBE NO. 1	2	3	4	5	6	RAKE NO.	TUBE NO. 1	2	3	4	5	6
1	0.907	0.912	0.915	0.950	0.938	0.910	2	0.923	0.930	0.936	0.949	0.948	0.924
3	0.954	0.939	0.964	0.948	0.942	0.920	4	0.960	0.951	0.963	0.931	0.940	0.908
5	0.918	0.920	0.932	0.964	0.959	0.900	6	0.945	0.917	0.908	0.956	0.951	0.883

TABLE II.- ENGINE-FACE PRESSURE RECOVERY DATA, p_{t_2}/p_{t_∞} - Continued

M_∞ = 2.75 α = 0.0° m_o/m_∞ = 0.955 Exit setting = B

$\bar{p}_{t_2}/p_{t_\infty}$ = 0.888 m_{bl}/m_∞ = 0.099 Δp_{t_2} = 0.111 p_2/p_∞ = 19.9

RAKE NO.	TUBE NO. 1	2	3	4	5	6	RAKE NO.	TUBE NO. 1	2	3	4	5	6
1	0.878	0.858	0.857	0.873	0.867	0.904	2	0.905	0.886	0.890	0.851	0.858	0.907
3	0.935	0.900	0.925	0.870	0.866	0.877	4	0.945	0.910	0.927	0.865	0.867	0.890
5	0.929	0.869	0.886	0.894	0.892	0.907	6	0.916	0.848	0.846	0.881	0.889	0.882

M_∞ = 2.75 α = 0.0° m_o/m_∞ = 0.955 Exit setting = C

$\bar{p}_{t_2}/p_{t_\infty}$ = 0.940 m_{bl}/m_∞ = 0.104 Δp_{t_2} = 0.110 p_2/p_∞ = 21.2

RAKE NO.	TUBE NO. 1	2	3	4	5	6	RAKE NO.	TUBE NO. 1	2	3	4	5	6
1	0.925	0.923	0.929	0.956	0.951	0.898	2	0.934	0.939	0.942	0.952	0.952	0.925
3	0.967	0.949	0.980	0.955	0.951	0.912	4	0.953	0.955	0.980	0.949	0.950	0.882
5	0.915	0.927	0.937	0.972	0.966	0.905	6	0.960	0.923	0.922	0.962	0.965	0.877

M_∞ = 2.75 α = 0.0° m_o/m_∞ = 0.955 Exit setting = C

$\bar{p}_{t_2}/p_{t_\infty}$ = 0.906 m_{bl}/m_∞ = 0.088 Δp_{t_2} = 0.099 p_2/p_∞ = 20.3

RAKE NO.	TUBE NO. 1	2	3	4	5	6	RAKE NO.	TUBE NO. 1	2	3	4	5	6
1	0.889	0.883	0.873	0.910	0.892	0.896	2	0.930	0.891	0.896	0.897	0.887	0.909
3	0.946	0.922	0.949	0.911	0.897	0.907	4	0.949	0.914	0.952	0.906	0.893	0.901
5	0.892	0.896	0.880	0.938	0.920	0.889	6	0.931	0.887	0.862	0.924	0.912	0.883

M_∞ = 2.50 α = 0.0° m_o/m_∞ = 0.871 Exit setting = A

$\bar{p}_{t_2}/p_{t_\infty}$ = 0.948 m_{bl}/m_∞ = 0.127 Δp_{t_2} = 0.075 p_2/p_∞ = 15.2

RAKE NO.	TUBE NO. 1	2	3	4	5	6	RAKE NO.	TUBE NO. 1	2	3	4	5	6
1	0.907	0.907	0.929	0.975	0.977	0.978	2	0.914	0.923	0.934	0.961	0.972	0.967
3	0.915	0.928	0.961	0.962	0.966	0.965	4	0.927	0.927	0.958	0.965	0.966	0.969
5	0.925	0.917	0.950	0.973	0.974	0.970	6	0.925	0.916	0.913	0.969	0.971	0.971

TABLE II.- ENGINE-FACE PRESSURE RECOVERY DATA, p_{t_2}/p_{t_∞} - Continued

M_∞ = 2.50 α = 0.0° m_0/m_∞ = 0.871 Exit setting = A

$\bar{p}_{t_2}/p_{t_\infty}$ = 0.932 m_{b1}/m_∞ = 0.109 Δp_{t_2} = 0.088 p_2/p_∞ = 15.0

RAKE NO.	TUBE NO. 1	2	3	4	5	6	RAKE NO.	TUBE NO. 1	2	3	4	5	6
1	0.893	0.889	0.911	0.952	0.963	0.971	2	0.902	0.897	0.905	0.942	0.958	0.960
3	0.906	0.906	0.934	0.949	0.953	0.954	4	0.918	0.906	0.934	0.951	0.956	0.963
5	0.908	0.897	0.926	0.958	0.964	0.962	6	0.912	0.897	0.898	0.951	0.960	0.964

M_∞ = 2.50 α = 0.0° m_0/m_∞ = 0.871 Exit setting = A

$\bar{p}_{t_2}/p_{t_\infty}$ = 0.881 m_{b1}/m_∞ = 0.091 Δp_{t_2} = 0.189 p_2/p_∞ = 13.5

RAKE NO.	TUBE NO. 1	2	3	4	5	6	RAKE NO.	TUBE NO. 1	2	3	4	5	6
1	0.783	0.836	0.898	0.938	0.918	0.945	2	0.779	0.786	0.817	0.869	0.909	0.919
3	0.788	0.837	0.916	0.928	0.927	0.928	4	0.807	0.856	0.917	0.935	0.931	0.935
5	0.802	0.833	0.877	0.927	0.936	0.928	6	0.793	0.822	0.872	0.933	0.938	0.937

M_∞ = 2.50 α = 0.0° m_0/m_∞ = 0.871 Exit setting = B

$\bar{p}_{t_2}/p_{t_\infty}$ = 0.945 m_{b1}/m_∞ = 0.110 Δp_{t_2} = 0.080 p_2/p_∞ = 15.1

RAKE NO.	TUBE NO. 1	2	3	4	5	6	RAKE NO.	TUBE NO. 1	2	3	4	5	6
1	0.903	0.902	0.932	0.971	0.975	0.978	2	0.917	0.917	0.926	0.961	0.969	0.968
3	0.915	0.927	0.956	0.958	0.962	0.962	4	0.932	0.928	0.955	0.962	0.964	0.968
5	0.917	0.907	0.943	0.969	0.970	0.969	6	0.918	0.911	0.914	0.966	0.969	0.970

M_∞ = 2.50 α = 0.0° m_0/m_∞ = 0.871 Exit setting = B

$\bar{p}_{t_2}/p_{t_\infty}$ = 0.932 m_{b1}/m_∞ = 0.100 Δp_{t_2} = 0.087 p_2/p_∞ = 14.9

RAKE NO.	TUBE NO. 1	2	3	4	5	6	RAKE NO.	TUBE NO. 1	2	3	4	5	6
1	0.887	0.886	0.913	0.955	0.961	0.968	2	0.898	0.899	0.906	0.952	0.957	0.960
3	0.907	0.911	0.945	0.949	0.952	0.953	4	0.913	0.908	0.943	0.953	0.954	0.960
5	0.902	0.897	0.927	0.957	0.962	0.962	6	0.905	0.894	0.900	0.952	0.959	0.964

TABLE II.- ENGINE-FACE PRESSURE RECOVERY DATA, p_{t_2}/p_{t_∞} - Continued

M_∞ = 2.50 α = 0.0° m_o/m_∞ = 0.871 Exit setting = B

$\bar{p}_{t_2}/p_{t_\infty}$ = 0.884 m_{bl}/m_∞ = 0.085 Δp_{t_2} = 0.185 p_2/p_∞ = 13.7

RAKE NO.	TUBE NO. 1	2	3	4	5	6	RAKE NO.	TUBE NO. 1	2	3	4	5	6
1	0.793	0.814	0.871	0.933	0.926	0.951	2	0.789	0.787	0.811	0.874	0.915	0.930
3	0.797	0.849	0.918	0.930	0.927	0.923	4	0.823	0.861	0.917	0.935	0.927	0.940
5	0.813	0.825	0.876	0.925	0.934	0.931	6	0.811	0.849	0.912	0.940	0.938	0.941

M_∞ = 2.50 α = 0.0° m_o/m_∞ = 0.871 Exit setting = C

$\bar{p}_{t_2}/p_{t_\infty}$ = 0.944 m_{bl}/m_∞ = 0.099 Δp_{t_2} = 0.092 p_2/p_∞ = 15.0

RAKE NO.	TUBE NO. 1	2	3	4	5	6	RAKE NO.	TUBE NO. 1	2	3	4	5	6
1	0.892	0.897	0.933	0.977	0.977	0.979	2	0.904	0.909	0.923	0.966	0.972	0.970
3	0.918	0.928	0.958	0.960	0.959	0.960	4	0.927	0.926	0.956	0.964	0.959	0.957
5	0.911	0.904	0.940	0.967	0.966	0.964	6	0.913	0.906	0.919	0.969	0.969	0.969

M_∞ = 2.50 α = 0.0° m_o/m_∞ = 0.871 Exit setting = C

$\bar{p}_{t_2}/p_{t_\infty}$ = 0.929 m_{bl}/m_∞ = 0.083 Δp_{t_2} = 0.103 p_2/p_∞ = 14.7

RAKE NO.	TUBE NO. 1	2	3	4	5	6	RAKE NO.	TUBE NO. 1	2	3	4	5	6
1	0.878	0.874	0.904	0.956	0.967	0.970	2	0.889	0.887	0.899	0.950	0.962	0.965
3	0.896	0.903	0.935	0.952	0.956	0.956	4	0.898	0.900	0.936	0.955	0.960	0.960
5	0.885	0.884	0.921	0.964	0.966	0.959	6	0.890	0.882	0.895	0.957	0.963	0.960

M_∞ = 2.50 α = 0.0° m_o/m_∞ = 0.871 Exit setting = C

$\bar{p}_{t_2}/p_{t_\infty}$ = 0.876 m_{bl}/m_∞ = 0.072 Δp_{t_2} = 0.257 p_2/p_∞ = 13.4

RAKE NO.	TUBE NO. 1	2	3	4	5	6	RAKE NO.	TUBE NO. 1	2	3	4	5	6
1	0.752	0.782	0.842	0.924	0.954	0.968	2	0.743	0.780	0.838	0.919	0.957	0.963
3	0.752	0.799	0.876	0.943	0.948	0.957	4	0.759	0.802	0.872	0.946	0.946	0.955
5	0.767	0.805	0.871	0.948	0.956	0.959	6	0.772	0.799	0.846	0.927	0.954	0.957

TABLE II.- ENGINE-FACE PRESSURE RECOVERY DATA, p_{t_2}/p_{t_∞} - Continued

M_∞ = 2.25 α = 0.0° m_o/m_∞ = 0.808 Exit setting = A

$\bar{p}_{t_2}/p_{t_\infty}$ = 0.948 m_{bl}/m_∞ = 0.112 Δp_{t_2} = 0.067 p_2/p_∞ = 10.2

RAKE NO.	TUBE NO.						RAKE NO.	TUBE NO.					
	1	2	3	4	5	6		1	2	3	4	5	6
1	0.911	0.910	0.934	0.968	0.969	0.973	2	0.911	0.916	0.934	0.957	0.967	0.971
3	0.922	0.930	0.962	0.964	0.973	0.973	4	0.920	0.926	0.956	0.967	0.972	0.972
5	0.926	0.921	0.956	0.964	0.969	0.968	6	0.913	0.917	0.936	0.959	0.967	0.973

M_∞ = 2.25 α = 0.0° m_o/m_∞ = 0.808 Exit setting = A

$\bar{p}_{t_2}/p_{t_\infty}$ = 0.937 m_{bl}/m_∞ = 0.098 Δp_{t_2} = 0.104 p_2/p_∞ = 10.0

RAKE NO.	TUBE NO.						RAKE NO.	TUBE NO.					
	1	2	3	4	5	6		1	2	3	4	5	6
1	0.884	0.886	0.921	0.968	0.972	0.973	2	0.878	0.884	0.915	0.962	0.970	0.971
3	0.876	0.897	0.960	0.963	0.972	0.972	4	0.902	0.917	0.955	0.968	0.970	0.962
5	0.891	0.906	0.945	0.965	0.968	0.960	6	0.879	0.888	0.916	0.963	0.969	0.970

M_∞ = 2.25 α = 0.0° m_o/m_∞ = 0.808 Exit setting = A

$\bar{p}_{t_2}/p_{t_\infty}$ = 0.886 m_{bl}/m_∞ = 0.078 Δp_{t_2} = 0.162 p_2/p_∞ = 9.2

RAKE NO.	TUBE NO.						RAKE NO.	TUBE NO.					
	1	2	3	4	5	6		1	2	3	4	5	6
1	0.795	0.831	0.880	0.917	0.933	0.932	2	0.792	0.828	0.866	0.902	0.921	0.929
3	0.813	0.865	0.901	0.920	0.916	0.928	4	0.799	0.831	0.889	0.915	0.926	0.927
5	0.818	0.869	0.912	0.934	0.936	0.936	6	0.799	0.843	0.891	0.927	0.936	0.929

M_∞ = 2.25 α = 0.0° m_o/m_∞ = 0.808 Exit setting = B

$\bar{p}_{t_2}/p_{t_\infty}$ = 0.948 m_{bl}/m_∞ = 0.102 Δp_{t_2} = 0.078 p_2/p_∞ = 10.2

RAKE NO.	TUBE NO.						RAKE NO.	TUBE NO.					
	1	2	3	4	5	6		1	2	3	4	5	6
1	0.904	0.913	0.942	0.965	0.974	0.975	2	0.901	0.909	0.930	0.967	0.972	0.973
3	0.915	0.924	0.963	0.970	0.976	0.974	4	0.926	0.930	0.959	0.968	0.973	0.972
5	0.919	0.919	0.954	0.967	0.971	0.969	6	0.905	0.916	0.938	0.964	0.969	0.973

TABLE II.- ENGINE-FACE PRESSURE RECOVERY DATA, p_{t_2}/p_{t_∞} - Continued

M_∞ = 2.25 α = 0.0° m_o/m_∞ = 0.808 Exit setting = B

$\bar{p}_{t_2}/p_{t_\infty}$ = 0.938 m_{bl}/m_∞ = 0.090 Δp_{t_2} = 0.102 p_2/p_∞ = 9.9

RAKE NO.	TUBE NO. 1	2	3	4	5	6	RAKE NO.	TUBE NO. 1	2	3	4	5	6
1	0.881	0.903	0.936	0.969	0.972	0.972	2	0.877	0.891	0.921	0.962	0.970	0.970
3	0.880	0.903	0.955	0.964	0.972	0.972	4	0.895	0.918	0.951	0.969	0.970	0.965
5	0.894	0.906	0.944	0.967	0.969	0.963	6	0.878	0.893	0.925	0.963	0.970	0.970

M_∞ = 2.25 α = 0.0° m_o/m_∞ = 0.808 Exit setting = B

$\bar{p}_{t_2}/p_{t_\infty}$ = 0.894 m_{bl}/m_∞ = 0.074 Δp_{t_2} = 0.161 p_2/p_∞ = 9.3

RAKE NO.	TUBE NO. 1	2	3	4	5	6	RAKE NO.	TUBE NO. 1	2	3	4	5	6
1	0.806	0.851	0.903	0.931	0.940	0.939	2	0.798	0.827	0.870	0.910	0.930	0.937
3	0.829	0.877	0.911	0.923	0.928	0.930	4	0.817	0.862	0.904	0.923	0.930	0.931
5	0.824	0.876	0.916	0.936	0.939	0.942	6	0.805	0.845	0.896	0.933	0.937	0.933

M_∞ = 2.25 α = 0.0° m_o/m_∞ = 0.808 Exit setting = C

$\bar{p}_{t_2}/p_{t_\infty}$ = 0.938 m_{bl}/m_∞ = 0.084 Δp_{t_2} = 0.100 p_2/p_∞ = 10.0

RAKE NO.	TUBE NO. 1	2	3	4	5	6	RAKE NO.	TUBE NO. 1	2	3	4	5	6
1	0.885	0.899	0.937	0.963	0.965	0.973	2	0.880	0.896	0.927	0.953	0.965	0.971
3	0.895	0.916	0.944	0.957	0.967	0.973	4	0.902	0.911	0.940	0.960	0.971	0.972
5	0.895	0.902	0.939	0.959	0.966	0.968	6	0.884	0.901	0.932	0.957	0.964	0.969

M_∞ = 2.25 α = 0.0° m_o/m_∞ = 0.888 Exit setting = C

$\bar{p}_{t_2}/p_{t_\infty}$ = 0.903 m_{bl}/m_∞ = 0.069 Δp_{t_2} = 0.145 p_2/p_∞ = 9.4

RAKE NO.	TUBE NO. 1	2	3	4	5	6	RAKE NO.	TUBE NO. 1	2	3	4	5	6
1	0.827	0.866	0.912	0.937	0.941	0.942	2	0.814	0.844	0.890	0.924	0.937	0.940
3	0.839	0.881	0.925	0.929	0.933	0.937	4	0.833	0.876	0.918	0.932	0.932	0.937
5	0.844	0.879	0.922	0.939	0.945	0.945	6	0.821	0.847	0.894	0.935	0.941	0.939

TABLE II.- ENGINE-FACE PRESSURE RECOVERY DATA, p_{t_2}/p_{t_∞} - Continued

M_∞ = 2.00 α = 0.0° m_o/m_∞ = --- Exit setting = A

$\bar{p}_{t_2}/p_{t_\infty}$ = .897 m_{bl}/m_∞ = 0.106 Δp_{t_2} = 0.101 p_2/p_∞ = 6.4

RAKE NO.	TUBE NO. 1	2	3	4	5	6	RAKE NO.	TUBE NO. 1	2	3	4	5	6
1	0.915	0.927	0.921	0.884	0.862	0.852	2	0.912	0.928	0.922	0.892	0.868	0.849
3	0.912	0.930	0.939	0.898	0.866	0.854	4	0.894	0.921	0.935	0.916	0.885	0.863
5	0.908	0.926	0.934	0.899	0.867	0.852	6	0.908	0.926	0.917	0.888	0.867	0.852

M_∞ = 2.00 α = 0.0° m_o/m_∞ = 0.696 Exit setting = A

$\bar{p}_{t_2}/p_{t_\infty}$ = 0.095 m_{bl}/m_∞ = 0.897 Δp_{t_2} = .078 p_2/p_∞ = 6.8

RAKE NO.	TUBE NO. 1	2	3	4	5	6	RAKE NO.	TUBE NO. 1	2	3	4	5	6
1	0.899	0.914	0.941	0.957	0.959	0.956	2	0.893	0.911	0.940	0.953	0.957	0.953
3	0.897	0.920	0.949	0.956	0.958	0.958	4	0.897	0.919	0.946	0.955	0.959	0.963
5	0.902	0.920	0.948	0.961	0.963	0.962	6	0.897	0.914	0.934	0.948	0.963	0.965

M_∞ = 2.00 α = 0.0° m_o/m_∞ = 0.696 Exit setting = A

$\bar{p}_{t_2}/p_{t_\infty}$ = .890 m_{bl}/m_∞ = 0.076 Δp_{t_2} = 0.170 p_2/p_∞ = 6.4

RAKE NO.	TUBE NO. 1	2	3	4	5	6	RAKE NO.	TUBE NO. 1	2	3	4	5	6
1	0.830	0.861	0.886	0.922	0.941	0.939	0 2	0.812	0.827	0.865	0.899	0.925	0.936
3	0.818	0.837	0.886	0.914	0.933	0.948	4	0.817	0.837	0.875	0.917	0.939	0.954
5	0.827	0.854	0.884	0.937	0.959	0.963	6	0.823	0.844	0.862	0.896	0.933	0.945

M_∞ = 2.00 α = 0.0° m_o/m_∞ = --- Exit setting = B

$\bar{p}_{t_2}/p_{t_\infty}$ = .889 m_{bl}/m_∞ = 0.094 Δp_{t_2} = 0.101 p_2/p_∞ = 6.3

RAKE NO.	TUBE NO. 1	2	3	4	5	6	RAKE NO.	TUBE NO. 1	2	3	4	5	6
1	0.906	0.920	0.913	0.877	0.857	0.849	2	0.900	0.919	0.918	0.879	0.855	0.847
3	0.904	0.923	0.936	0.888	0.862	0.848	4	0.889	0.917	0.930	0.897	0.866	0.850
5	0.902	0.920	0.919	0.884	0.857	0.846	6	0.903	0.920	0.911	0.880	0.858	0.849

TABLE II.- ENGINE-FACE PRESSURE RECOVERY DATA, p_{t_2}/p_{t_∞} - Continued

M_∞ = 2.00 α = 0.0° m_o/m_∞ = 0.696 Exit setting = B

$\bar{p}_{t_2}/p_{t_\infty}$ = 0.935 m_{bl}/m_∞ = 0.084 Δp_{t_2} = 0.082 p_2/p_∞ = 6.7

RAKE NO.	TUBE NO. 1	2	3	4	5	6	RAKE NO.	TUBE NO. 1	2	3	4	5	6
1	0.892	0.912	0.940	0.957	0.955	0.950	2	0.887	0.909	0.938	0.951	0.955	0.947
3	0.890	0.917	0.948	0.957	0.955	0.949	4	0.889	0.914	0.944	0.951	0.953	0.958
5	0.893	0.917	0.946	0.956	0.961	0.958	6	0.886	0.910	0.931	0.952	0.960	0.962

M_∞ = 2.00 α = 0.0° m_o/m_∞ = 0.696 Exit setting = B

$\bar{p}_{t_2}/p_{t_\infty}$ = 0.916 m_{bl}/m_∞ = 0.075 Δp_{t_2} = 0.146 p_2/p_∞ = 6.5

RAKE NO.	TUBE NO. 1	2	3	4	5	6	RAKE NO.	TUBE NO. 1	2	3	4	5	6
1	0.844	0.864	0.903	0.959	0.970	0.966	2	0.837	0.853	0.881	0.926	0.954	0.964
3	0.843	0.861	0.921	0.951	0.968	0.967	4	0.836	0.862	0.916	0.957	0.966	0.962
5	0.843	0.875	0.928	0.965	0.965	0.957	6	0.840	0.869	0.903	0.956	0.970	0.970

M_∞ = 2.00 α = 0.0° m_o/m_∞ = 0.696 Exit setting = C

$\bar{p}_{t_2}/p_{t_\infty}$ = 0.931 m_{bl}/m_∞ = 0.073 Δp_{t_2} = 0.092 p_2/p_∞ = 6.6

RAKE NO.	TUBE NO. 1	2	3	4	5	6	RAKE NO.	TUBE NO. 1	2	3	4	5	6
1	0.880	0.911	0.944	0.954	0.956	0.947	2	0.871	0.901	0.940	0.950	0.953	0.946
3	0.882	0.915	0.948	0.955	0.954	0.948	4	0.883	0.910	0.945	0.951	0.949	0.949
5	0.881	0.911	0.946	0.957	0.956	0.953	6	0.873	0.904	0.930	0.956	0.956	0.956

M_∞ = 2.00 α = 0.0° m_o/m_∞ = 0.696 Exit setting = C

$\bar{p}_{t_2}/p_{t_\infty}$ = 0.896 m_{bl}/m_∞ = 0.064 Δp_{t_2} = 0.181 p_2/p_∞ = 6.2

RAKE NO.	TUBE NO. 1	2	3	4	5	6	RAKE NO.	TUBE NO. 1	2	3	4	5	6
1	0.818	0.851	0.888	0.925	0.952	0.961	2	0.807	0.838	0.868	0.905	0.941	0.958
3	0.806	0.829	0.897	0.917	0.945	0.964	4	0.806	0.847	0.893	0.937	0.956	0.968
5	0.818	0.847	0.883	0.924	0.954	0.966	6	0.822	0.855	0.886	0.915	0.934	0.964

TABLE II.- ENGINE-FACE PRESSURE RECOVERY DATA, p_{t_2}/p_{t_∞} - Continued

M_∞ = 1.75 α = 0.0° m_o/m_∞ = --- Exit setting = A

$\bar{p}_{t_2}/p_{t_\infty}$ = 0.942 m_{bl}/m_∞ = 0.096 Δp_{t_2} = 0.053 p_2/p_∞ = 4.7

RAKE NO.	TUBE NO.						RAKE NO.	TUBE NO.					
	1	2	3	4	5	6		1	2	3	4	5	6
1	0.964	0.950	0.936	0.934	0.935	0.927	2	0.976	0.959	0.941	0.930	0.931	0.926
3	0.968	0.954	0.941	0.931	0.932	0.930	4	0.965	0.953	0.937	0.933	0.933	0.932
5	0.963	0.951	0.938	0.937	0.937	0.934	6	0.955	0.947	0.940	0.936	0.936	0.936

M_∞ = 1.75 α = 0.0° m_o/m_∞ = 0.606 Exit setting = A

$\bar{p}_{t_2}/p_{t_\infty}$ = 0.951 m_{bl}/m_∞ = 0.081 Δp_{t_2} = 0.044 p_2/p_∞ = 4.7

RAKE NO.	TUBE NO.						RAKE NO.	TUBE NO.					
	1	2	3	4	5	6		1	2	3	4	5	6
1	0.927	0.933	0.950	0.954	0.962	0.961	2	0.938	0.936	0.950	0.957	0.967	0.958
3	0.939	0.941	0.956	0.962	0.965	0.962	4	0.932	0.937	0.950	0.957	0.962	0.963
5	0.932	0.939	0.961	0.953	0.956	0.957	6	0.925	0.936	0.956	0.959	0.965	0.960

M_∞ = 1.75 α = 0.0° m_o/m_∞ = 0.606 Exit setting = A

$\bar{p}_{t_2}/p_{t_\infty}$ = 0.915 m_{bl}/m_∞ = 0.067 Δp_{t_2} = 0.120 p_2/p_∞ = 4.4

RAKE NO.	TUBE NO.						RAKE NO.	TUBE NO.					
	1	2	3	4	5	6		1	2	3	4	5	6
1	0.866	0.881	0.925	0.959	0.949	0.950	2	0.855	0.874	0.912	0.959	0.963	0.948
3	0.899	0.914	0.939	0.930	0.915	0.900	4	0.867	0.895	0.927	0.942	0.925	0.915
5	0.856	0.867	0.901	0.953	0.962	0.954	6	0.852	0.874	0.906	0.933	0.939	0.935

M_∞ = 1.75 α = 0.0° m_o/m_∞ = --- Exit setting = B

$\bar{p}_{t_2}/p_{t_\infty}$ = 0.940 m_{bl}/m_∞ = 0.087 Δp_{t_2} = 0.053 p_2/p_∞ = 4.6

RAKE NO.	TUBE NO.						RAKE NO.	TUBE NO.					
	1	2	3	4	5	6		1	2	3	4	5	6
1	0.958	0.945	0.935	0.935	0.936	0.925	2	0.971	0.953	0.936	0.928	0.931	0.922
3	0.961	0.950	0.939	0.932	0.933	0.928	4	0.957	0.946	0.934	0.933	0.933	0.932
5	0.955	0.945	0.936	0.937	0.937	0.932	6	0.947	0.942	0.937	0.937	0.938	0.936

TABLE II.- ENGINE-FACE PRESSURE RECOVERY DATA, p_{t_2}/p_{t_∞} - Continued

M_∞ = 1.75 α = 0.0° m_o/m_∞ = 0.606 Exit setting = B

$\bar{p}_{t_2}/p_{t_\infty}$ = 0.949 m_{bl}/m_∞ = 0.078 Δp_{t_2} = 0.078 p_2/p_∞ = 4.6

RAKE NO.	TUBE NO. 1	2	3	4	5	6	RAKE NO.	TUBE NO. 1	2	3	4	5	6
1	0.903	0.925	0.957	0.974	0.972	0.961	2	0.901	0.926	0.959	0.967	0.971	0.958
3	0.907	0.936	0.959	0.973	0.971	0.966	4	0.901	0.922	0.953	0.972	0.972	0.970
5	0.905	0.927	0.958	0.974	0.972	0.966	6	0.900	0.920	0.947	0.966	0.969	0.968

M_∞ = 1.75 α = 0.0° m_o/m_∞ = 0.606 Exit setting = B

$\bar{p}_{t_2}/p_{t_\infty}$ = 0.920 m_{bl}/m_∞ = 0.065 Δp_{t_2} = 0.120 p_2/p_∞ = 4.4

RAKE NO.	TUBE NO. 1	2	3	4	5	6	RAKE NO.	TUBE NO. 1	2	3	4	5	6
1	0.879	0.890	0.919	0.948	0.958	0.944	2	0.876	0.902	0.941	0.963	0.958	0.939
3	0.908	0.922	0.948	0.936	0.918	0.900	4	0.889	0.914	0.945	0.939	0.917	0.899
5	0.864	0.877	0.906	0.937	0.953	0.957	6	0.853	0.869	0.894	0.933	0.955	0.963

M_∞ = 1.75 α = 0.0° m_o/m_∞ = --- Exit setting = C

$\bar{p}_{t_2}/p_{t_\infty}$ = 0.944 m_{bl}/m_∞ = 0.079 Δp_{t_2} = 0.052 p_2/p_∞ = 4.7

RAKE NO.	TUBE NO. 1	2	3	4	5	6	RAKE NO.	TUBE NO. 1	2	3	4	5	6
1	0.971	0.955	0.939	0.936	0.936	0.926	2	0.972	0.965	0.948	0.929	0.933	0.923
3	0.969	0.961	0.946	0.934	0.934	0.930	4	0.964	0.956	0.941	0.934	0.933	0.933
5	0.967	0.954	0.940	0.938	0.936	0.932	6	0.964	0.951	0.939	0.936	0.937	0.936

M_∞ = 1.75 α = 0.0° m_o/m_∞ = 0.606 Exit setting = C

$\bar{p}_{t_2}/p_{t_\infty}$ 0.947 m_{bl}/m_∞ = 0.069 Δp_{t_2} = 0.086 p_2/p_∞ = 4.6

RAKE NO.	TUBE NO. 1	2	3	4	5	6	RAKE NO.	TUBE NO. 1	2	3	4	5	6
1	0.899	0.924	0.956	0.975	0.974	0.960	2	0.899	0.921	0.956	0.966	0.970	0.956
3	0.905	0.939	0.959	0.974	0.971	0.965	4	0.895	0.919	0.953	0.972	0.972	0.969
5	0.897	0.920	0.956	0.975	0.972	0.966	6	0.893	0.918	0.948	0.969	0.971	0.971

TABLE II.- ENGINE-FACE PRESSURE RECOVERY DATA, p_{t_2}/p_{t_∞} - Continued

M_∞ = 1.75 α = 0.0° m_0/m_∞ = 0.606 Exit setting = C

$\bar{p}_{t_2}/p_{t_\infty}$ = 0.915 m_{bl}/m_∞ = 0.057 Δp_{t_2} = 0.128 p_2/p_∞ = 4.1

RAKE NO.	TUBE NO. 1	2	3	4	5	6	RAKE NO.	TUBE NO. 1	2	3	4	5	6
1	0.852	0.873	0.907	0.942	0.951	0.955	2	0.856	0.887	0.924	0.953	0.961	0.951
3	0.853	0.883	0.916	0.958	0.963	0.953	4	0.848	0.869	0.909	0.949	0.952	0.954
5	0.847	0.869	0.902	0.939	0.951	0.954	6	0.846	0.866	0.895	0.935	0.946	0.963

M_∞ = 1.55 α = 0.0° m_0/m_∞ = --- Exit setting = A

$\bar{p}_{t_2}/p_{t_\infty}$ = 0.900 m_{bl}/m_∞ = 0.076 Δp_{t_2} = 0.105 p_2/p_∞ = 3.3

RAKE NO.	TUBE NO. 1	2	3	4	5	6	RAKE NO.	TUBE NO. 1	2	3	4	5	6
1	0.881	0.881	0.884	0.903	0.902	0.894	2	0.864	0.866	0.872	0.885	0.905	0.888
3	0.889	0.900	0.901	0.900	0.914	0.901	4	0.874	0.871	0.882	0.884	0.908	0.895
5	0.906	0.917	0.926	0.943	0.949	0.959	6	0.898	0.901	0.907	0.926	0.916	0.917

M_∞ = 1.55 α = 0.0° m_0/m_∞ = 0.540 Exit setting = A

$\bar{p}_{t_2}/p_{t_\infty}$ = 0.981 m_{bl}/m_∞ = 0.094 Δp_{t_2} = 0.028 p_2/p_∞ = 3.7

RAKE NO.	TUBE NO. 1	2	3	4	5	6	RAKE NO.	TUBE NO. 1	2	3	4	5	6
1	0.987	0.987	0.984	0.978	0.978	0.968	2	0.990	0.987	0.991	0.971	0.979	0.963
3	0.991	0.989	0.984	0.981	0.981	0.976	4	0.982	0.982	0.983	0.977	0.977	0.977
5	0.989	0.986	0.983	0.979	0.978	0.973	6	0.986	0.985	0.981	0.976	0.976	0.976

M_∞ = 1.55 α = 0.0° m_0/m_∞ = 0.540 Exit setting = A

$\bar{p}_{t_2}/p_{t_\infty}$ = 0.961 m_{bl}/m_∞ = 0.067 Δp_{t_2} = 0.075 p_2/p_∞ = 3.5

RAKE NO.	TUBE NO. 1	2	3	4	5	6	RAKE NO.	TUBE NO. 1	2	3	4	5	6
1	0.921	0.937	0.967	0.983	0.984	0.971	2	0.921	0.941	0.970	0.975	0.982	0.966
3	0.928	0.952	0.962	0.986	0.985	0.981	4	0.915	0.931	0.963	0.984	0.985	0.984
5	0.920	0.938	0.966	0.982	0.982	0.978	6	0.915	0.935	0.959	0.976	0.981	0.982

TABLE II.- ENGINE-FACE PRESSURE RECOVERY DATA, p_{t_2}/p_{t_∞} - Continued

M_∞ = 1.55 α = 0.0° m_o/m_∞ = --- Exit setting = B

$\bar{p}_{t_2}/p_{t_\infty}$ = 0.895 m_{bl}/m_∞ = 0.074 Δp_{t_2} = 0.092 p_2/p_∞ = 3.3

RAKE NO.	TUBE NO. 1	2	3	4	5	6	RAKE NO.	TUBE NO. 1	2	3	4	5	6
1	0.881	0.912	0.885	0.889	0.890	0.885	2	0.872	0.882	0.877	0.881	0.895	0.878
3	0.871	0.870	0.902	0.886	0.890	0.893	4	0.864	0.882	0.888	0.888	0.888	0.907
5	0.900	0.917	0.933	0.930	0.947	0.909	6	0.883	0.902	0.906	0.901	0.926	0.911

M_∞ = 1.55 α = 0.0° m_o/m_∞ = 0.540 Exit setting = B

$\bar{p}_{t_2}/p_{t_\infty}$ = 0.981 m_{bl}/m_∞ = 0.086 Δp_{t_2} = 0.030 p_2/p_∞ = 3.7

RAKE NO.	TUBE NO. 1	2	3	4	5	6	RAKE NO.	TUBE NO. 1	2	3	4	5	6
1	0.983	0.985	0.982	0.979	0.978	0.967	2	0.987	0.986	0.991	0.972	0.979	0.961
3	0.990	0.989	0.985	0.982	0.983	0.977	4	0.982	0.981	0.984	0.978	0.978	0.977
5	0.989	0.984	0.984	0.981	0.979	0.974	6	0.985	0.986	0.980	0.976	0.977	0.977

M_∞ = 1.55 α = 0.0° m_o/m_∞ = 0.540 Exit setting = B

$\bar{p}_{t_2}/p_{t_\infty}$ = 0.956 m_{bl}/m_∞ = 0.071 Δp_{t_2} = 0.068 p_2/p_∞ = 3.5

RAKE NO.	TUBE NO. 1	2	3	4	5	6	RAKE NO.	TUBE NO. 1	2	3	4	5	6
1	0.926	0.926	0.952	0.980	0.980	0.963	2	0.923	0.930	0.951	0.964	0.973	0.957
3	0.921	0.942	0.961	0.979	0.979	0.977	4	0.917	0.928	0.961	0.980	0.982	0.981
5	0.922	0.922	0.956	0.982	0.980	0.976	6	0.918	0.923	0.941	0.981	0.982	0.981

M_∞ = 1.55 α = 0.0° m_o/m_∞ = --- Exit setting = C

$\bar{p}_{t_2}/p_{t_\infty}$ = 0.894 m_{bl}/m_∞ = 0.066 Δp_{t_2} = 0.101 p_2/p_∞ = 3.3

RAKE NO.	TUBE NO. 1	2	3	4	5	6	RAKE NO.	TUBE NO. 1	2	3	4	5	6
1	0.870	0.875	0.882	0.890	0.890	0.887	2	0.857	0.872	0.879	0.884	0.894	0.879
3	0.862	0.865	0.887	0.883	0.897	0.902	4	0.870	0.878	0.902	0.887	0.897	0.895
5	0.895	0.914	0.938	0.947	0.944	0.902	6	0.897	0.912	0.918	0.914	0.905	0.914

TABLE II.- ENGINE-FACE PRESSURE RECOVERY DATA, p_{t_2}/p_{t_∞} - Continued

M_∞ = 1.55 α = 0.0° m_o/m_∞ = 0.540 Exit setting = C

$\bar{p}_{t_2}/p_{t_\infty}$ = 0.977 m_{bl}/m_∞ = 0.077 Δp_{t_2} = 0.030 p_2/p_∞ = 3.7

RAKE NO.	TUBE NO. 1	2	3	4	5	6	RAKE NO.	TUBE NO. 1	2	3	4	5	6
1	0.987	0.981	0.975	0.976	0.976	0.964	2	0.983	0.983	0.982	0.967	0.974	0.959
3	0.987	0.985	0.977	0.979	0.980	0.976	4	0.979	0.976	0.975	0.974	0.975	0.975
5	0.986	0.979	0.976	0.977	0.976	0.973	6	0.981	0.980	0.973	0.973	0.975	0.975

M_∞ = 1.55 α = 0.0° m_o/m_∞ = 0.540 Exit setting = C

$\bar{p}_{t_2}/p_{t_\infty}$ = 0.940 m_{bl}/m_∞ = 0.050 Δp_{t_2} = 0.112 p_2/p_∞ = 3.4

RAKE NO.	TUBE NO. 1	2	3	4	5	6	RAKE NO.	TUBE NO. 1	2	3	4	5	6
1	0.890	0.911	0.938	0.960	0.962	0.964	2	0.893	0.923	0.959	0.967	0.976	0.958
3	0.898	0.935	0.932	0.979	0.980	0.975	4	0.878	0.897	0.926	0.955	0.963	0.973
5	0.882	0.910	0.941	0.965	0.973	0.974	6	0.874	0.901	0.929	0.959	0.970	0.976

M_∞ = 3.00 α = 2.0° m_o/m_∞ = --- Exit setting = A

$\bar{p}_{t_2}/p_{t_\infty}$ = 0.876 m_{bl}/m_∞ = 0.111 Δp_{t_2} = 0.140 p_2/p_∞ = 30.5

RAKE NO.	TUBE NO. 1	2	3	4	5	6	RAKE NO.	TUBE NO. 1	2	3	4	5	6
1	0.818	0.879	0.875	0.907	0.907	0.900	2	0.864	0.904	0.877	0.900	0.902	0.916
3	0.881	0.878	0.814	0.864	0.873	0.856	4	0.924	0.848	0.822	0.805	0.802	0.804
5	0.911	0.901	0.909	0.870	0.885	0.877	6	0.898	0.898	0.876	0.912	0.920	0.876

M_∞ = 3.00 α = 2.0° m_o/m_∞ = --- Exit setting = B

$\bar{p}_{t_2}/p_{t_\infty}$ = 0.886 m_{bl}/m_∞ = 0.097 Δp_{t_2} = 0.108 p_2/p_∞ = 30.2

RAKE NO.	TUBE NO. 1	2	3	4	5	6	RAKE NO.	TUBE NO. 1	2	3	4	5	6
1	0.844	0.887	0.878	0.898	0.898	0.870	2	0.841	0.877	0.861	0.892	0.885	0.891
3	0.906	0.904	0.906	0.891	0.894	0.893	4	0.922	0.917	0.901	0.862	0.868	0.827
5	0.883	0.909	0.912	0.885	0.896	0.905	6	0.883	0.894	0.871	0.899	0.900	0.866

TABLE II.- ENGINE-FACE PRESSURE RECOVERY DATA, p_{t_2}/p_{t_∞} - Continued

M_∞ = 3.00 α = 2.0° m_o/m_∞ = --- Exit setting = C

$\bar{p}_{t_2}/p_{t_\infty}$ = 0.875 m_{bl}/m_∞ = 0.077 Δp_{t_2} = 0.104 p_2/p_∞ = 29.2

RAKE NO.	TUBE NO.						RAKE NO.	TUBE NO.					
	1	2	3	4	5	6		1	2	3	4	5	6
1	0.829	0.864	0.850	0.886	0.879	0.856	2	0.858	0.875	0.862	0.865	0.866	0.868
3	0.880	0.887	0.901	0.881	0.884	0.906	4	0.900	0.887	0.902	0.867	0.869	0.862
5	0.843	0.896	0.888	0.881	0.889	0.920	6	0.852	0.863	0.842	0.888	0.894	0.849

M_∞ = 2.75 α = 2.0° m_o/m_∞ = --- Exit setting = A

$\bar{p}_{t_2}/p_{t_\infty}$ = 0.921 m_{bl}/m_∞ = 0.123 Δp_{t_2} = 0.137 p_2/p_∞ = 21.5

RAKE NO.	TUBE NO.						RAKE NO.	TUBE NO.					
	1	2	3	4	5	6		1	2	3	4	5	6
1	0.841	0.873	0.864	0.916	0.962	0.963	2	0.867	0.900	0.873	0.930	0.964	0.967
3	0.887	0.912	0.936	0.949	0.953	0.955	4	0.863	0.907	0.923	0.943	0.941	0.952
5	0.908	0.919	0.935	0.944	0.948	0.945	6	0.880	0.912	0.870	0.945	0.942	0.949

M_∞ = 2.75 α = 2.0° m_o/m_∞ = --- Exit setting = B

$\bar{p}_{t_2}/p_{t_\infty}$ = 0.919 m_{bl}/m_∞ = 0.108 Δp_{t_2} = 0.141 p_2/p_∞ = 21.3

RAKE NO.	TUBE NO.						RAKE NO.	TUBE NO.					
	1	2	3	4	5	6		1	2	3	4	5	6
1	0.837	0.869	0.857	0.905	0.964	0.966	2	0.856	0.891	0.867	0.935	0.962	0.966
3	0.903	0.910	0.930	0.956	0.959	0.956	4	0.853	0.903	0.923	0.951	0.949	0.960
5	0.902	0.912	0.932	0.941	0.941	0.951	6	0.876	0.904	0.862	0.946	0.942	0.949

M_∞ = 2.75 α = 2.0° m_o/m_∞ = --- Exit setting = C

$\bar{p}_{t_2}/p_{t_\infty}$ = 0.914 m_{bl}/m_∞ = 0.098 Δp_{t_2} = 0.150 p_2/p_∞ = 21.0

RAKE NO.	TUBE NO.						RAKE NO.	TUBE NO.					
	1	2	3	4	5	6		1	2	3	4	5	6
1	0.828	0.860	0.846	0.910	0.964	0.965	2	0.848	0.884	0.865	0.944	0.959	0.966
3	0.891	0.898	0.911	0.953	0.942	0.954	4	0.871	0.891	0.917	0.955	0.941	0.954
5	0.890	0.910	0.934	0.931	0.928	0.946	6	0.871	0.889	0.850	0.941	0.944	0.950

TABLE II.- ENGINE-FACE PRESSURE RECOVERY DATA, p_{t_2}/p_{t_∞} - Continued

M_∞ = 2.50 α = 2.0° m_o/m_∞ ≐ --- Exit setting = A

$\bar{p}_{t_2}/p_{t_\infty}$ = 0.940 m_{bl}/m_∞ = 0.120 Δp_{t_2} = 0.080 p_2/p_∞ = 15.1

RAKE NO.	TUBE NO.						RAKE NO.	TUBE NO.					
	1	2	3	4	5	6		1	2	3	4	5	6
1	0.909	0.905	0.928	0.958	0.962	0.966	2	0.905	0.923	0.947	0.958	0.964	0.963
3	0.910	0.907	0.930	0.956	0.957	0.959	4	0.893	0.910	0.929	0.952	0.957	0.962
5	0.907	0.919	0.951	0.968	0.968	0.968	6	0.906	0.914	0.924	0.964	0.965	0.968

M_∞ = 2.50 α = 2.0° m_o/m_∞ = --- Exit setting = B

$\bar{p}_{t_2}/p_{t_\infty}$ = 0.937 m_{bl}/m_∞ = 0.108 Δp_{t_2} = 0.128 p_2/p_∞ = 15.0

RAKE NO.	TUBE NO.						RAKE NO.	TUBE NO.					
	1	2	3	4	5	6		1	2	3	4	5	6
1	0.901	0.898	0.924	0.960	0.963	0.967	2	0.901	0.921	0.944	0.956	0.964	0.963
3	0.897	0.908	0.929	0.964	0.956	0.959	4	0.853	0.881	0.928	0.959	0.968	0.972
5	0.888	0.916	0.956	0.973	0.960	0.970	6	0.901	0.911	0.929	0.965	0.966	0.970

M_∞ = 2.50 α = 2.0° m_o/m_∞ = --- Exit setting = C

$\bar{p}_{t_2}/p_{t_\infty}$ = 0.929 m_{bl}/m_∞ = 0.092 Δp_{t_2} = 0.170 p_2/p_∞ = 14.8

RAKE NO.	TUBE NO.						RAKE NO.	TUBE NO.					
	1	2	3	4	5	6		1	2	3	4	5	6
1	0.896	0.889	0.925	0.961	0.963	0.967	2	0.893	0.918	0.951	0.959	0.958	0.963
3	0.872	0.898	0.899	0.958	0.921	0.963	4	0.821	0.846	0.895	0.951	0.972	0.979
5	0.863	0.897	0.943	0.967	0.923	0.968	6	0.895	0.912	0.943	0.967	0.960	0.971

M_∞ = 2.25 α = 2.0° m_o/m_∞ = --- Exit setting = A

$\bar{p}_{t_2}/p_{t_\infty}$ = 0.934 m_{bl}/m_∞ = 0.102 Δp_{t_2} = 0.118 p_2/p_∞ = 10.0

RAKE NO.	TUBE NO.						RAKE NO.	TUBE NO.					
	1	2	3	4	5	6		1	2	3	4	5	6
1	0.906	0.905	0.919	0.945	0.948	0.958	2	0.922	0.922	0.933	0.935	0.945	0.956
3	0.886	0.896	0.938	0.967	0.970	0.971	4	0.862	0.885	0.932	0.966	0.972	0.972
5	0.894	0.912	0.950	0.970	0.956	0.947	6	0.909	0.913	0.931	0.937	0.941	0.948

TABLE II.- ENGINE-FACE PRESSURE RECOVERY DATA, p_{t_2}/p_{t_∞} - Continued

M_∞ = 2.25 α = 2.0° m_o/m_∞ = --- Exit setting = B

$\bar{p}_{t_2}/p_{t_\infty}$ = 0.935 m_{bl}/m_∞ = 0.097 Δp_{t_2} = 0.122 p_2/p_∞ = 9.9

RAKE NO.	TUBE NO. 1	2	3	4	5	6	RAKE NO.	TUBE NO. 1	2	3	4	5	6
1	0.918	0.911	0.941	0.955	0.959	0.968	.2	0.909	0.914	0.937	0.956	0.960	0.965
3	0.889	0.912	0.929	0.957	0.959	0.958	4	0.854	0.877	0.919	0.949	0.954	0.955
5	0.885	0.907	0.934	0.952	0.962	0.958	6	0.914	0.923	0.947	0.955	0.959	0.961

M_∞ = 2.25 α = 2.0° m_o/m_∞ = --- Exit setting = C

$\bar{p}_{t_2}/p_{t_\infty}$ = 0.924 m_{bl}/m_∞ = 0.082 Δp_{t_2} = 0.147 p_2/p_∞ = 9.7

RAKE NO.	TUBE NO. 1	2	3	4	5	6	RAKE NO.	TUBE NO. 1	2	3	4	5	6
1	0.908	0.899	0.940	0.953	0.956	0.965	2	0.897	0.911	0.934	0.954	0.961	0.963
3	0.859	0.881	0.878	0.948	0.935	0.962	4	0.829	0.843	0.876	0.926	0.942	0.960
5	0.869	0.892	0.926	0.953	0.937	0.961	6	0.900	0.919	0.953	0.954	0.956	0.960

M_∞ = 2.00 α = 2.0° m_o/m_∞ = --- Exit setting = A

$\bar{p}_{t_2}/p_{t_\infty}$ = 0.934 m_{bl}/m_∞ = 0.092 Δp_{t_2} = 0.085 p_2/p_∞ = 6.8

RAKE NO.	TUBE NO. 1	2	3	4	5	6	RAKE NO.	TUBE NO. 1	2	3	4	5	6
1	0.884	0.903	0.935	0.957	0.962	0.951	2	0.886	0.906	0.938	0.948	0.954	0.947
3	0.898	0.927	0.950	0.958	0.952	0.944	4	0.895	0.916	0.941	0.954	0.943	0.939
5	0.903	0.917	0.947	0.963	0.957	0.951	6	0.894	0.909	0.936	0.945	0.944	0.957

M_∞ = 2.00 α = 2.0° m_o/m_∞ = --- Exit setting = B

$\bar{p}_{t_2}/p_{t_\infty}$ = 0.934 m_{bl}/m_∞ = 0.084 Δp_{t_2} = 0.087 p_2/p_∞ = 6.7

RAKE NO.	TUBE NO. 1	2	3	4	5	6	RAKE NO.	TUBE NO. 1	2	3	4	5	6
1	0.883	0.901	0.937	0.958	0.963	0.951	2	0.887	0.911	0.943	0.949	0.956	0.948
3	0.886	0.921	0.950	0.960	0.957	0.946	4	0.885	0.913	0.944	0.958	0.949	0.947
5	0.889	0.915	0.948	0.964	0.957	0.950	6	0.889	0.904	0.937	0.946	0.949	0.960

TABLE II.- ENGINE-FACE PRESSURE RECOVERY DATA, p_{t_2}/p_{t_∞} - Continued

M_∞ = 2.00 α = 2.0° m_o/m_∞ = --- Exit setting = C

$\bar{p}_{t_2}/p_{t_\infty}$ = 0.929 m_{bl}/m_∞ = 0.074 Δp_{t_2} = 0.117 p_2/p_∞ = 6.6

RAKE NO.	TUBE NO.						RAKE NO.	TUBE NO.					
	1	2	3	4	5	6		1	2	3	4	5	6
1	0.884	0.904	0.944	0.958	0.961	0.952	2	0.888	0.918	0.950	0.951	0.955	0.950
3	0.879	0.907	0.915	0.943	0.942	0.950	4	0.857	0.877	0.909	0.932	0.945	0.950
5	0.877	0.912	0.945	0.955	0.951	0.956	6	0.887	0.909	0.947	0.951	0.957	0.965

M_∞ = 1.75 α = 2.0° m_o/m_∞ = --- Exit setting = A

$\bar{p}_{t_2}/p_{t_\infty}$ = 0.942 m_{bl}/m_∞ = 0.080 Δp_{t_2} = 0.070 p_2/p_∞ = 4.6

RAKE NO.	TUBE NO.						RAKE NO.	TUBE NO.					
	1	2	3	4	5	6		1	2	3	4	5	6
1	0.914	0.932	0.962	0.972	0.968	0.960	2	0.923	0.932	0.953	0.956	0.966	0.956
3	0.935	0.942	0.938	0.950	0.945	0.938	4	0.926	0.933	0.936	0.934	0.925	0.915
5	0.925	0.939	0.957	0.956	0.940	0.932	6	0.906	0.926	0.948	0.954	0.961	0.959

M_∞ = 1.75 α = 2.0° m_o/m_∞ = --- Exit setting = B

$\bar{p}_{t_2}/p_{t_\infty}$ = 0.938 m_{bl}/m_∞ = .072 Δp_{t_2} = 0.078 p_2/p_∞ = 4.6

RAKE NO.	TUBE NO.						RAKE NO.	TUBE NO.					
	1	2	3	4	5	6		1	2	3	4	5	6
1	0.910	0.927	0.957	0.971	0.968	0.956	2	0.917	0.935	0.948	0.949	0.960	0.953
3	0.926	0.938	0.942	0.953	0.938	0.926	4	0.915	0.931	0.938	0.929	0.916	0.904
5	0.903	0.926	0 952	0.958	0.940	0.929	6	0.898	0.923	0.950	0.952	0.953	0.956

M_∞ = 1.75 α = 2.0° m_o/m_∞ = --- Exit setting = C

$\bar{p}_{t_2}/p_{t_\infty}$ = 0.934 m_{bl}/m_∞ = 0.071 Δp_{t_2} = 0.097 p_2/p_∞ = 4.5

RAKE NO.	TUBE NO.						RAKE NO.	TUBE NO.					
	1	2	3	4	5	6		1	2	3	4	5	6
1	0.941	0.932	0.923	0.926	0.927	0.921	2	0.941	0.927	0.921	0.921	0.928	0.919
3	0.913	0.913	0.943	0.950	0.955	0.950	4	0.888	0.896	0.937	0.972	0.973	0 970
5	0.900	0.900	0.936	0.978	0.973	0.968	6	0.915	0.918	0.924	0.940	0.943	0.941

TABLE II.- ENGINE-FACE PRESSURE RECOVERY DATA, p_{t_2}/p_{t_∞} - Continued

M_∞ = 1.55 α = 2.0° m_o/m_∞ = --- Exit setting = A

$\bar{p}_{t_2}/p_{t_\infty}$ = 0.966 m_{bl}/m_∞ = 0.088 Δp_{t_2} = 0.052 p_2/p_∞ = 3.6

RAKE NO.	TUBE NO. 1	2	3	4	5	6	RAKE NO.	TUBE NO. 1	2	3	4	5	6
1	0.992	0.980	0.971	0.969	0.970	0.949	2	0.992	0.978	0.964	0.954	0.966	0.942
3	0.970	0.965	0.963	0.967	0.971	0.969	4	0.949	0.954	0.961	0.968	0.970	0.971
5	0.963	0.962	0.964	0.968	0.968	0.966	6	0.973	0.968	0.961	0.964	0.967	0.968

M_∞ = 1.55 α = 2.0° m_o/m_∞ = --- Exit setting = B

$\bar{p}_{t_2}/p_{t_\infty}$ = 0.965 m_{bl}/m_∞ = 0.082 Δp_{t_2} = 0.071 p_2/p_∞ = 3.6

RAKE NO.	TUBE NO. 1	2	3	4	5	6	RAKE NO.	TUBE NO. 1	2	3	4	5	6
1	0.983	0.978	0.975	0.970	0.971	0.953	2	0.992	0.971	0.923	0.950	0.967	0.947
3	0.972	0.965	0.946	0.958	0.973	0.970	4	0.950	0.950	0.962	0.968	0.970	0.971
5	0.966	0.961	0.964	0.969	0.969	0.967	6	0.978	0.969	0.962	0.965	0.968	0.970

M_∞ = 1.55 α = 2.0° m_o/m_∞ = --- Exit setting = C

$\bar{p}_{t_2}/p_{t_\infty}$ = 0.967 m_{bl}/m_∞ = 0.073 Δp_{t_2} = 0.045 p_2/p_∞ = 3.6

RAKE NO.	TUBE NO. 1	2	3	4	5	6	RAKE NO.	TUBE NO. 1	2	3	4	5	6
1	0.992	0.980	0.971	0.970	0.971	0.955	2	0.990	0.977	0.964	0.957	0.967	0.949
3	0.970	0.964	0.965	0.968	0.972	0.970	4	0.950	0.948	0.964	0.970	0.971	0.972
5	0.963	0.959	0.964	0.969	0.970	0.967	6	0.978	0.967	0.962	0.965	0.968	0.970

M_∞ = 3.00 α = 5.0° m_o/m_∞ = --- Exit setting = A

$\bar{p}_{t_2}/p_{t_\infty}$ = 0.830 m_{bl}/m_∞ = 0.098 Δp_{t_2} = 0.201 p_2/p_∞ = 29.6

RAKE NO.	TUBE NO. 1	2	3	4	5	6	RAKE NO.	TUBE NO. 1	2	3	4	5	6
1	0.803	0.820	0.838	0.879	0.904	0.926	2	0.833	0.855	0.883	0.861	0.845	0.904
3	0.767	0.785	0.766	0.843	0.833	0.816	4	0.791	0.782	0.759	0.776	0.763	0.762
5	0.780	0.805	0.832	0.840	0 825	0.800	6	0.834	0.859	0.898	0.877	0.855	0.887

TABLE II.- ENGINE-FACE PRESSURE RECOVERY DATA, p_{t_2}/p_{t_∞} - Continued

M_∞ = 3.00 α = 5.0° m_o/m_∞ = --- Exit setting = B

$\bar{p}_{t_2}/p_{t_\infty}$ = 0.833 m_{bl}/m_∞ = 0.098 Δp_{t_2} = 0.255 p_2/p_∞ = 28.5

RAKE NO.	TUBE NO. 1	2	3	4	5	6	RAKE NO.	TUBE NO. 1	2	3	4	5	6
1	0.812	0.824	0.844	0.889	0.895	0.904	2	0.773	0.813	0.872	0.922	0.913	0.899
3	0.719	0.737	0.787	0.829	0.864	0.864	4	0.720	0.745	0.792	0.837	0.851	0.862
5	0.722	0.734	0.775	0.828	0.858	0.859	6	0.786	0.816	0.865	0.931	0.930	0.904

M_∞ = 3.00 α = 5.0° m_o/m_∞ = --- Exit setting = C

$\bar{p}_{t_2}/p_{t_\infty}$ = 0.812 m_{bl}/m_∞ = 0.077 Δp_{t_2} = 0.304 p_2/p_∞ = 27.9

RAKE NO.	TUBE NO. 1	2	3	4	5	6	RAKE NO.	TUBE NO. 1	2	3	4	5	6
1	0.799	0.810	0.830	0.888	0.893	0.913	2	0.732	0.762	0.841	0.919	0.914	0.914
3	0.682	0.689	0.763	0.809	0.837	0.858	4	0.682	0.700	0.743	0.811	0.840	0.861
5	0.680	0.690	0.737	0.805	0.837	0.845	6	0.737	0.786	0.861	0.927	0.913	0.919

M_∞ = 2.75 α = 5.0° m_o/m_∞ = --- Exit setting = A

$\bar{p}_{t_2}/p_{t_\infty}$ = 0.874 m_{bl}/m_∞ = 0.120 Δp_{t_2} = 0.160 p_2/p_∞ = 20.7

RAKE NO.	TUBE NO. 1	2	3	4	5	6	RAKE NO.	TUBE NO. 1	2	3	4	5	6
1	0.849	0.855	0.880	0.906	0.910	0.914	2	0.845	0.868	0.901	0.923	0.910	0.939
3	0.806	0.830	0.854	0.875	0.875	0.873	4	0.800	0.818	0.854	0.877	0.889	0.889
5	0.805	0.828	0.862	0.876	0.877	0.879	6	0.840	0.856	0.896	0.930	0.934	0.931

M_∞ = 2.75 α = 5.0° m_o/m_∞ = --- Exit setting = B

$\bar{p}_{t_2}/p_{t_\infty}$ = 0.852 m_{bl}/m_∞ = 0.105 Δp_{t_2} = 0.212 p_2/p_∞ = 20.1

RAKE NO.	TUBE NO. 1	2	3	4	5	6	RAKE NO.	TUBE NO. 1	2	3	4	5	6
1	0.841	0.843	0.875	0.892	0.895	0.901	2	0.820	0.844	0.889	0.922	0.918	0.907
3	0.758	0.784	0.805	0.851	0.870	0.872	4	0.748	0.776	0.810	0.846	0.874	0.878
5	0.760	0.778	0.817	0.852	0.873	0.882	6	0.810	0.835	0.883	0.927	0.929	0.919

TABLE II.- ENGINE-FACE PRESSURE RECOVERY DATA, p_{t_2}/p_{t_∞} - Continued

M_∞ = 2.75 α = 5.0° m_o/m_∞ = --- Exit setting = C

$\bar{p}_{t_2}/p_{t_\infty}$ = 0.837 m_{bl}/m_∞ = 0.086 Δp_{t_2} = 0.262 p_2/p_∞ = 19.6

RAKE NO.	TUBE NO.						RAKE NO.	TUBE NO.					
	1	2	3	4	5	6		1	2	3	4	5	6
1	0.838	0.839	0.877	0.891	0.891	0.899	2	0.793	0.821	0.880	0.926	0.928	0.869
3	0.718	0.736	0.777	0.819	0.864	0.878	4	0.715	0.735	0.771	0.828	0.868	0.891
5	0.726	0.734	0.767	0.828	0.876	0.883	6	0.791	0.813	0.870	0.935	0.934	0.909

M_∞ = 2.50 α = 5.0 m_o/m_∞ = --- Exit setting = A

$\bar{p}_{t_2}/p_{t_\infty}$ 0.880 m_{bl}/m_∞ = 0.118 Δp_{t_2} = 0.175 p_2/p_∞ = 14.2

RAKE NO.	TUBE NO.						RAKE NO.	TUBE NO.					
	1	2	3	4	5	6		1	2	3	4	5	6
1	0.868	0.864	0.898	0.908	0.914	0.921	2	0.866	0.891	0.926	0.935	0.898	0.936
3	0.817	0.830	0.853	0.855	0.870	0.880	4	0.794	0.821	0.847	0.874	0.896	0.883
5	0.819	0.829	0.856	0.883	0.896	0.892	6	0.861	0.880	0.907	0.946	0.902	0.947

M_∞ = 2.50 α = 5.0° m_o/m_∞ = --- Exit setting = B

$\bar{p}_{t_2}/p_{t_\infty}$ = 0.865 m_{bl}/m_∞ = 0.105 Δp_{t_2} = 0.215 p_2/p_∞ = 14.0

RAKE NO.	TUBE NO.						RAKE NO.	TUBE NO.					
	1	2	3	4	5	6		1	2	3	4	5	6
1	0.860	0.855	0.890	0.909	0.917	0.924	2	0.851	0.870	0.914	0.932	0.901	0.942
3	0.782	0.795	0.809	0.844	0.869	0.882	4	0.761	0.776	0.804	0.842	0.876	0.889
5	0.783	0.793	0.820	0.854	0.881	0.904	6	0.844	0.861	0.905	0.947	0.918	0.929

M_∞ = 2.50 α = 5.0° m_o/m_∞ = --- Exit setting = C

$\bar{p}_{t_2}/p_{t_\infty}$ = 0.846 m_{bl}/m_∞ = 0.091 Δp_{t_2} = 0.264 p_2/p_∞ = 13.6

RAKE NO.	TUBE NO.						RAKE NO.	TUBE NO.					
	1	2	3	4	5	6		1	2	3	4	5	6
1	0.848	0.849	0.879	0.898	0.910	0.926	2	0.830	0.852	0.901	0.929	0.900	0.928
3	0.744	0.749	0.769	0.813	0.859	0.890	4	0.721	0.736	0.767	0.804	0.852	0.880
5	0.750	0.756	0.784	0.820	0.871	0.903	6	0.824	0.848	0.895	0.945	0.918	0.912

TABLE II.- ENGINE-FACE PRESSURE RECOVERY DATA, p_{t_2}/p_{t_∞} - Continued

M_∞ = 2.25 α = 5.0° m_o/m_∞ = --- Exit setting = A

$\bar{p}_{t_2}/p_{t_\infty}$ = 0.868 m_{bl}/m_∞ = 0.086 Δp_{t_2} = 0.195 p_2/p_∞ = 5.0

RAKE NO.	TUBE NO. 1	2	3	4	5	6	RAKE NO.	TUBE NO. 1	2	3	4	5	6
1	0.882	0.900	0.917	0.904	0.900	0.938	2	0.841	0.878	0.917	0.946	0.901	0.935
3	0.808	0.806	0.806	0.855	0.878	0.891	4	0.777	0.780	0.795	0.815	0.826	0.827
5	0.826	0.818	0.835	0.854	0.863	0.865	6	0.876	0.919	0.936	0.922	0.903	0.910

M_∞ = 2.25 α = 5.0° m_o/m_∞ = --- Exit setting = B

$\bar{p}_{t_2}/p_{t_\infty}$ = 0.877 m_{bl}/m_∞ = 0.087 Δp_{t_2} = 0.162 p_2/p_∞ = 9.2

RAKE NO.	TUBE NO. 1	2	3	4	5	6	RAKE NO.	TUBE NO. 1	2	3	4	5	6
1	0.889	0.888	0.918	0.924	0.926	0.931	2	0.886	0.906	0.916	0.922	0.910	0.928
3	0.833	0.817	0.834	0.836	0.856	0.856	4	0.793	0.803	0.826	0.853	0.874	0.878
5	0.829	0.825	0.842	0.855	0.871	0.884	6	0.870	0.896	0.930	0.932	0.908	0.935

M_∞ = 2.25 α = 5.0° m_o/m_∞ = --- Exit setting = C

$\bar{p}_{t_2}/p_{t_\infty}$ = 0.867 m_{bl}/m_∞ = 0.073 Δp_{t_2} = 0.198 p_2/p_∞ = 9.0

RAKE NO.	TUBE NO. 1	2	3	4	5	6	RAKE NO.	TUBE NO. 1	2	3	4	5	6
1	0.876	0.885	0.916	0.918	0.922	0.927	2	0.884	0.907	0.910	0.914	0.898	0.926
3	0.808	0.800	0.807	0.832	0.852	0.872	4	0.762	0.776	0.801	0.826	0.859	0.865
5	0.808	0.802	0.820	0.842	0.868	0.887	6	0.865	0.897	0.928	0.930	0.881	0.934

M_∞ = 2.00 α = 5.0° m_o/m_∞ = --- Exit setting = A

$\bar{p}_{t_2}/p_{t_\infty}$ = 0.888 m_{bl}/m_∞ = 0.090 Δp_{t_2} = 0.160 p_2/p_∞ = 6.4

RAKE NO.	TUBE NO. 1	2	3	4	5	6	RAKE NO.	TUBE NO. 1	2	3	4	5	6
1	0.900	0.917	0.937	0.940	0.914	0.829	2	0.890	0.866	0.838	0.833	0.834	0.825
3	0.859	0.871	0.901	0.943	0.964	0.955	4	0.876	0.885	0.890	0.886	0.876	0.860
5	0.869	0.908	0.951	0.967	0.955	0.948	6	0.881	0.856	0.835	0.835	0.836	0.833

TABLE II.- ENGINE-FACE PRESSURE RECOVERY DATA, p_{t_2}/p_{t_∞} - Continued

M_∞ = 2.00 α = 5.0° m_o/m_∞ = --- Exit setting = B

$\bar{p}_{t_2}/p_{t_\infty}$ = 0.882 m_{b1}/m_∞ = 0.083 Δp_{t_2} = 0.155 p_2/p_∞ = 6.3

RAKE NO.	TUBE NO. 1	2	3	4	5	6	RAKE NO.	TUBE NO. 1	2	3	4	5	6
1	0.898	0.913	0.936	0.935	0.893	0.830	2	0.886	0.863	0.837	0.834	0.836	0.827
3	0.859	0.878	0.848	0.944	0.946	0.949	4	0.821	0.829	0.848	0.871	0.889	0.906
5	0.866	0.910	0.947	0.959	0.953	0.958	6	0.878	0.856	0.836	0.838	0.837	0.833

M_∞ = 2.00 α = 5.0° m_o/m_∞ = --- Exit setting = C

$\bar{p}_{t_2}/p_{t_\infty}$ = 0.880 m_{b1}/m_∞ = 0.065 Δp_{t_2} = 0.190 p_2/p_∞ = 6.3

RAKE NO.	TUBE NO. 1	2	3	4	5	6	RAKE NO.	TUBE NO. 1	2	3	4	5	6
1	0.848	0.887	0.939	0.953	0.958	0.927	2	0.897	0.928	0.935	0.929	0.923	0.924
3	0.846	0.826	0.822	0.836	0.853	0.852	4	0.791	0.802	0.812	0.829	0.856	0.866
5	0.849	0.835	0.841	0.850	0.865	0.873	6	0.889	0.930	0.922	0.917	0.937	0.945

M_∞ = 1.75 α = 5.0° m_o/m_∞ = --- Exit setting = A

$\bar{p}_{t_2}/p_{t_\infty}$ = 0.934 m_{b1}/m_∞ = 0.086 Δp_{t_2} = 0.088 p_2/p_∞ = 4.6

RAKE NO.	TUBE NO. 1	2	3	4	5	6	RAKE NO.	TUBE NO. 1	2	3	4	5	6
1	0.973	0.967	0.973	0.937	0.916	0.916	2	0.944	0.926	0.917	0.917	0.920	0.913
3	0.914	0.941	0.906	0.978	0.968	0.965	4	0.896	0.904	0.902	0.905	0.910	0.909
5	0.915	0.939	0.969	0.976	0.964	0.961	6	0.920	0.914	0.927	0.936	0.937	0.933

M_∞ = 1.75 α = 5.0° m_o/m_∞ = --- Exit setting = B

$\bar{p}_{t_2}/p_{t_\infty}$ = 0.929 m_{b1}/m_∞ = 0.079 Δp_{t_2} = 0.108 p_2/p_∞ = 4.5

RAKE NO.	TUBE NO. 1	2	3	4	5	6	RAKE NO.	TUBE NO. 1	2	3	4	5	6
1	0.970	0.966	0.978	0.944	0.919	0.915	2	0.940	0.924	0.918	0.916	0.920	0.913
3	0.911	0.933	0.884	0.974	0.963	0.966	4	0.881	0.877	0.887	0.900	0.917	0.932
5	0.909	0.924	0.939	0.953	0.949	0.958	6	0.924	0.913	0.930	0.936	0.938	0.934

TABLE II.- ENGINE-FACE PRESSURE RECOVERY DATA, p_{t_2}/p_{t_∞} - Concluded

M_∞ = 1.75 α = 5.0° m_o/m_∞ = --- Exit setting = C

$\bar{p}_{t_2}/p_{t_\infty}$ = 0.924 m_{bl}/m_∞ = 0.072 Δp_{t_2} = 0.126 p_2/p_∞ = 4.5

RAKE NO.	TUBE NO. 1	2	3	4	5	6	RAKE NO.	TUBE NO. 1	2	3	4	5	6
1	0.964	0.963	0.982	0.946	0.924	0.915	2	0.940	0.920	0.918	0.915	0.921	0.912
3	0.908	0.931	0.878	0.951	0.947	0.962	4	0.865	0.867	0.876	0.882	0.902	0.909
5	0.910	0.916	0.929	0.937	0.936	0.954	6	0.921	0.915	0.930	0.937	0.937	0.933

M_∞ = 1.55 α = 5.0° m_o/m_∞ = --- Exit setting = A

$\bar{p}_{t_2}/p_{t_\infty}$ = 0.934 m_{bl}/m_∞ = 0.077 Δp_{t_2} = 0.112 p_2/p_∞ = 3.5

RAKE NO.	TUBE NO. 1	2	3	4	5	6	RAKE NO.	TUBE NO. 1	2	3	4	5	6
1	0.967	0.962	0.947	0.950	0.954	0.869	2	0.932	0.939	0.951	0.945	0.957	0.866
3	0.926	0.939	0.890	0.966	0.965	0.971	4	0.888	0.883	0.886	0.891	0.899	0.903
5	0.923	0.930	0.943	0.955	0.957	0.964	6	0.928	0.942	0.958	0.966	0.966	0.965

M_∞ = 1.55 α = 5.0° m_o/m_∞ = --- Exit setting = B

$\bar{p}_{t_2}/p_{t_\infty}$ = 0.921 m_{bl}/m_∞ = 0.068 Δp_{t_2} = 0.239 p_2/p_∞ = 3.4

RAKE NO.	TUBE NO. 1	2	3	4	5	6	RAKE NO.	TUBE NO. 1	2	3	4	5	6
1	0.952	0.949	0.943	0.950	0.951	0.769	2	0.929	0.947	0.954	0.943	0.958	0.751
3	0.925	0.923	0.878	0.942	0.953	0.958	4	0.867	0.867	0.876	0.880	0.889	0.896
5	0.916	0.914	0.918	0.931	0.937	0.945	6	0.919	0.944	0.962	0.971	0.970	0.969

M_∞ = 1.55 α = 5.0° m_o/m_∞ = --- Exit setting = C

$\bar{p}_{t_2}/p_{t_\infty}$ = 0.906 m_{bl}/m_∞ = 0.061 Δp_{t_2} = 0.464 p_2/p_∞ = 3.0

RAKE NO.	TUBE NO. 1	2	3	4	5	6	RAKE NO.	TUBE NO. 1	2	3	4	5	6
1	0.955	0.950	0.943	0.949	0.950	0.553	2	0.931	0.945	0.952	0.936	0.951	0.546
3	0.922	0.916	0.869	0.931	0.947	0.959	4	0.861	0.865	0.871	0.874	0.889	0.897
5	0.914	0.910	0.915	0.925	0.936	0.949	6	0.922	0.943	0.958	0.966	0.965	0.964

TABLE III.- INDEX TO FIGURES

Figure	
1	Model photograph
2(a)-2(b)	Sketches of model
3	Area distributions
4	Design flow field
5	Theoretical mass-flow ratio
6	Contraction ratio
7	Maximum design performance (variable $(x/R)_{lip}$)
8	Maximum design performance (maximum pressure recovery)
9	Supercritical performance (variable $(x/R)_{lip}$)
10(a)-10(i)	Supercritical performance (M_∞ = 3.20-1.55, α = 0°)
11	Maximum off-design performance, α = 0°
12(a)-12(g)	Supercritical performance at angle of attack
13(a)-13(c)	Maximum performance at angle of attack
14(a)-14(i)	Total-pressure distortion profiles at the engine face
15(a)-15(i)	Supercritical bleed flow, individual bleed zones
16(a)-16(i)	Bleed plenum chamber pressure recoveries
17(a)-17(d)	Maximum bleed plenum chamber pressure recoveries
18(a)-18(c)	Pitot pressure profiles, maximum pressure recovery
19-27	Static-pressure distributions
28-30	Effect of unstarting the inlet
31	Inlet tolerance to change in angle of attack
32(a)-32(h)	Transonic performance, M_∞ = 0.6-1.3
33(a)-33(c)	Transonic performance at angle of attack

Figure 1.- Model mounted in Supersonic Wind Tunnel.

A-36911

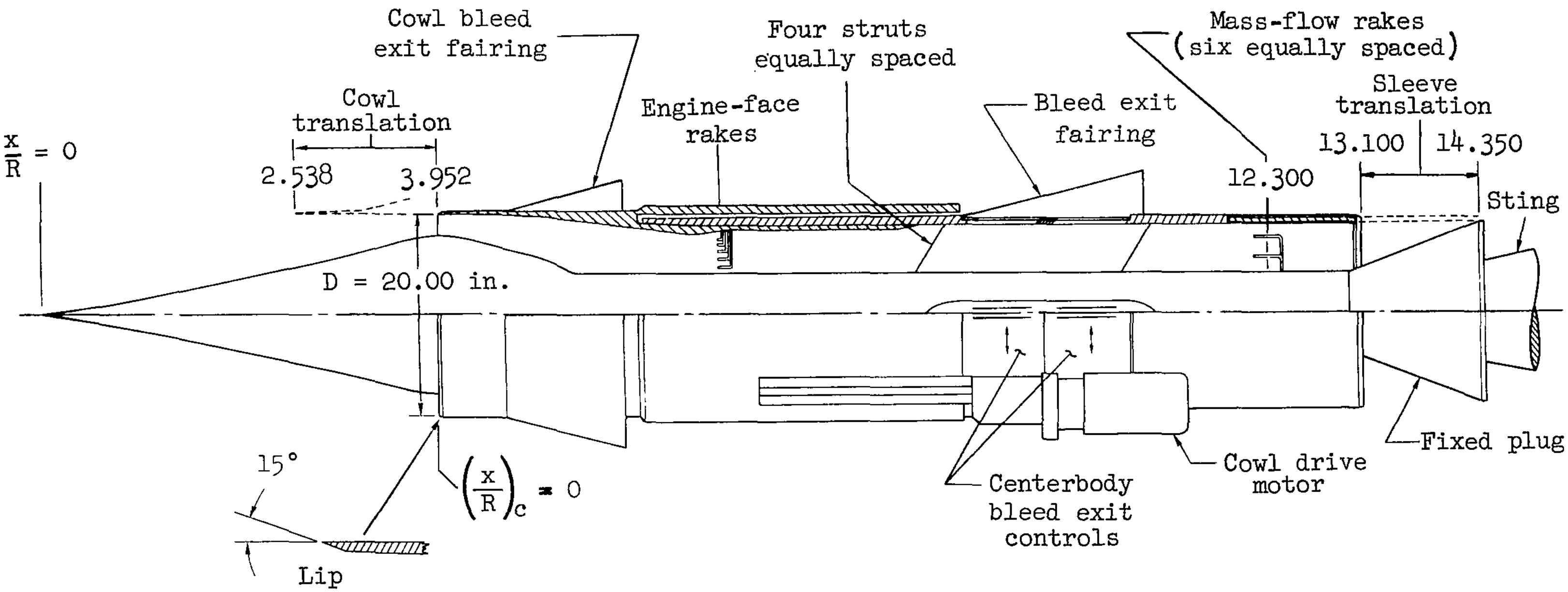

(a) Overall model.

Figure 2.- Model.

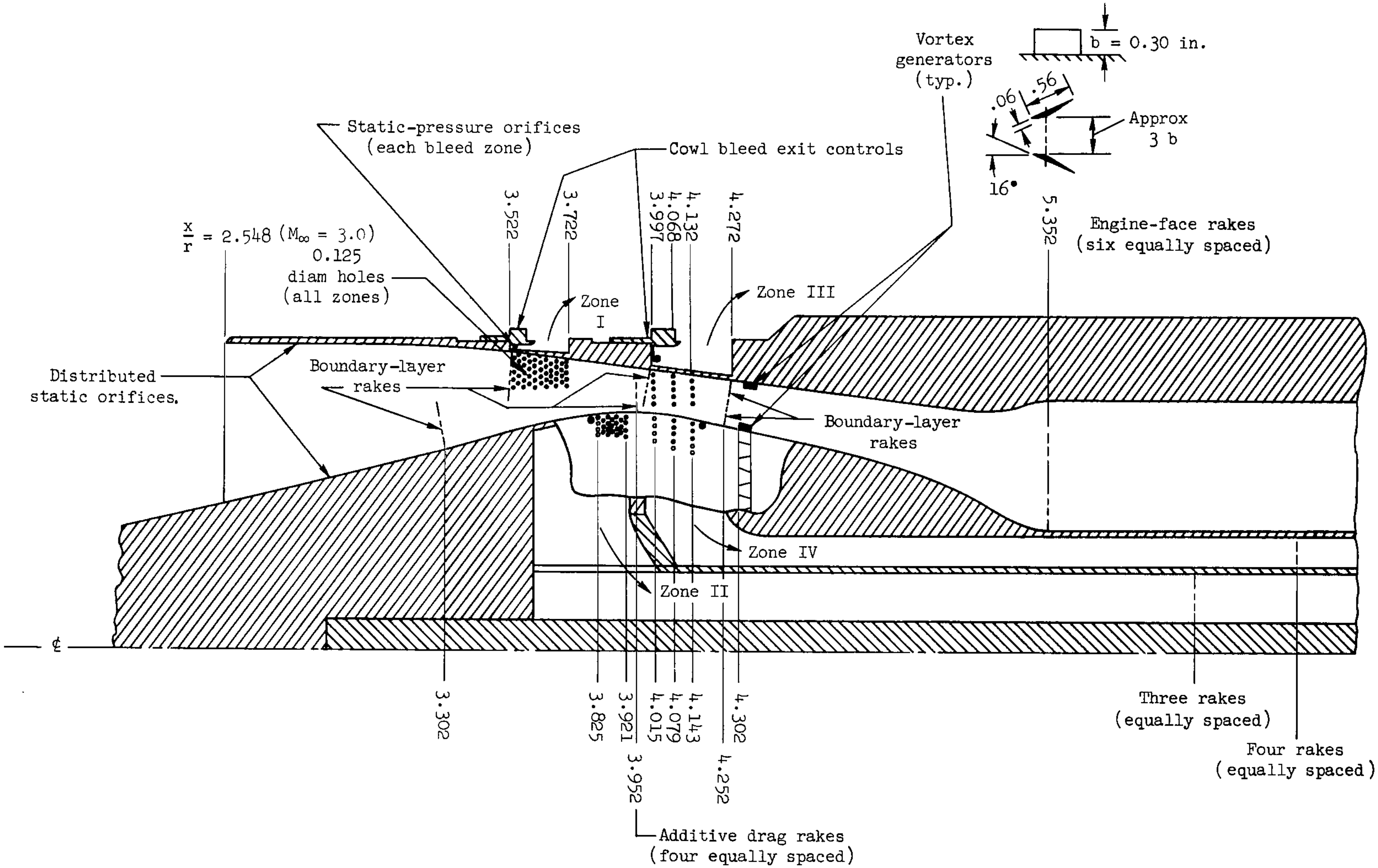

(b) Bleed configuration and instrumentation.

Figure 2.- Concluded.

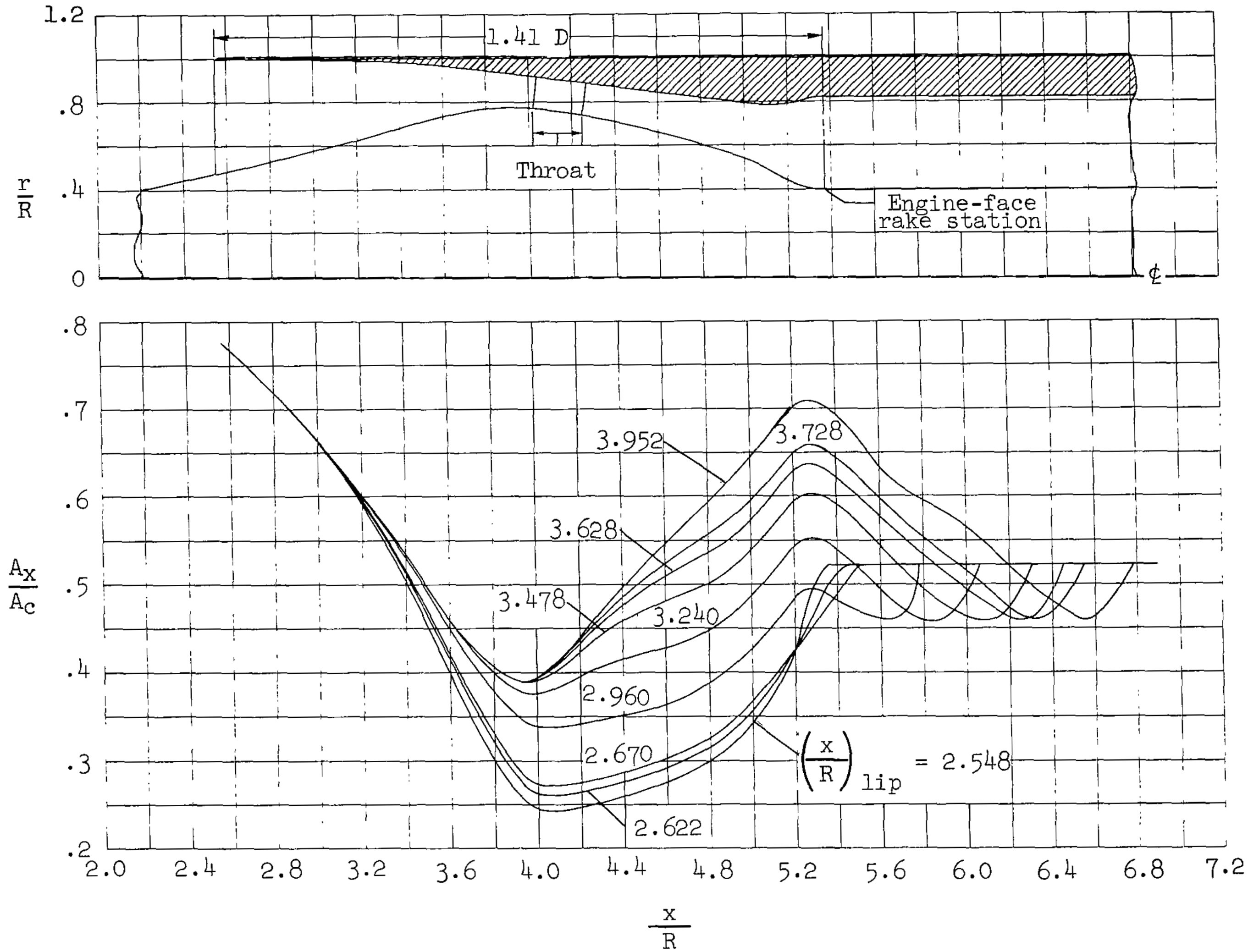

Figure 3.- Area distributions.

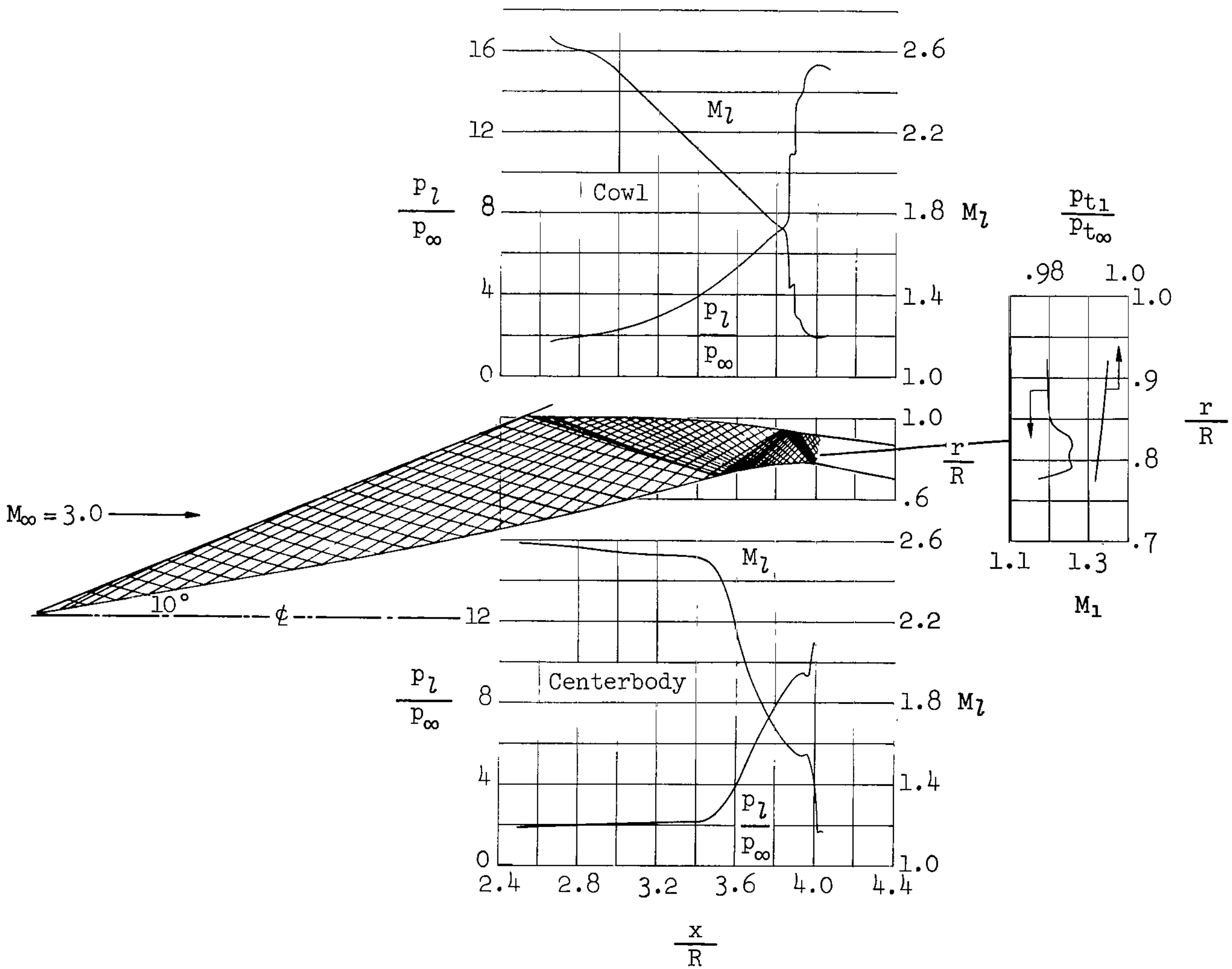

Figure 4.- Design theoretical flow field.

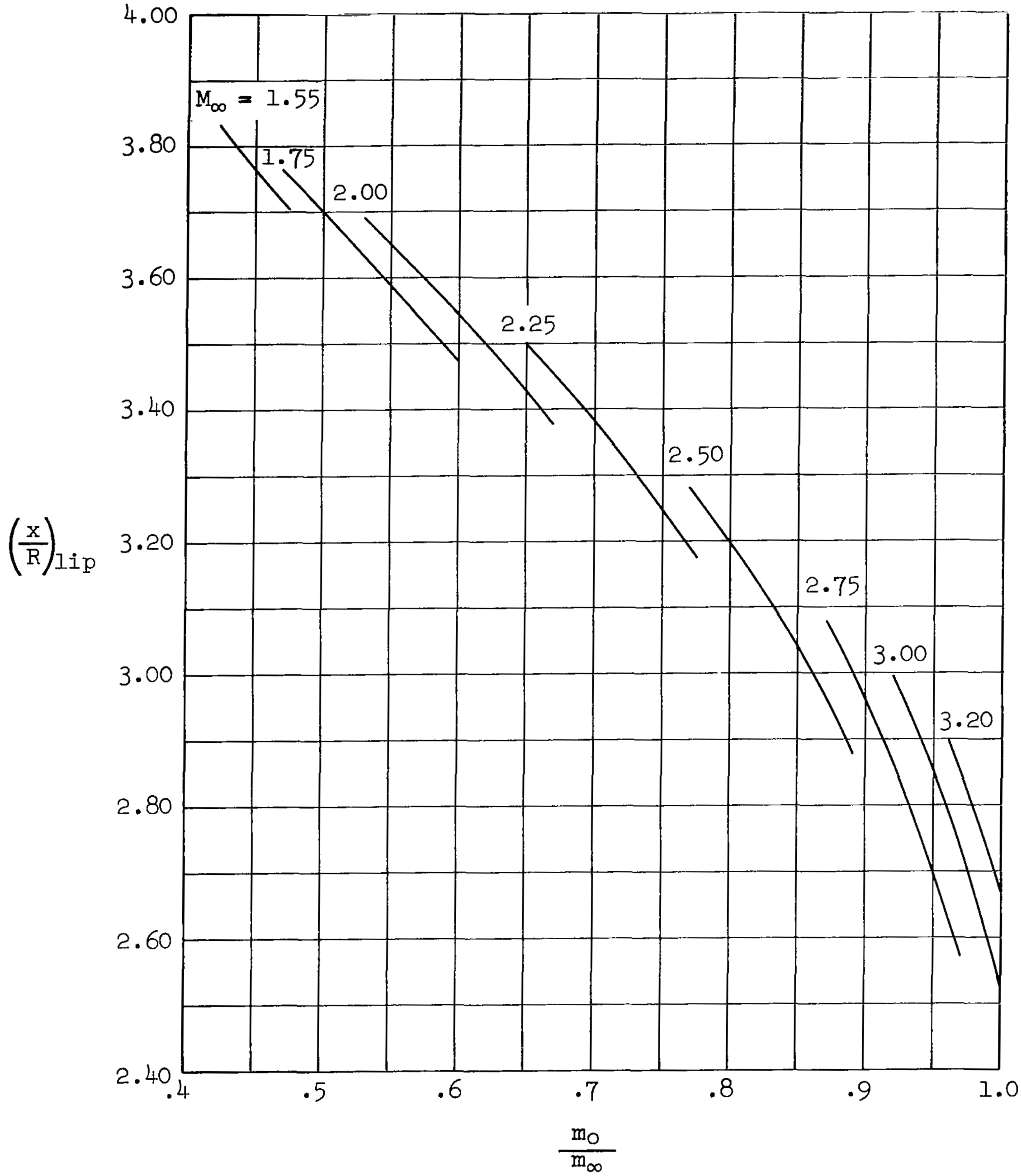

Figure 5.- Inlet theoretical mass-flow ratios; α = 0°.

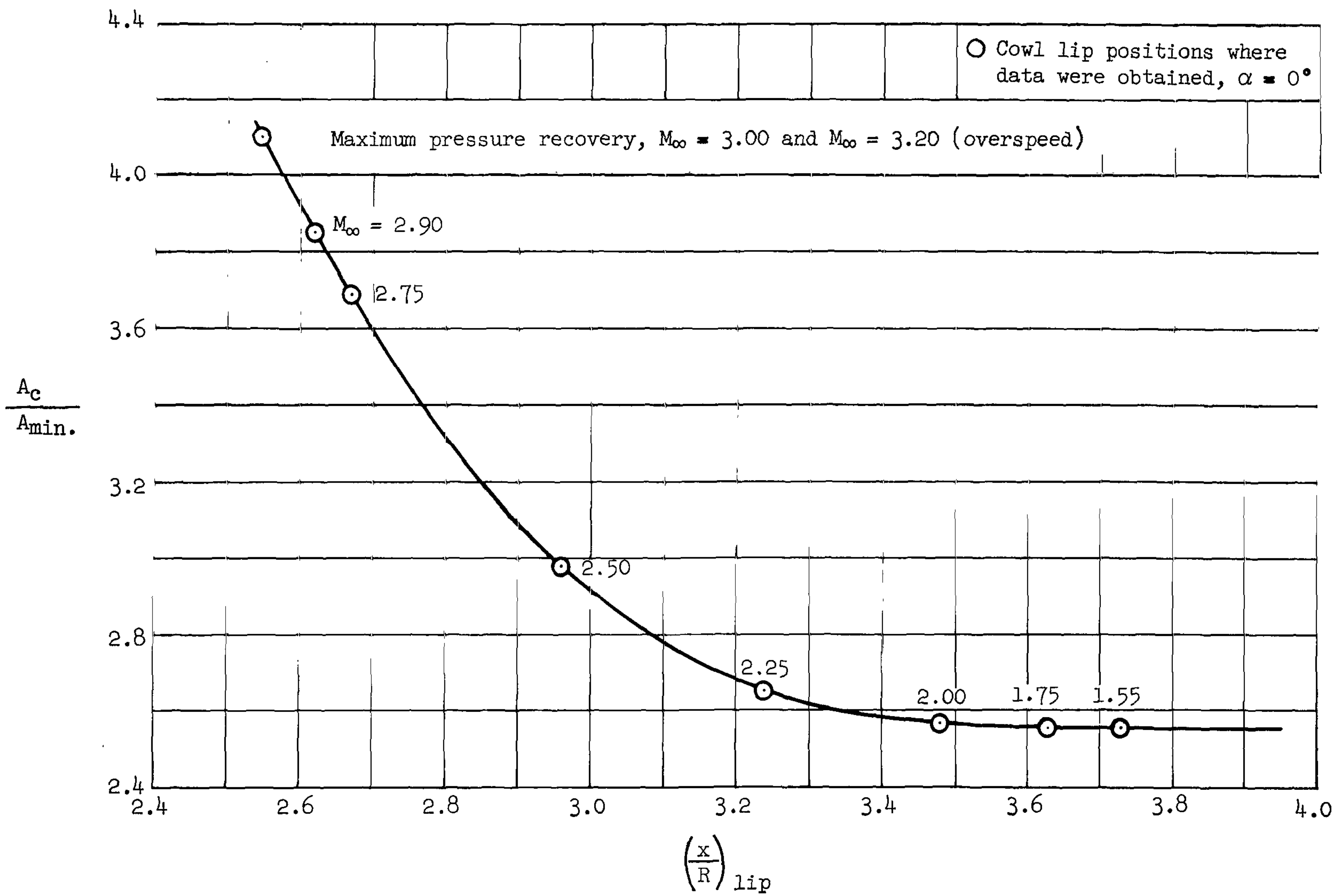

Figure 6.- Inlet contraction ratio.

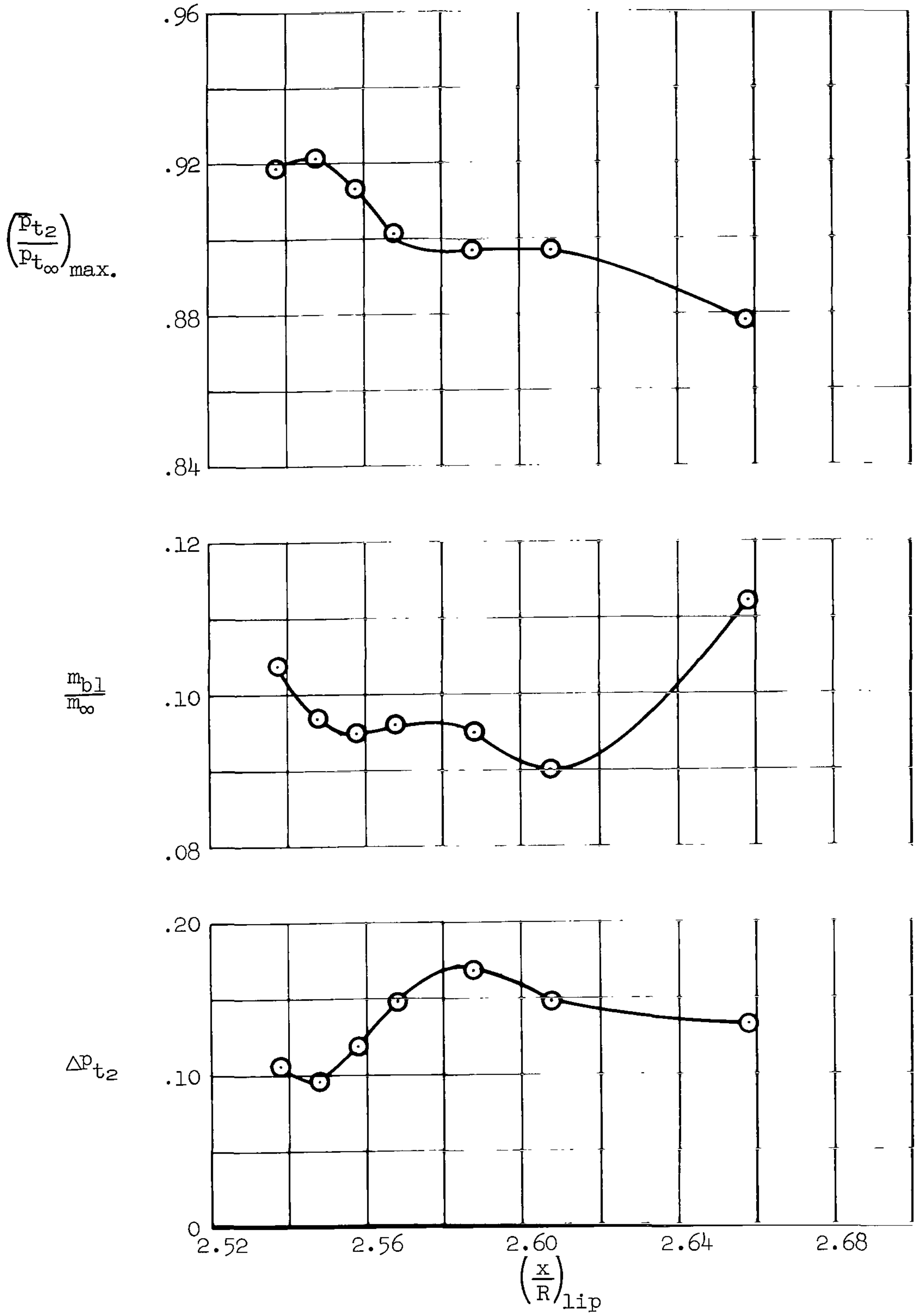

Figure 7.- Maximum performance at various cowl lip positions, bleed exit setting B; $M_\infty = 3.00$, $\alpha = 0°$.

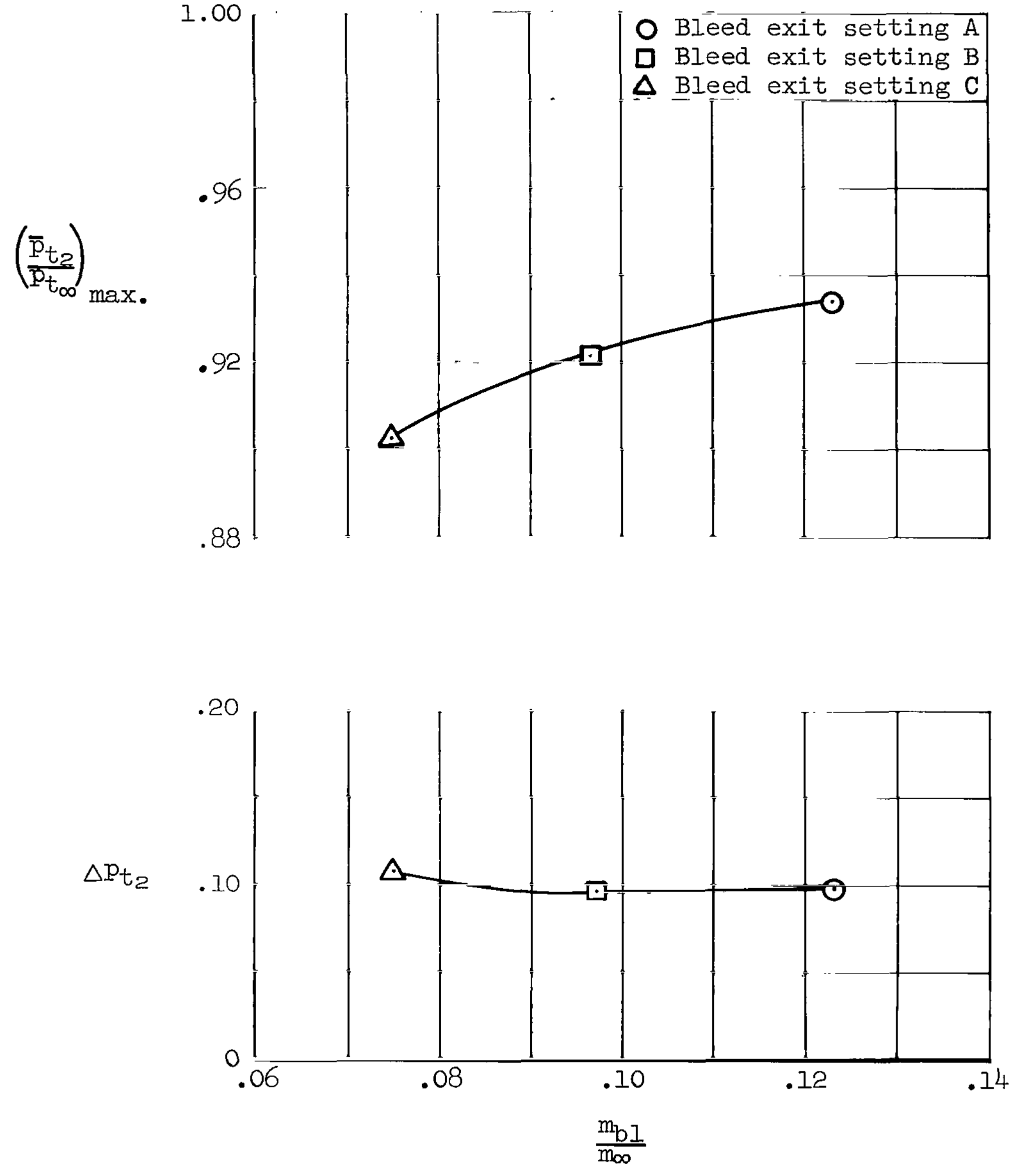

Figure 8.- Maximum performance for various boundary layer bleed exit settings; $(x/R)_{lip} = 2.548$; $M_\infty = 3.00$, $\alpha = 0°$.

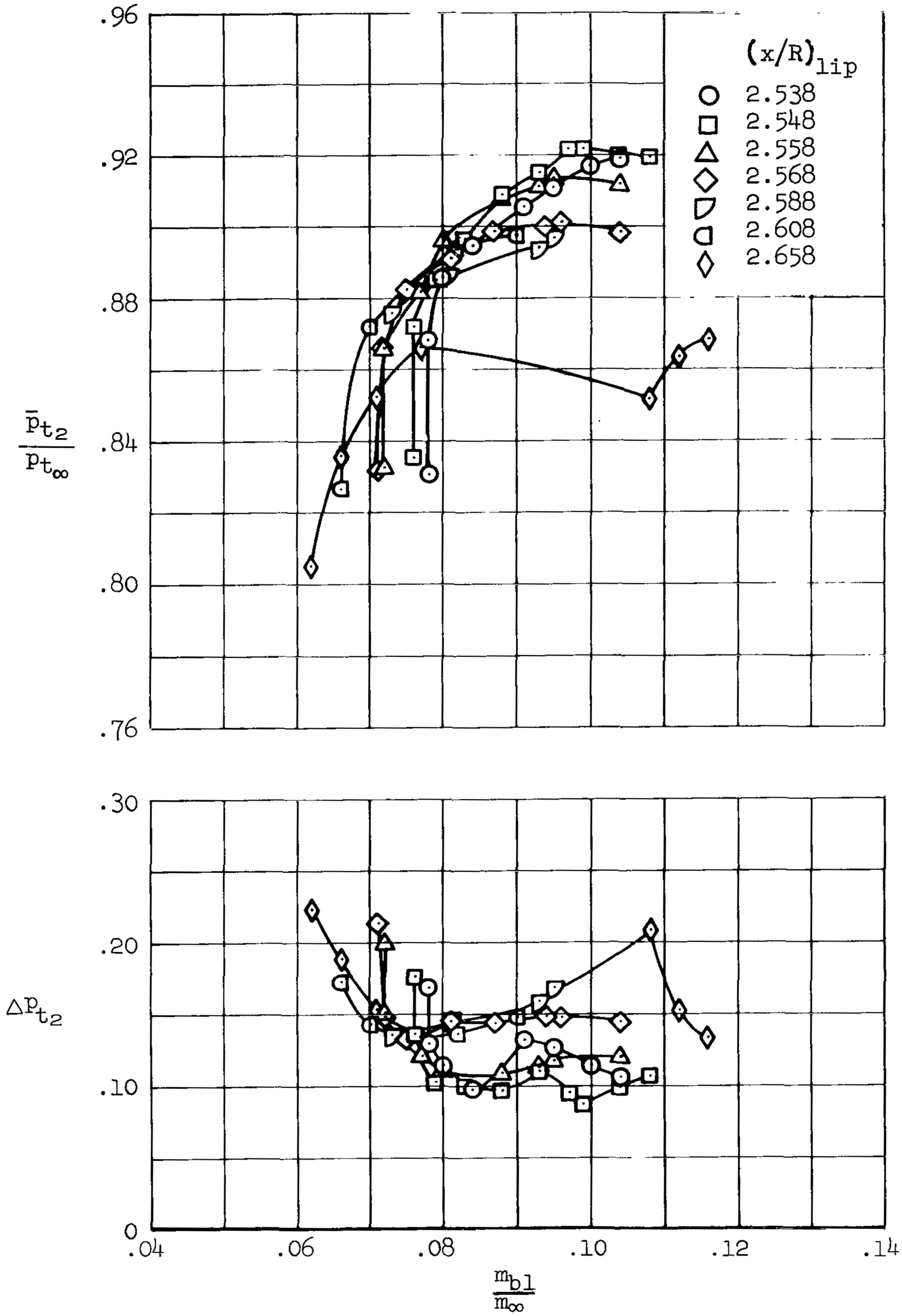

Figure 9.- Supercritical performance for various cowl positions, bleed exit setting B; $M_\infty = 3.00$, $\alpha = 0°$.

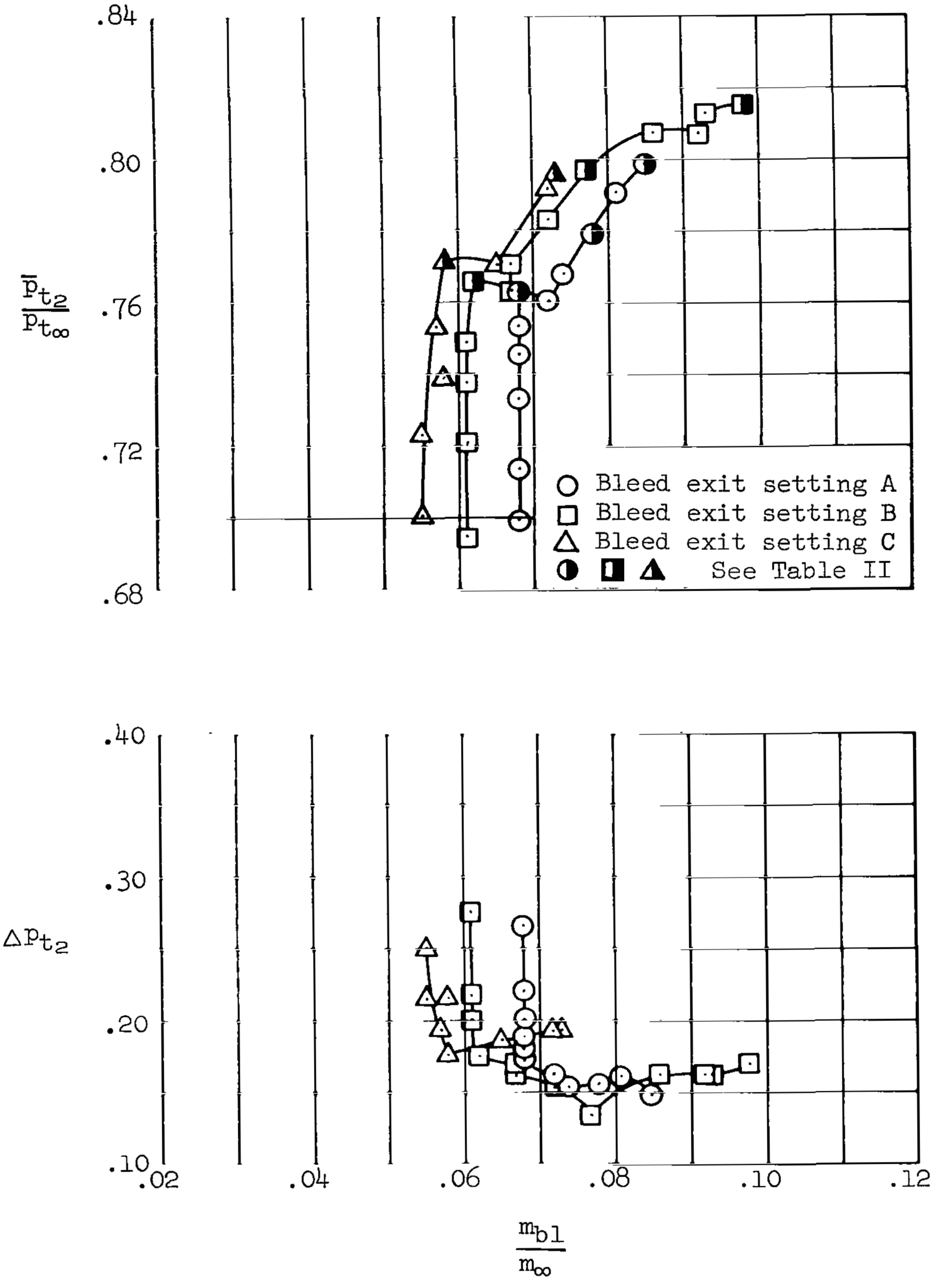

(a) $(x/R)_{lip} = 2.548$, $M_\infty = 3.20$

Figure 10.- Supercritical performance, $\alpha = 0^{\circ}$. (Tabulated pressure recoveries and mass-flow ratios are included in Table II for points with half-filled symbols.)

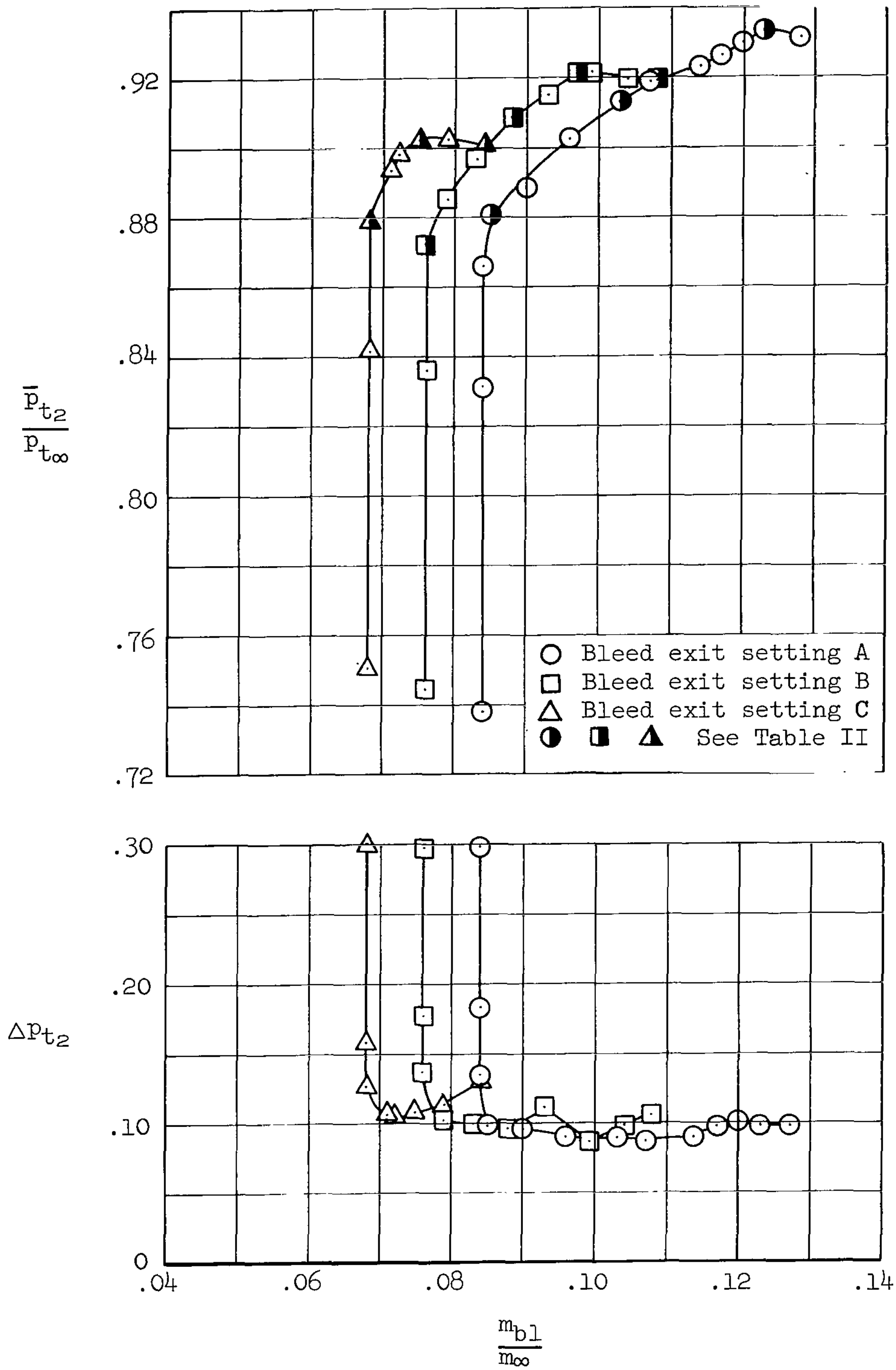

(b) $(x/R)_{lip} = 2.548$, $M_\infty = 3.00$.

Figure 10.- Continued.

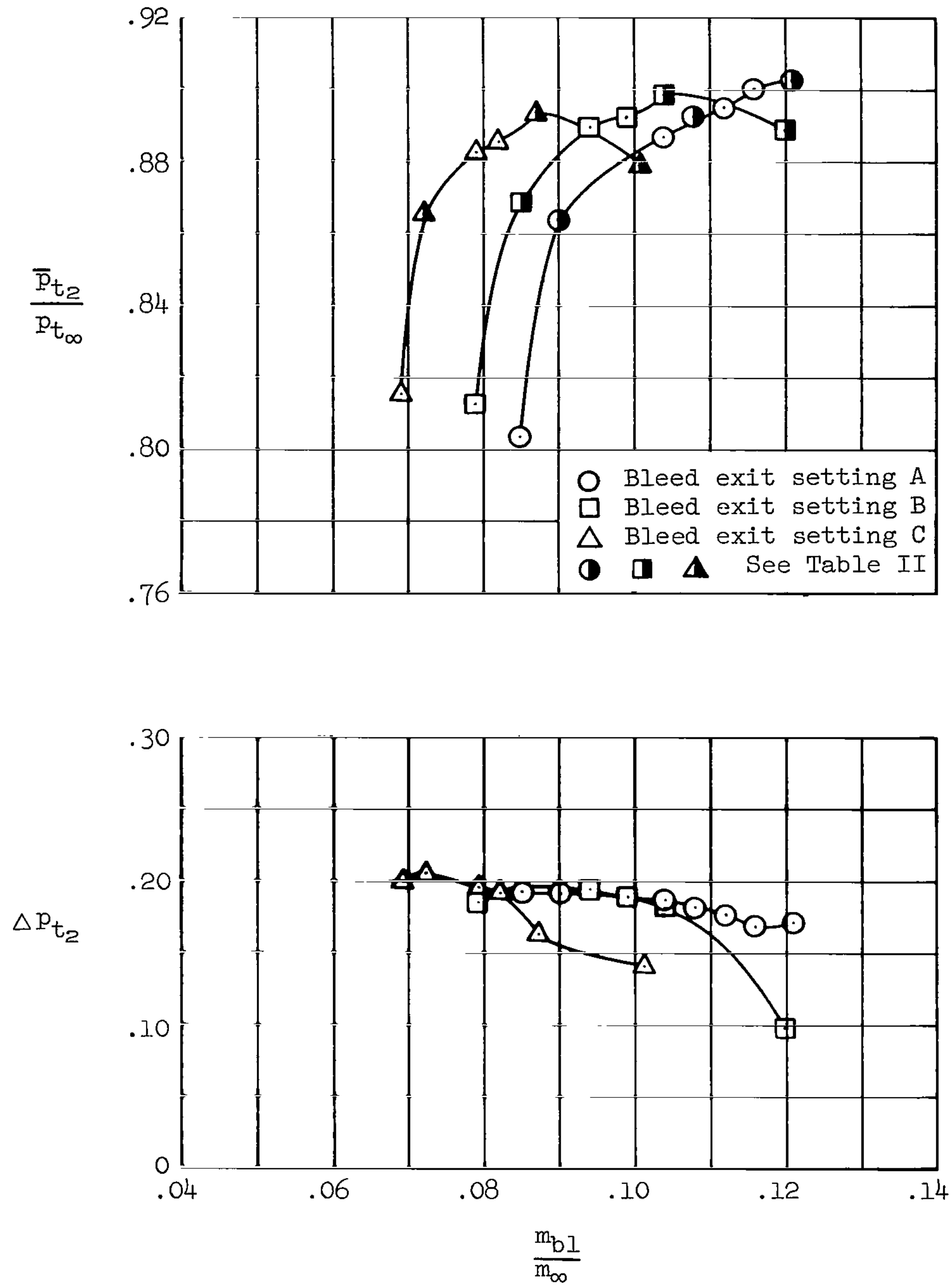

(c) $(x/R)_{lip} = 2.622$, $M_\infty = 2.90$.

Figure 10.- Continued.

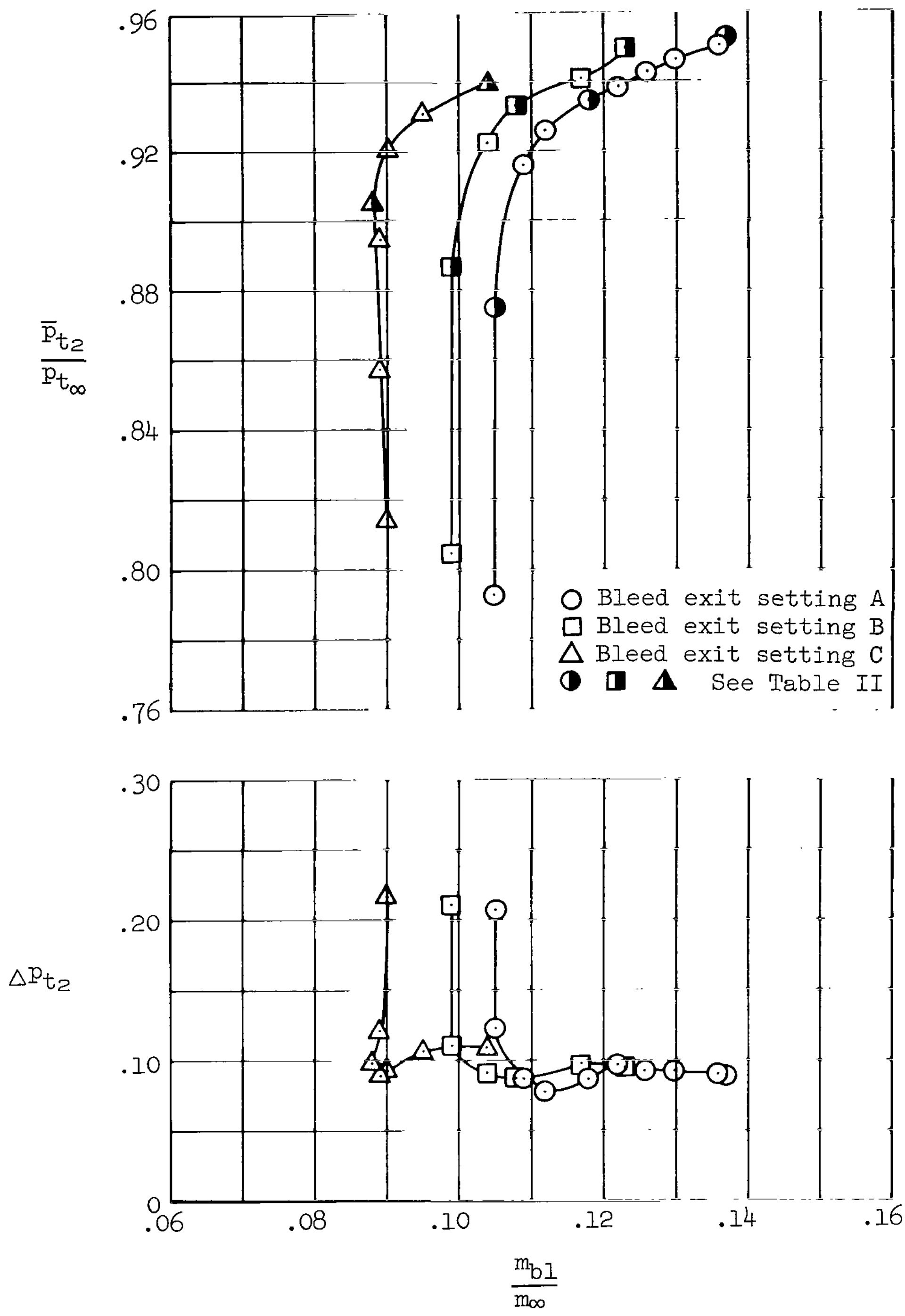

(d) $(x/R)_{lip} = 2.670$, $M_\infty = 2.75$.

Figure 10.- Continued.

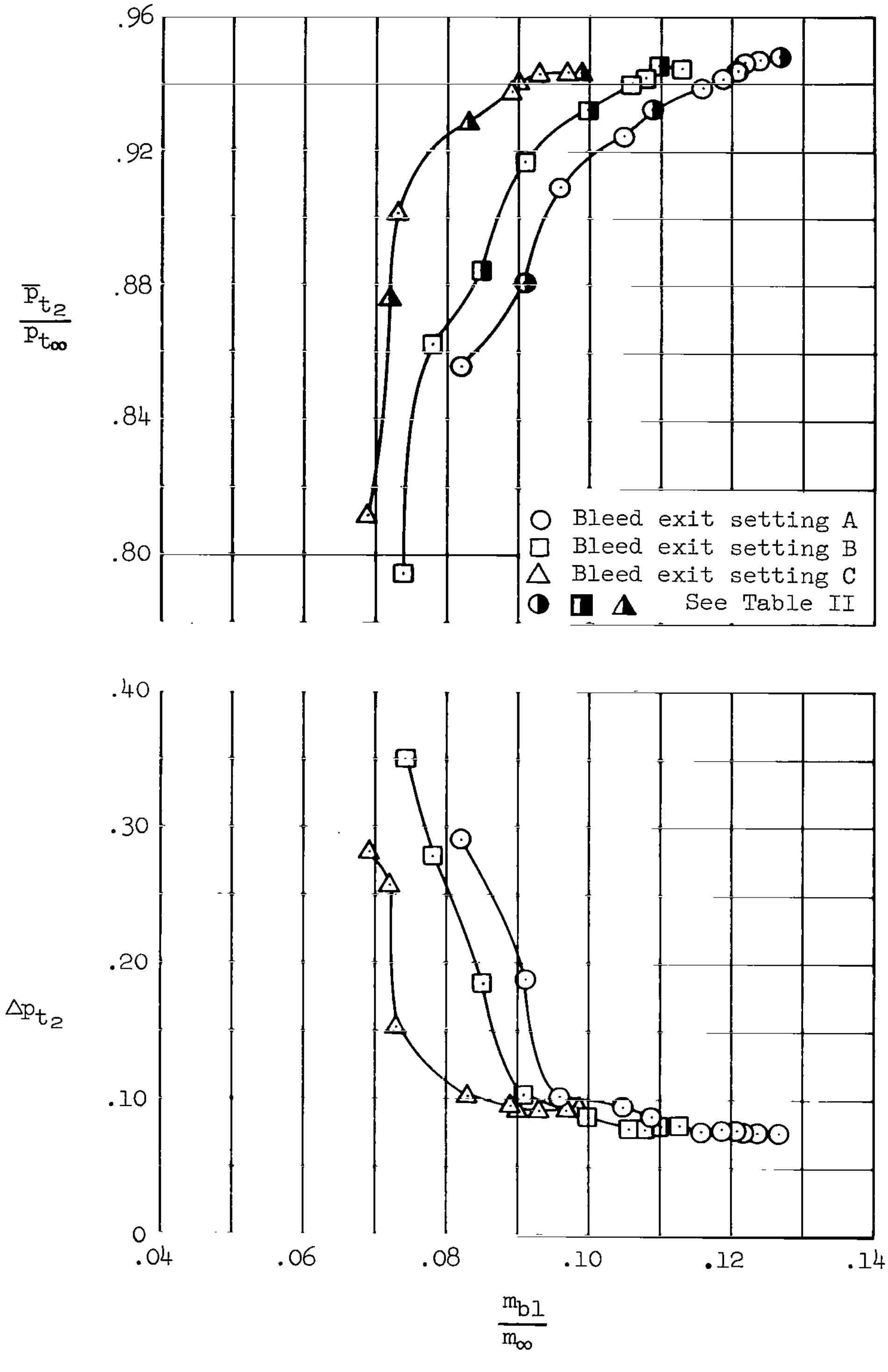

(e) $(x/R)_{lip} = 2.960$, $M_\infty = 2.50$

Figure 10.- Continued.

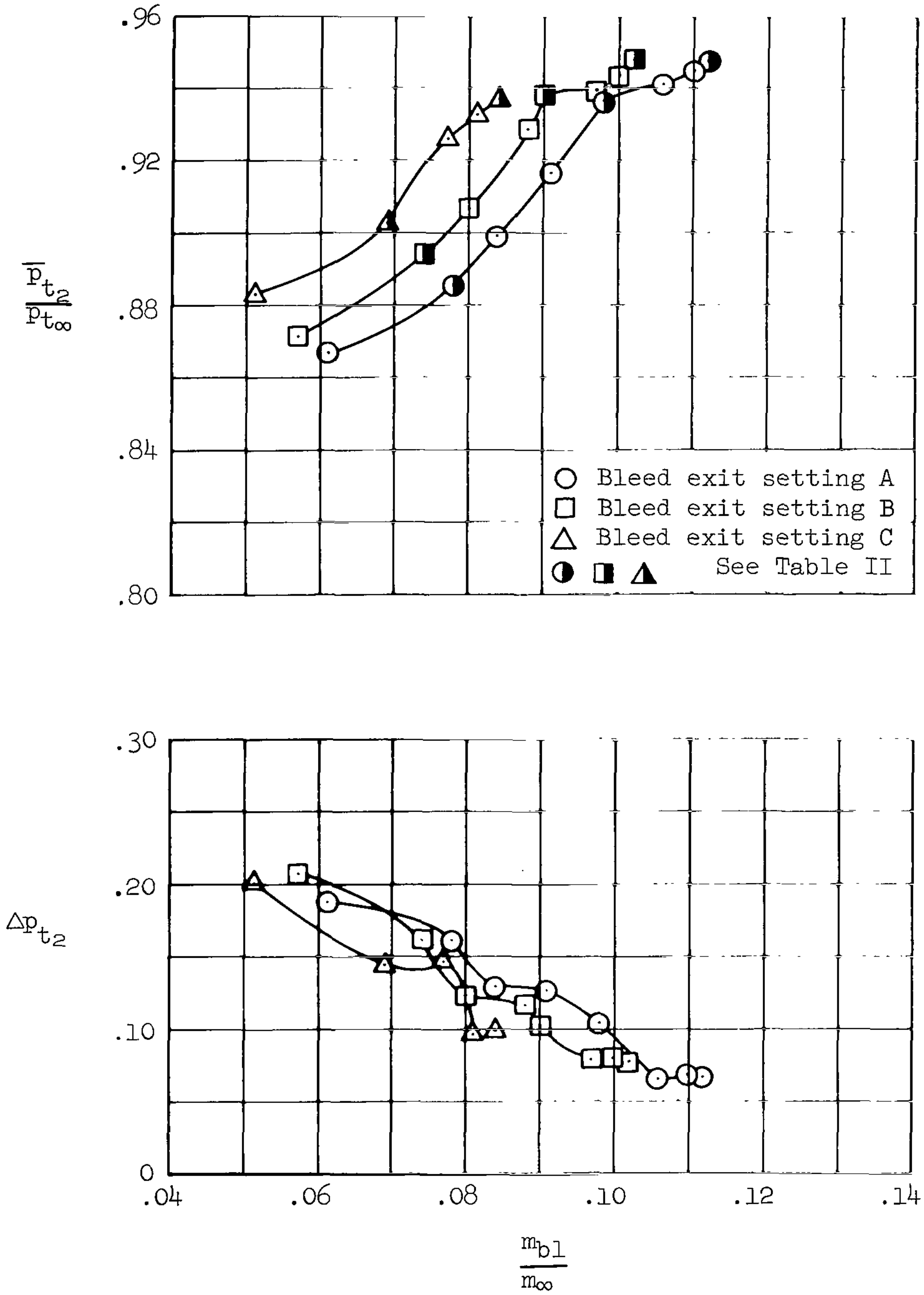

(f) $(x/R)_{lip} = 3.240$, $M_\infty = 2.25$

Figure 10.- Continued.

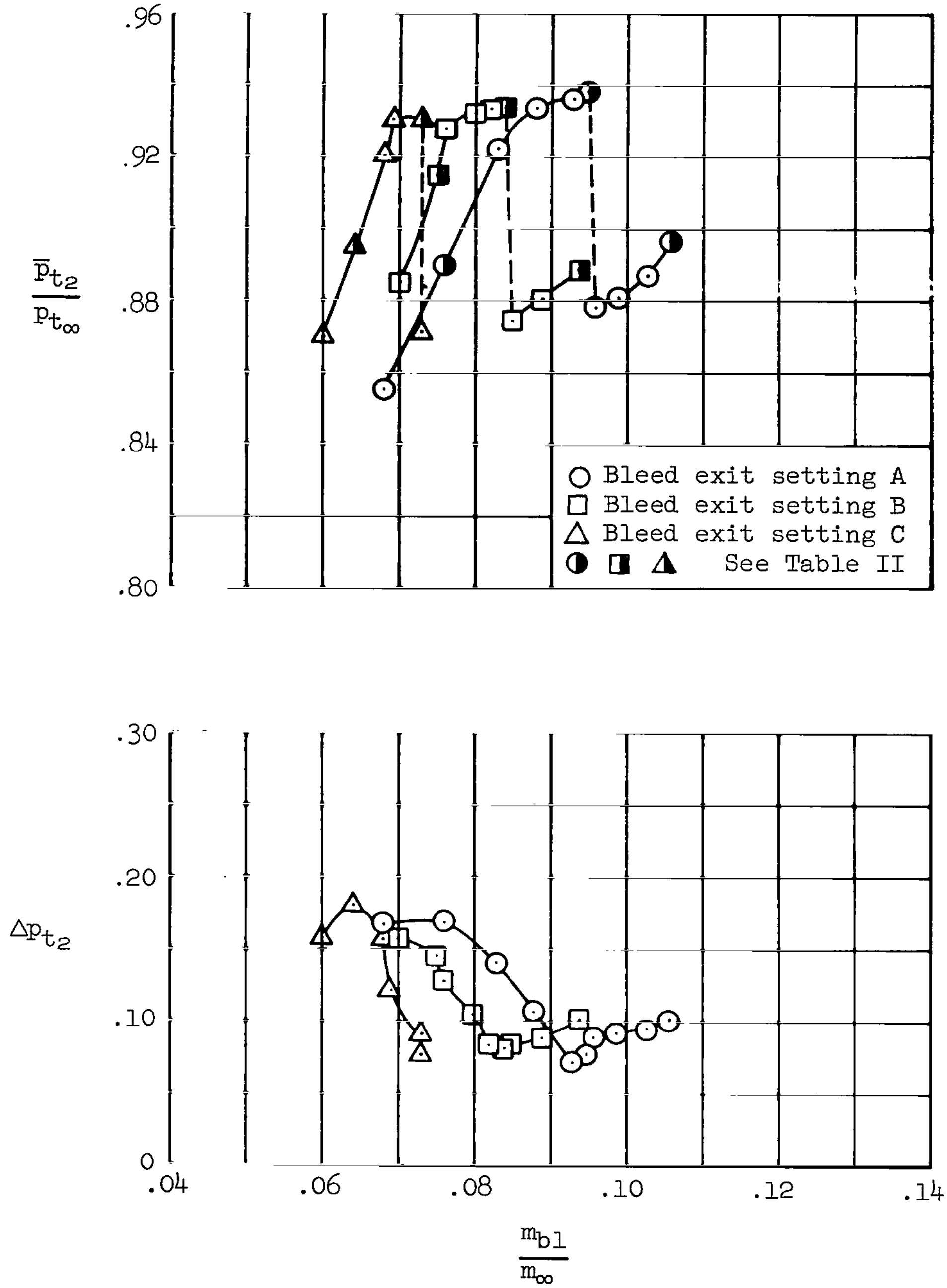

(g) $(x/R)_{lip} = 3.478$, $M_\infty = 2.00$

Figure 10.- Continued.

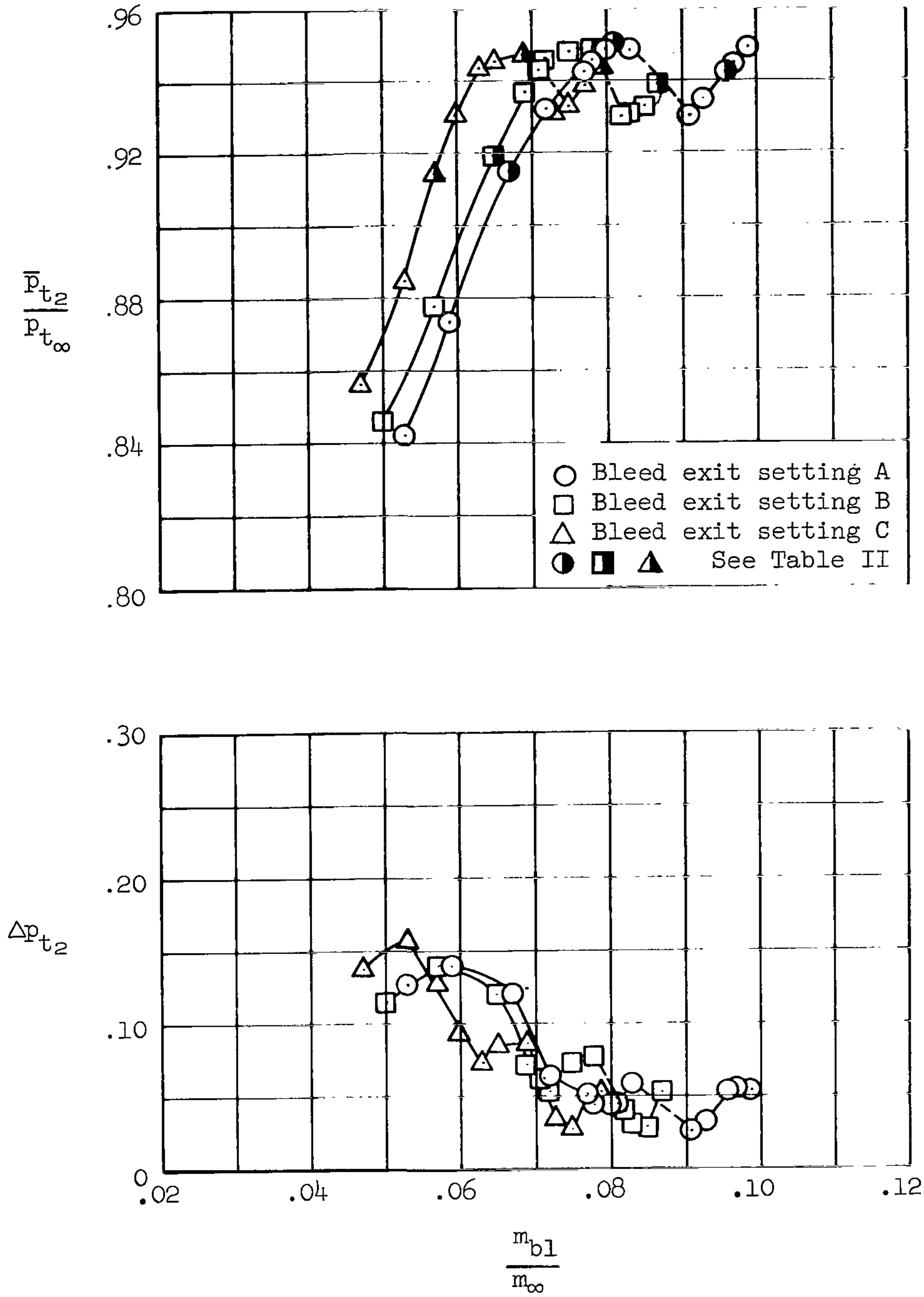

(h) $(x/R)_{lip} = 3.628$, $M_\infty = 1.75$

Figure 10.- Continued.

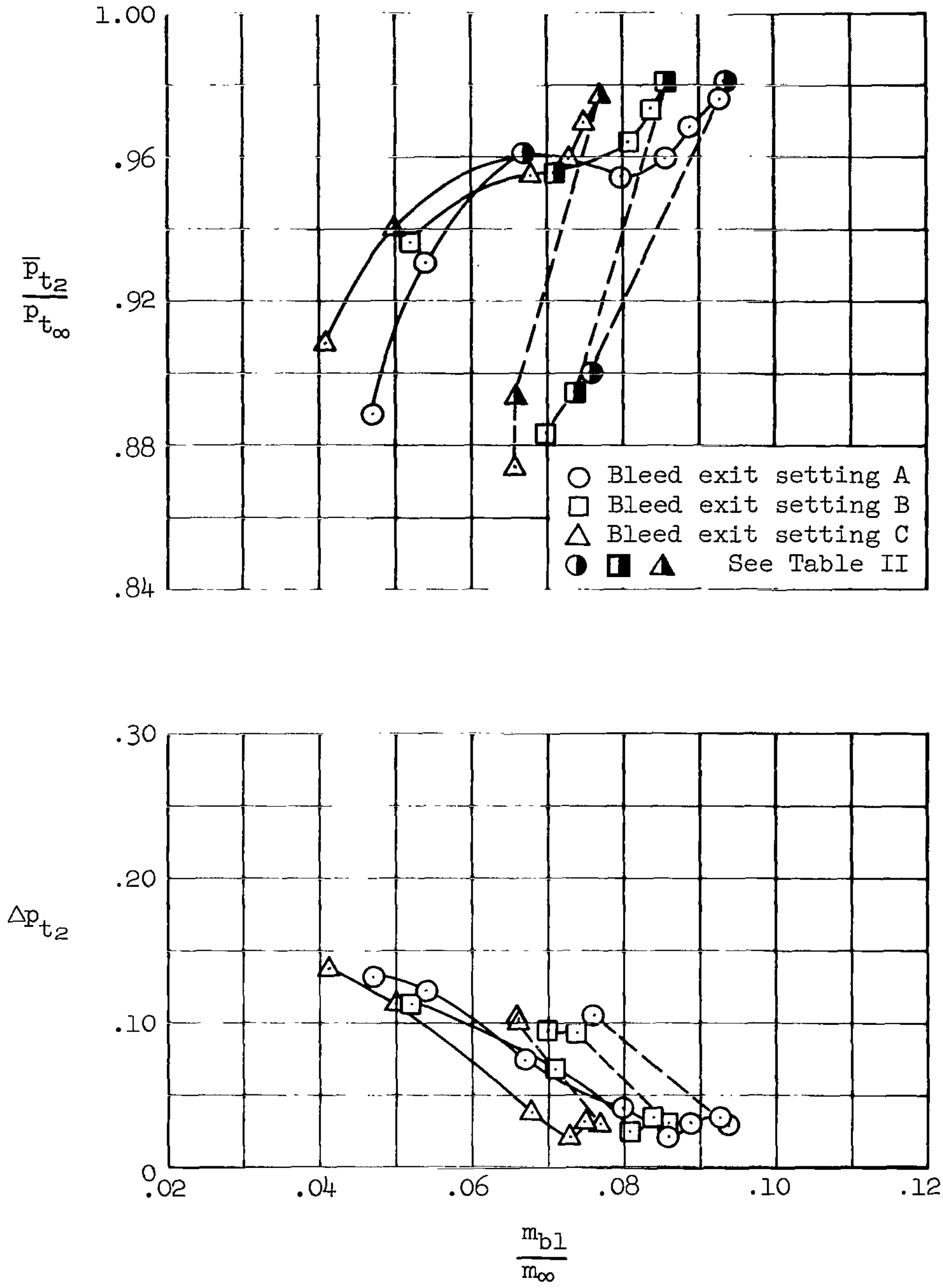

(i) $(x/R)_{lip} = 3.728$, $M_\infty = 1.55$

Figure 10.- Concluded.

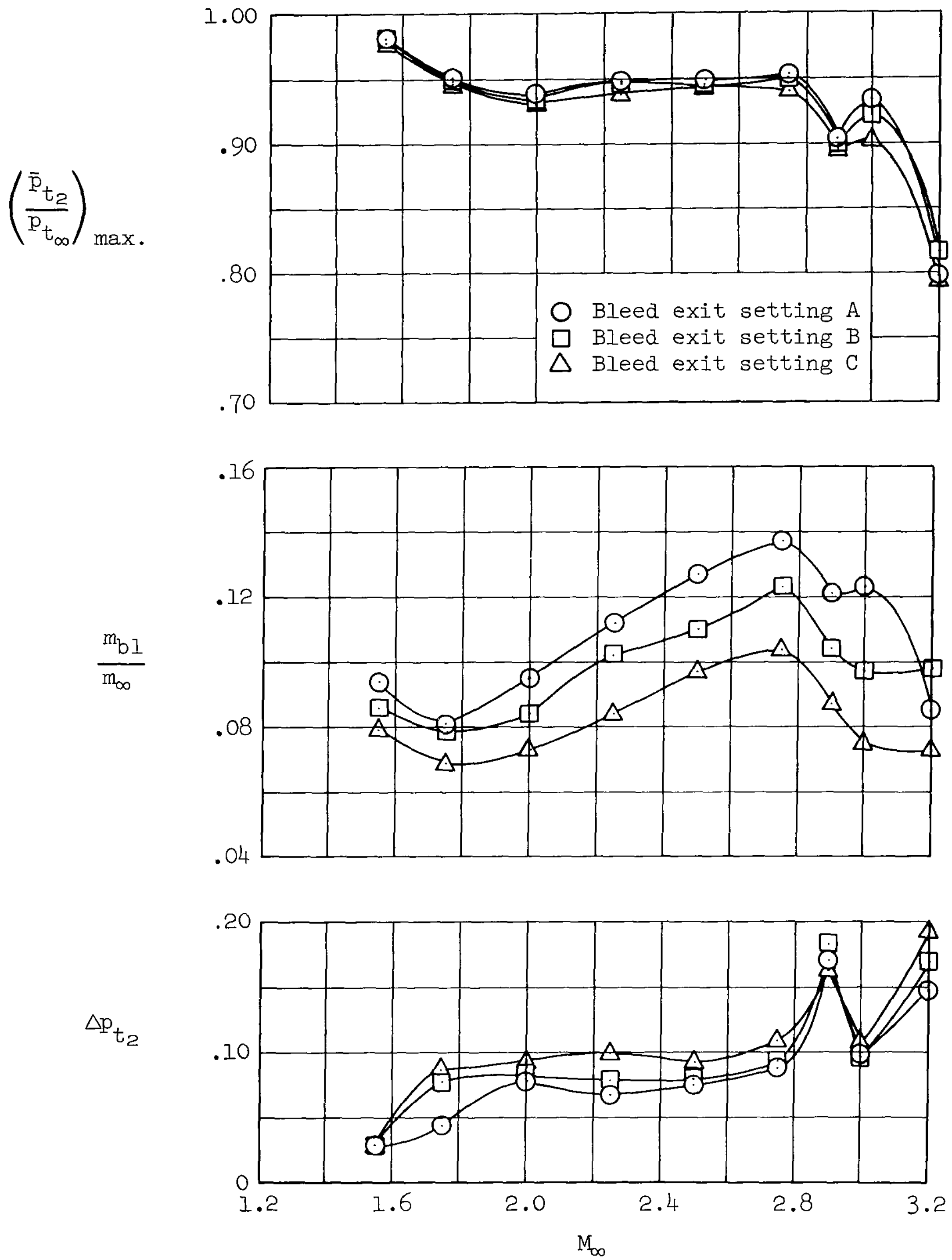

Figure 11.- Off-design maximum performance; α = 0°.

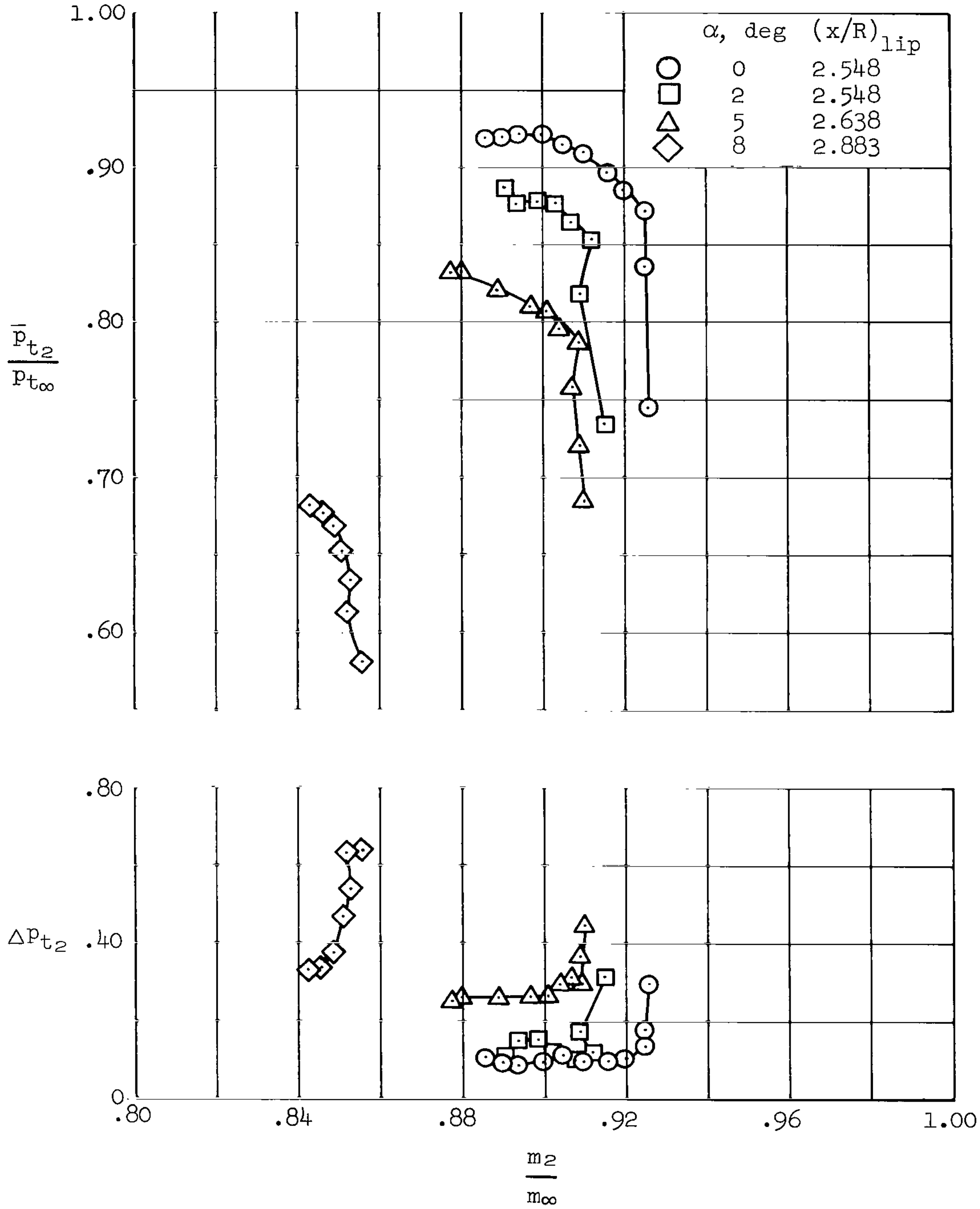

(a) $M_\infty = 3.00$

Figure 12.- Supercritical performance at angle of attack; bleed exit setting B.

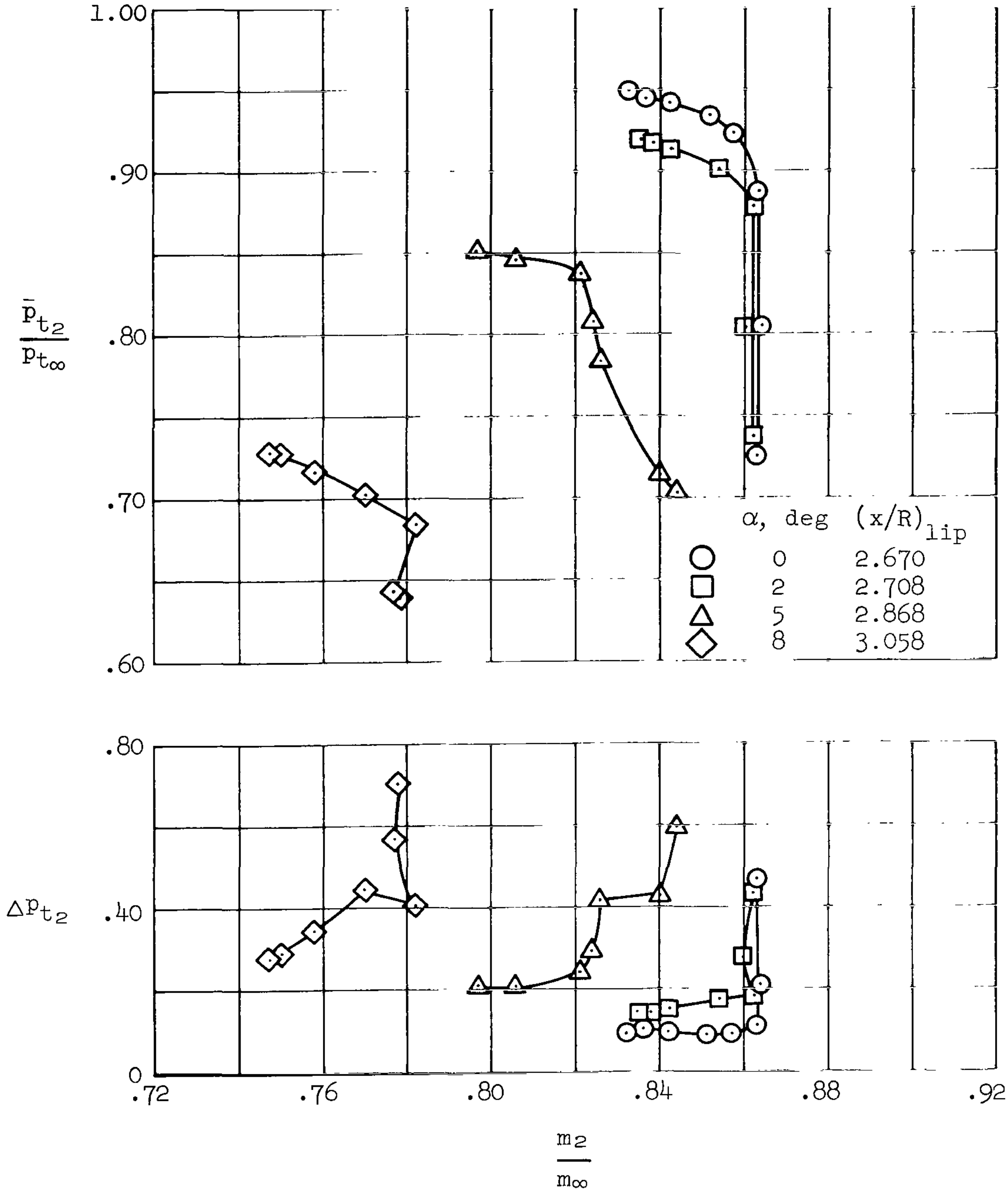

(b) $M_\infty = 2.75$

Figure 12.- Continued.

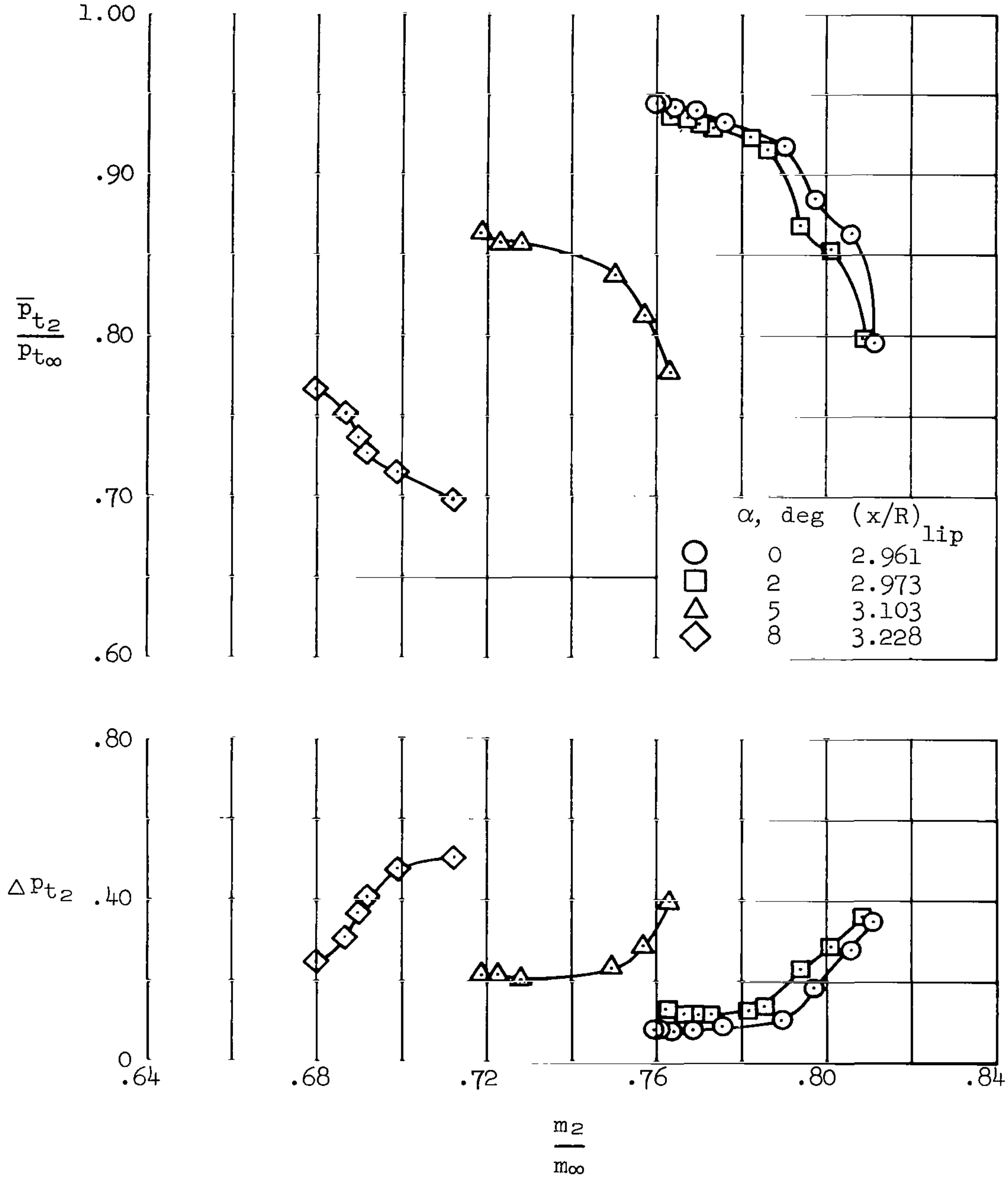

(c) $M_\infty = 2.50$

Figure 12.- Continued.

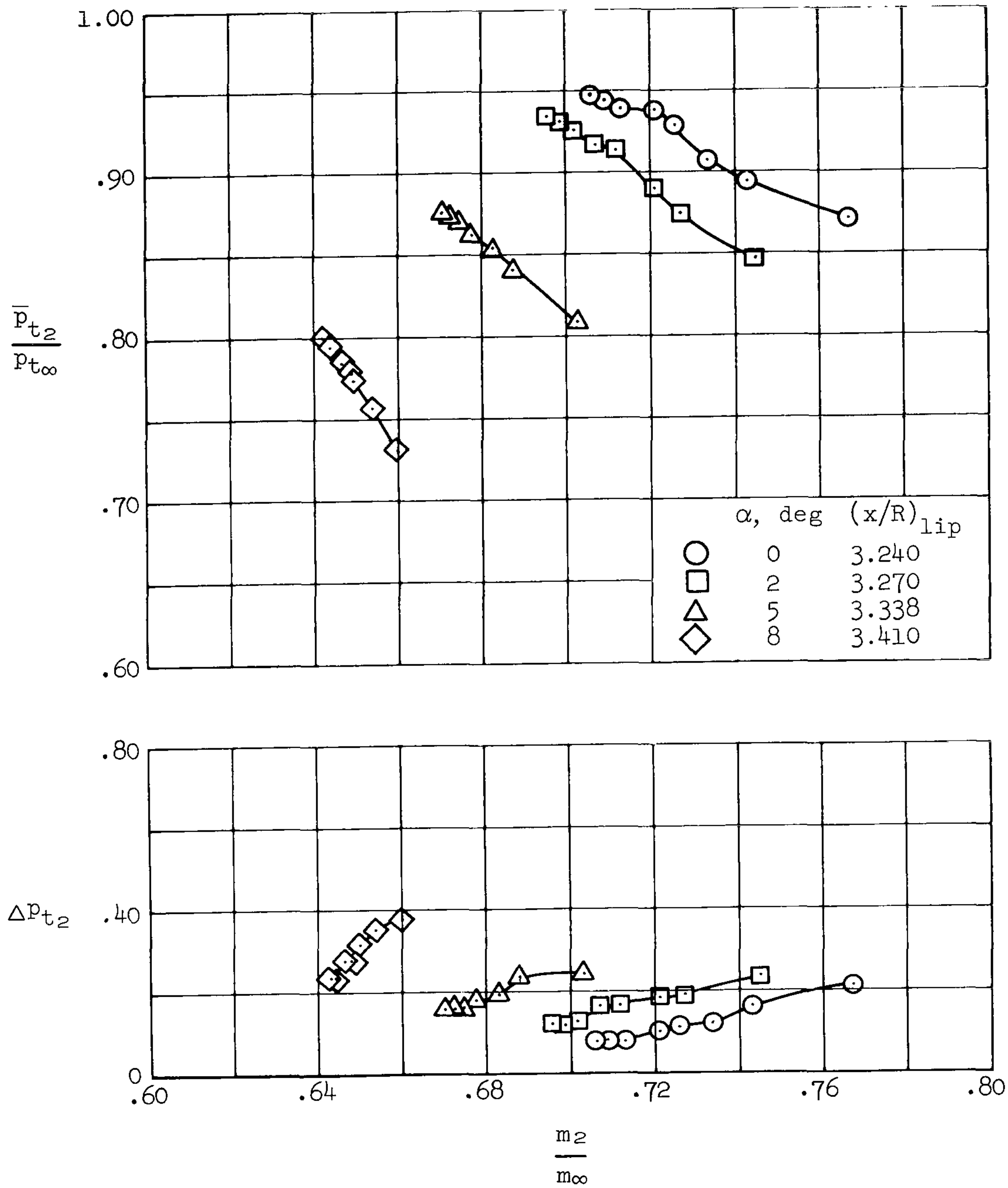

(d) $M_\infty = 2.25$

Figure 12.- Continued.

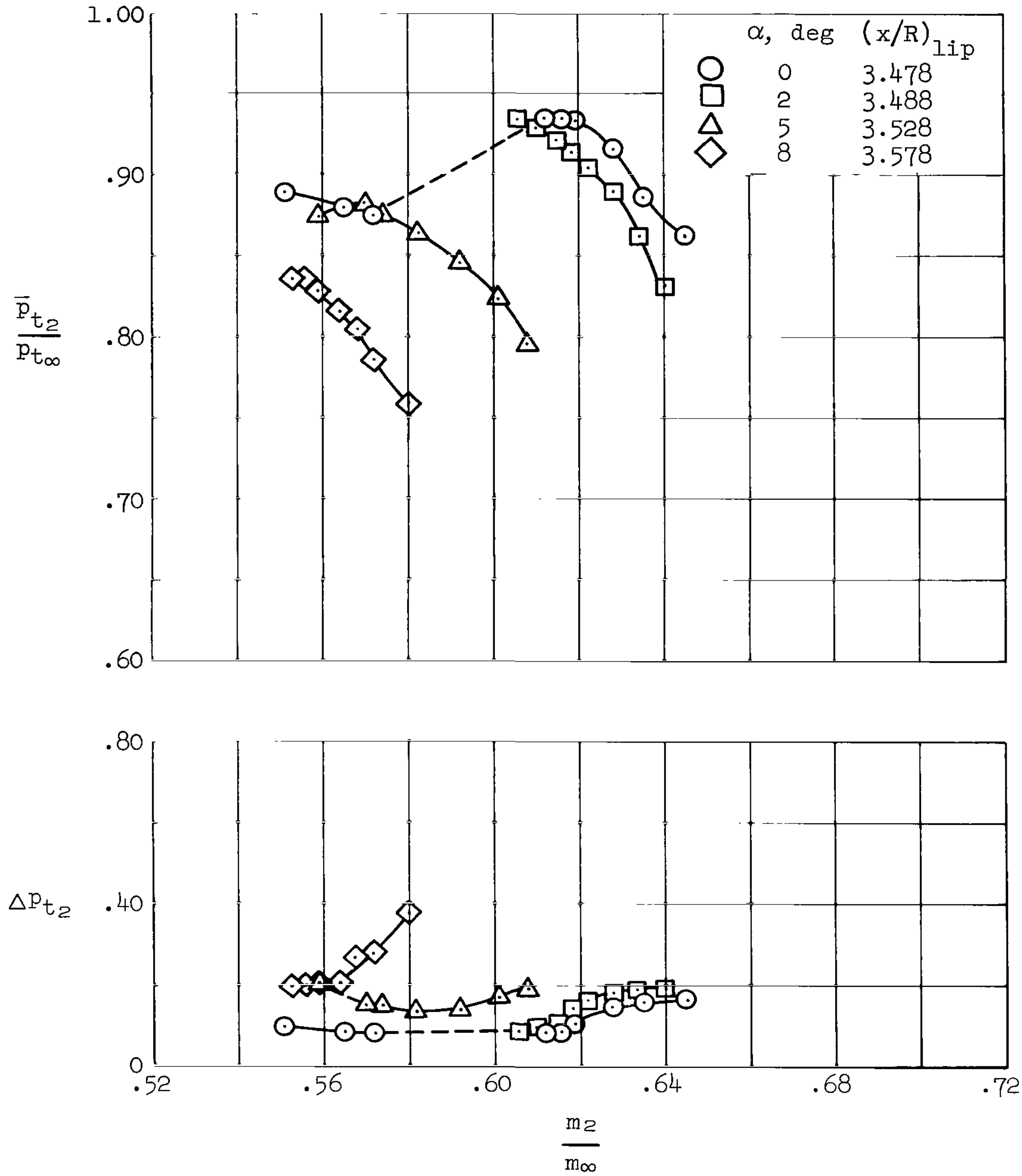

(e) $M_\infty = 2.00$

Figure 12.- Continued.

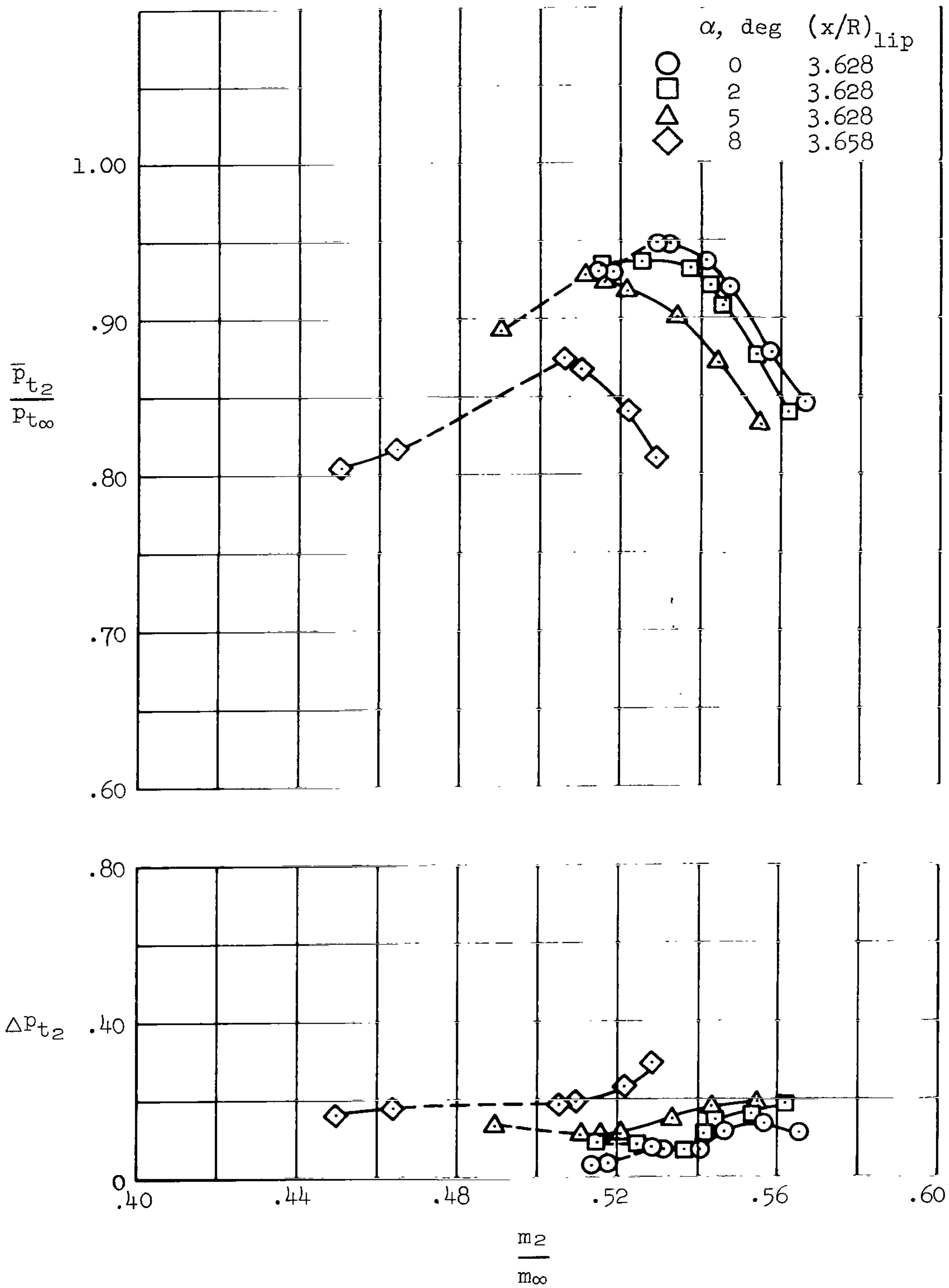

(f) $M_\infty = 1.75$

Figure 12.- Concluded.

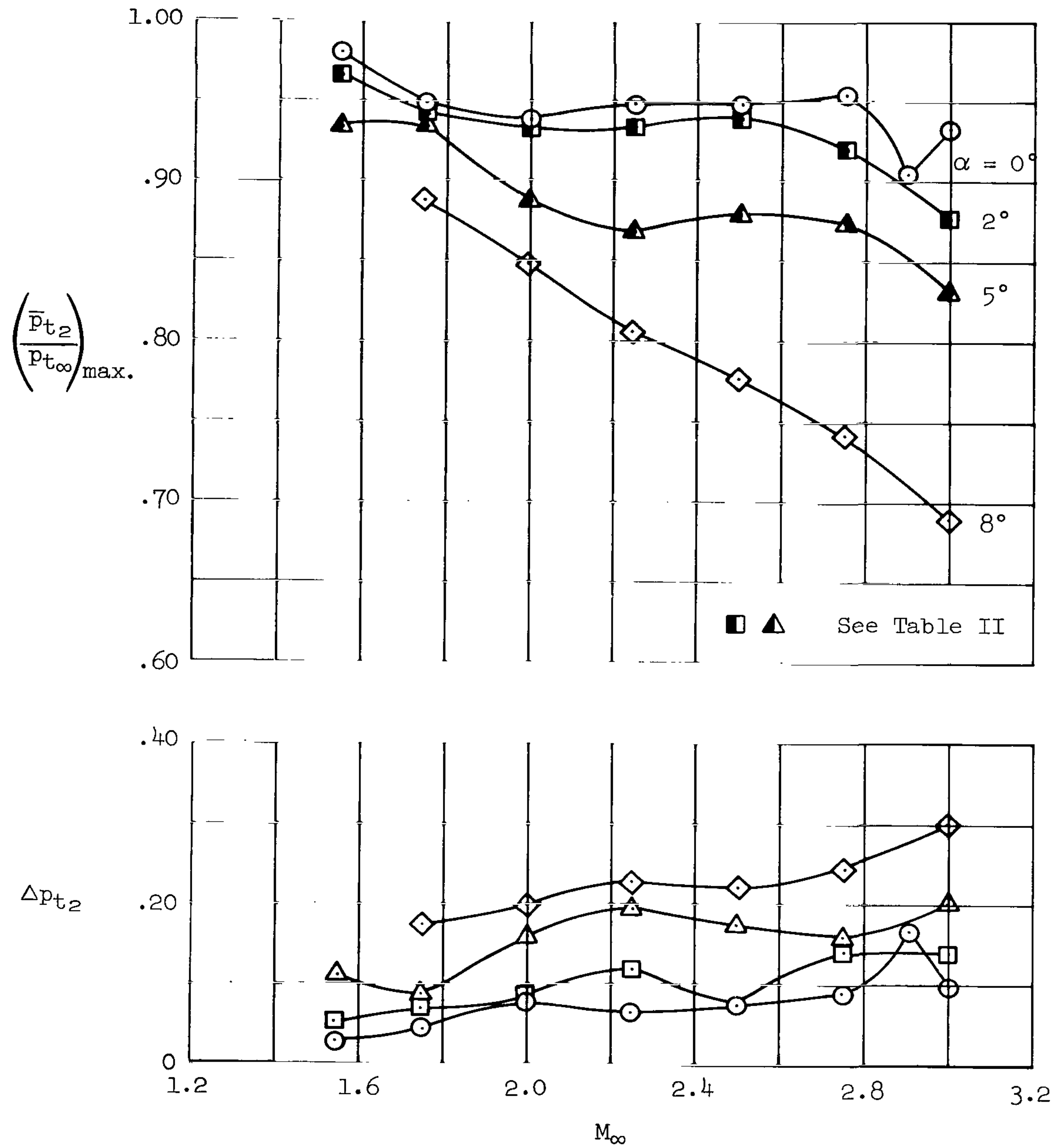

(a) Bleed exit setting A

Figure 13.- Maximum performance at angle of attack.

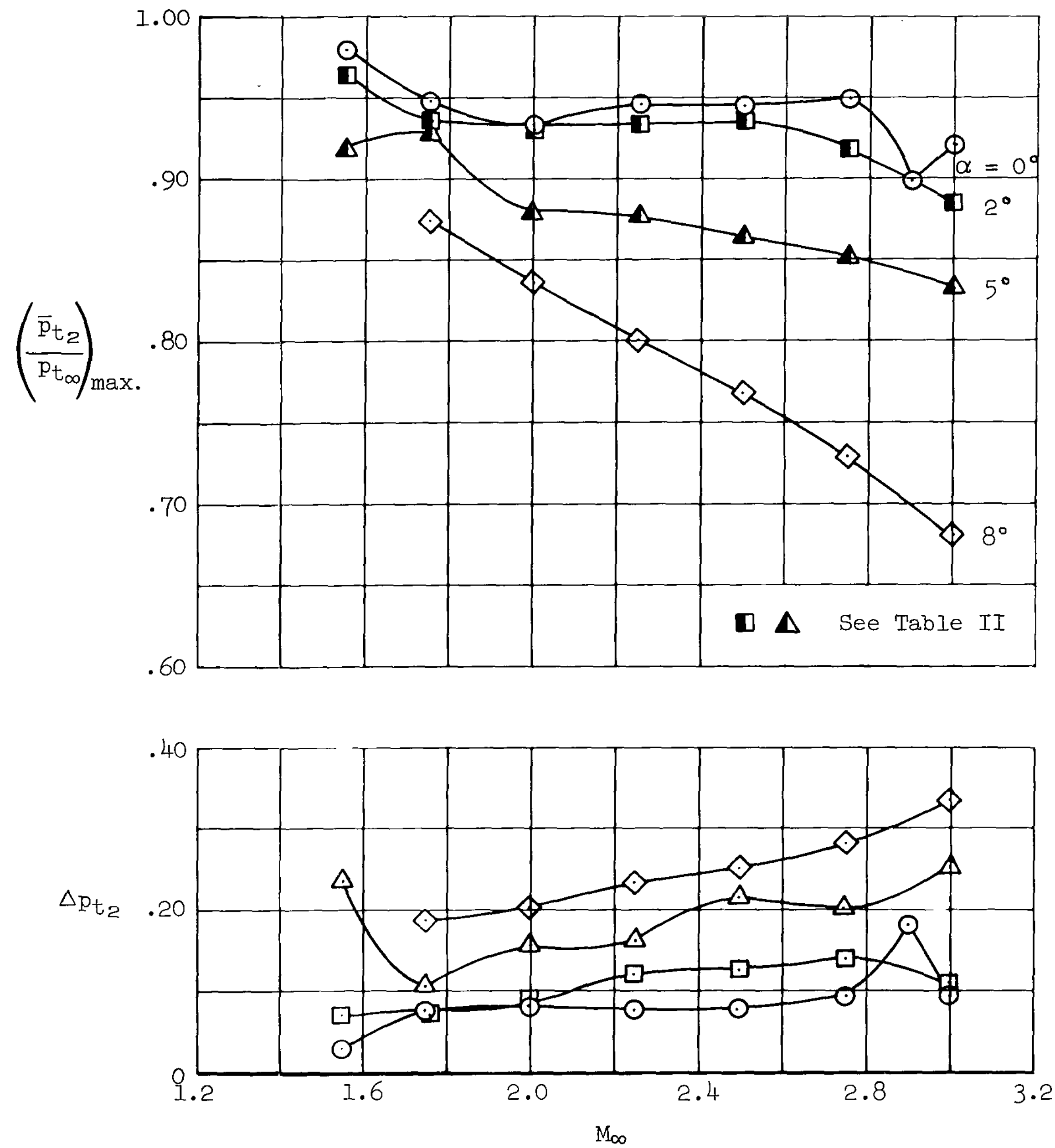

(b) Bleed exit setting B

Figure 13.- Continued.

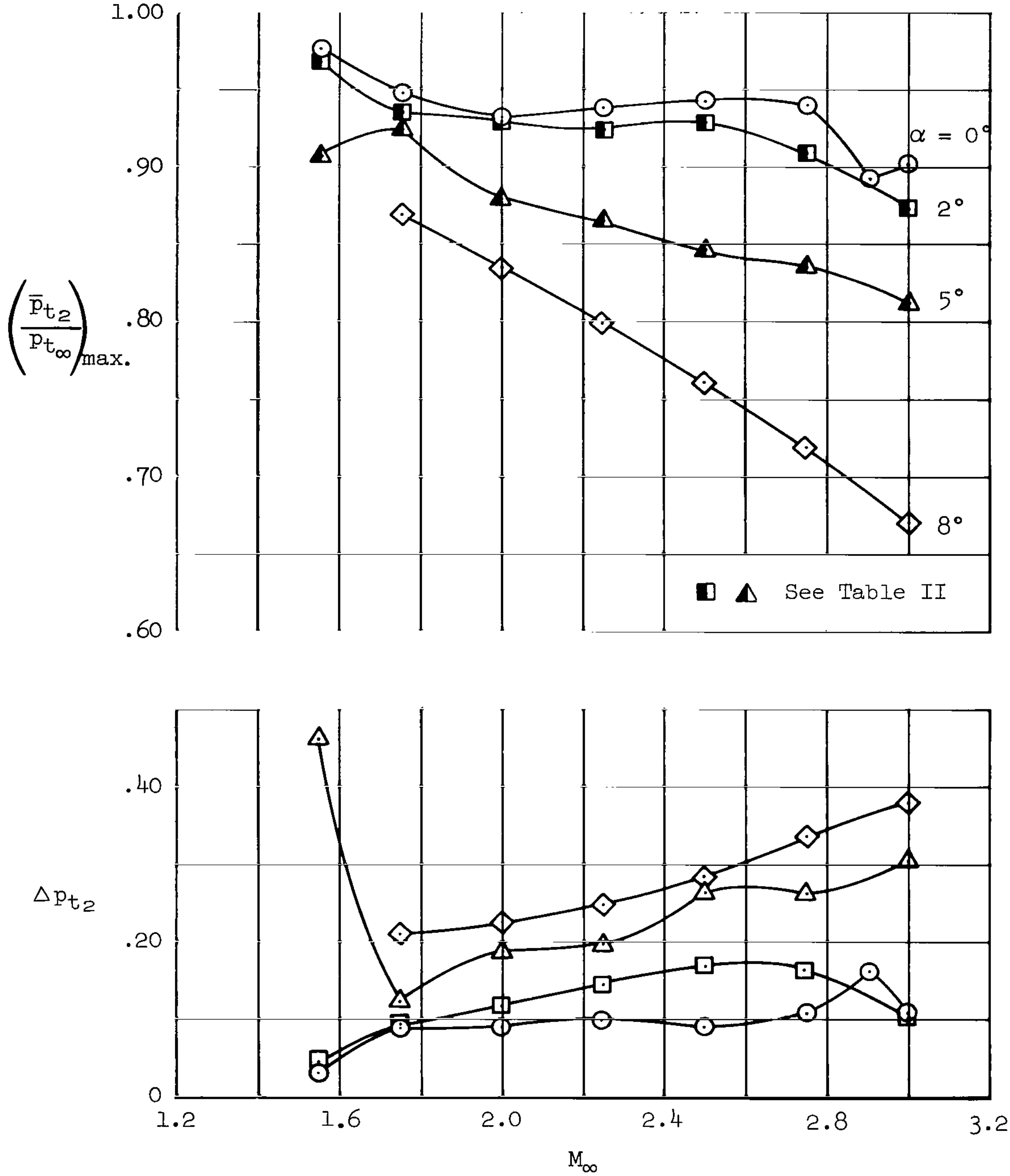

(c) Bleed exit setting C

Figure 13.- Concluded.

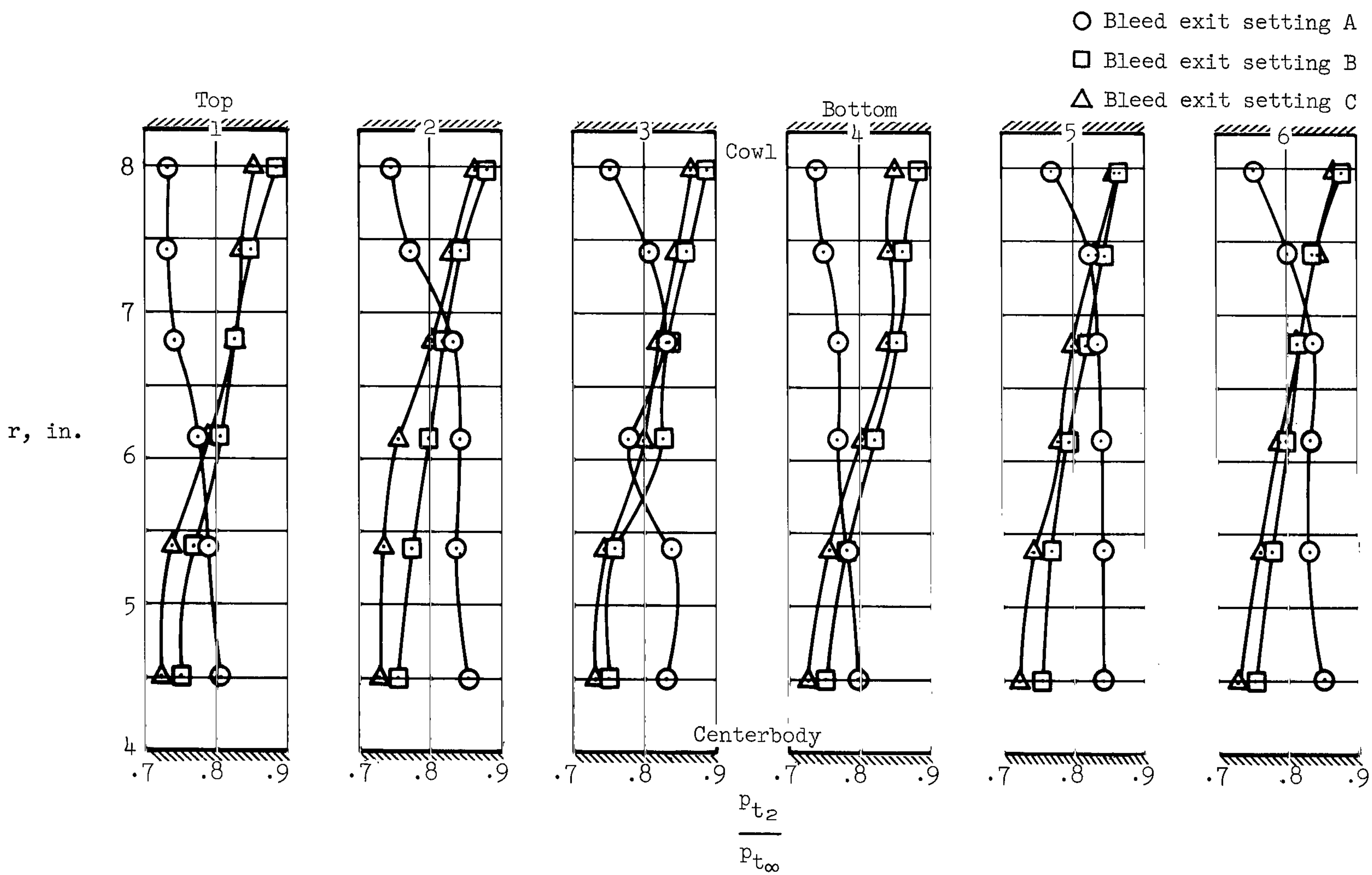

(a) $(x/R)_{lip} = 2.548$, $M_\infty = 3.20$

Figure 14.- Total-pressure recovery profiles at the engine-face, maximum pressure recovery; $\alpha = 0°$.

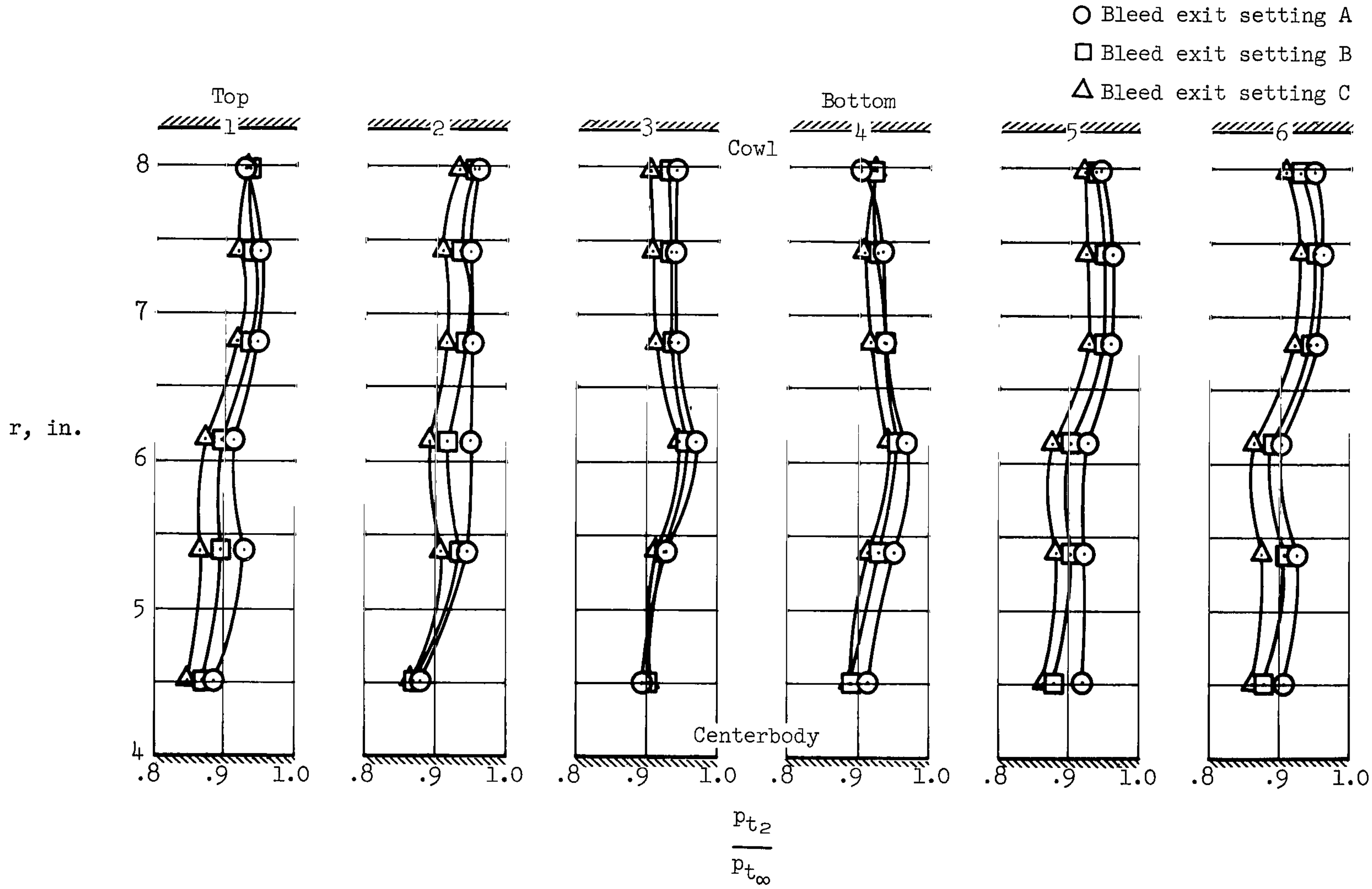

(b) $(x/R)_{lip} = 2.548$, $M_\infty = 3.00$

Figure 14.- Continued.

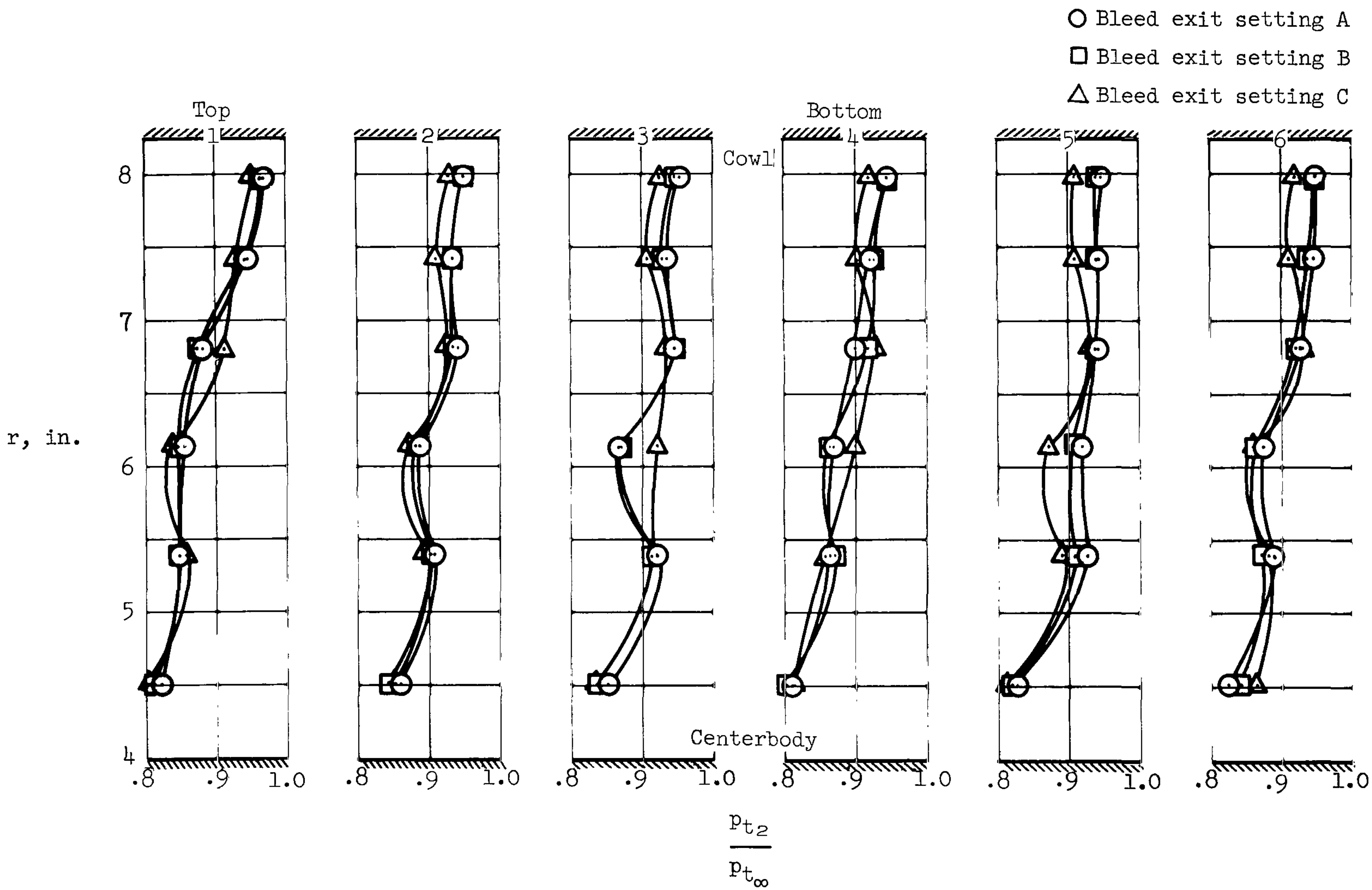

(c) $(x/R)_{lip} = 2.622$, $M_\infty = 2.90$

Figure 14.- Continued.

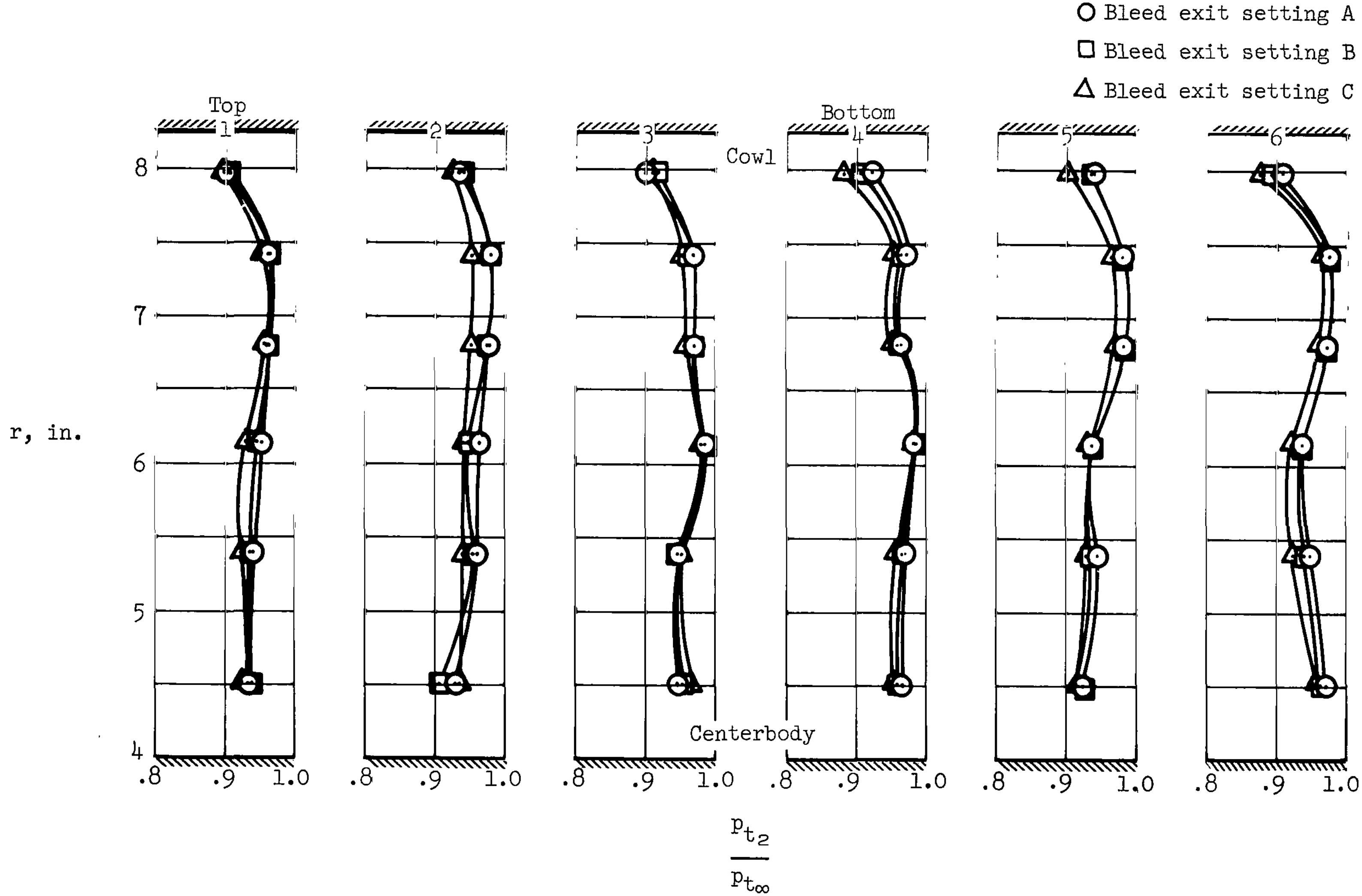

(d) $(x/R)_{lip} = 2.670$, $M_\infty = 2.75$

Figure 14.- Continued.

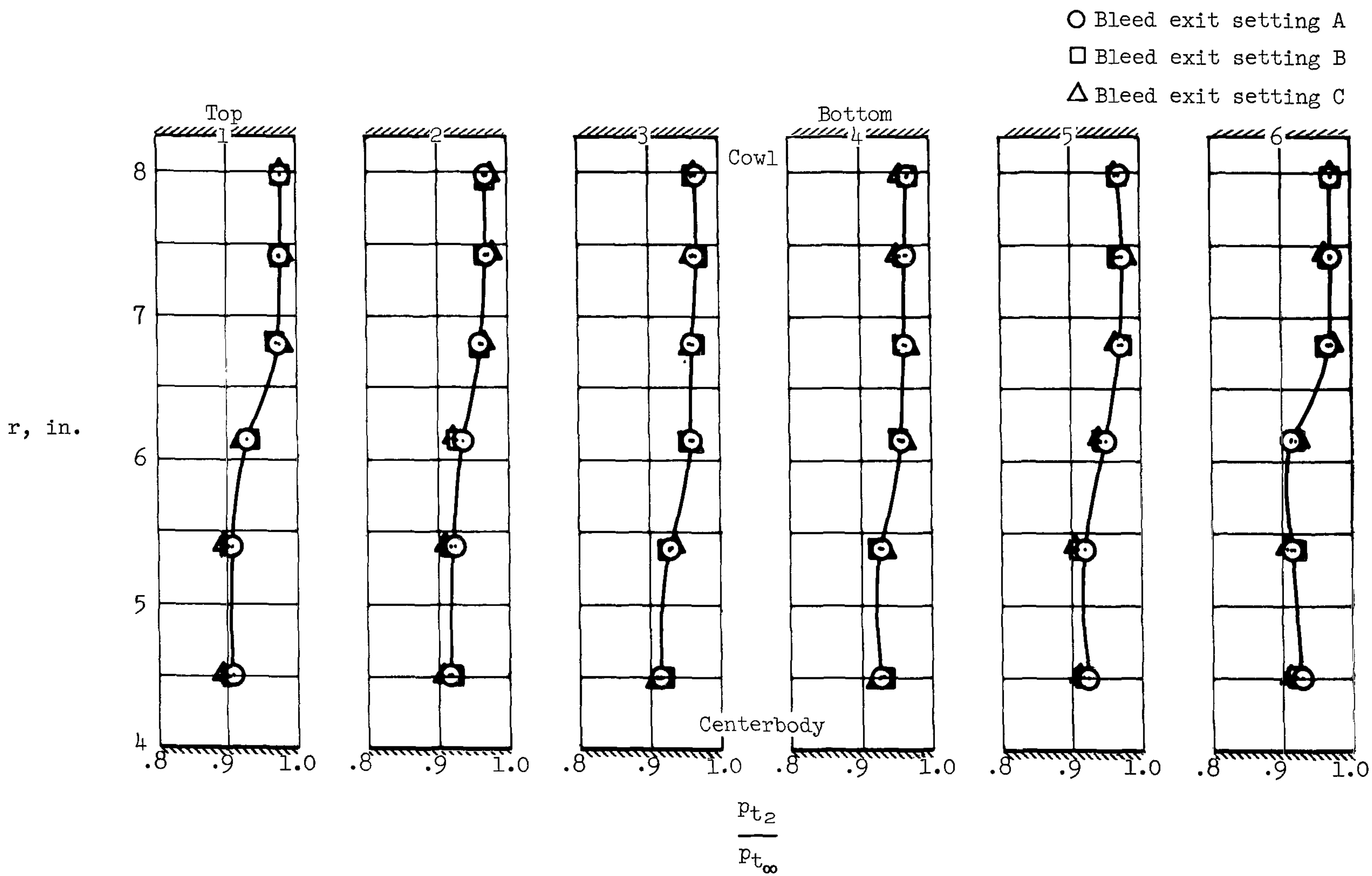

(e) $(x/R)_{lip} = 2.960$, $M_\infty = 2.50$

Figure 14.- Continued.

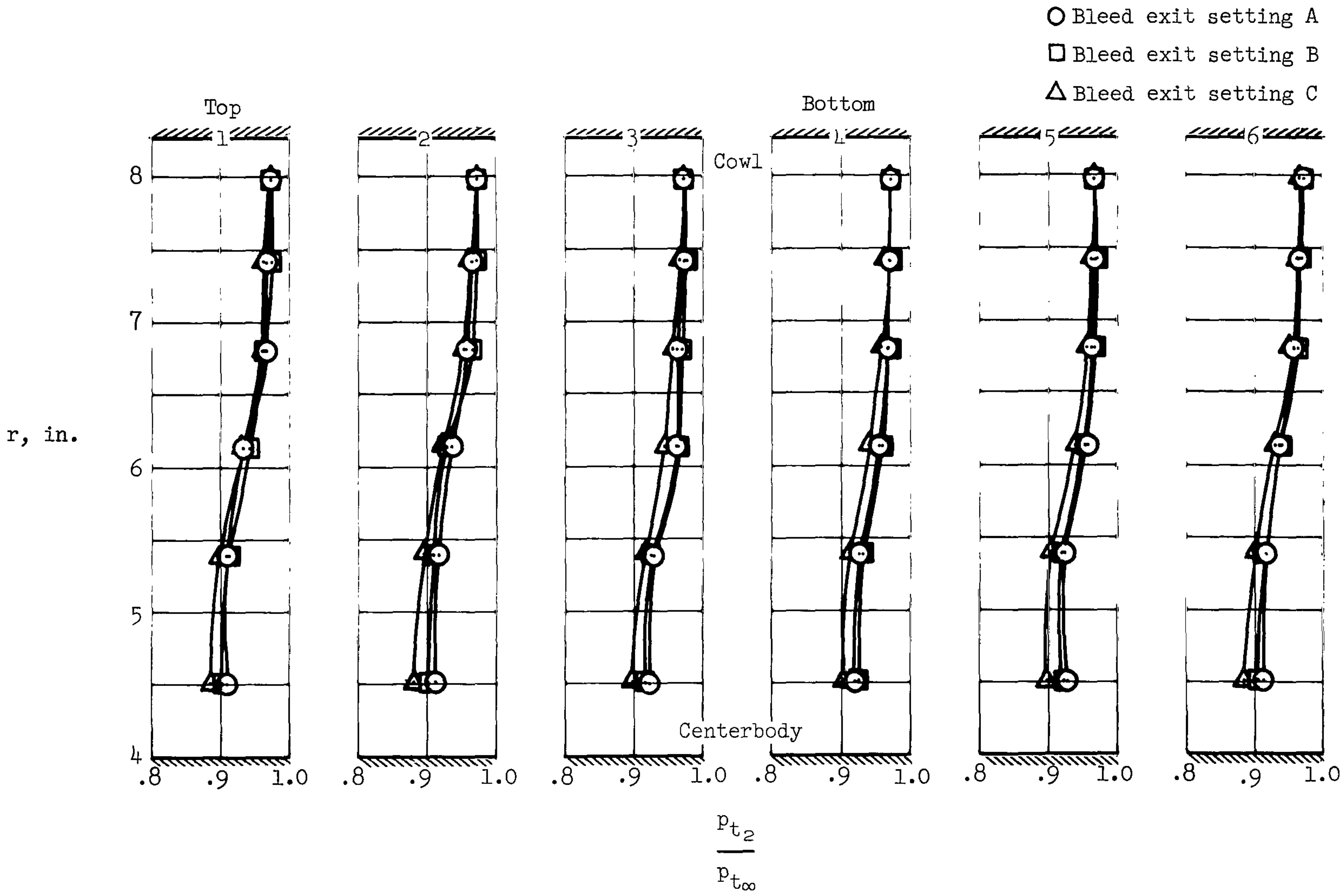

(f) $(x/R)_{lip} = 3.240$, $M_\infty = 2.25$

Figure 14.- Continued.

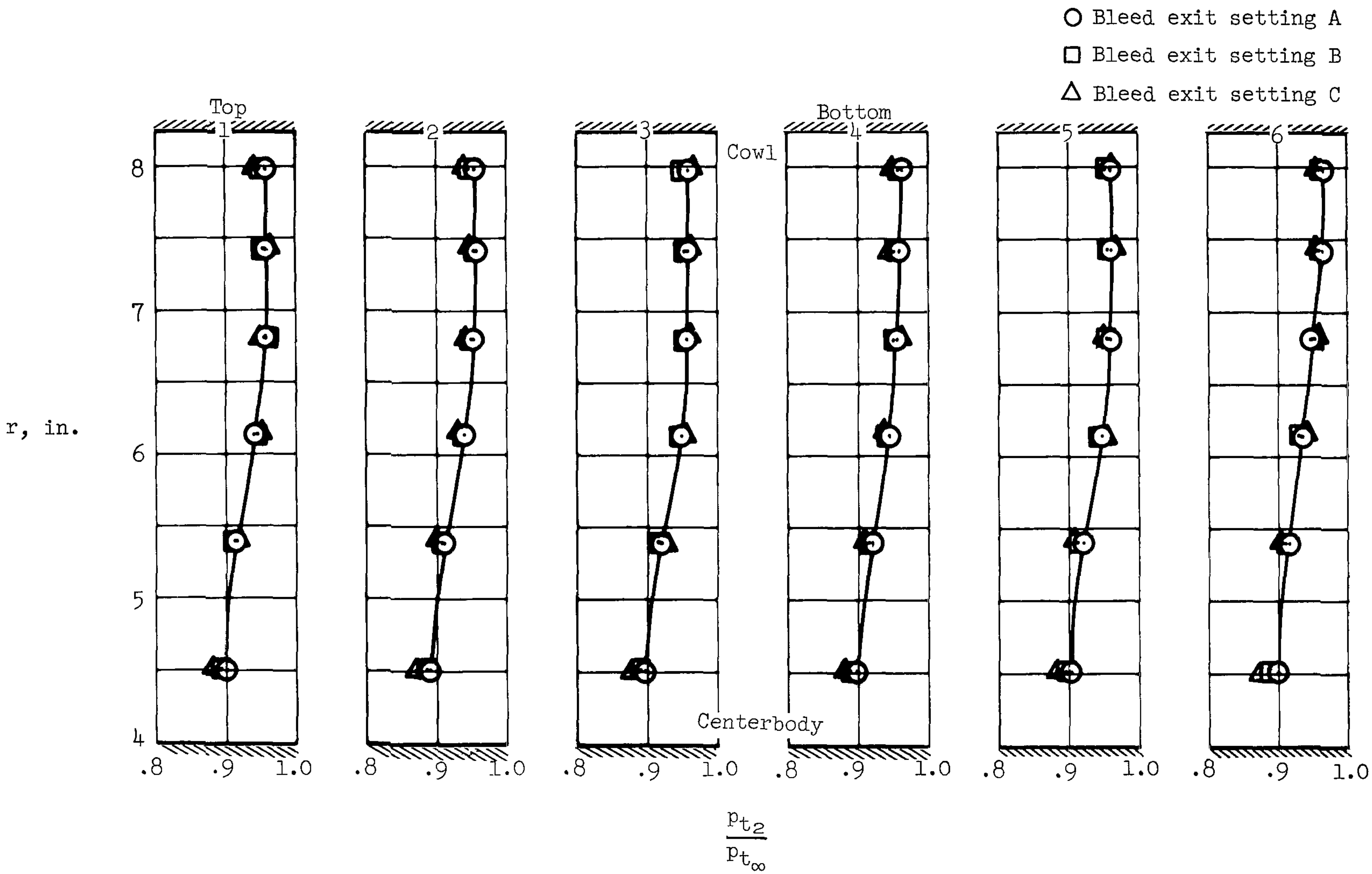

(g) $(x/R)_{lip} = 3.478$, $M_\infty = 2.00$

Figure 14.- Continued.

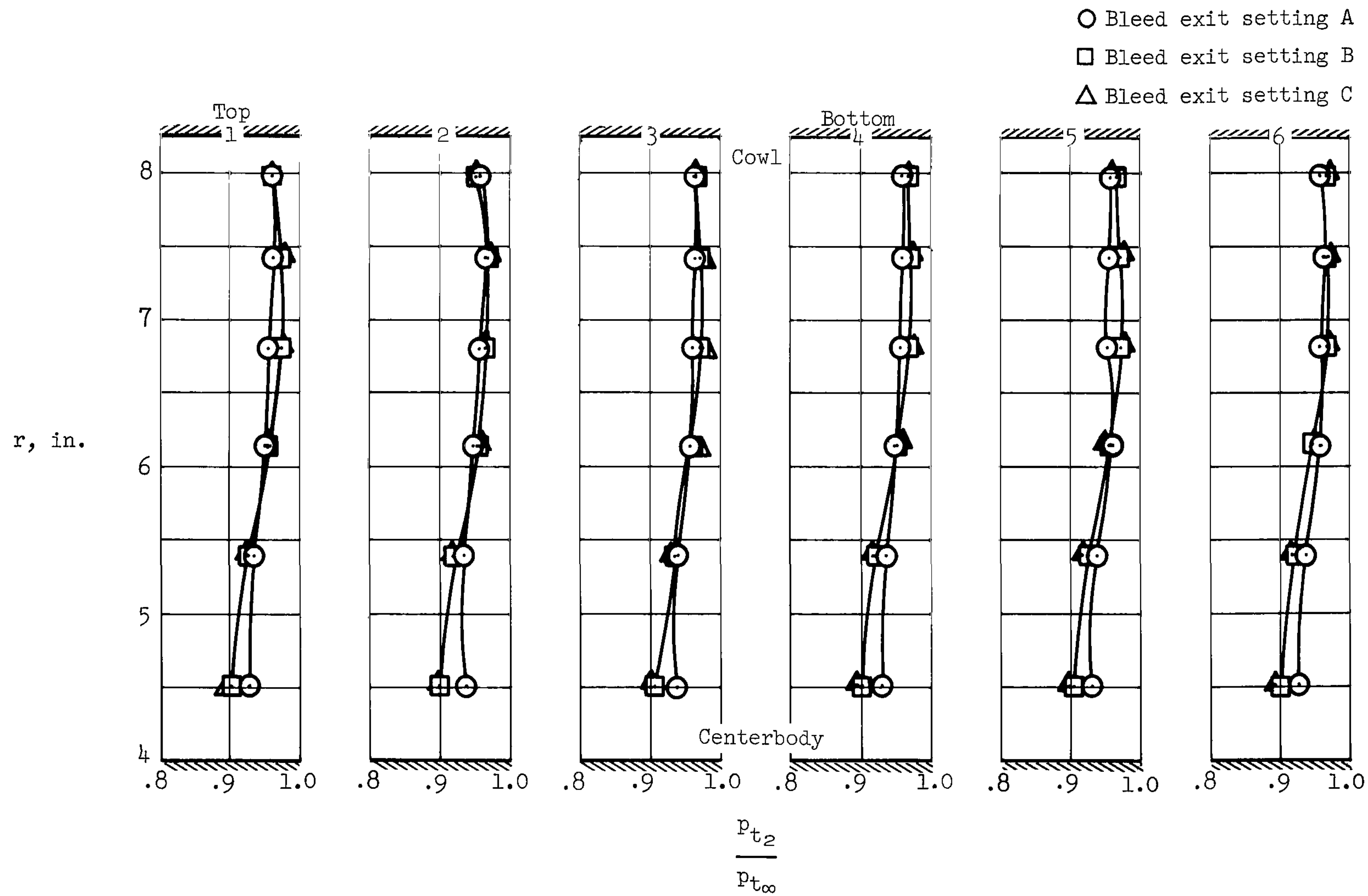

(h) $(x/R)_{lip} = 3.628$, $M_\infty = 1.75$

Figure 14.- Continued.

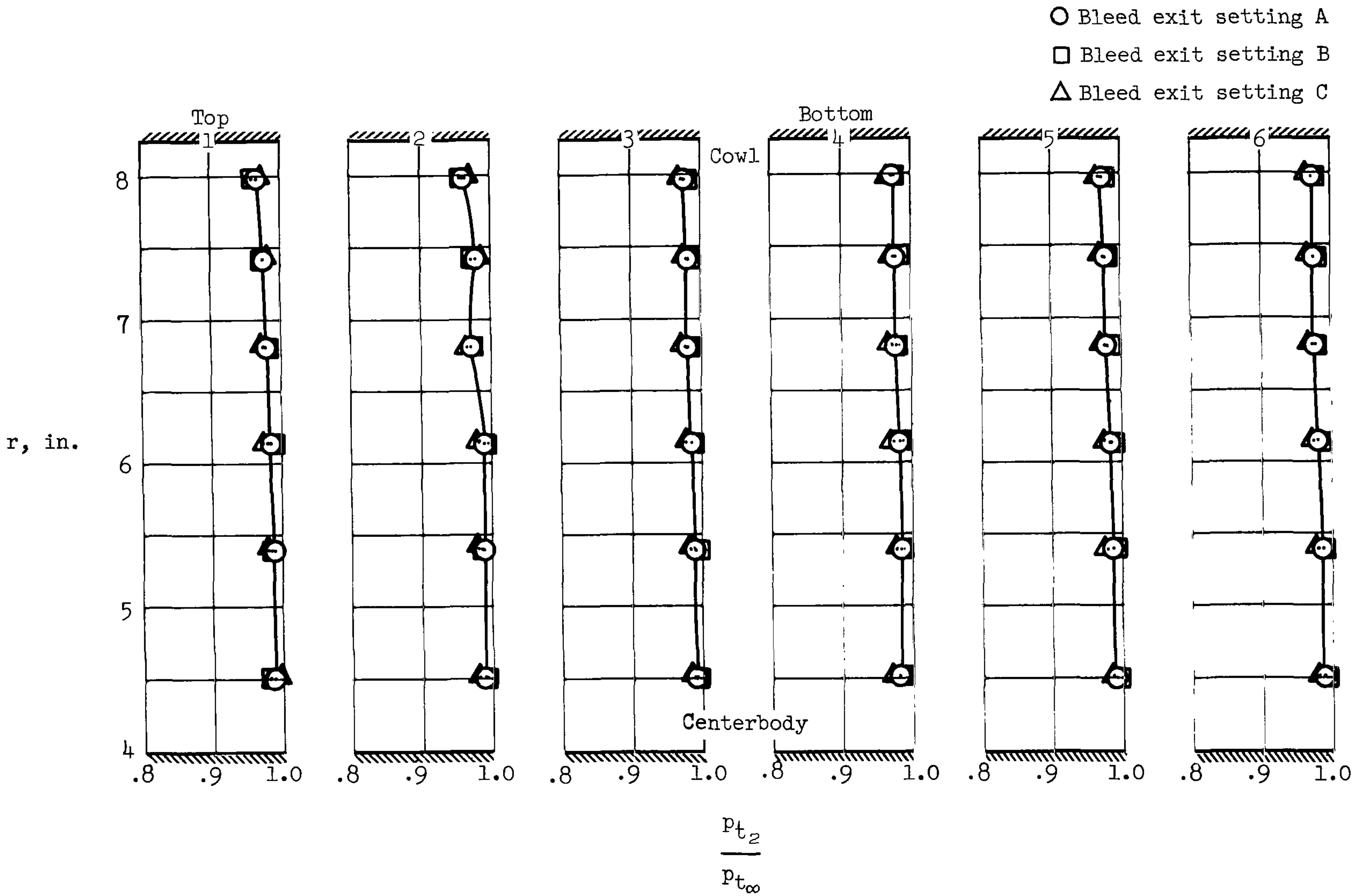

(i) $(x/R)_{lip} = 3.728$, $M_\infty = 1.55$

Figure 14.- Concluded.

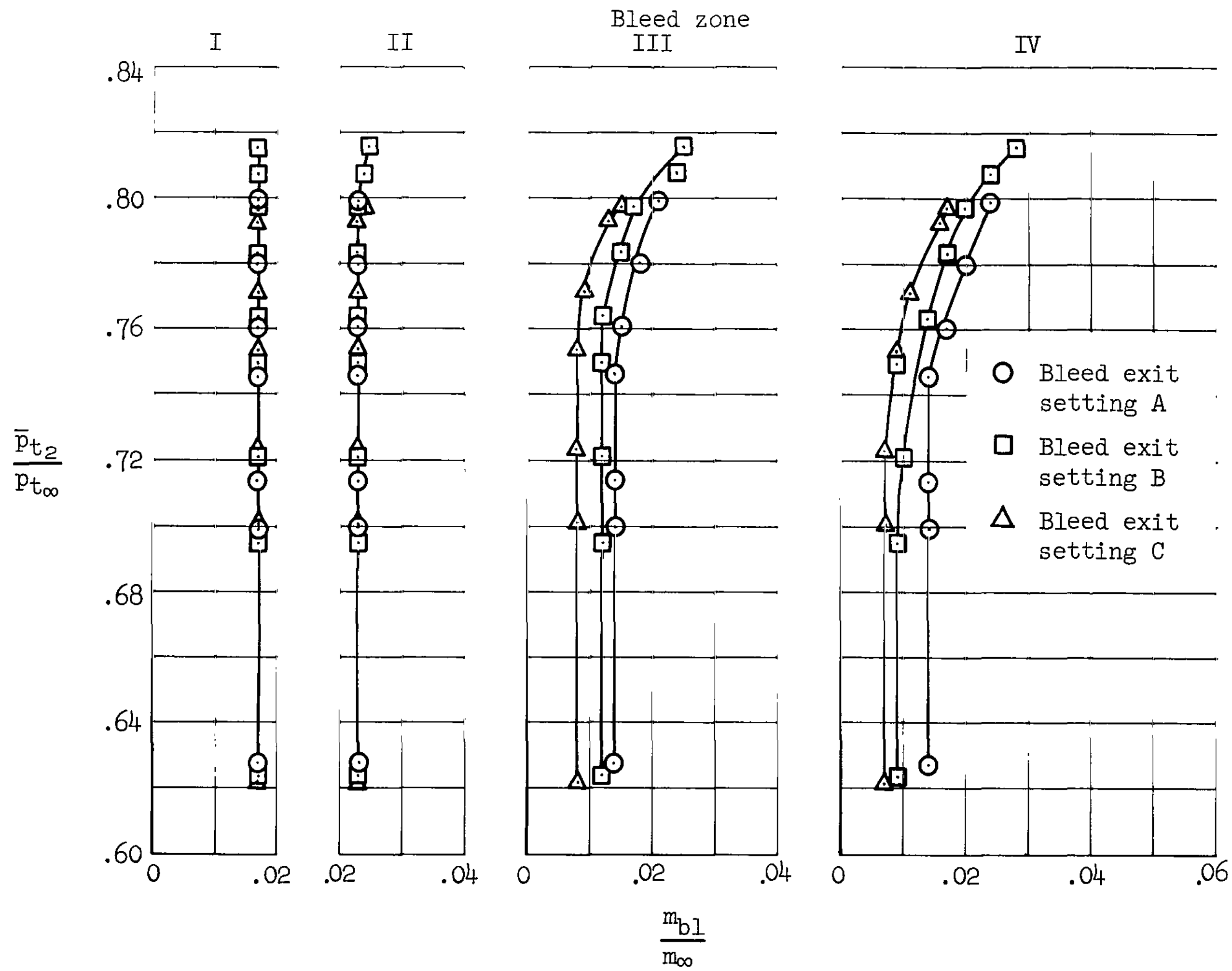

(a) $(x/R)_{lip} = 2.548$, $M_\infty = 3.20$

Figure 15.- Supercritical bleed flow, individual bleed zones; $\alpha = 0°$.

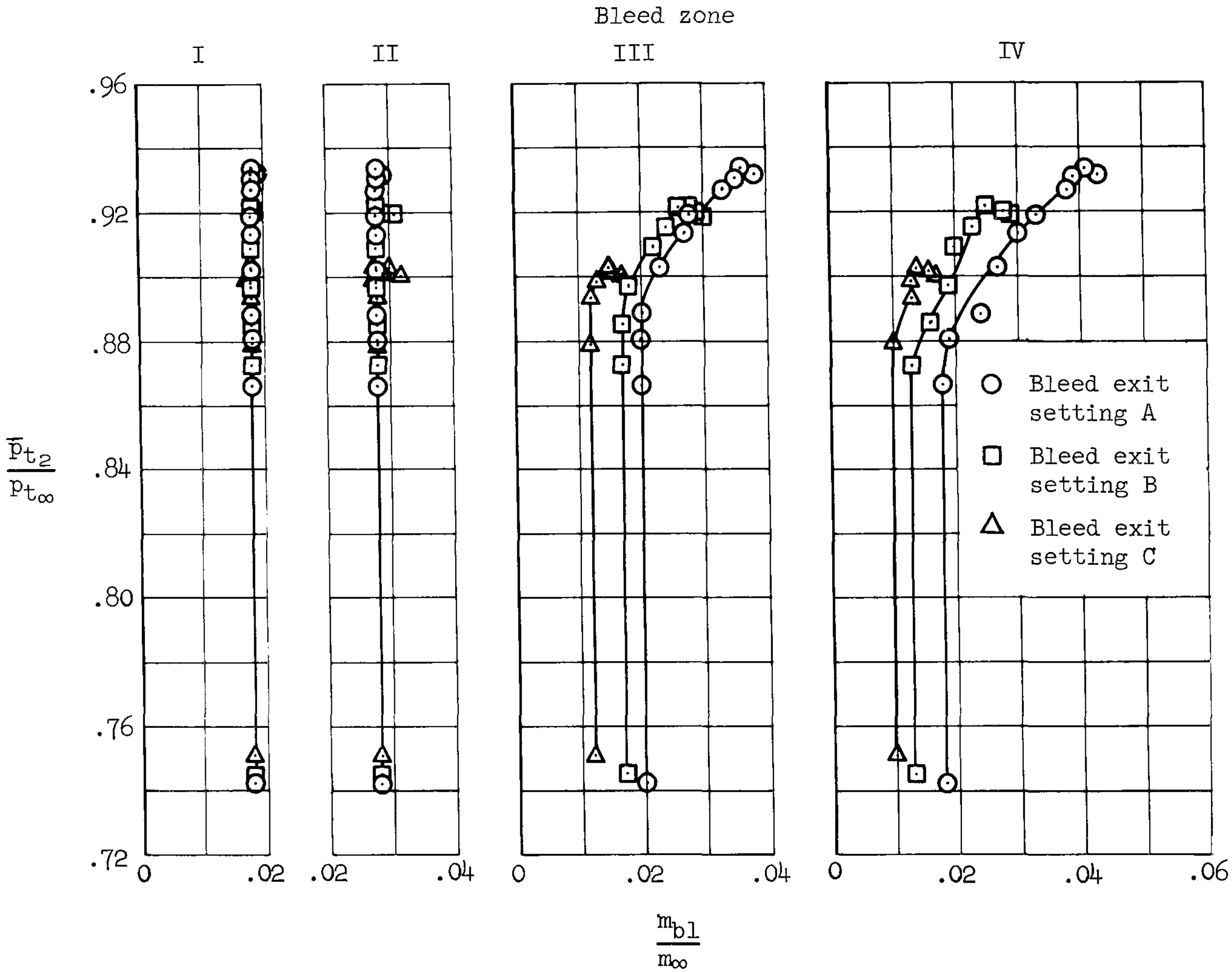

(b) $(x/R)_{lip} = 2.548$, $M_\infty = 3.00$

Figure 15.- Continued.

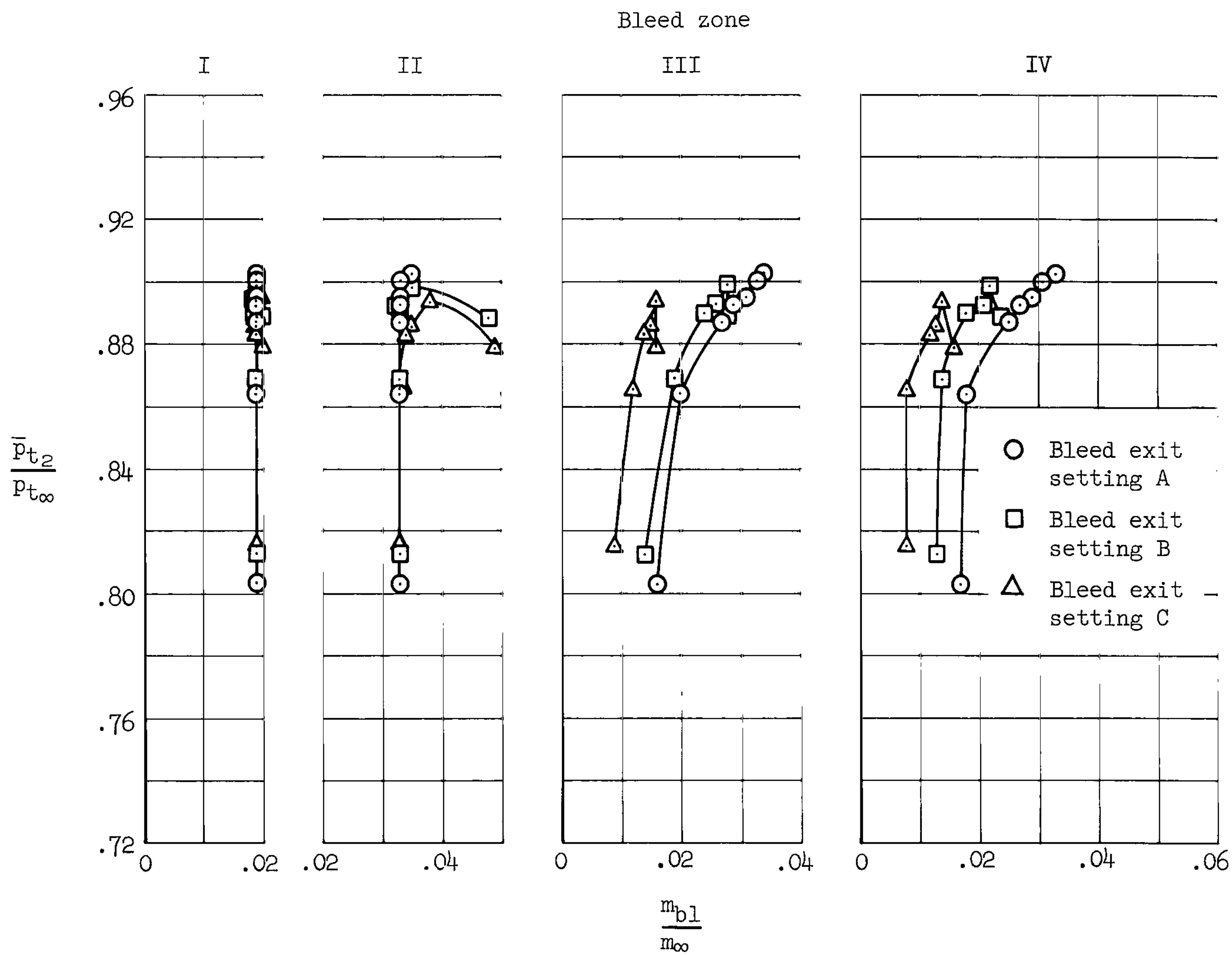

(c) $(x/R)_{lip} = 2.622$, $M_\infty = 2.90$

Figure 15.- Continued.

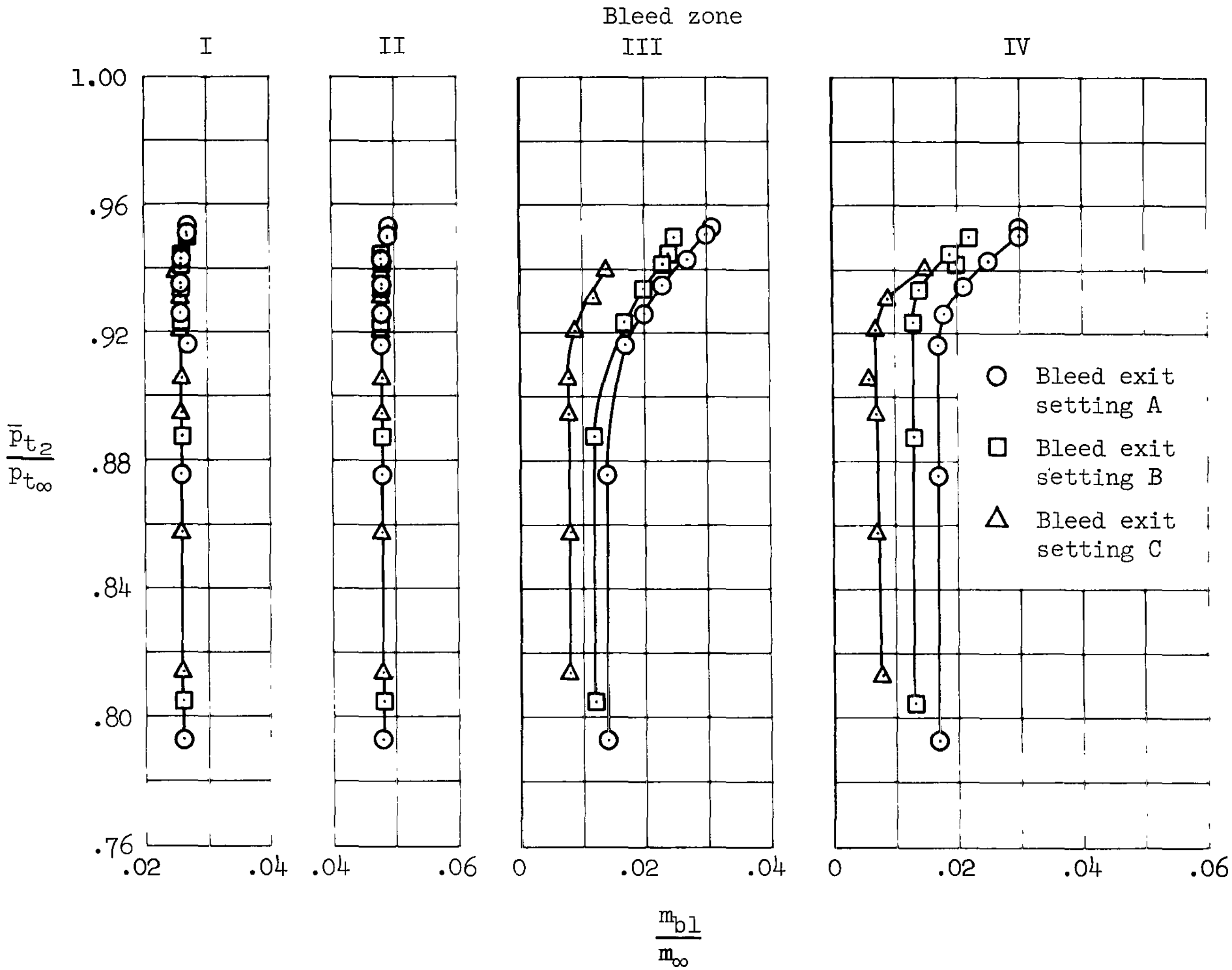

(d) $(x/R)_{lip} = 2.670$, $M_\infty = 2.75$

Figure 15.- Continued.

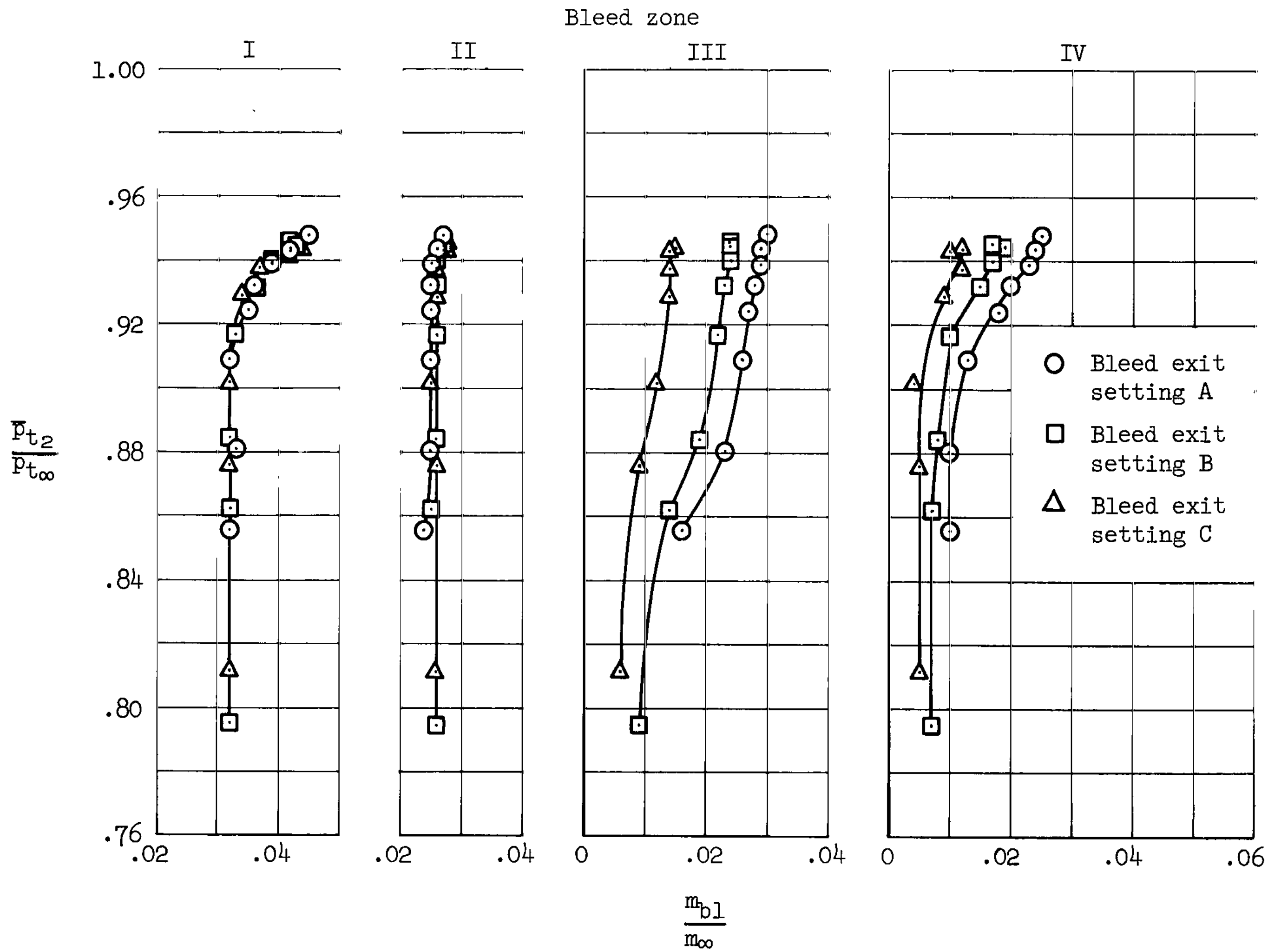

(e) $(x/R)_{lip} = 2.960$, $M_\infty = 2.50$

Figure 15.- Continued.

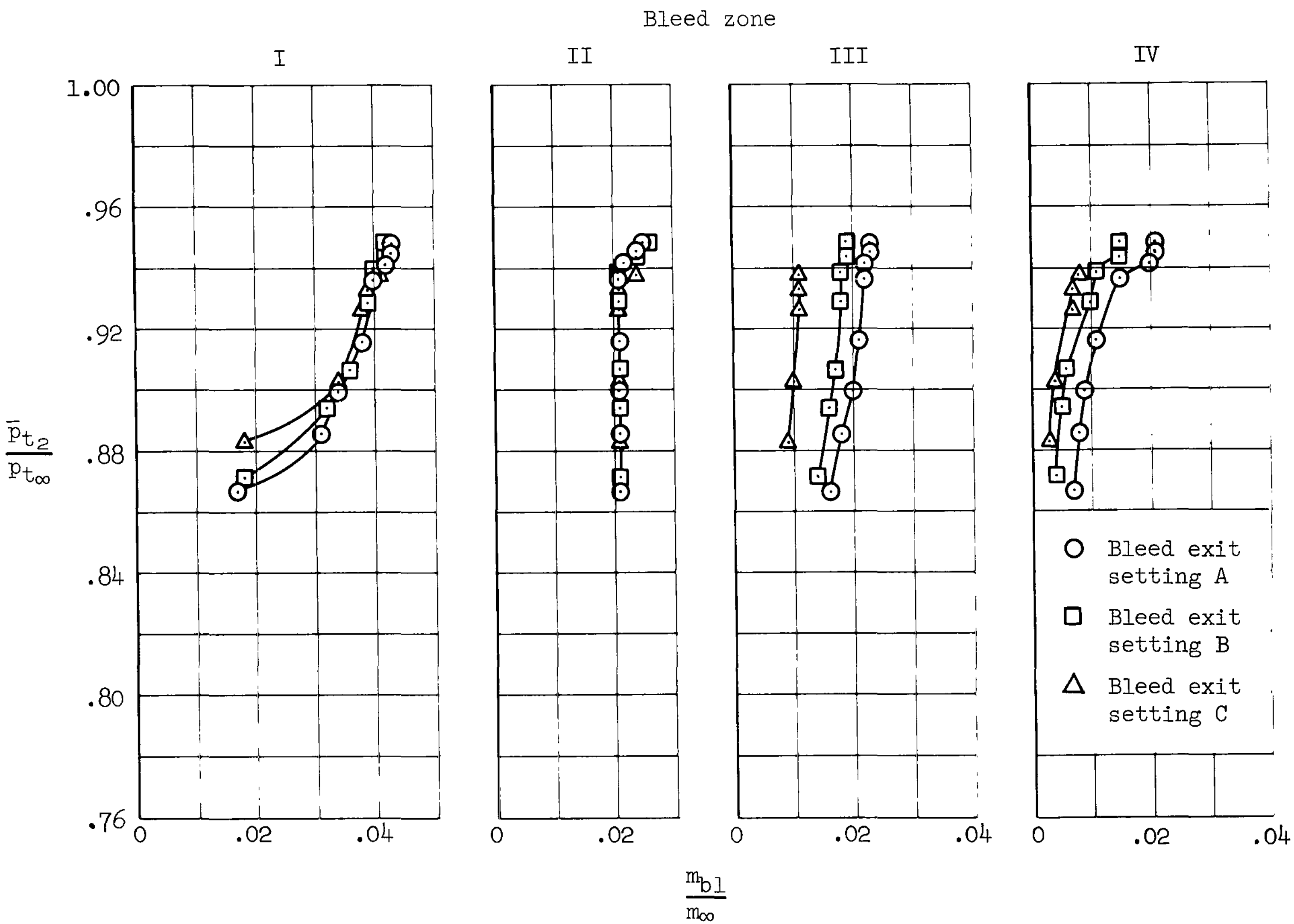

(f) $(x/R)_{lip} = 3.240$, $M_\infty = 2.25$

Figure 15.- Continued.

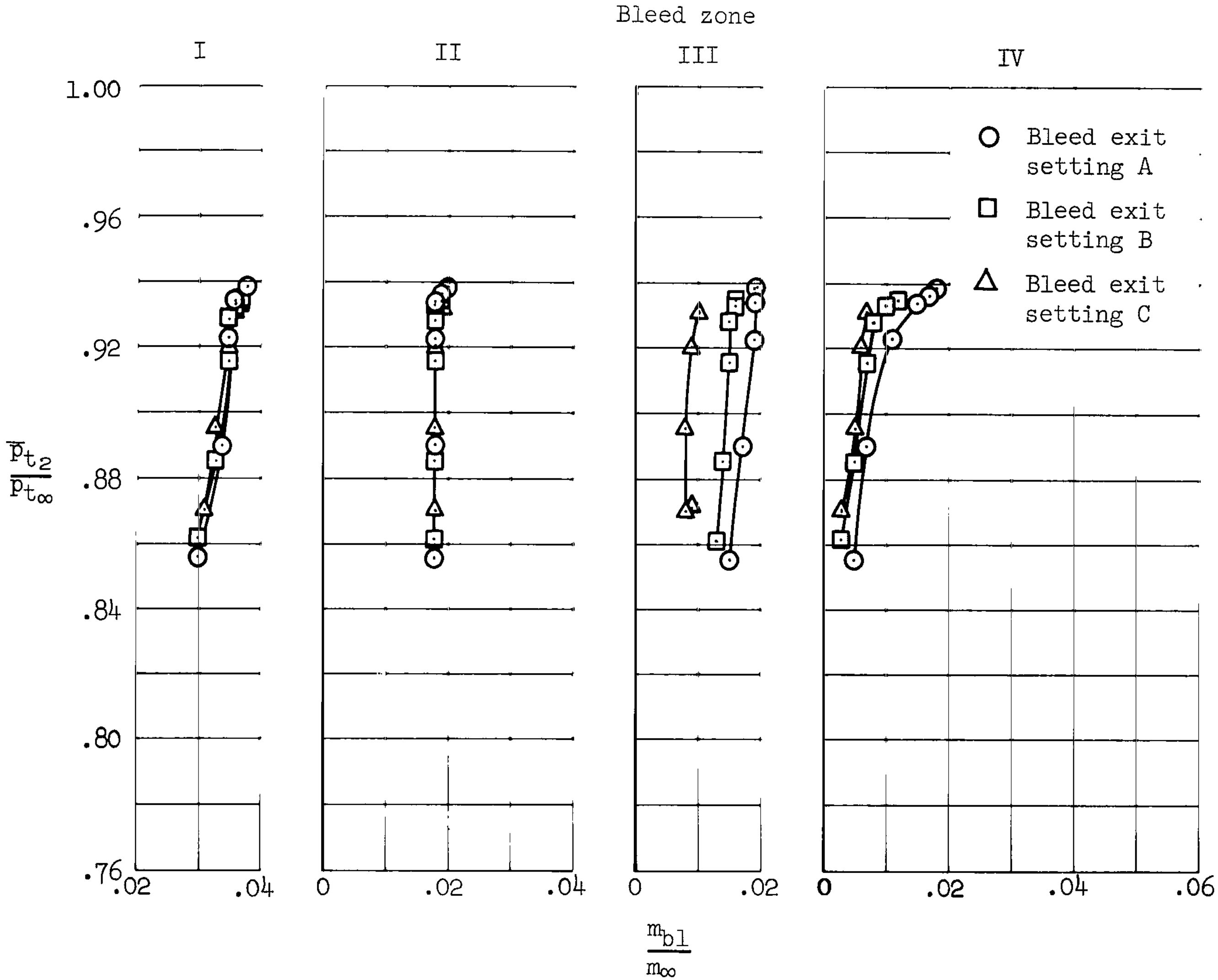

(g) $(x/R)_{lip} = 3.478$, $M_\infty = 2.00$

Figure 15.- Continued.

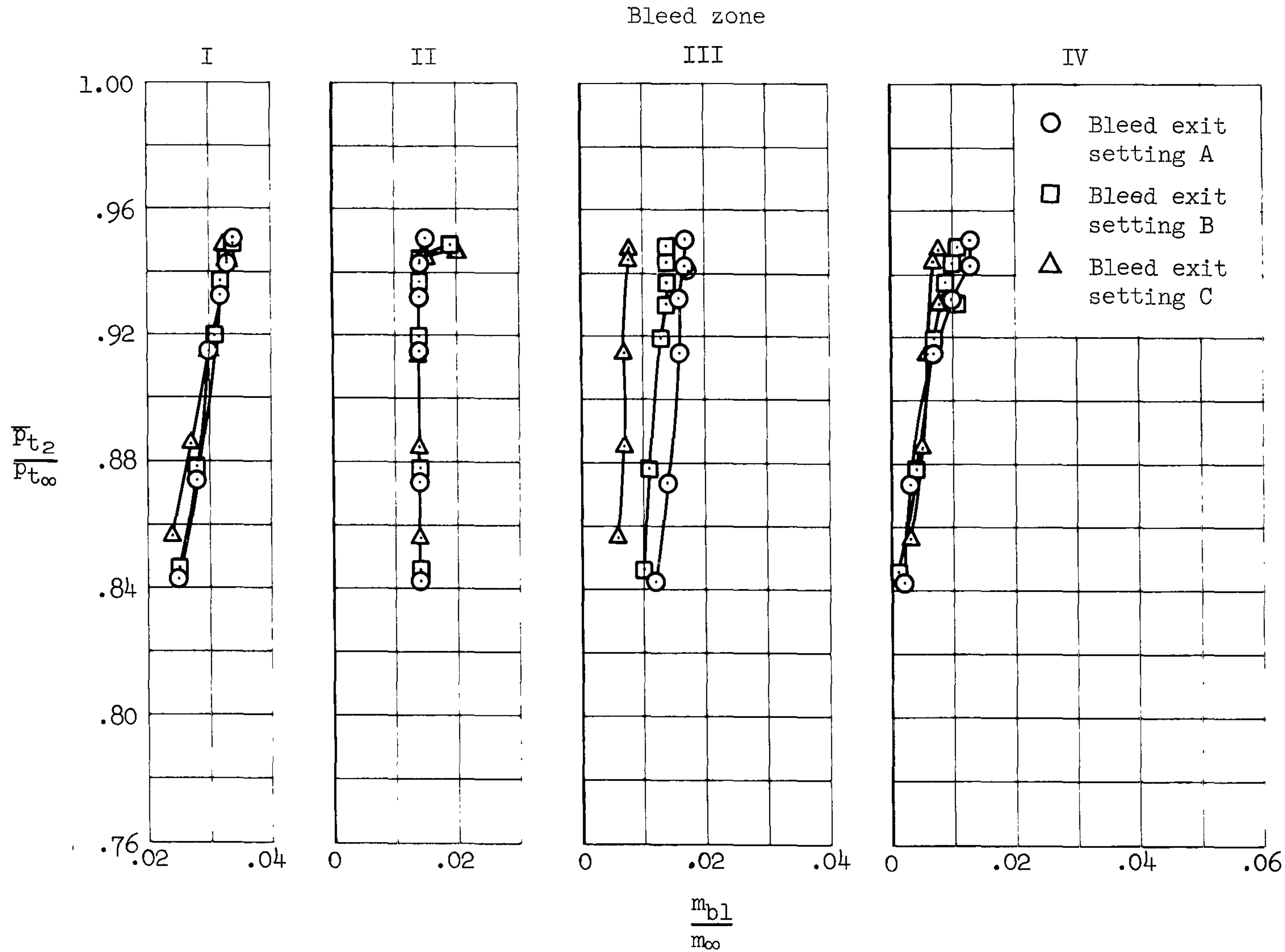

(h) $(x/R)_{lip} = 3.628$, $M_\infty = 1.75$

Figure 15.- Continued.

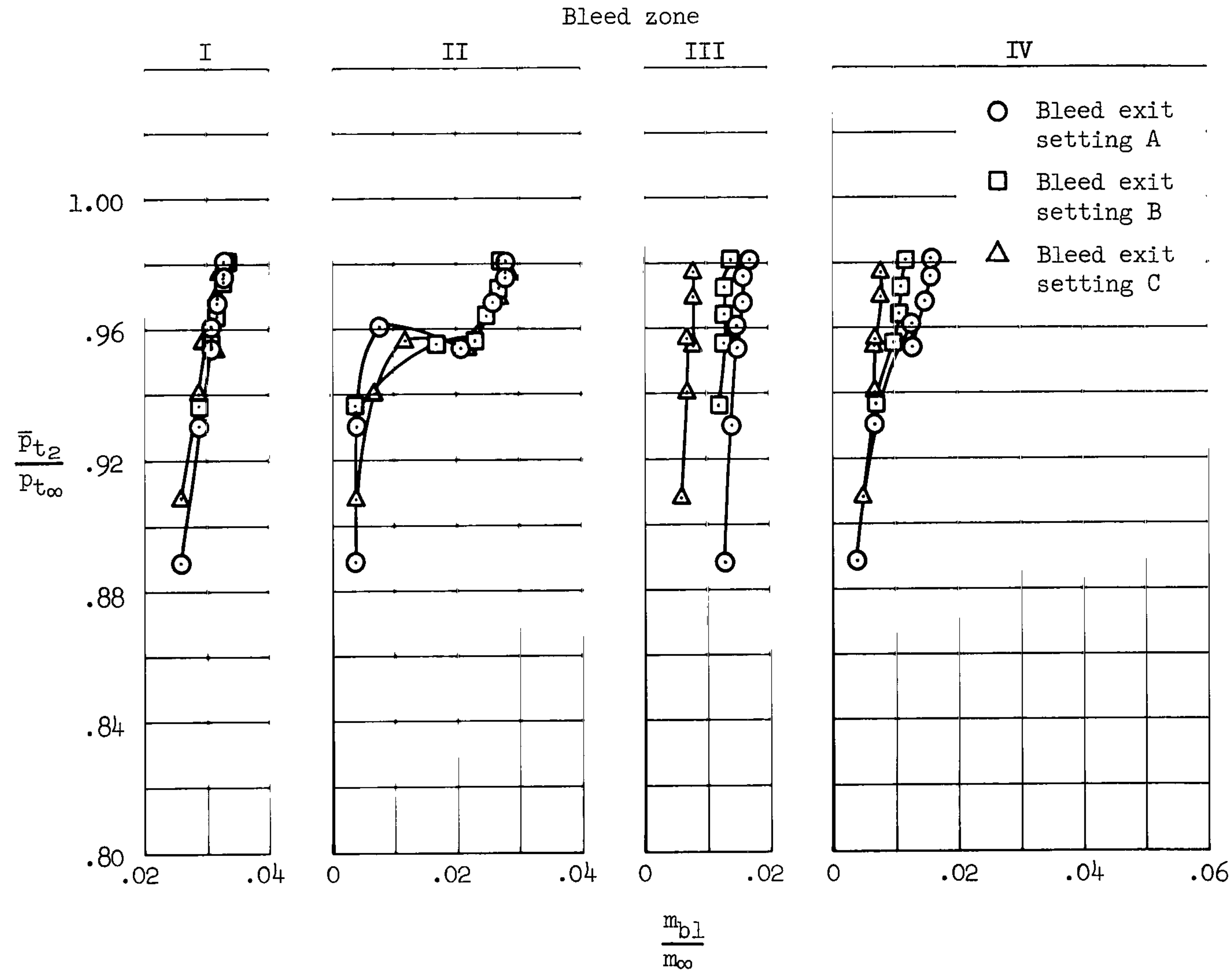

(i) $(x/R)_{lip} = 3.728$, $M_\infty = 1.55$

Figure 15.- Concluded.

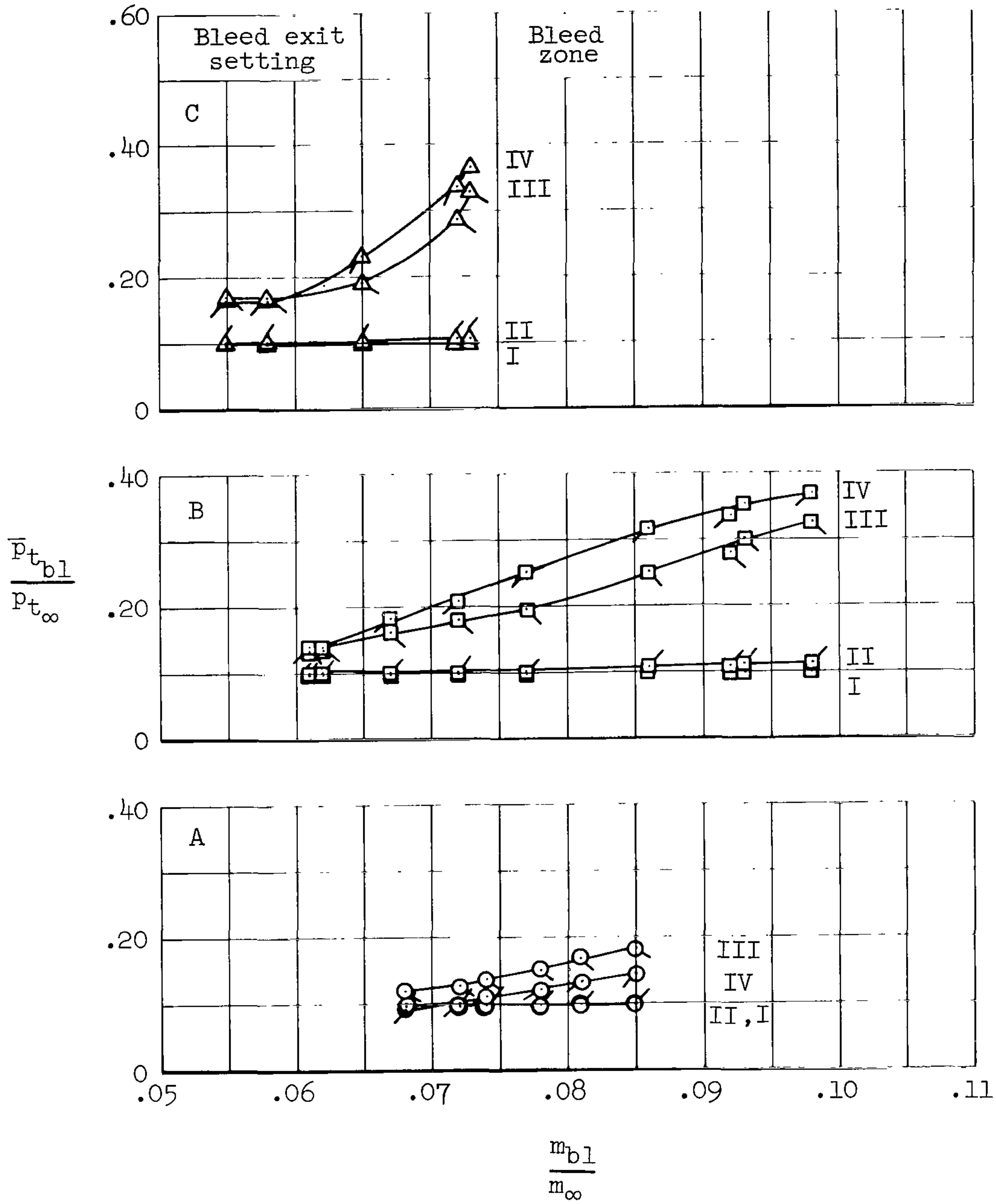

(a) $(x/R)_{lip} = 2.548$, $M_\infty = 3.20$

Figure 16.- Bleed plenum chamber pressure recoveries; $\alpha = 0°$.

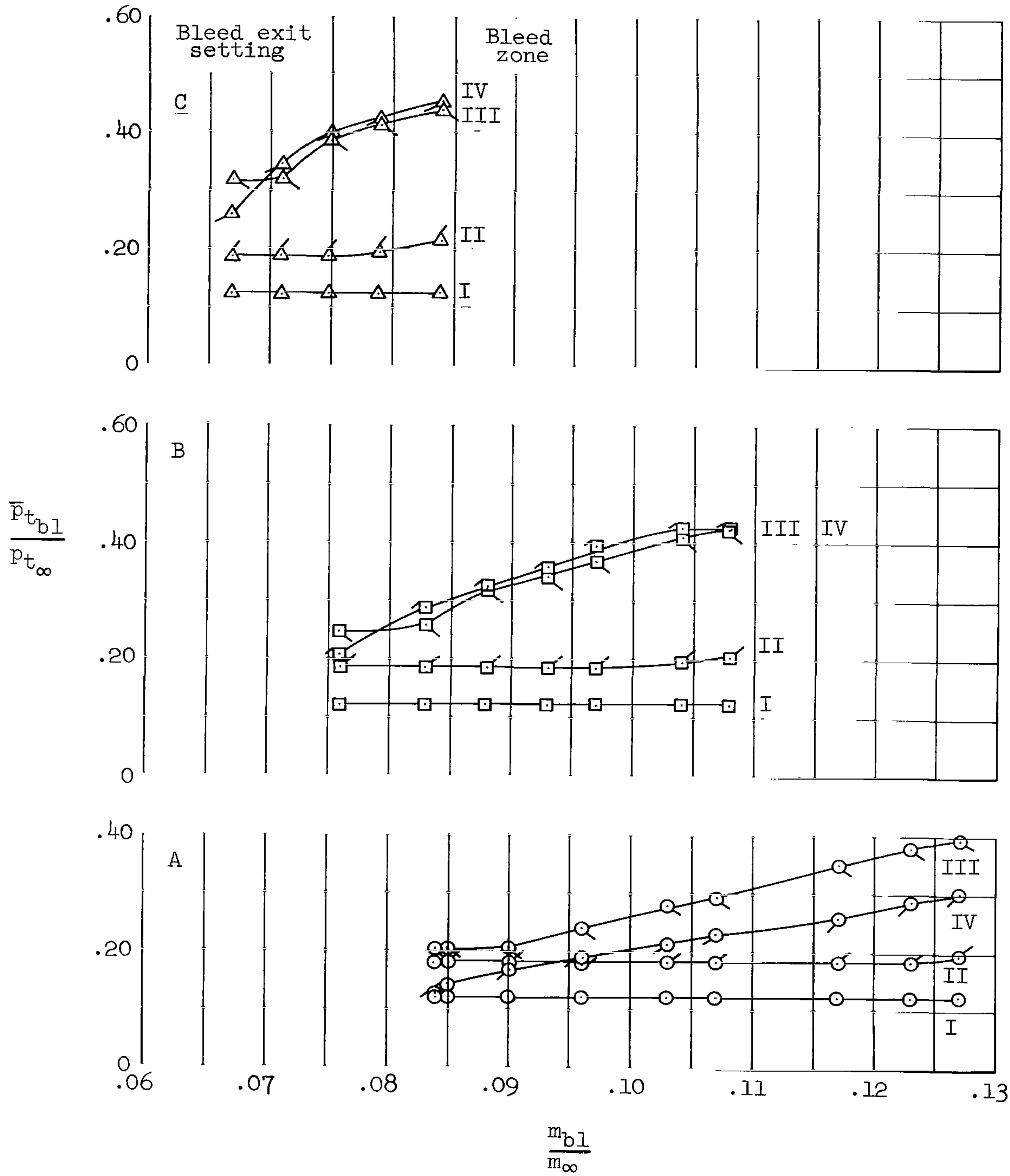

(b) $(x/R)_{lip} = 2.548$, $M_\infty = 3.00$

Figure 16.- Continued.

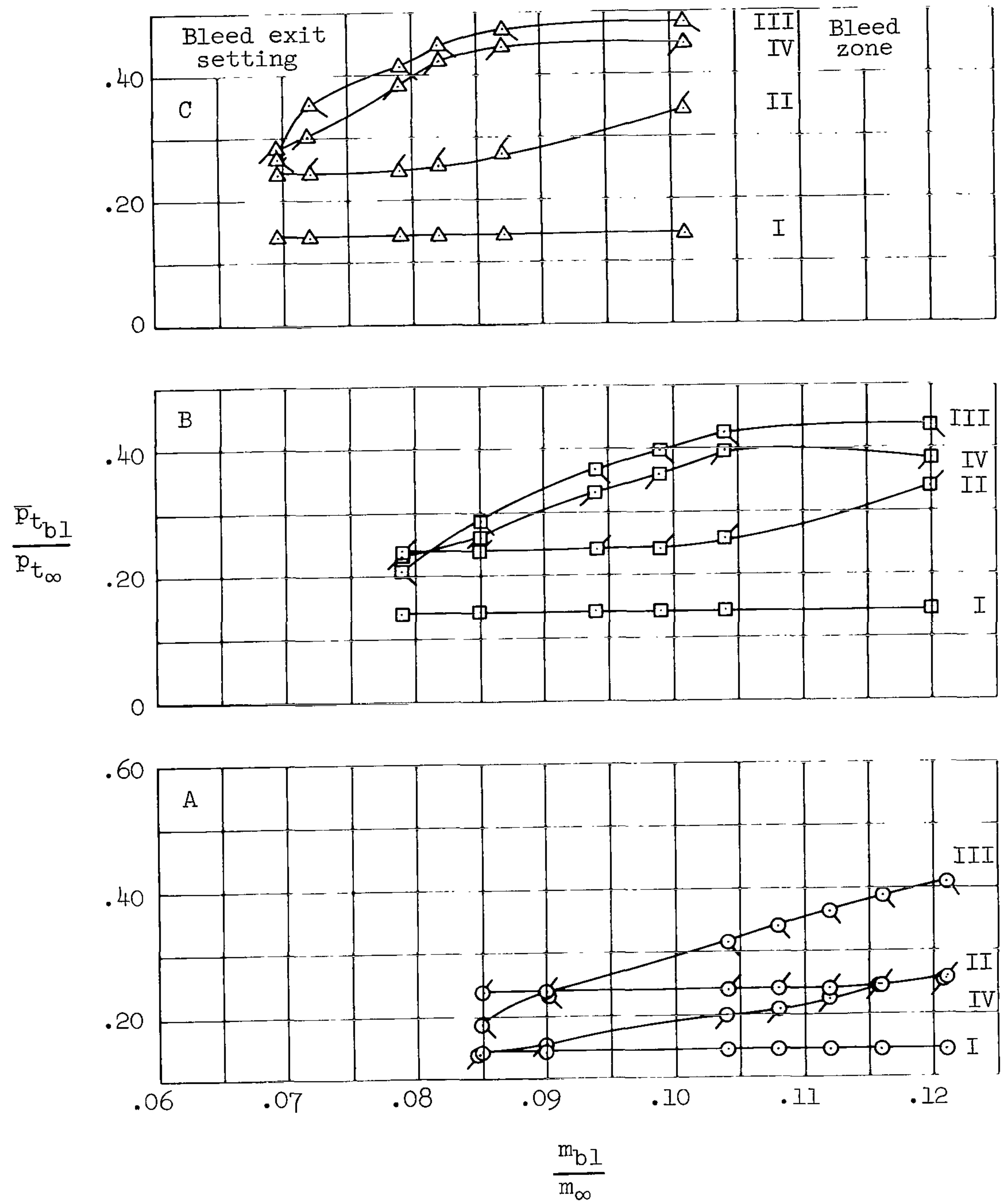

(c) $(x/R)_{lip} = 2.622$, $M_\infty = 2.90$

Figure 16.- Continued.

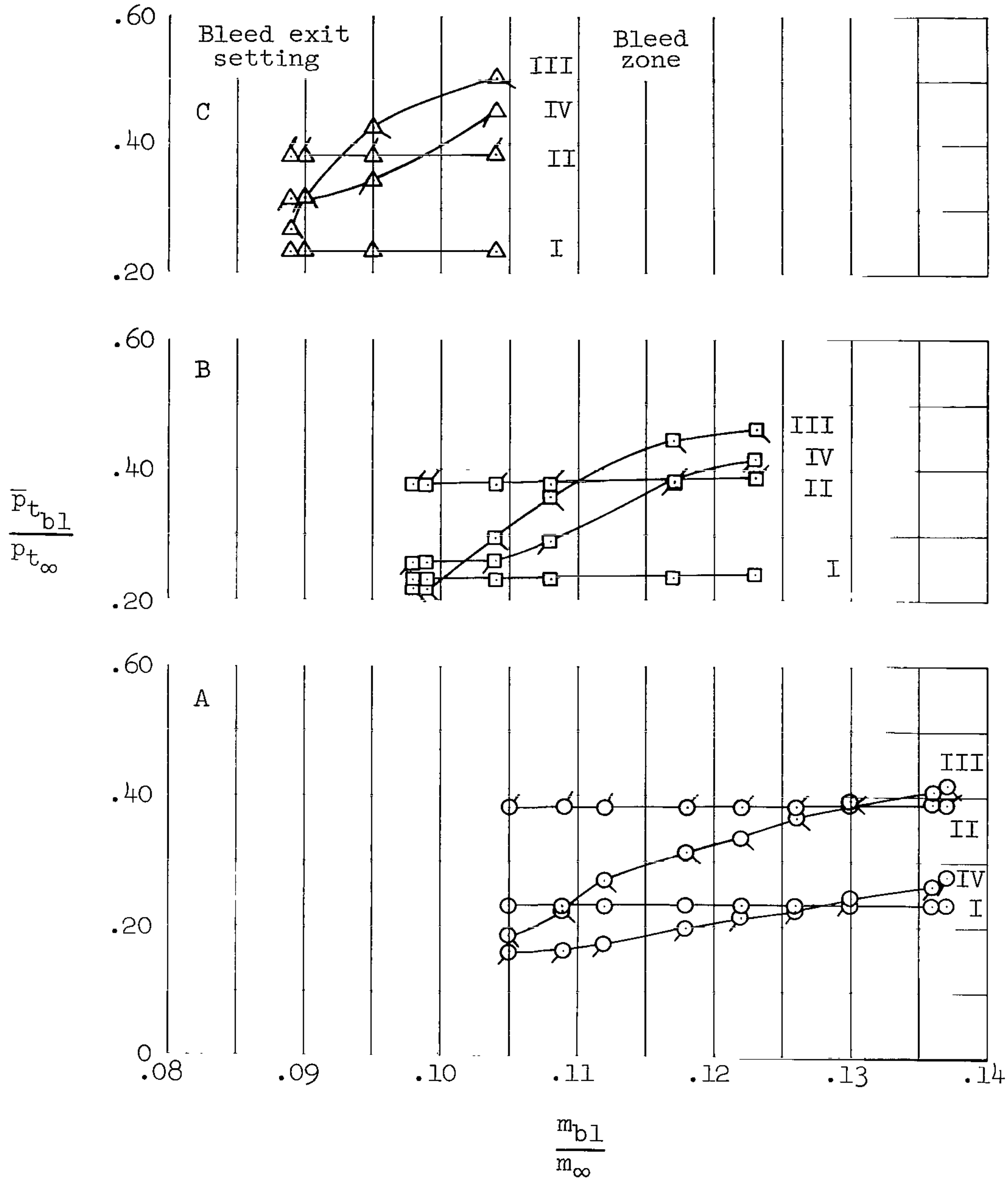

(d) $(x/R)_{lip} = 2.670$, $M_\infty = 2.75$

Figure 16.- Continued.

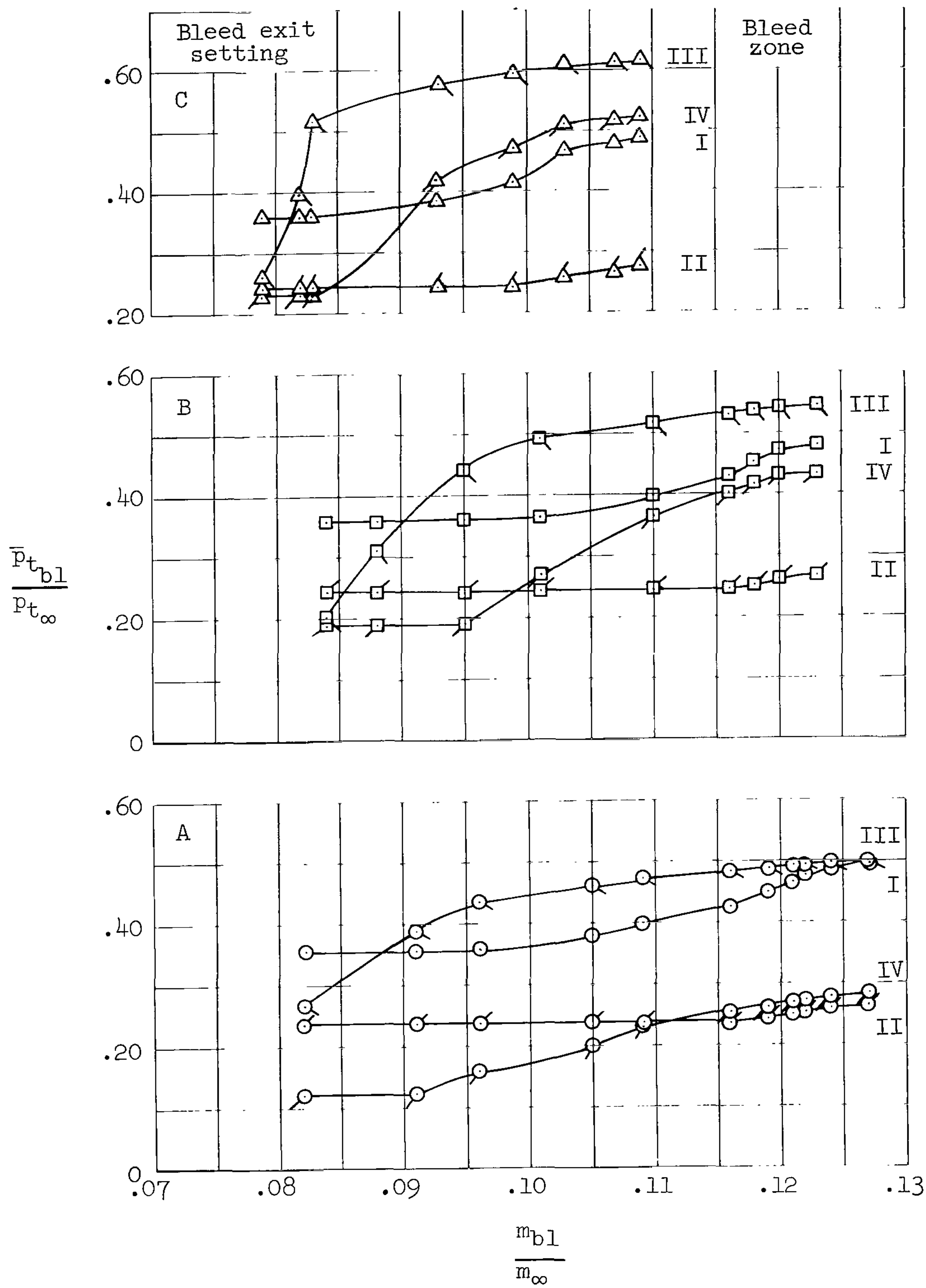

(e) $(x/R)_{lip} = 2.960$, $M_\infty = 2.50$

Figure 16.- Continued.

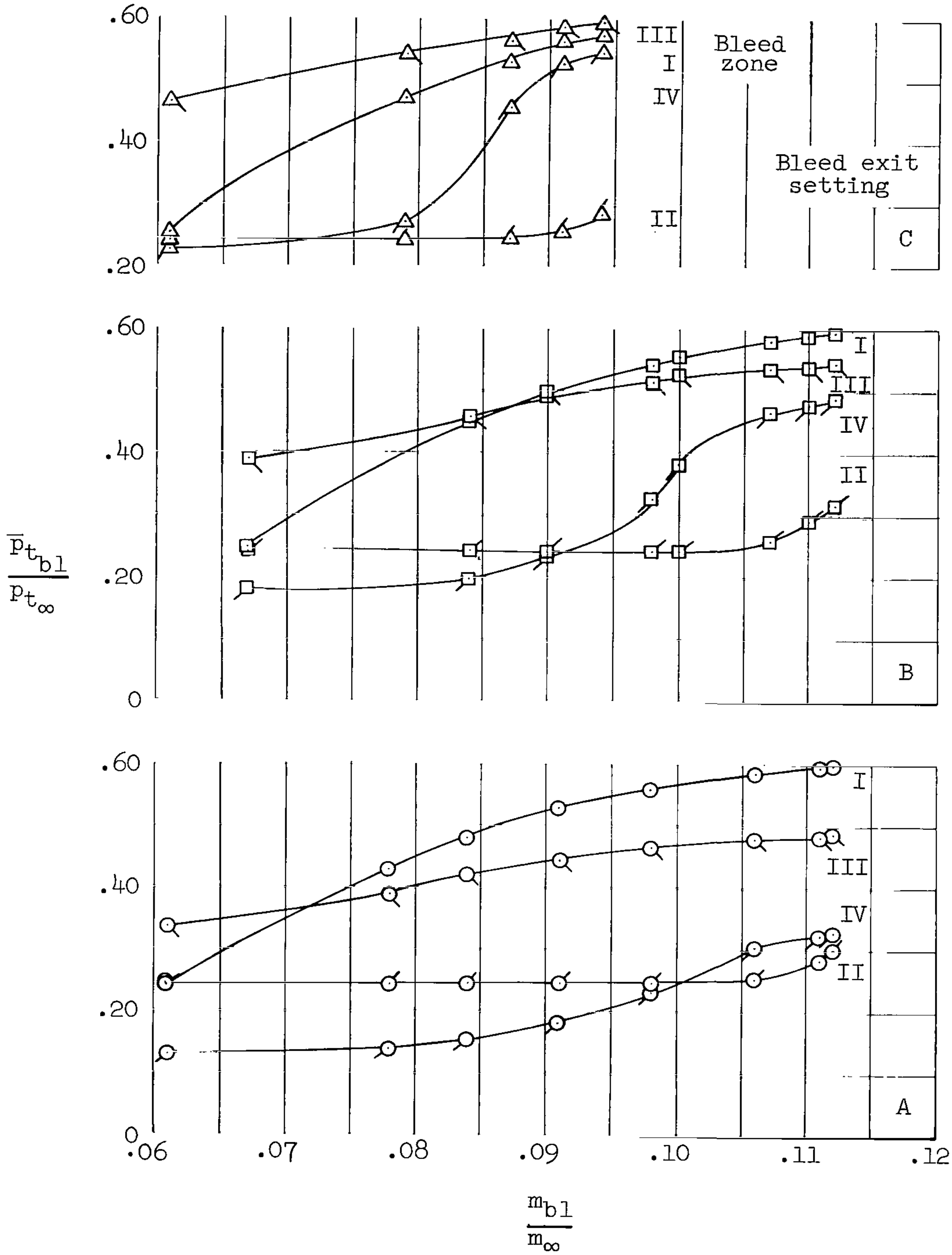

(f) $(x/R)_{lip} = 3.240$, $M_\infty = 2.25$

Figure 16.- Continued.

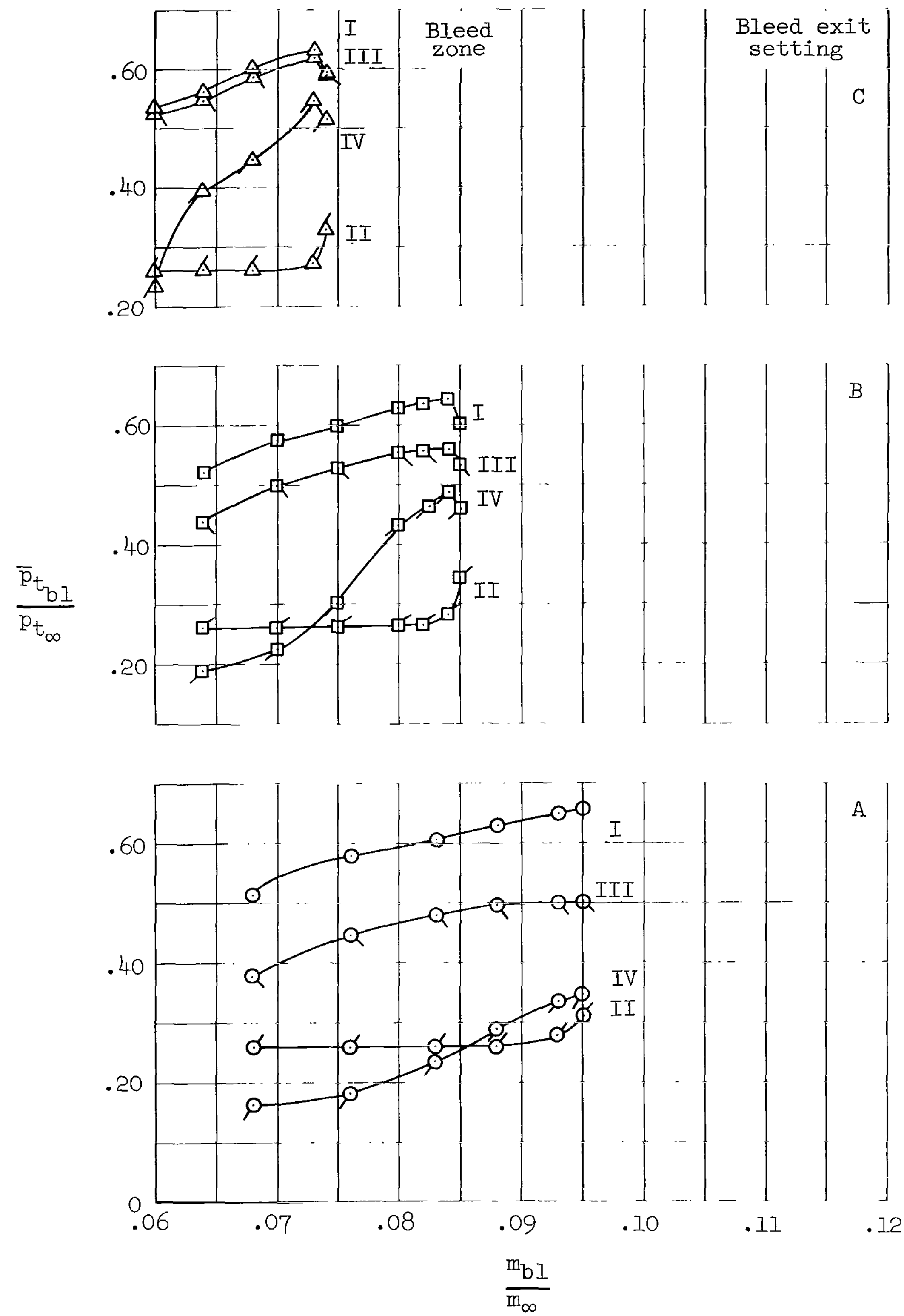

(g) $(x/R)_{lip} = 3.478$, $M_\infty = 2.00$

Figure 16.- Continued.

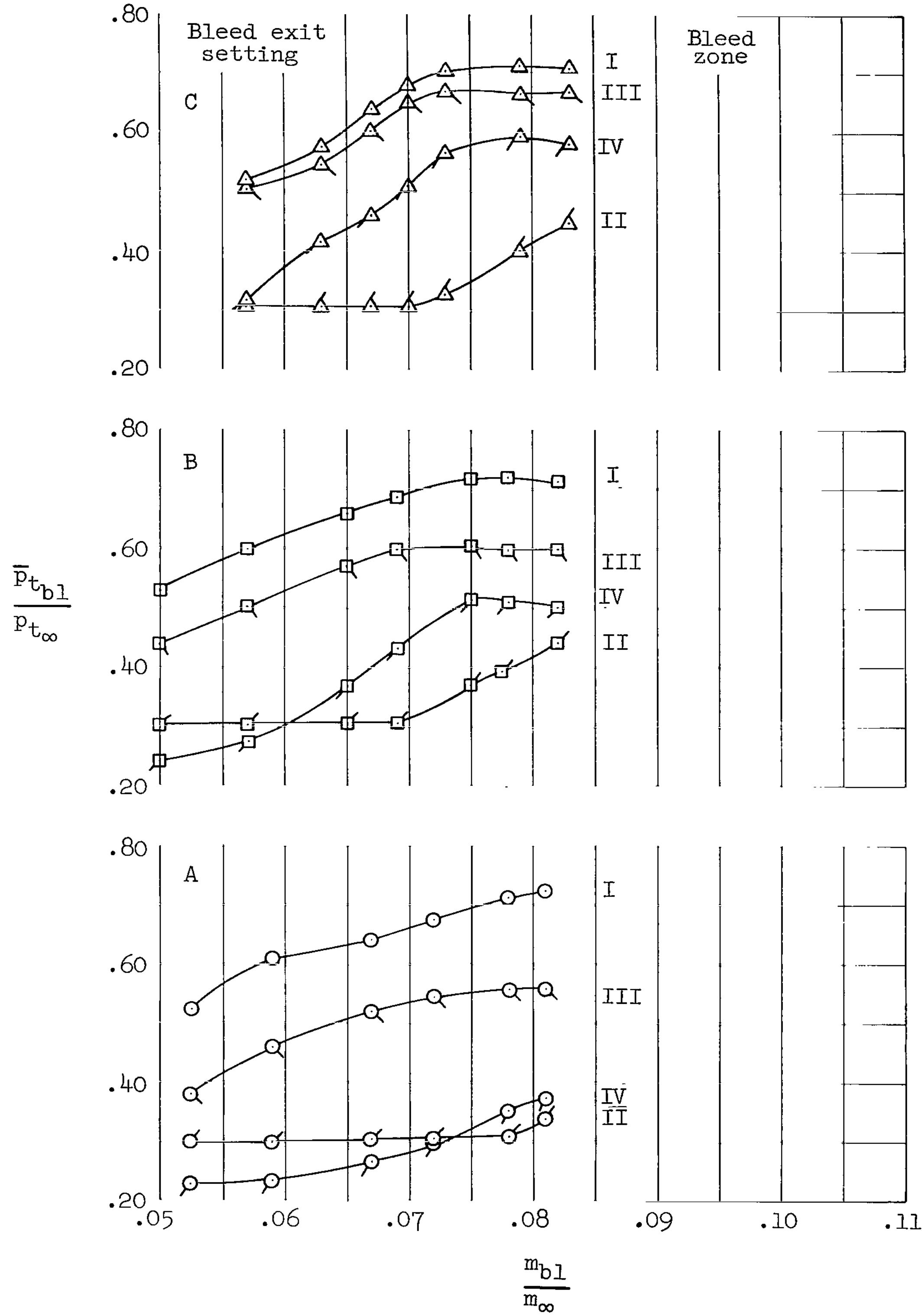

(h) $(x/R)_{lip} = 3.628$, $M_\infty = 1.75$

Figure 16.- Continued.

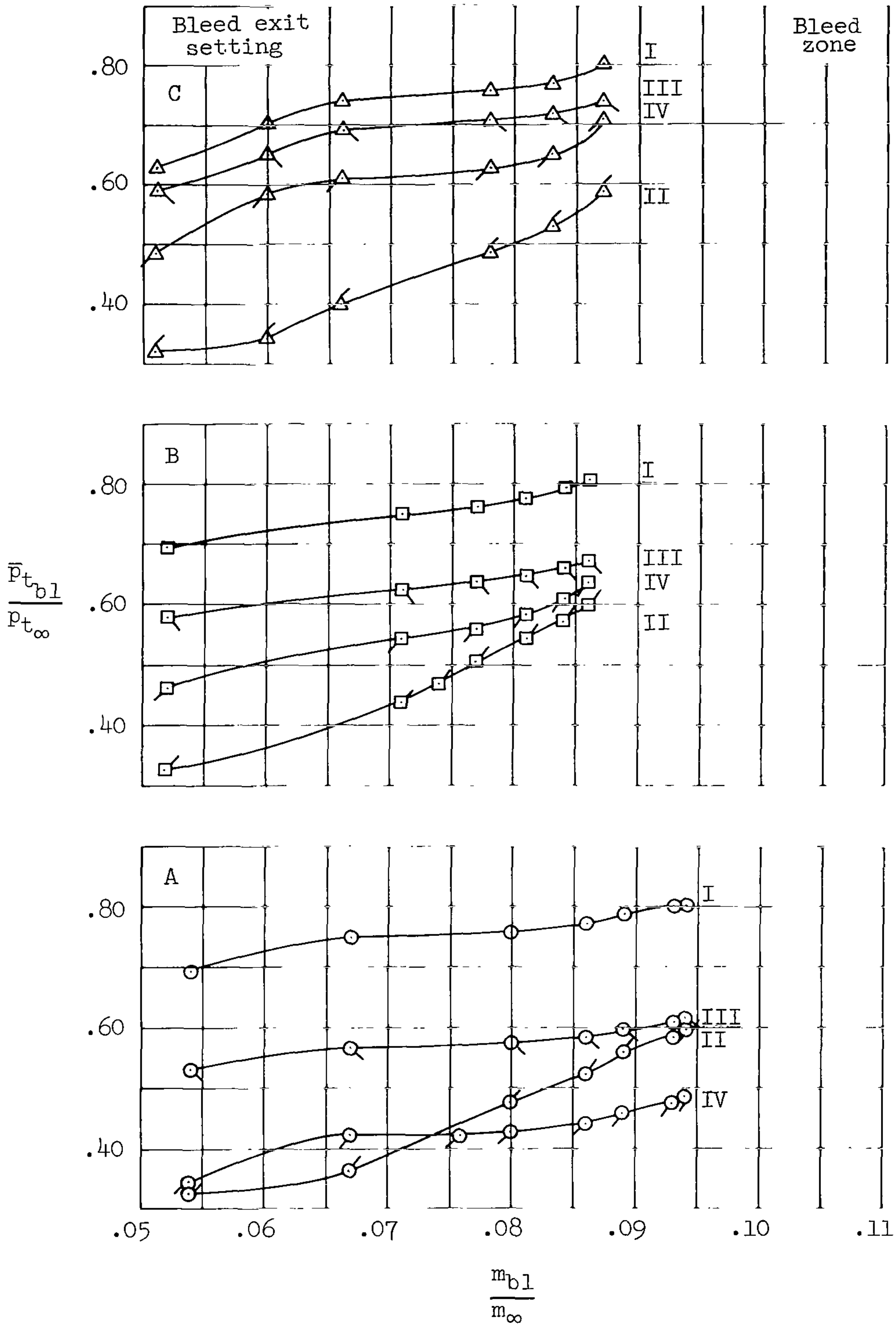

(i) $(x/R)_{lip} = 3.728$, $M_\infty = 1.55$

Figure 16.- Concluded.

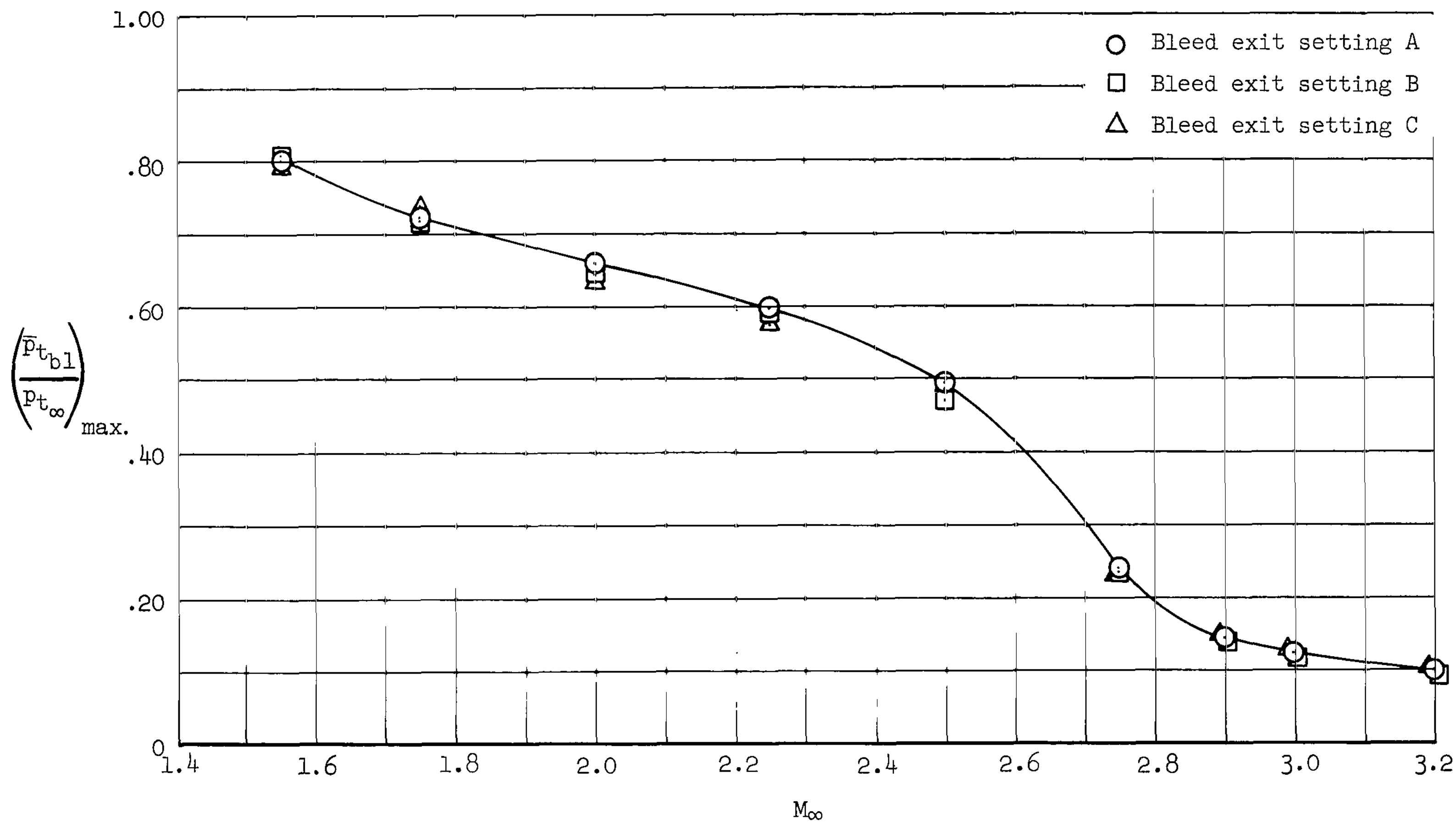

(a) Bleed zone I

Figure 17.- Maximum bleed plenum chamber pressure recoveries; $\alpha = 0°$.

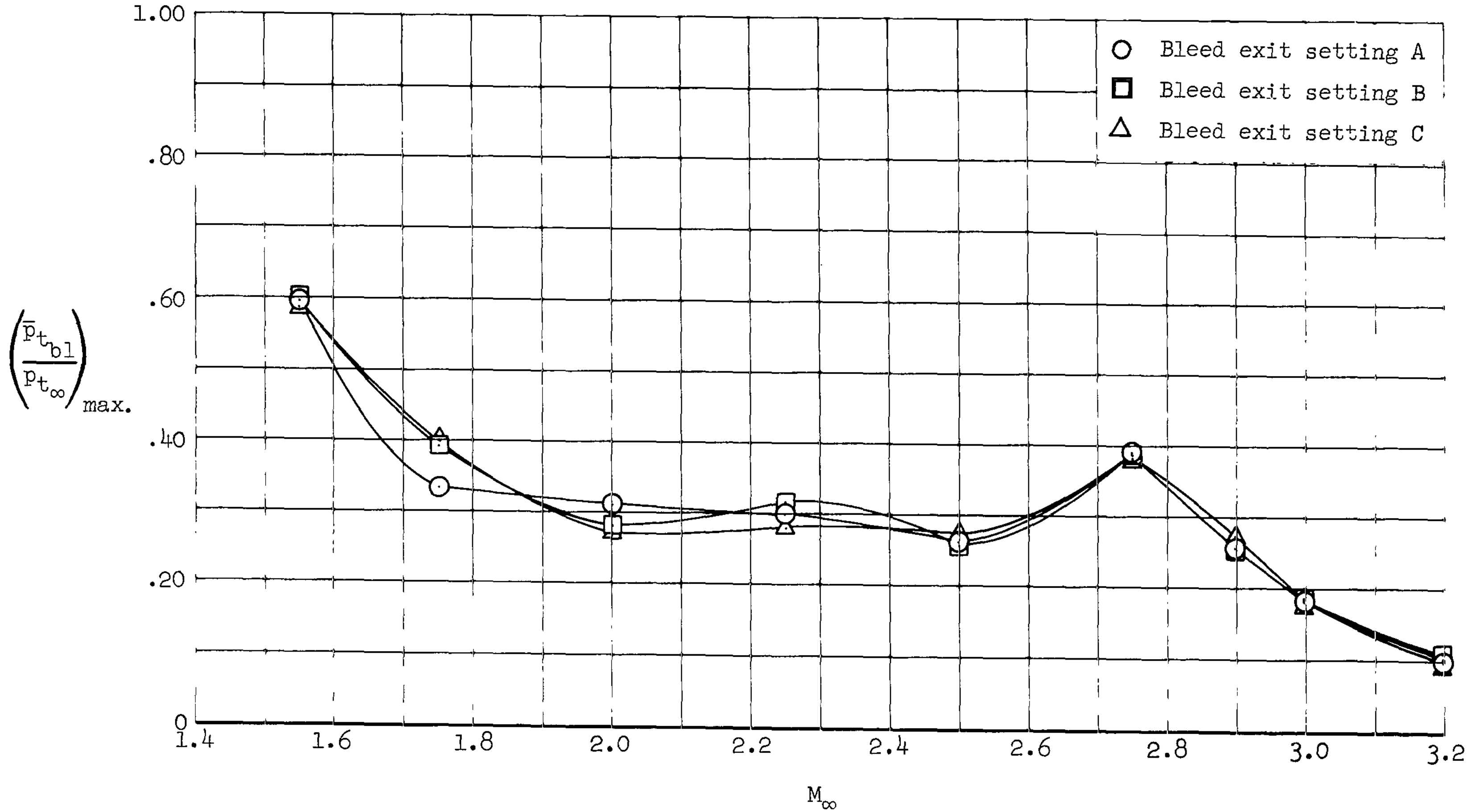

(b) Bleed zone II

Figure 17.- Continued.

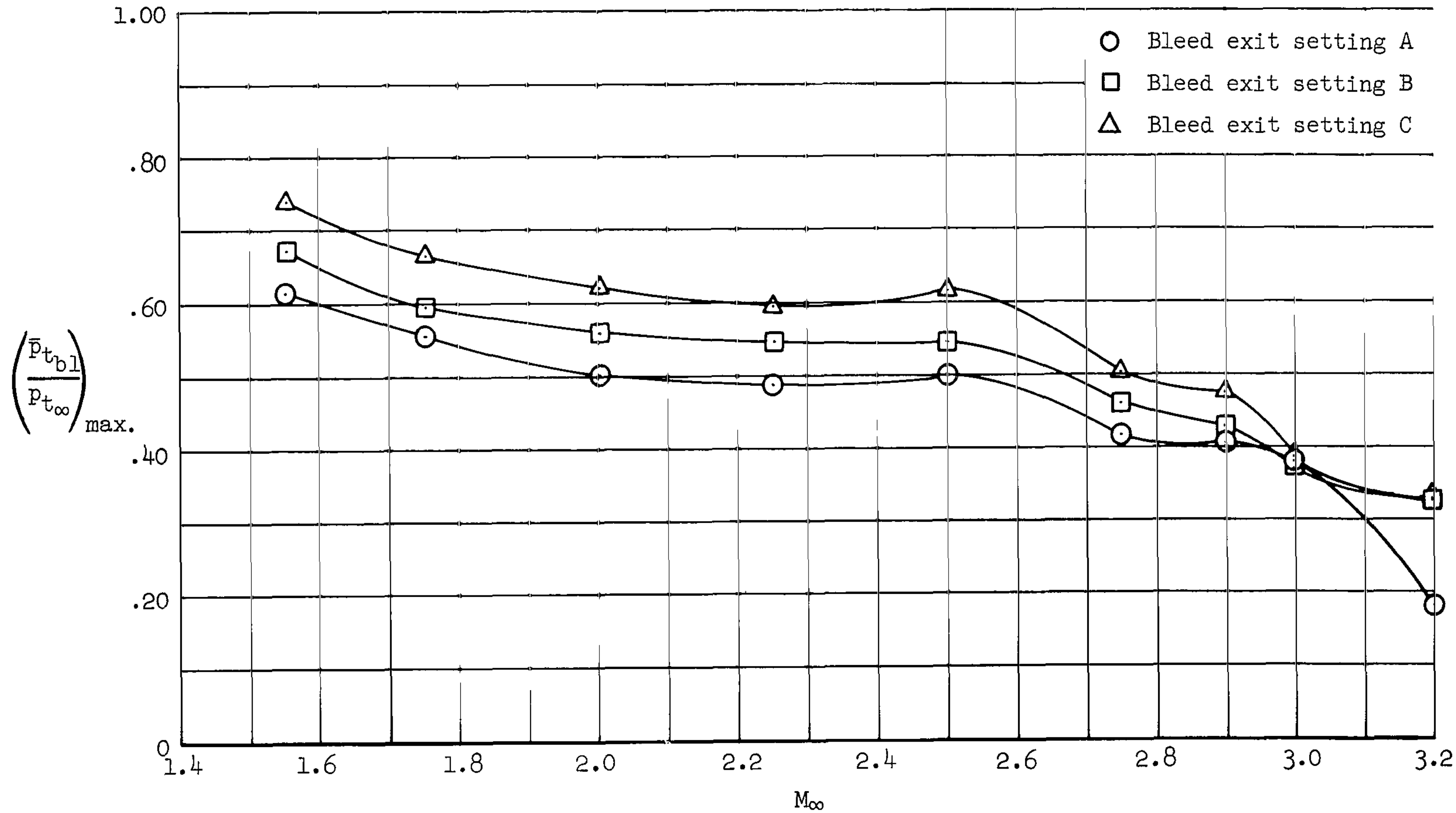

(c) Bleed zone III

Figure 17.- Continued.

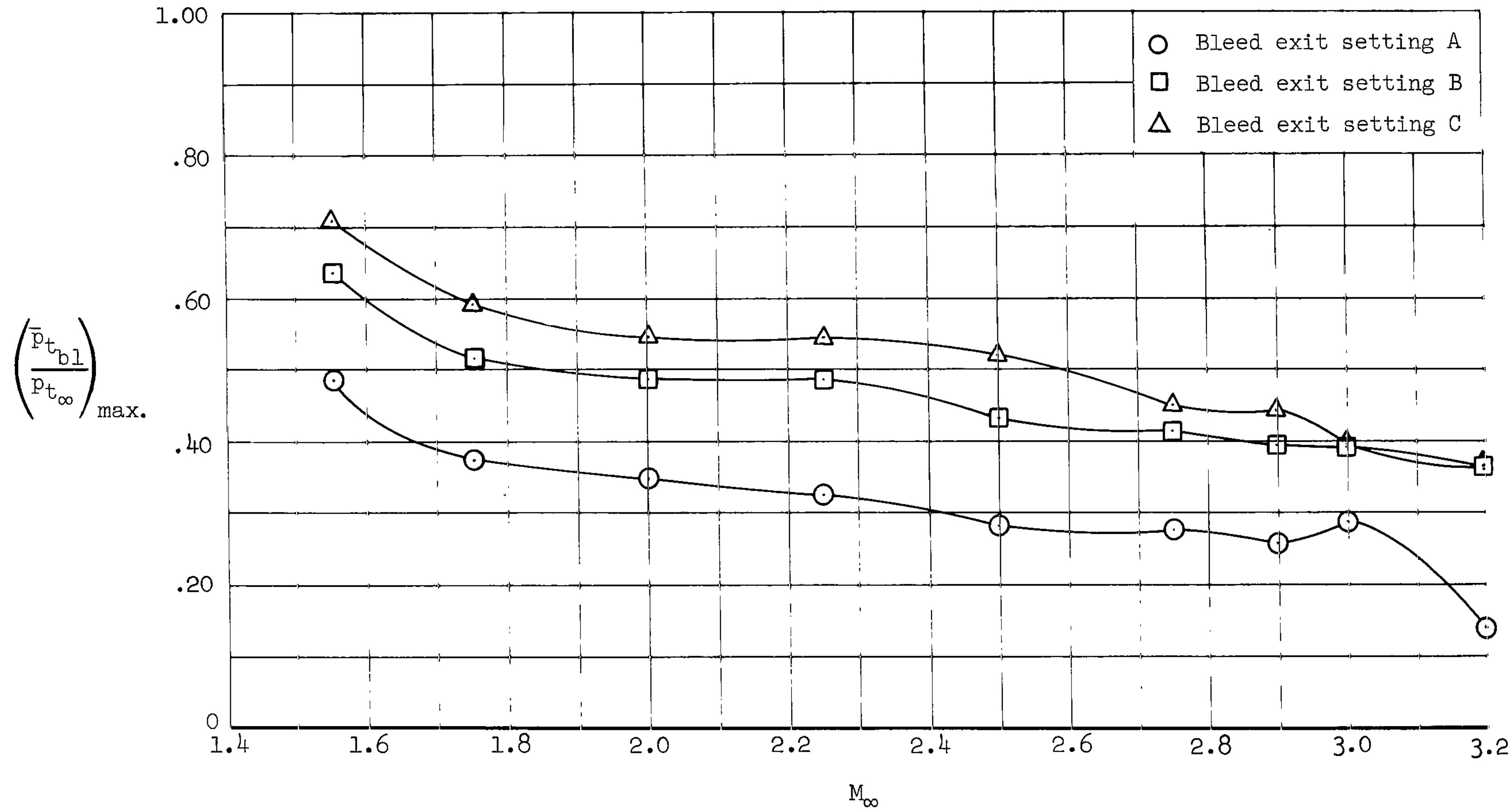

(d) Bleed zone IV

Figure 17.- Concluded.

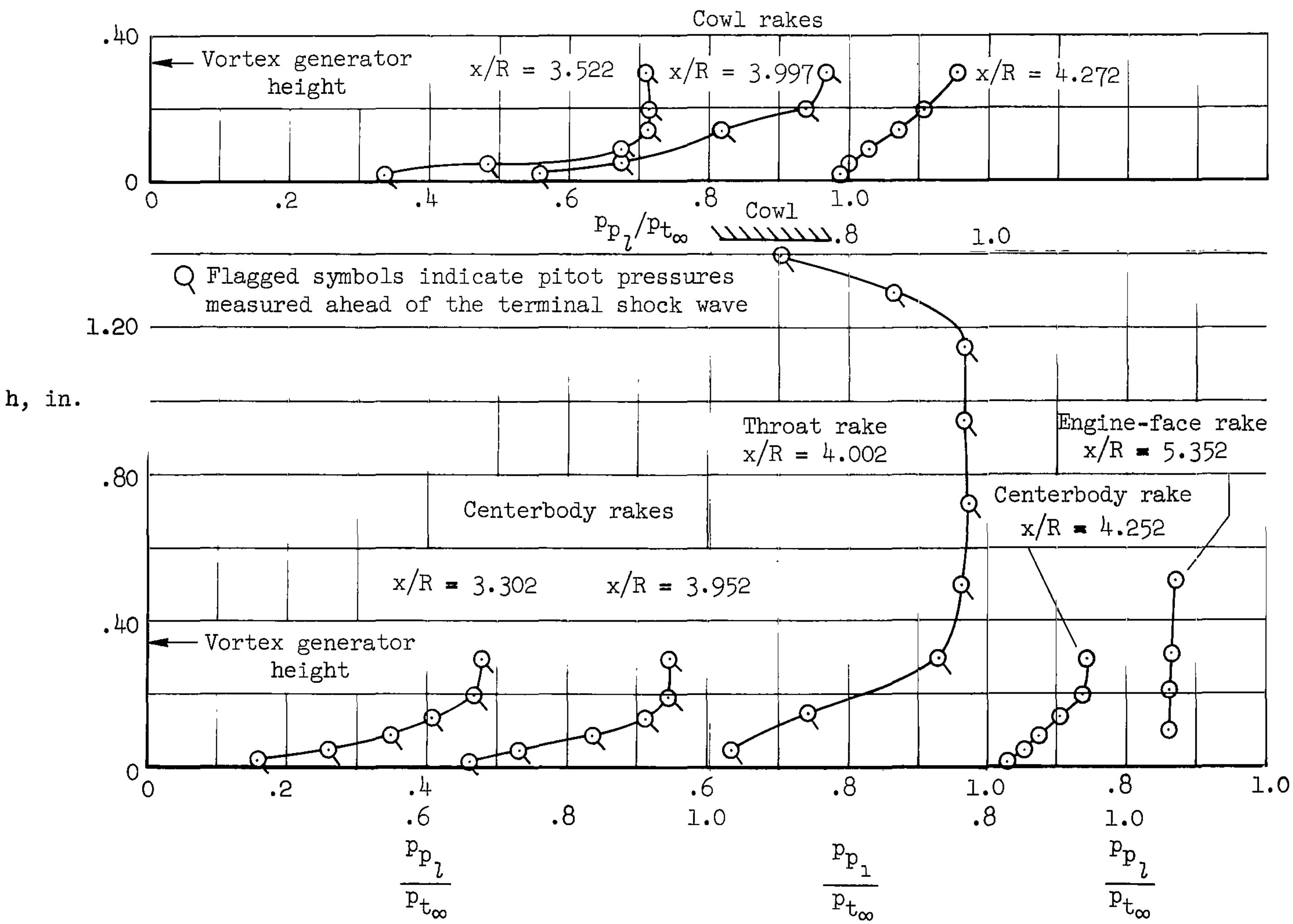

(a) $(x/R)_{lip} = 2.548$, $M_\infty = 3.00$

Figure 18.- Pitot pressure profiles, maximum pressure recovery; bleed exit setting B.

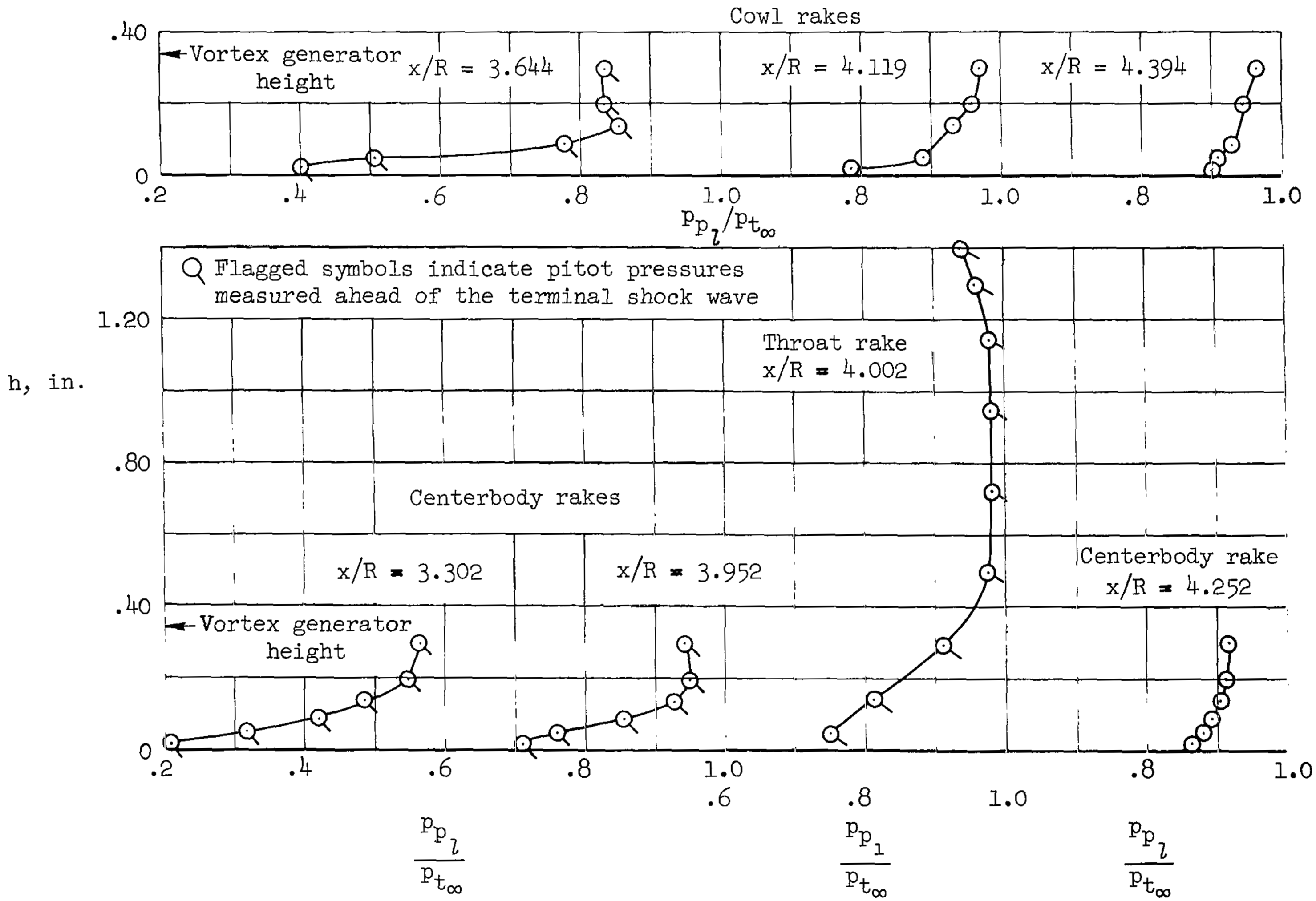

(b) $(x/R)_{lip} = 2.670$, $M_\infty = 2.75$

Figure 18.- Continued.

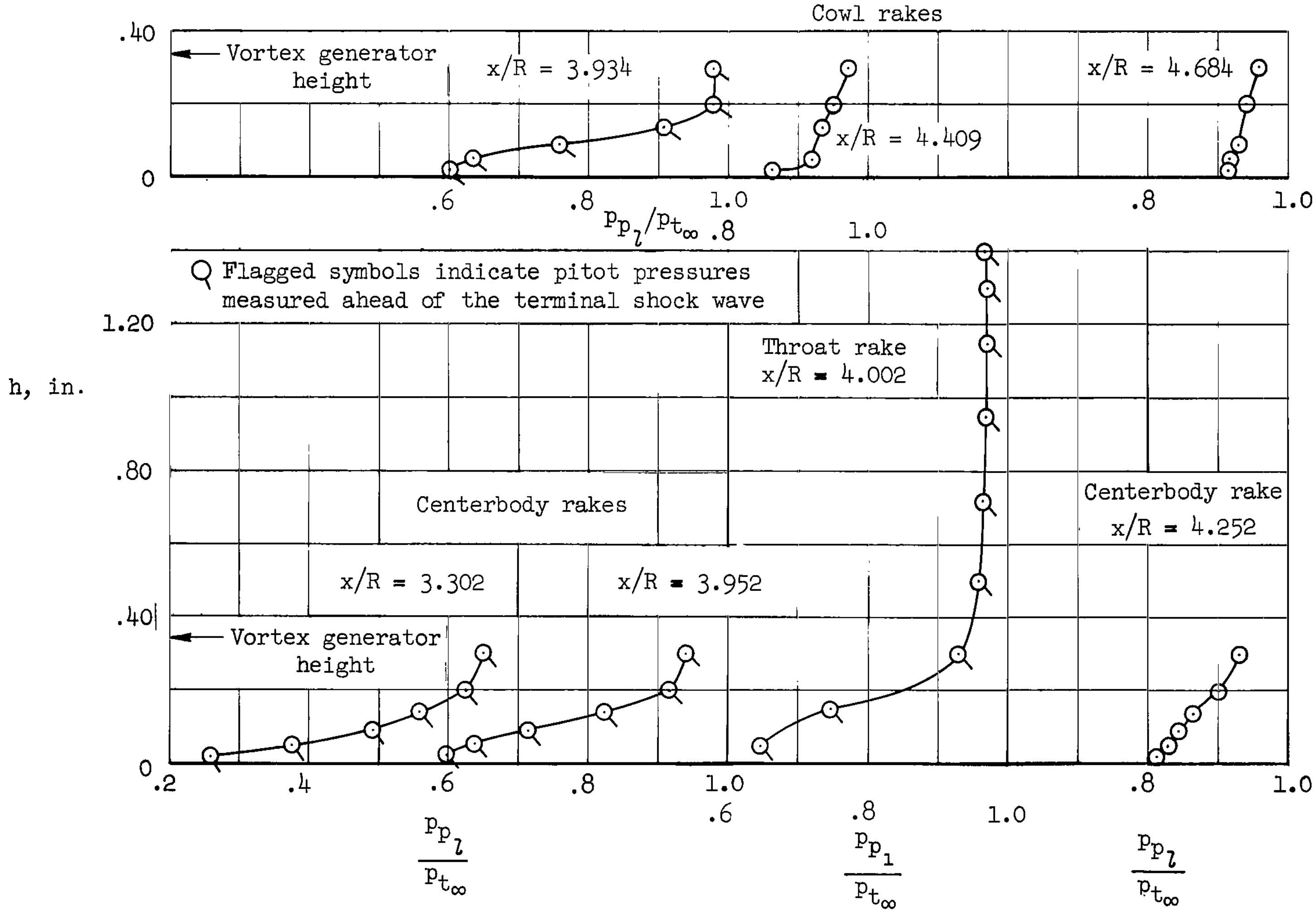

(c) $(x/R)_{lip} = 2.960$, $M_\infty = 2.50$

Figure 18.- Concluded.

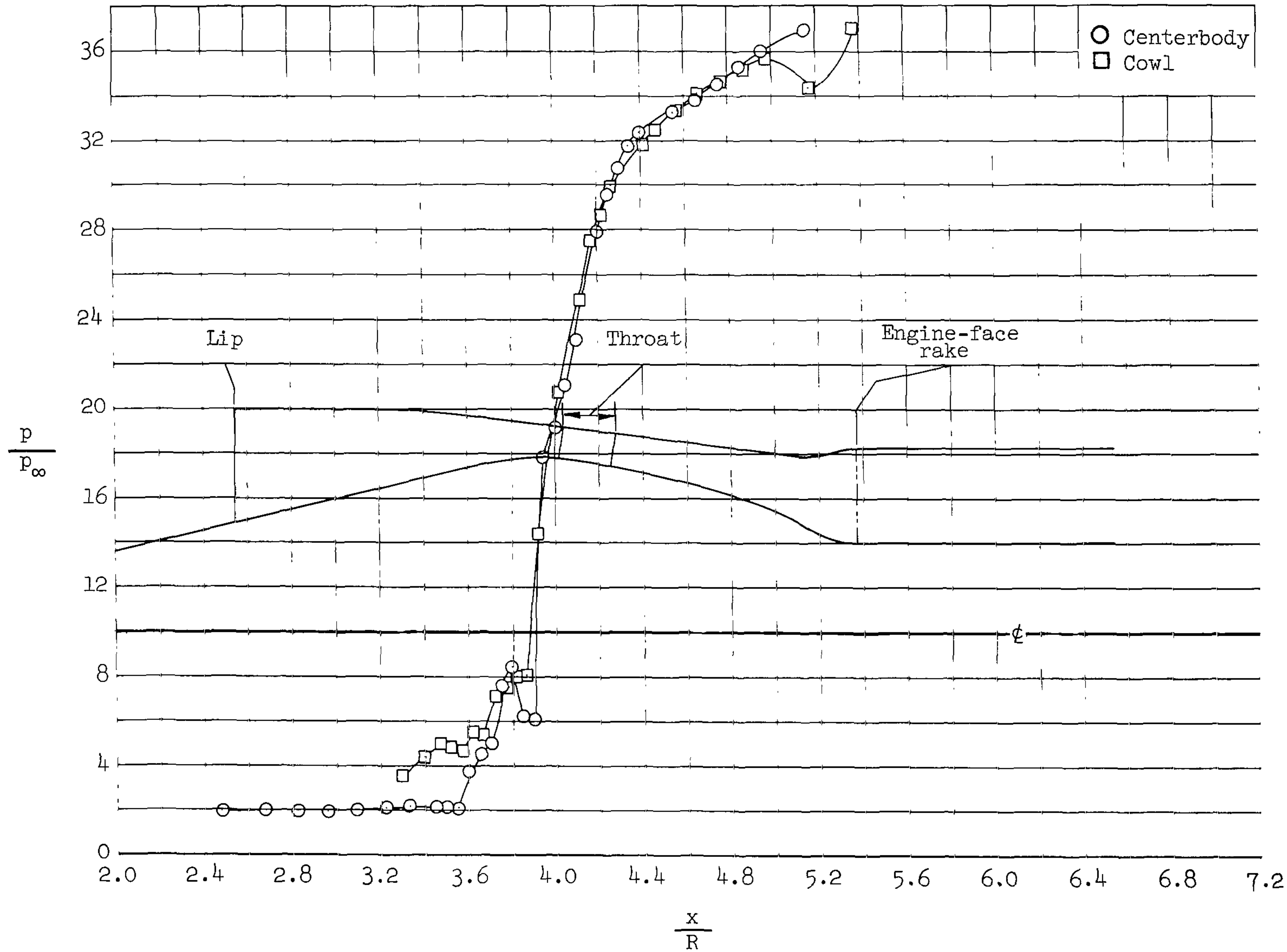

(a) $\bar{p}_{t_2}/p_{t_\infty} = 0.816$, $m_{bl}/m_\infty = 0.098$

Figure 19.- Static pressure distribution; bleed exit setting B, $(x/R)_{lip} = 2.548$; $M_\infty = 3.20$, $\alpha = 0°$.

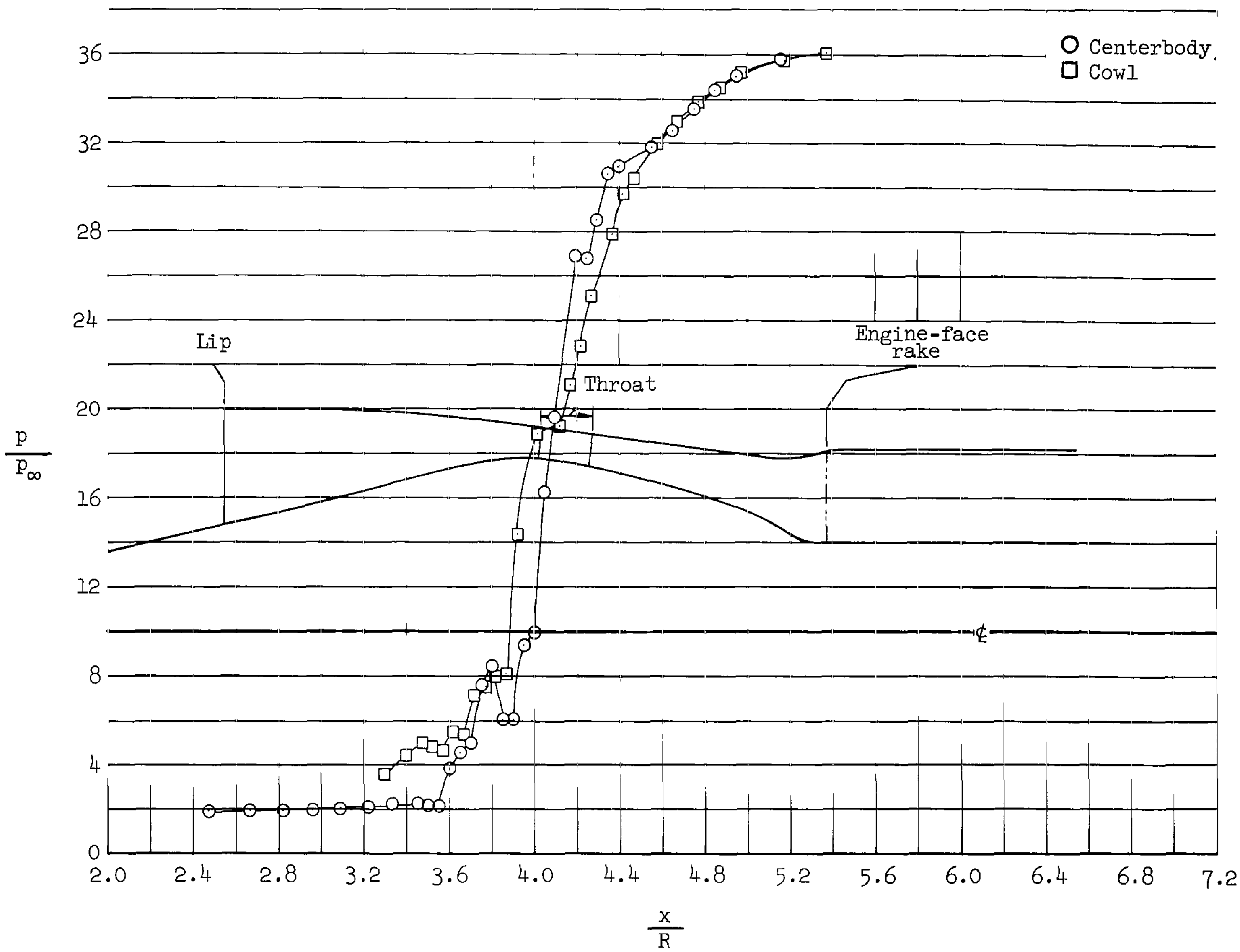

(b) $\bar{p}_{t_2}/p_{t_\infty} = 0.797$, $m_{bl}/m_\infty = 0.077$

Figure 19.- Continued.

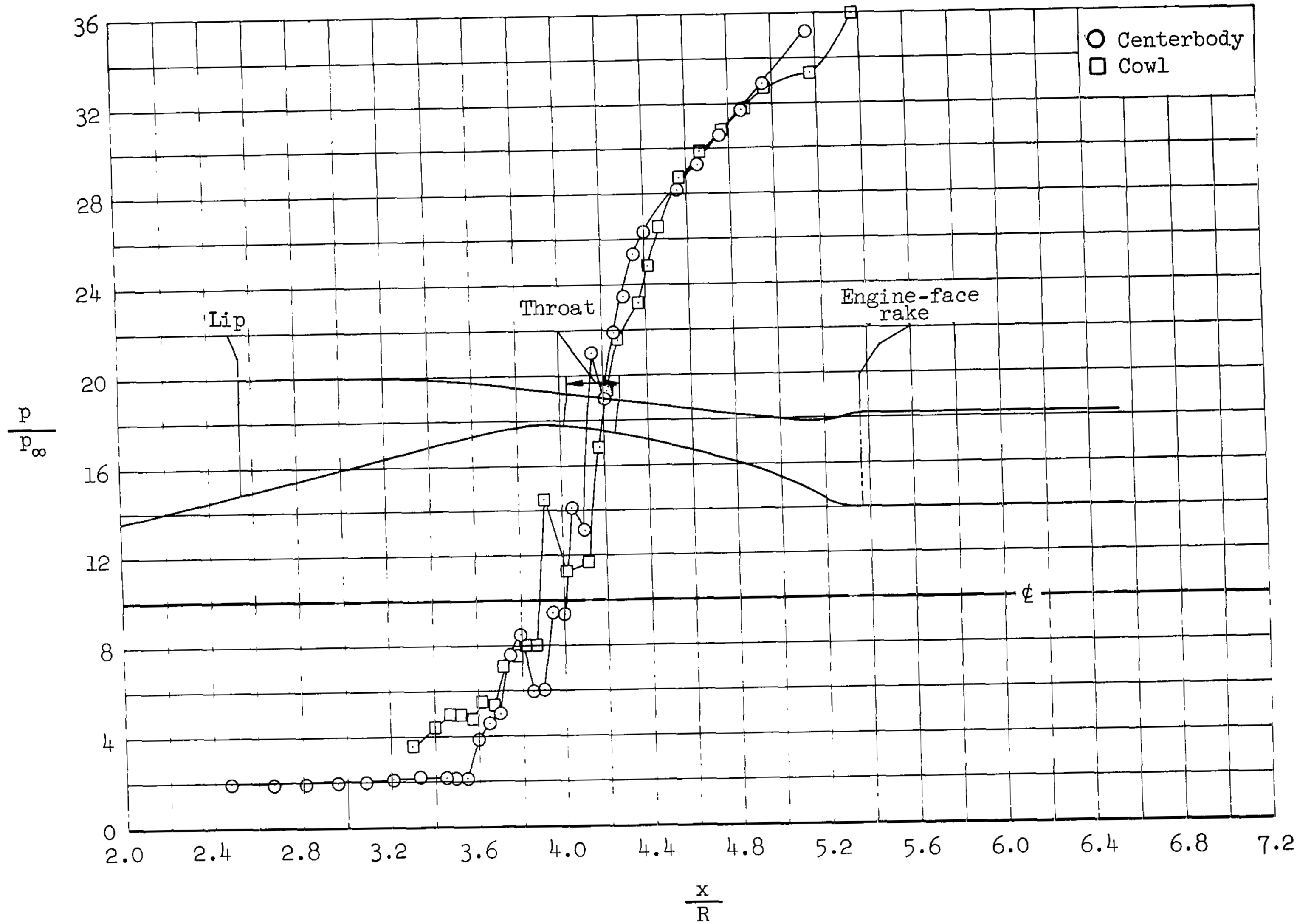

(c) $\bar{p}_{t_2}/p_{t_\infty} = 0.766$, $m_{bl}/m_\infty = 0.062$

Figure 19.- Concluded.

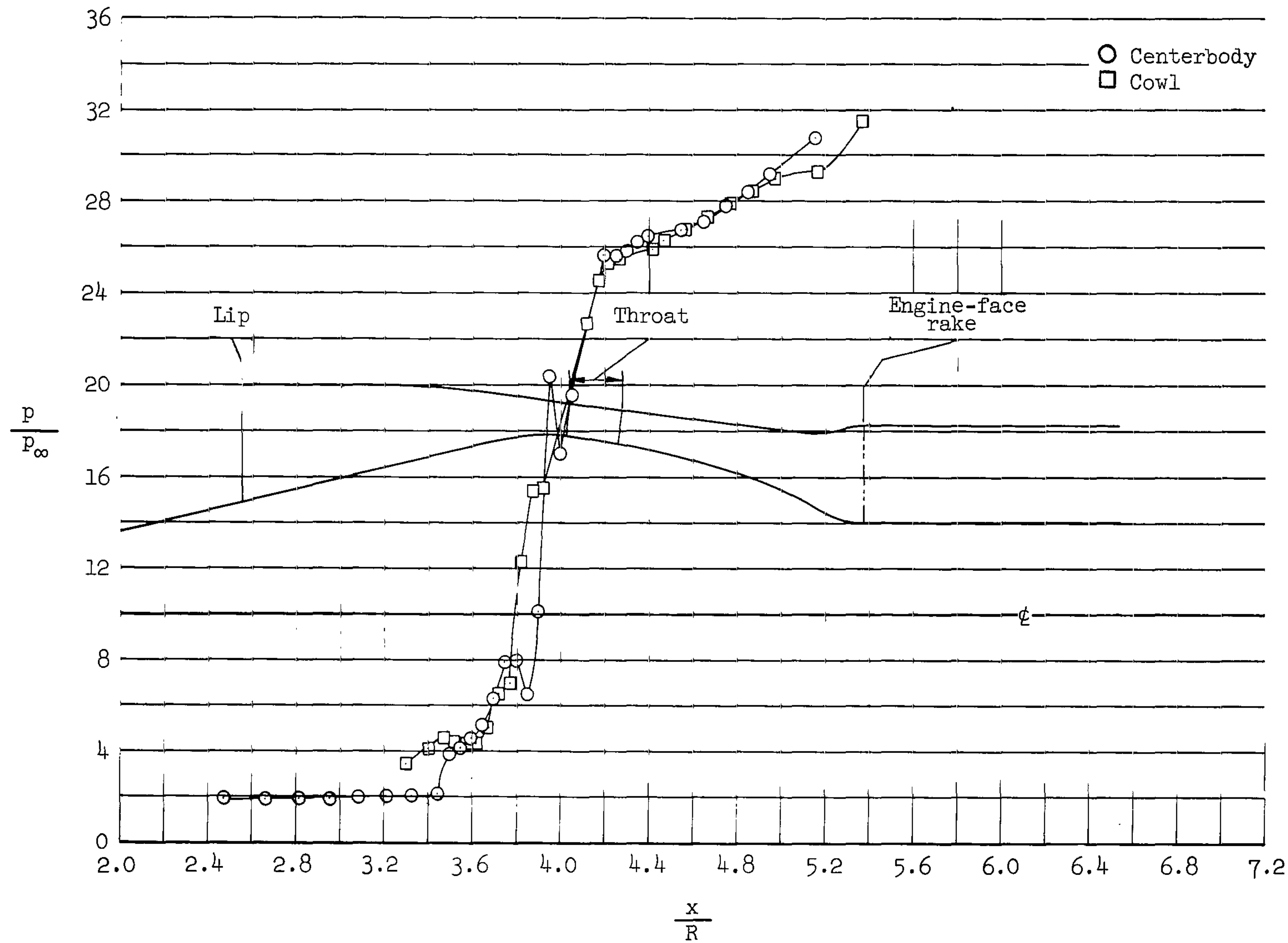

(a) $\bar{p}_{t_2}/p_{t_\infty} = 0.920$, $m_{bl}/m_\infty = 0.108$

Figure 20.- Static pressure distribution; bleed exit setting B, $(x/R)_{lip} = 2.548$; $M_\infty = 3.00$, $\alpha = 0°$.

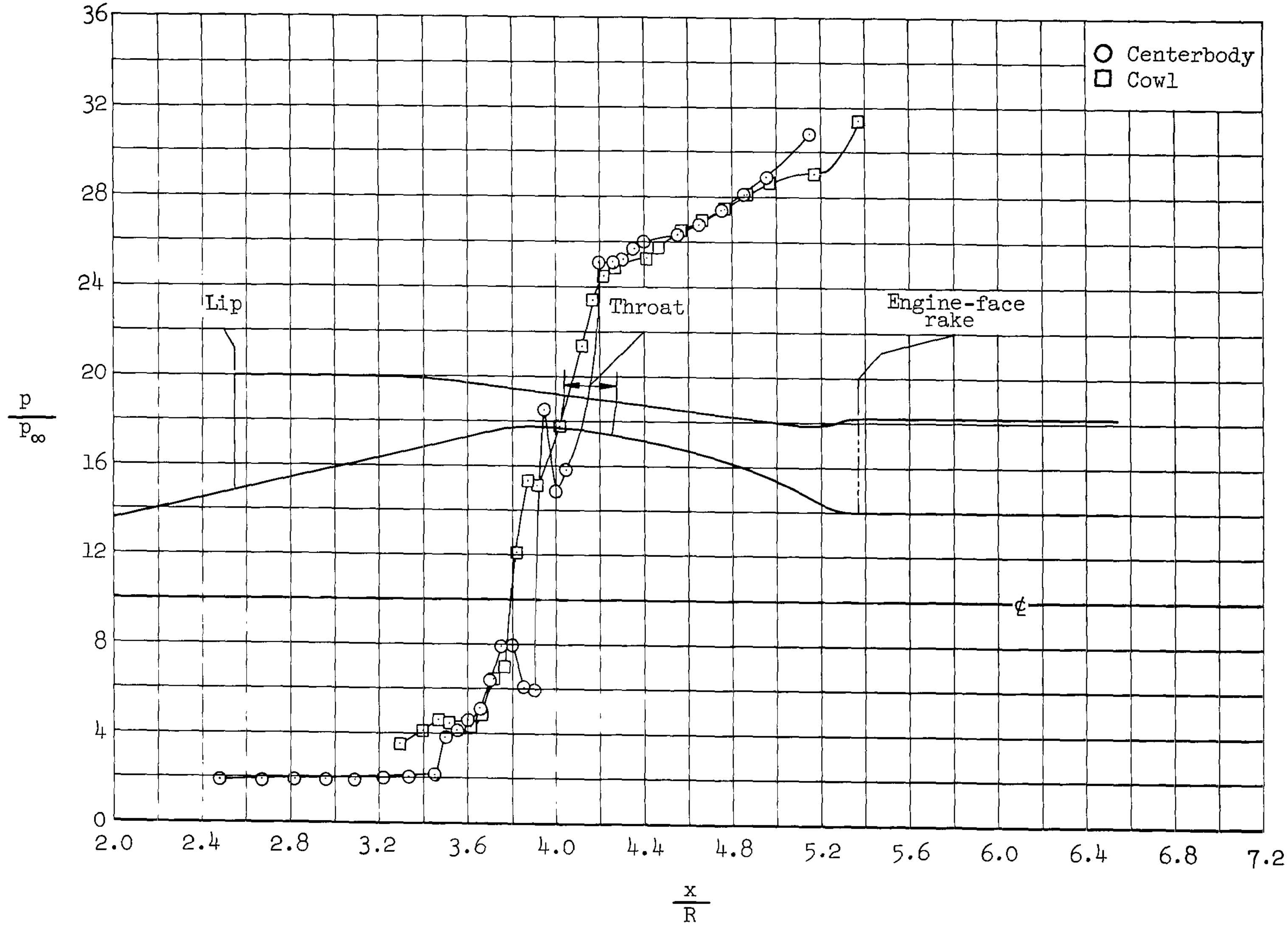

(b) $\bar{p}_{t_2}/p_{t_\infty} = 0.922$, $m_{bl}/m_\infty = 0.097$

Figure 20.- Continued.

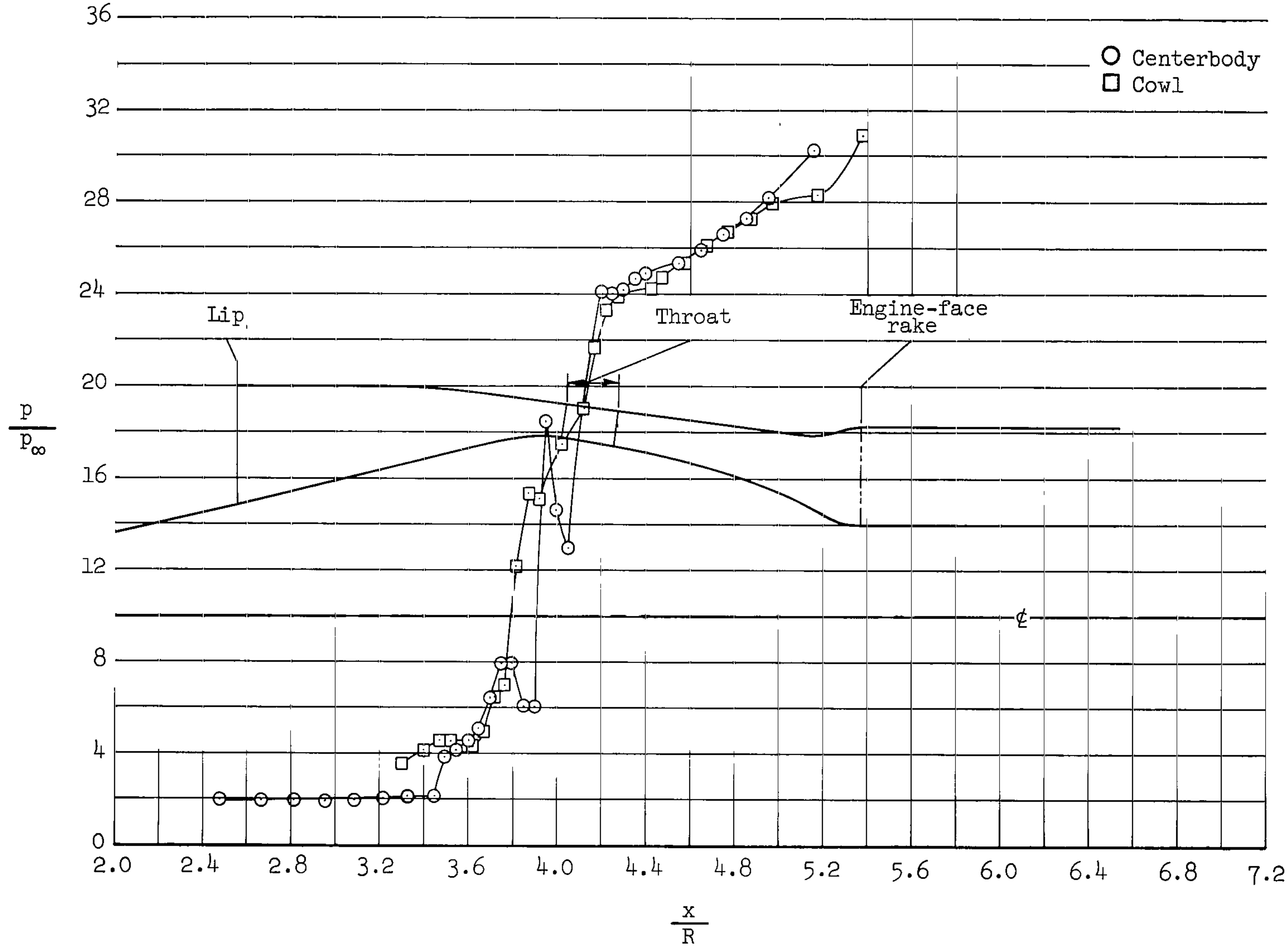

(c) $\bar{p}_{t_2}/p_{t_\infty} = 0.909$, $m_{bl}/m_\infty = 0.088$

Figure 20.- Continued.

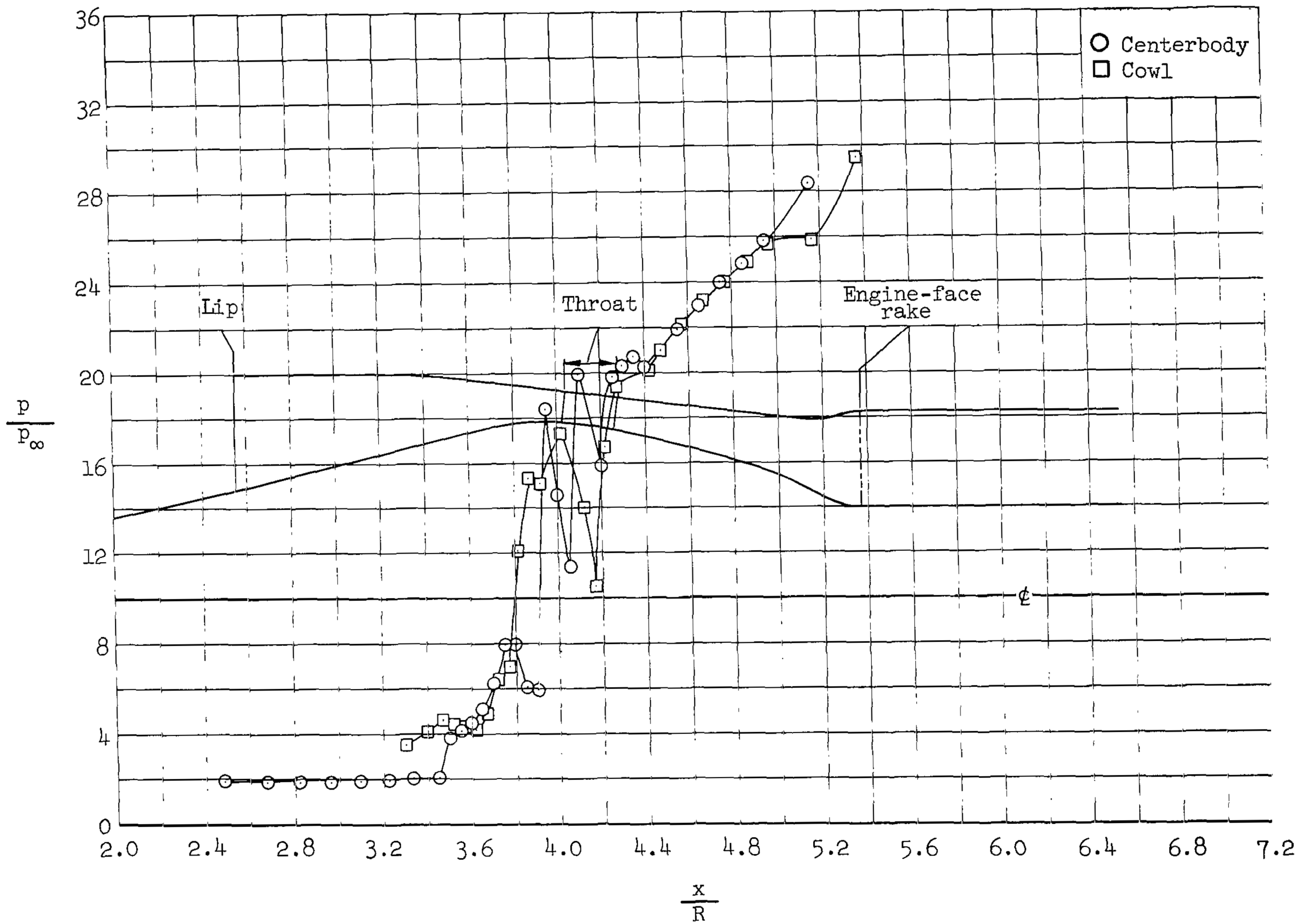

(d) $\bar{p}_{t_2}/p_{t_\infty} = 0.872$, $m_{bl}/m_\infty = 0.076$

Figure 20.- Concluded.

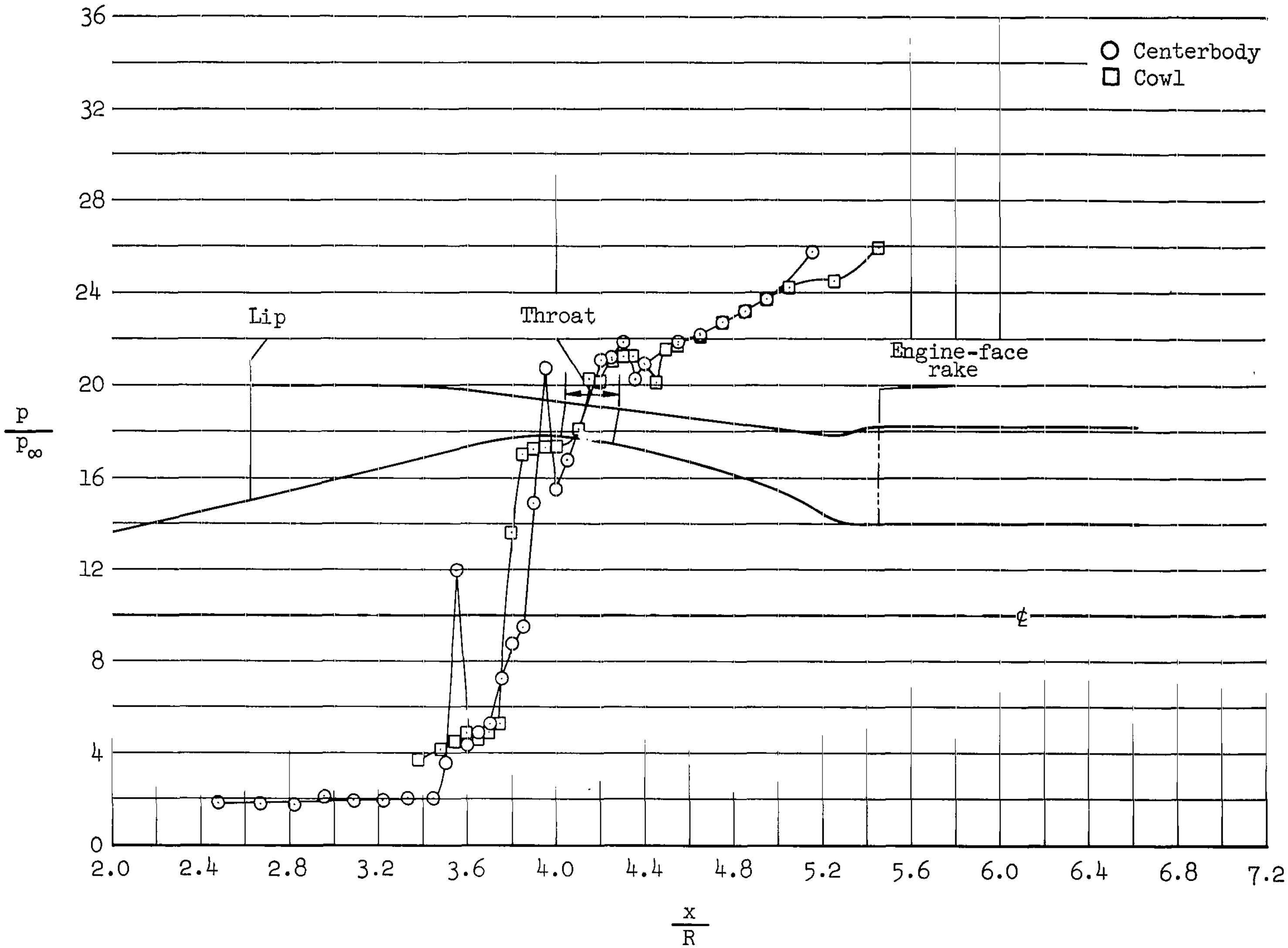

(a) $\bar{p}_{t_2}/p_{t_\infty} = 0.889$, $m_{bl}/m_\infty = 0.120$

Figure 21.- Static pressure distribution; bleed exit setting B, $(x/R)_{lip} = 2.622$; $M_\infty = 2.90$, $\alpha = 0°$.

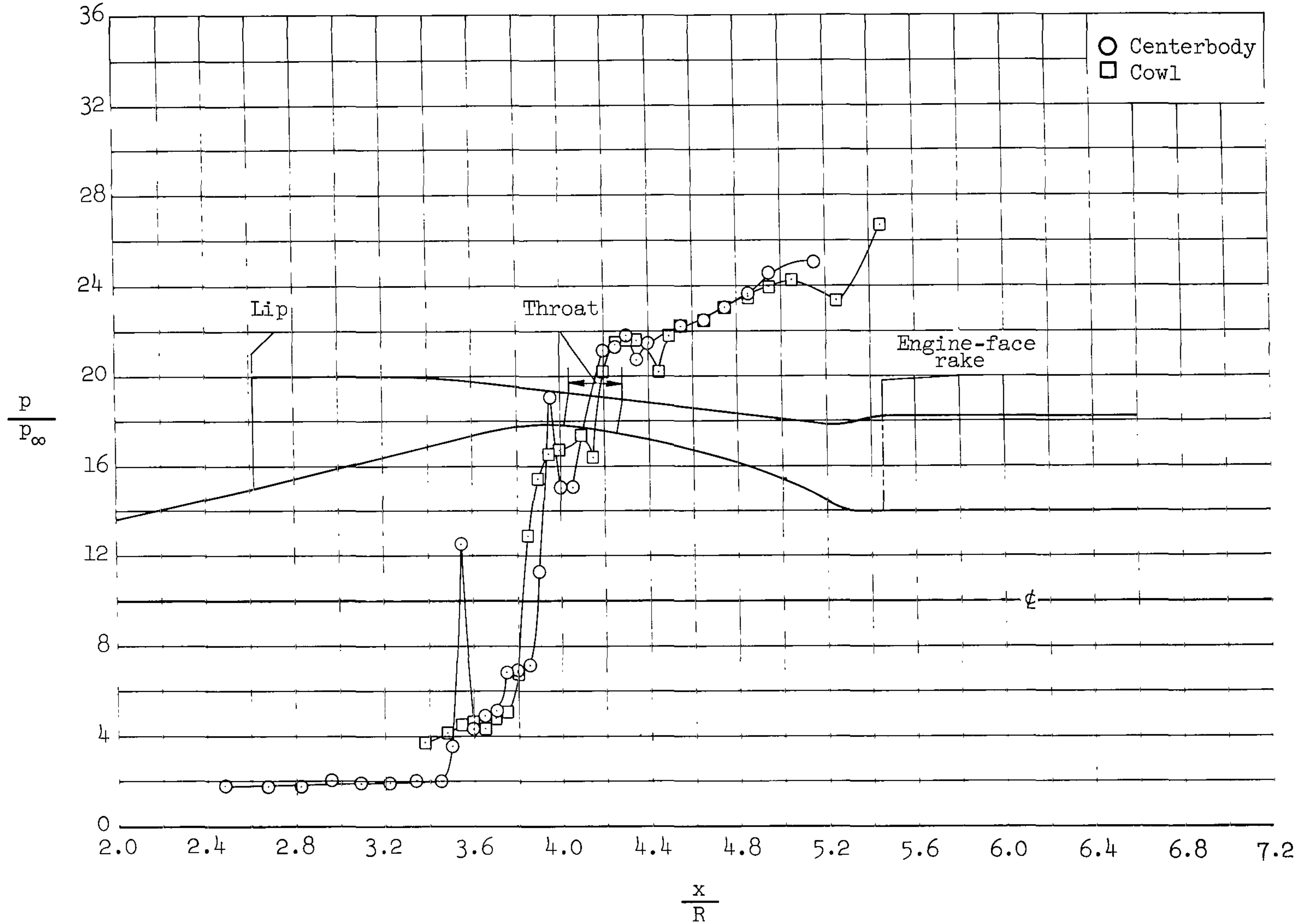

(b) $\bar{p}_{t_2}/p_{t_\infty} = 0.899$, $m_{bl}/m_\infty = 0.104$

Figure 21.- Continued.

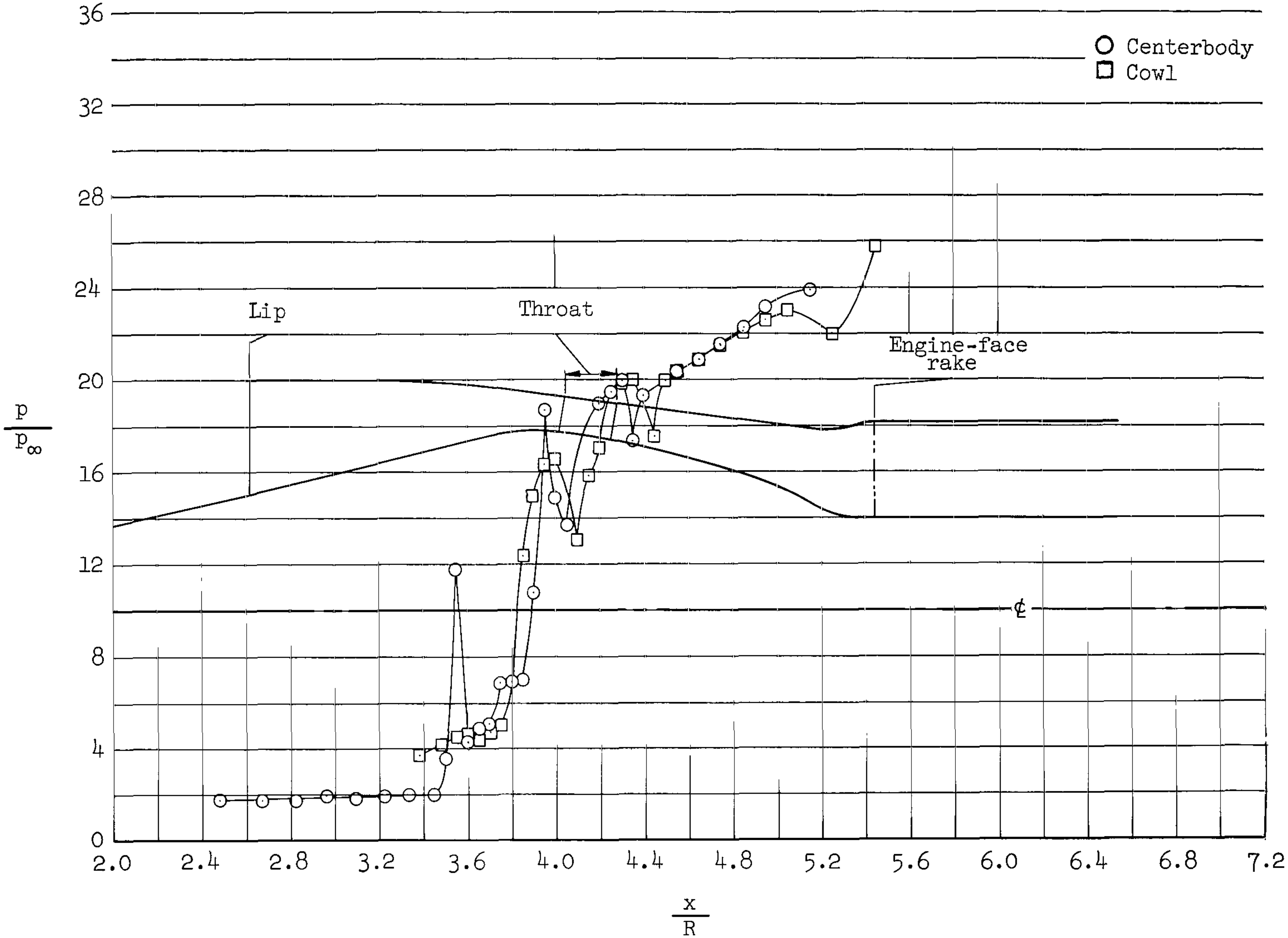

(c) $\bar{p}_{t_2}/p_{t_\infty} = 0.869$, $m_{bl}/m_\infty = 0.085$

Figure 21.- Concluded.

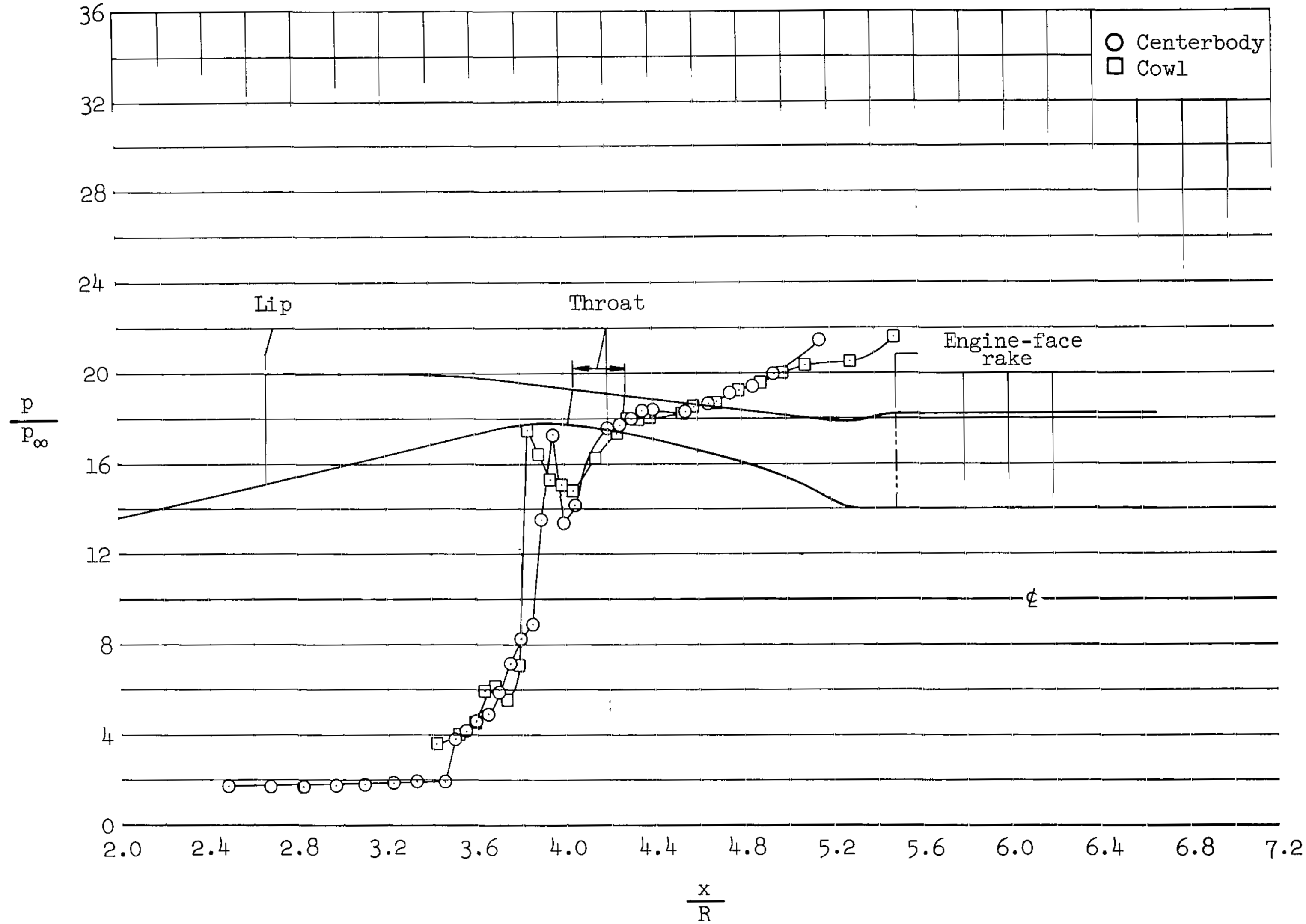

(a) $\bar{p}_{t_2}/p_{t_\infty} = 0.950$, $m_{bl}/m_\infty = 0.123$

Figure 22.- Static pressure distribution; bleed exit setting B, $(x/R)_{lip} = 2.670$; $M_\infty = 2.75$, $\alpha = 0°$.

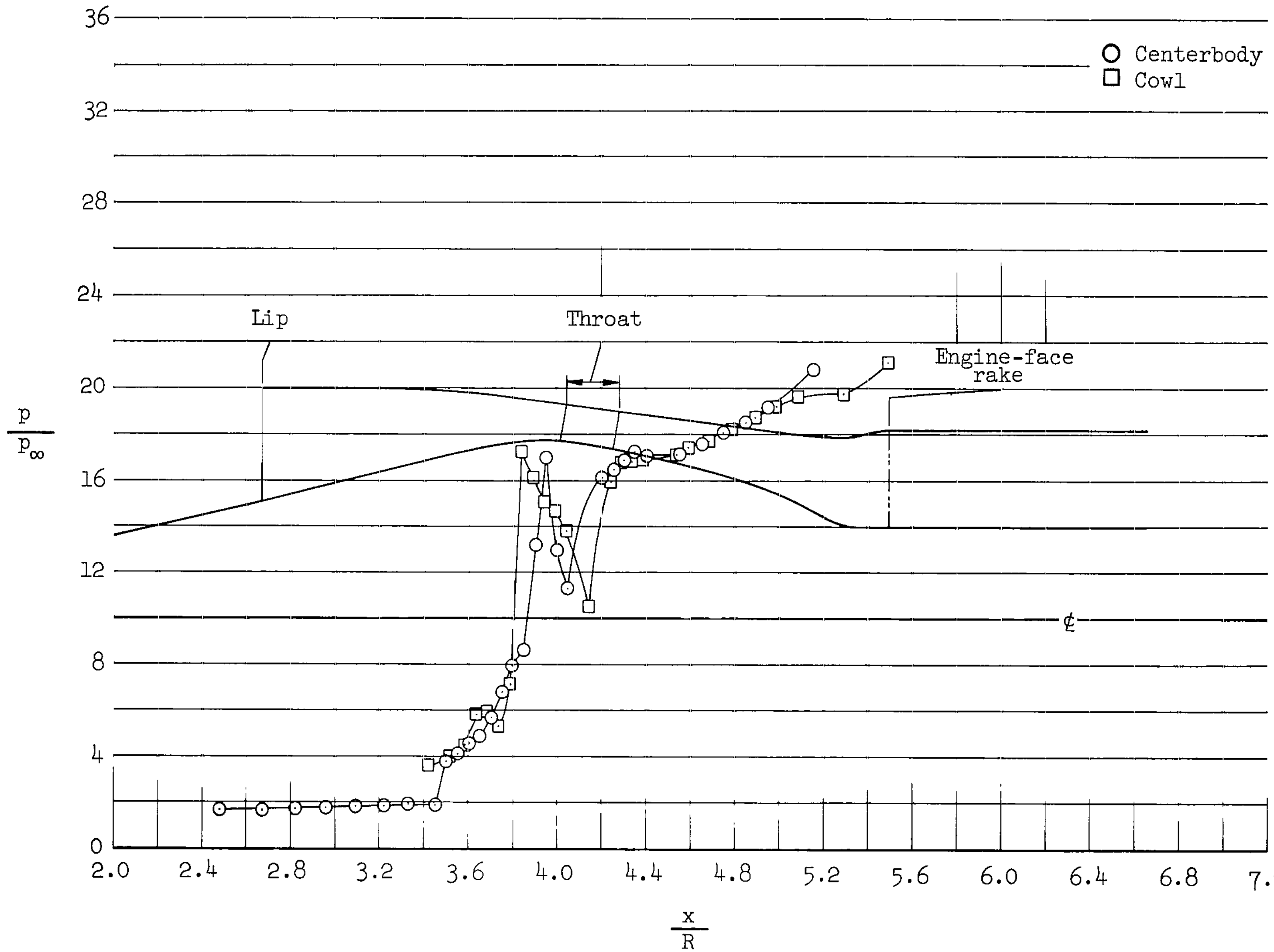

(b) $\bar{p}_{t_2}/p_{t_\infty} = 0.934$, $m_{bl}/m_\infty = 0.108$

Figure 22.- Continued.

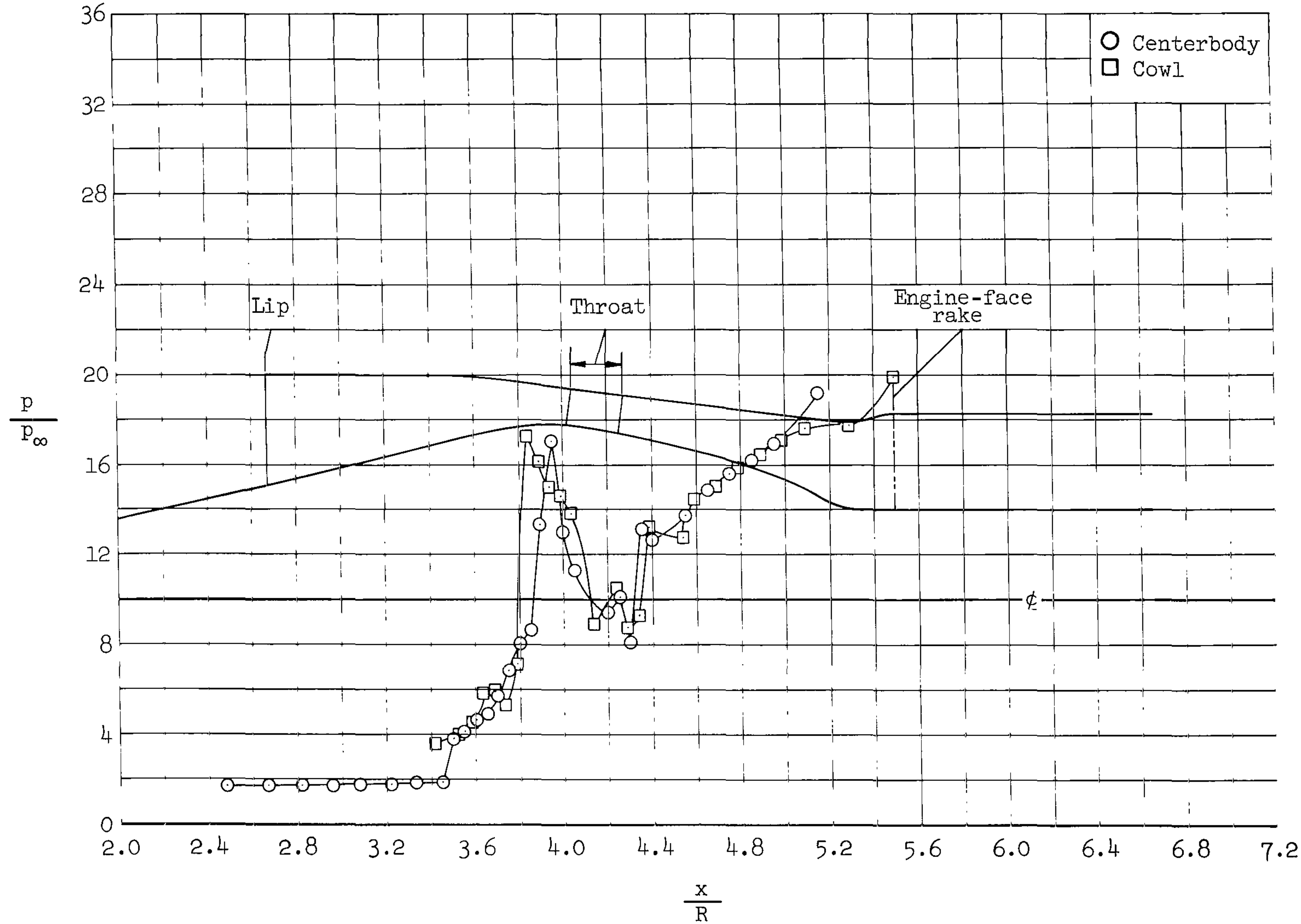

(c) $\bar{p}_{t_2}/p_{t_\infty} = 0.888$, $m_{bl}/m_\infty = 0.099$

Figure 22.- Concluded.

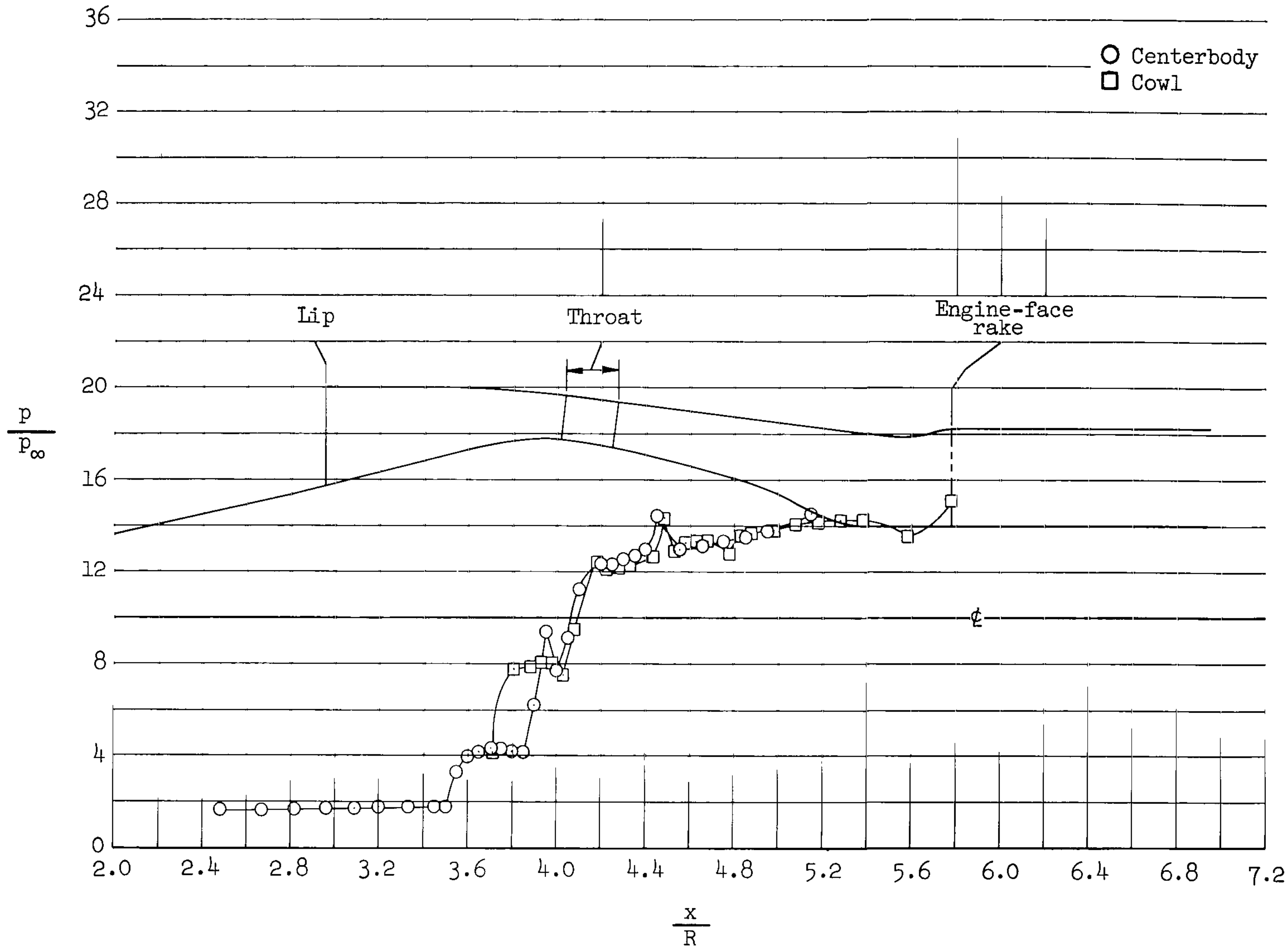

(a) $\bar{p}_{t_2}/p_{t_\infty} = 0.945$, $m_{bl}/m_\infty = 0.110$

Figure 23.- Static pressure distribution; bleed exit setting B, $(x/R)_{lip} = 2.960$; $M_\infty = 2.50$, $\alpha = 0°$.

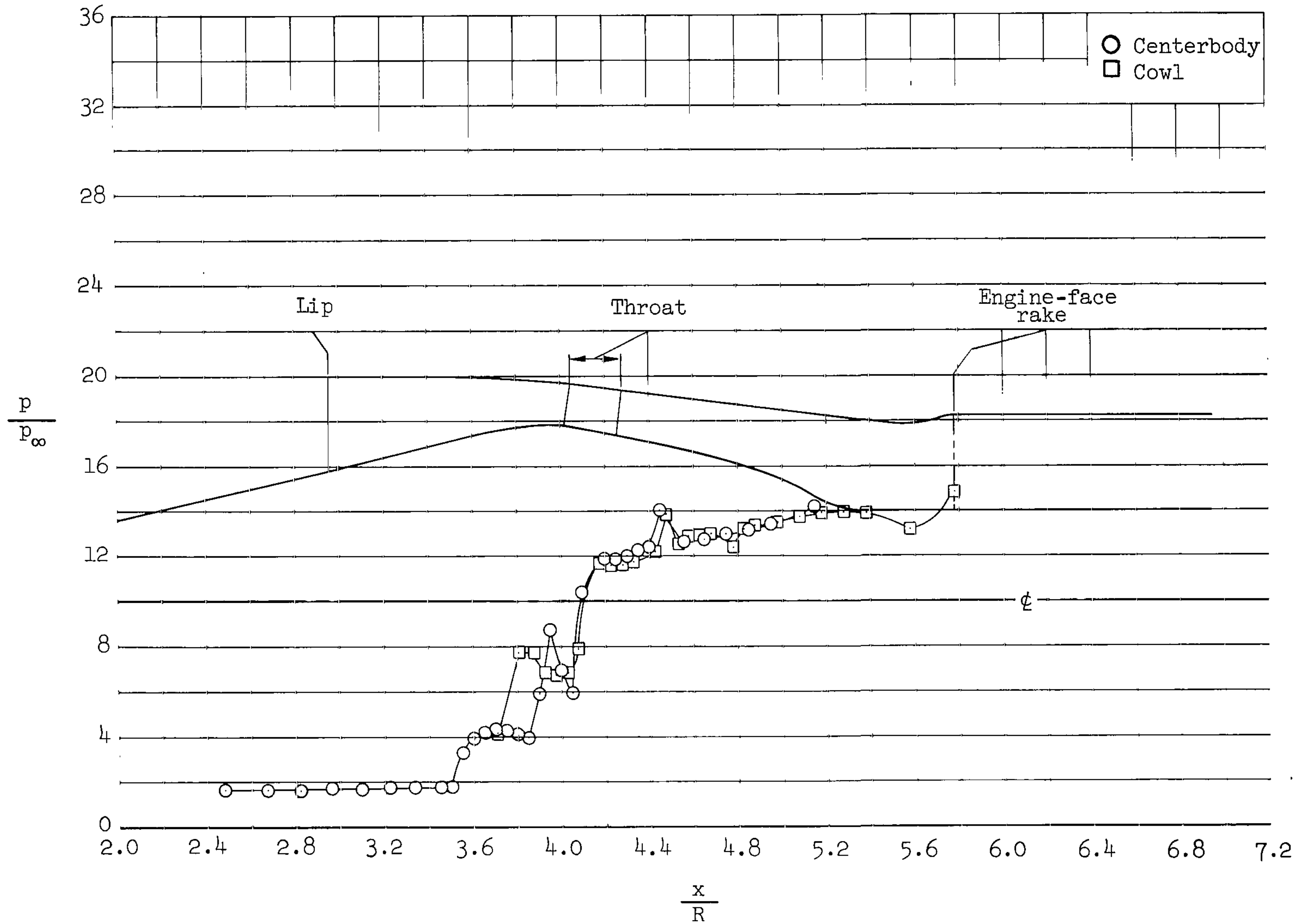

(b) $\bar{p}_{t_2}/p_{t_\infty} = 0.932$, $m_{bl}/m_\infty = 0.100$

Figure 23.- Continued.

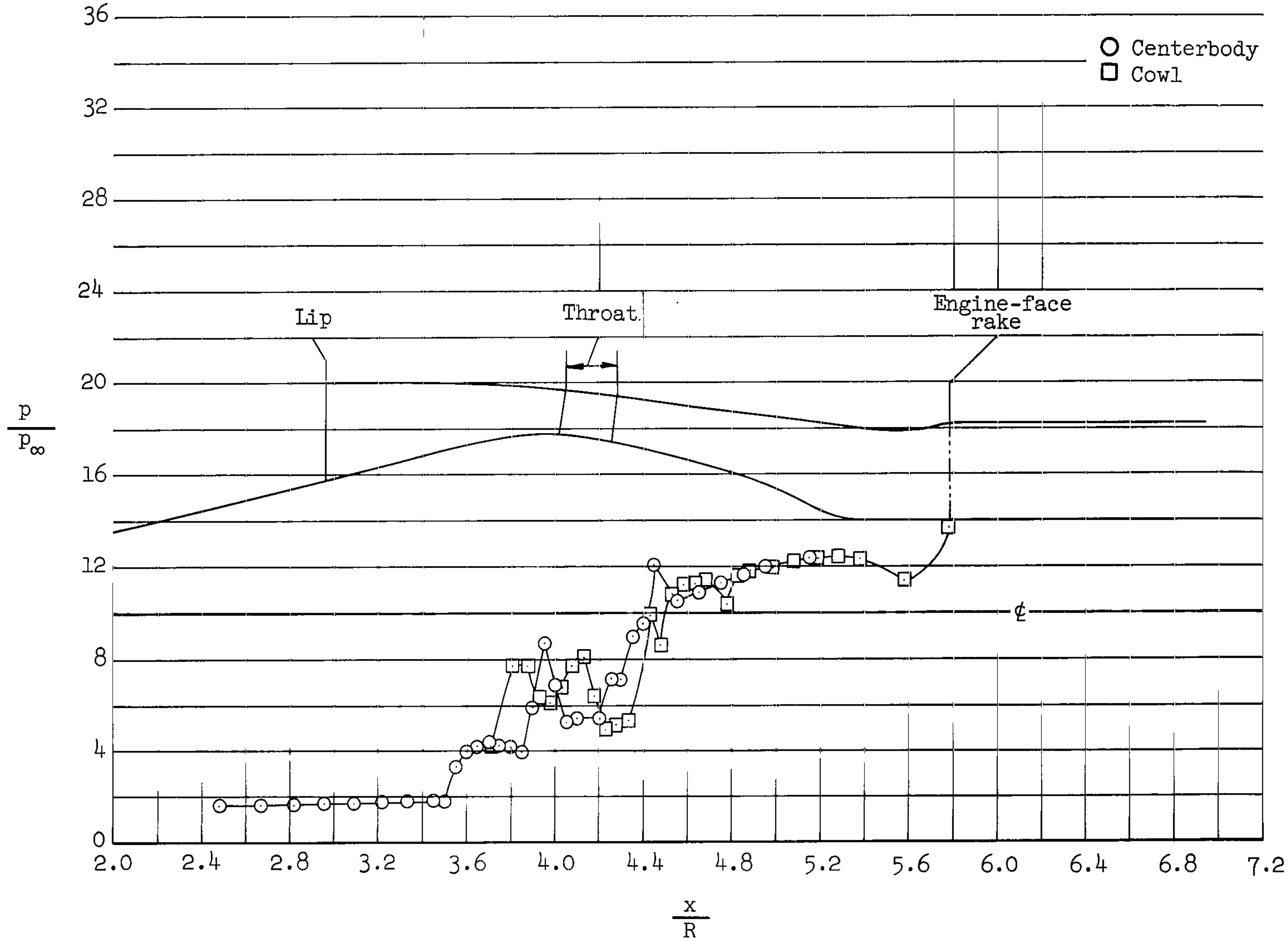

(c) $\bar{p}_{t_2}/p_{t_\infty} = 0.884$, $m_{bl}/m_\infty = 0.085$

Figure 23.- Concluded.

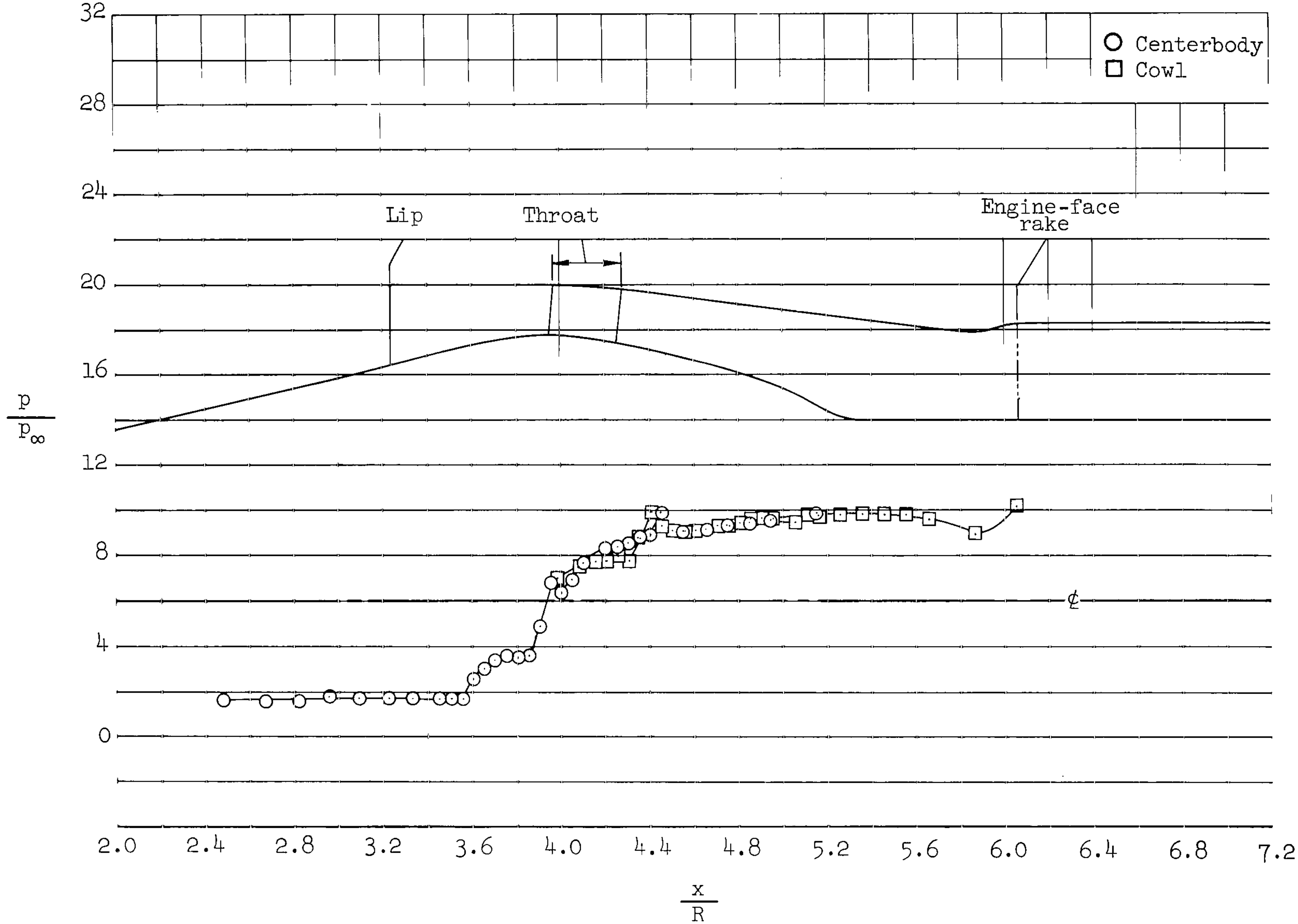

(a) $\bar{p}_{t_2}/p_{t_\infty} = 0.948$, $m_{bl}/m_\infty = 0.102$

Figure 24.- Static pressure distribution; bleed exit setting B, $(x/R)_{lip} = 3.240$; $M_\infty = 2.25$, $\alpha = 0°$.

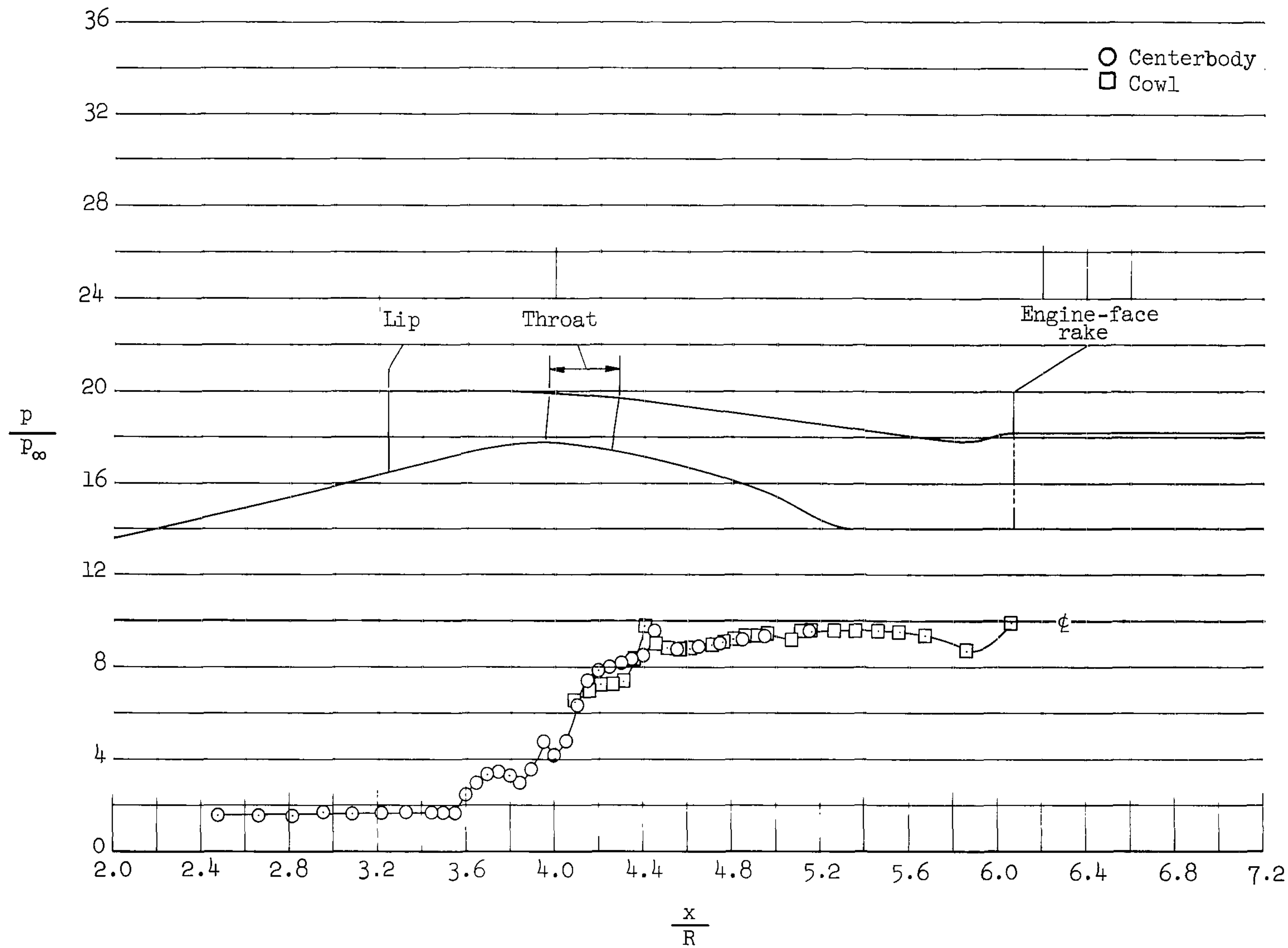

(b) $\bar{p}_{t_2}/p_{t_\infty} = 0.938$, $m_{bl}/m_\infty = 0.090$

Figure 24.- Continued.

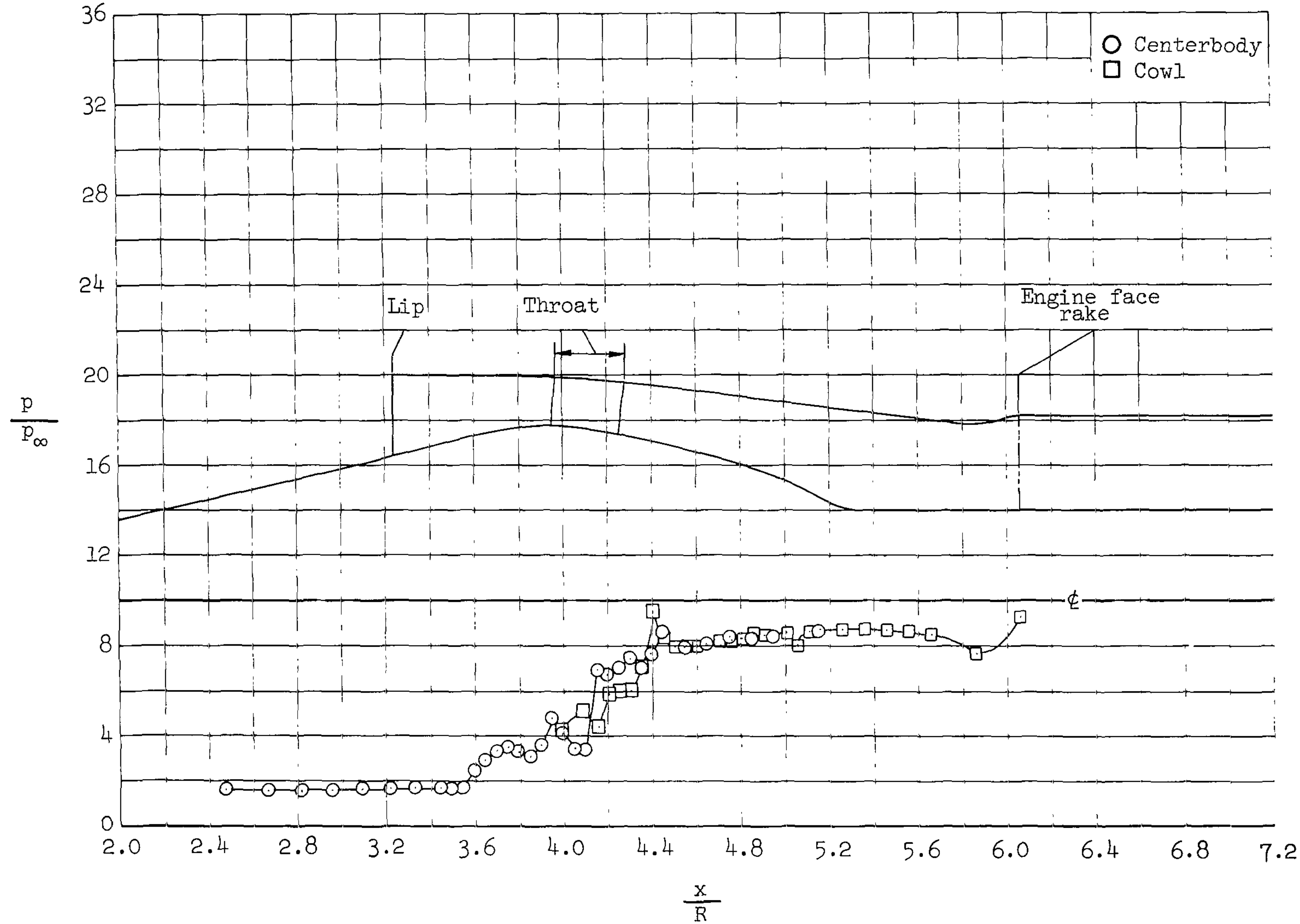

(c) $\bar{p}_{t_2}/p_{t_\infty} = 0.894$, $m_{bl}/m_\infty = 0.074$

Figure 24.- Concluded.

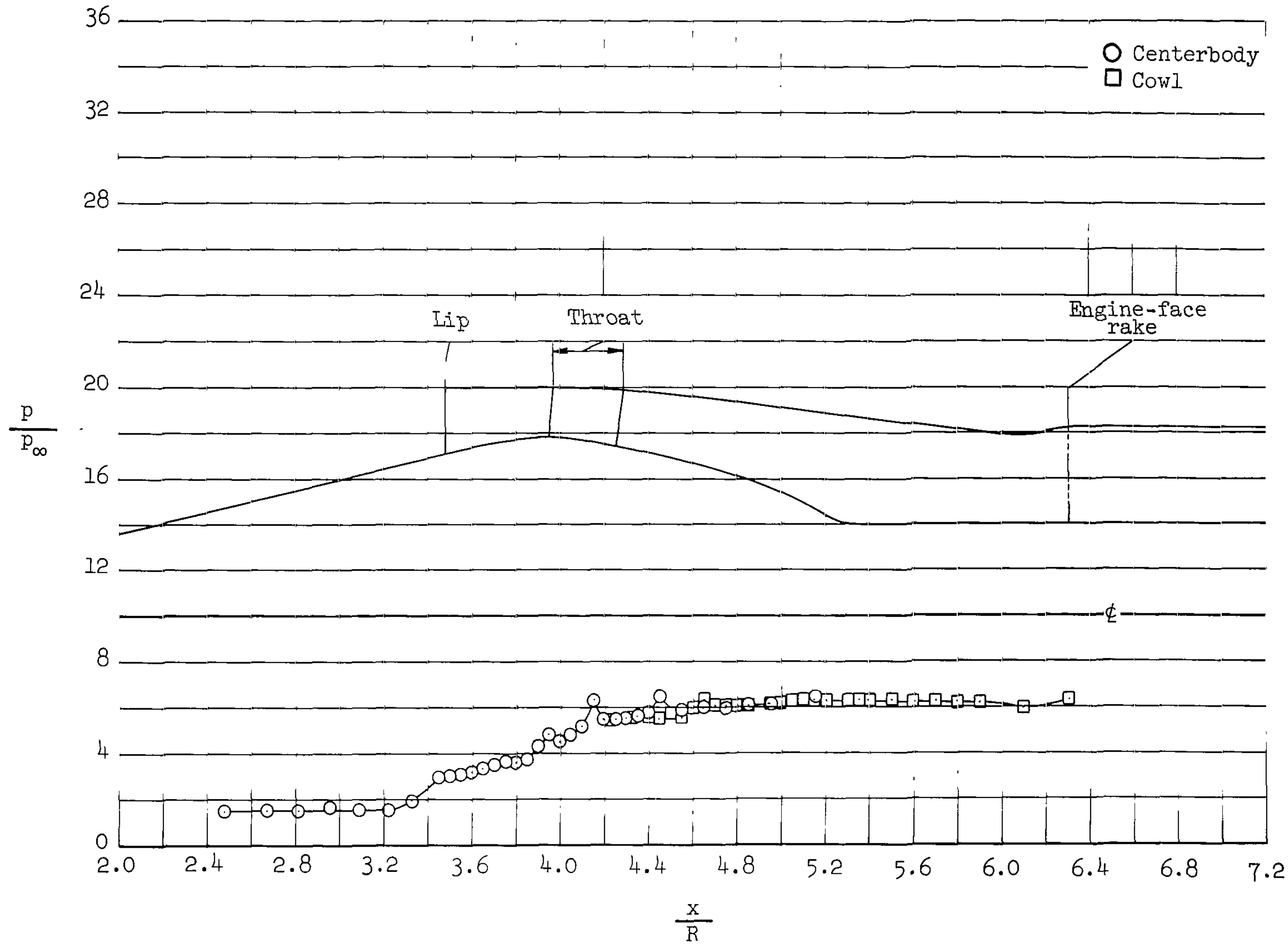

(a) $\bar{p}_{t_2}/p_{t_\infty} = 0.889$, $m_{bl}/m_\infty = 0.094$

Figure 25.- Static pressure distribution; bleed exit setting B, $(x/R)_{lip} = 3.478$; $M_\infty = 2.00$, $\alpha = 0°$.

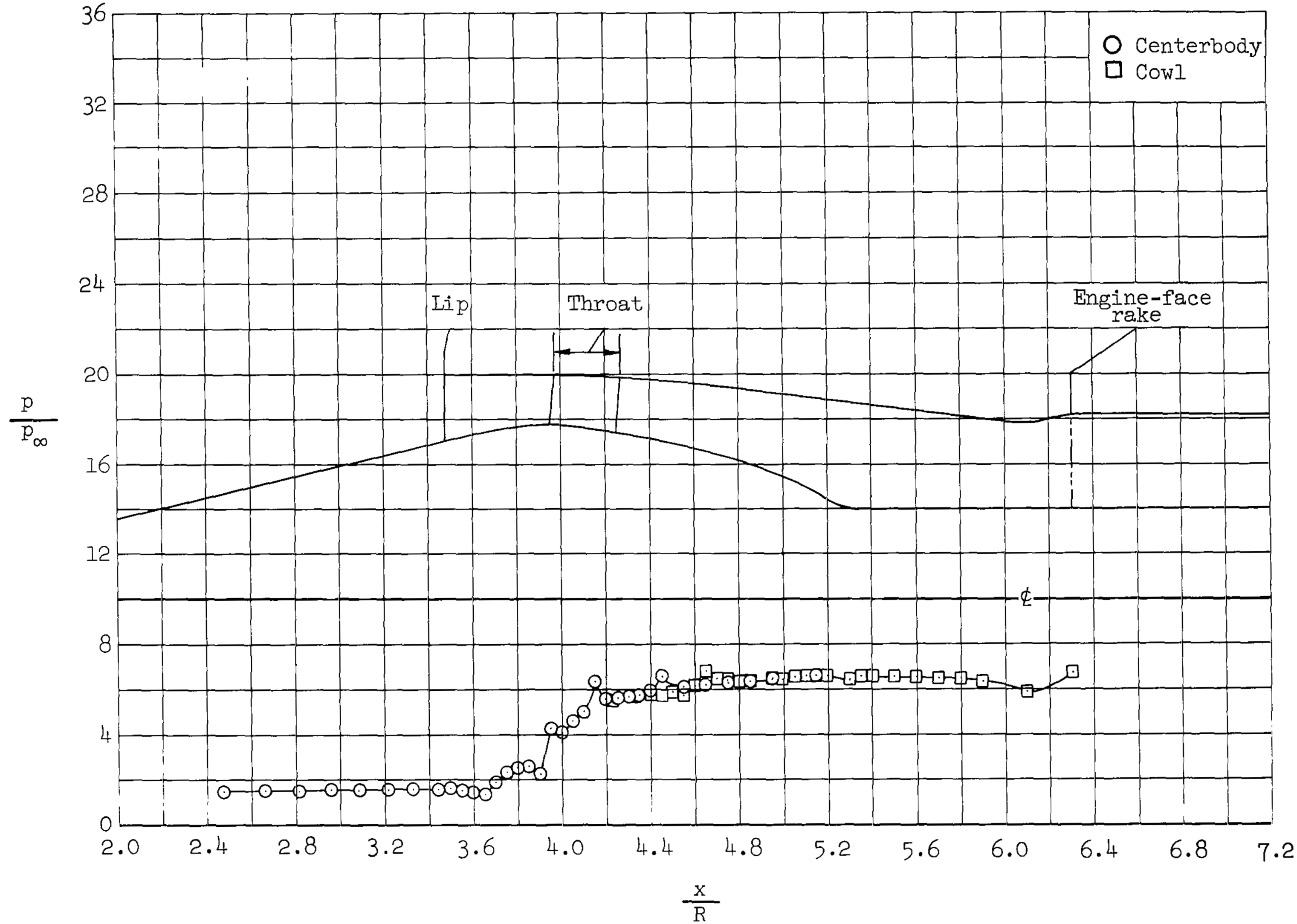

(b) $\bar{p}_{t_2}/p_{t_\infty} = 0.935$, $m_{bl}/m_\infty = 0.084$

Figure 25.- Continued.

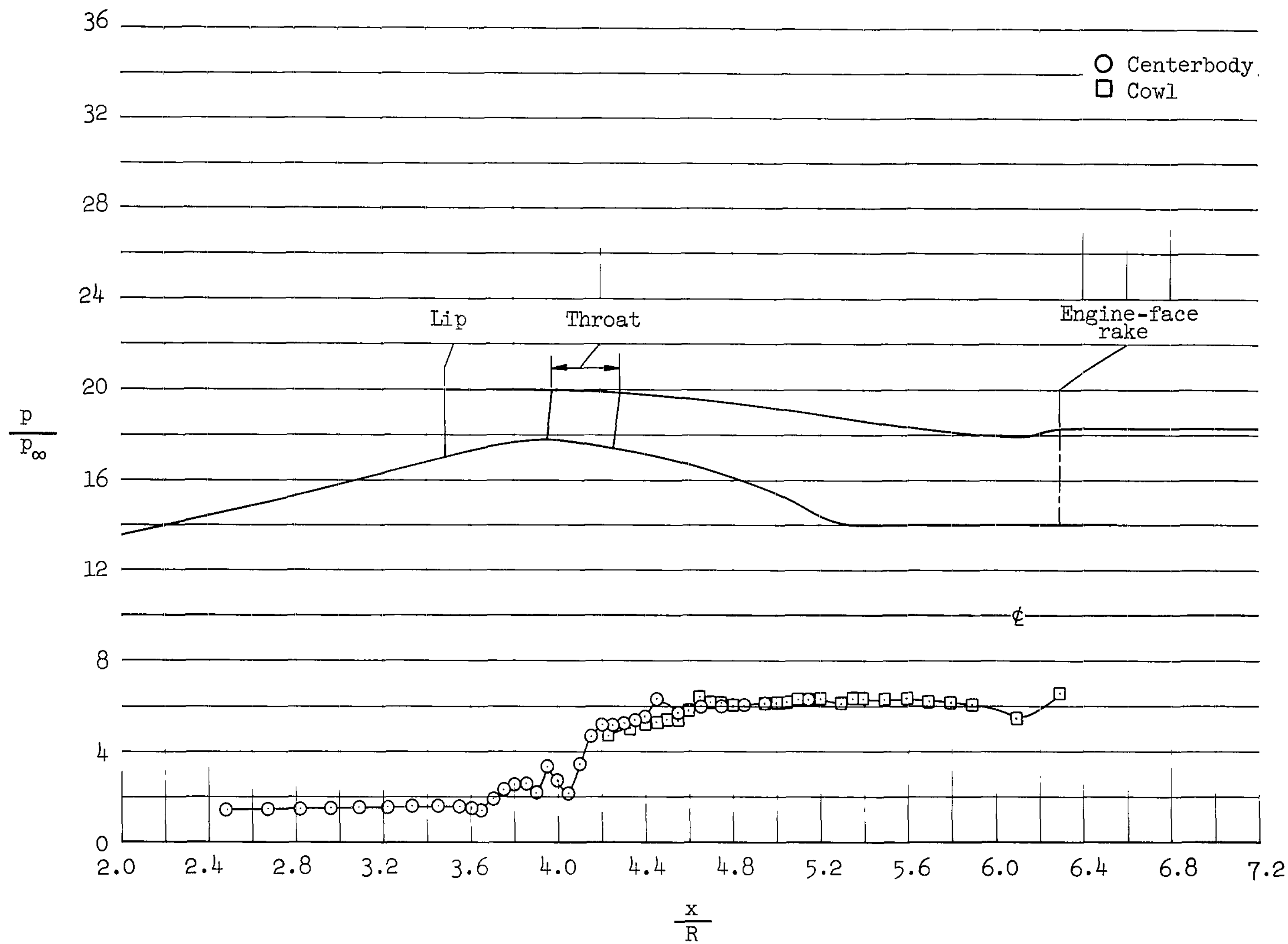

(c) $\bar{p}_{t_2}/p_{t_\infty} = 0.916$, $m_{bl}/m_\infty = 0.075$

Figure 25.- Concluded.

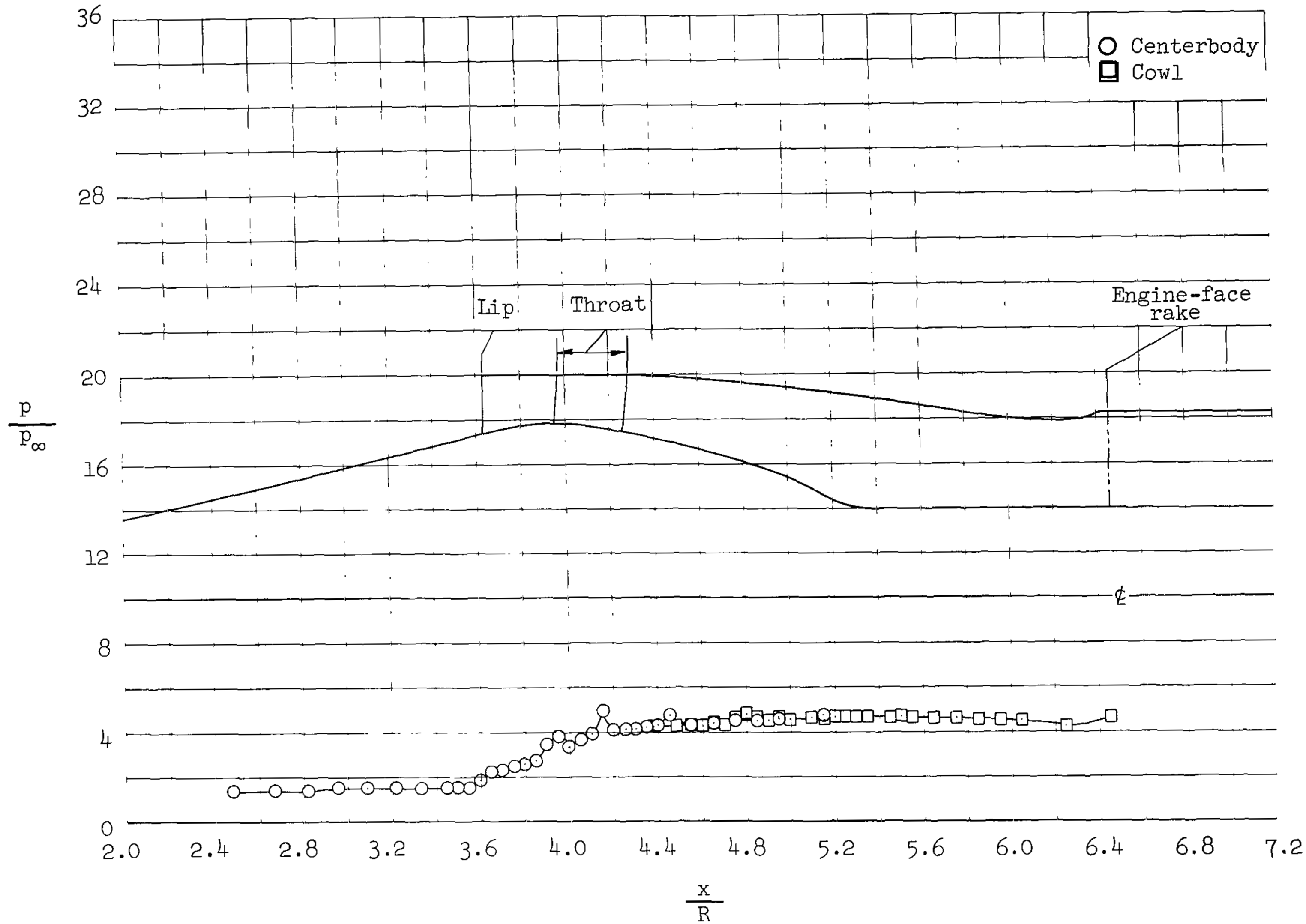

(a) $\bar{p}_{t_2}/p_{t_\infty} = 0.940$, $m_{bl}/m_\infty = 0.087$

Figure 26.- Static pressure distribution; bleed exit setting B, $(x/R)_{lip} = 3.628$; $M_\infty = 1.75$, $\alpha = 0°$.

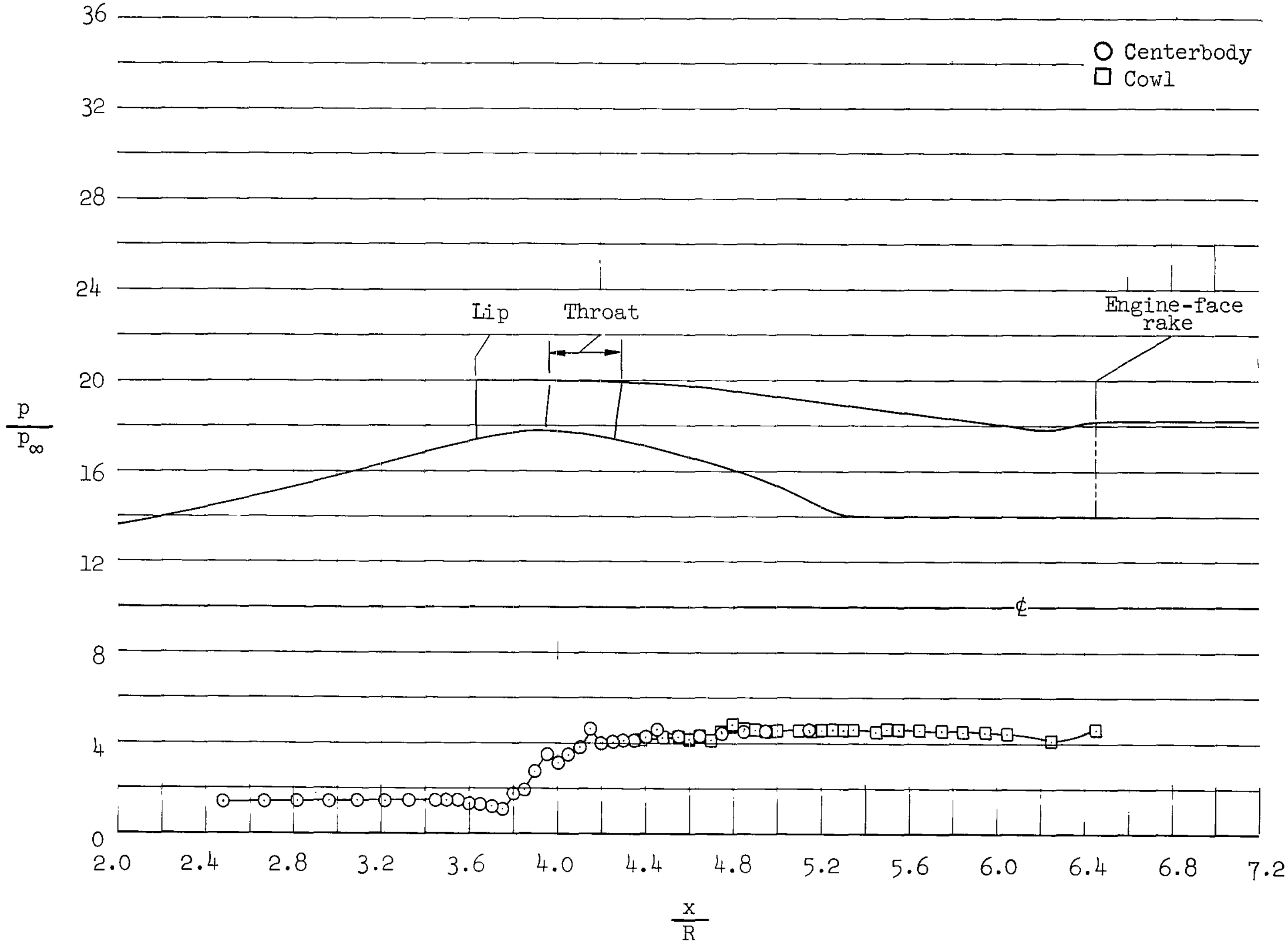

(b) $\bar{p}_{t_2}/p_{t_\infty} = 0.949$, $m_{bl}/m_\infty = 0.078$

Figure 26.- Continued.

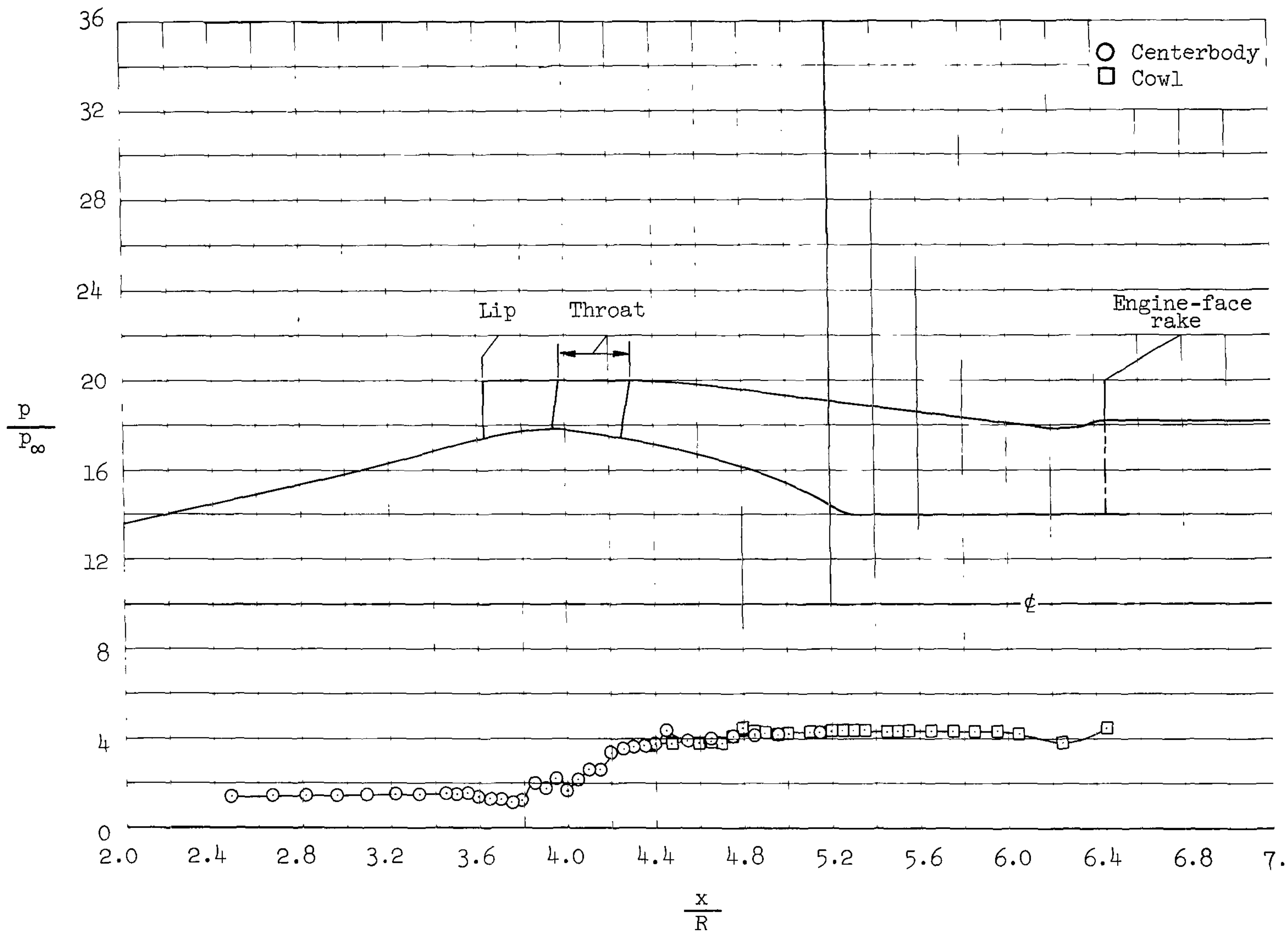

(c) $\bar{p}_{t_2}/p_{t_\infty} = 0.920$, $m_{bl}/m_\infty = 0.065$

Figure 26.- Concluded.

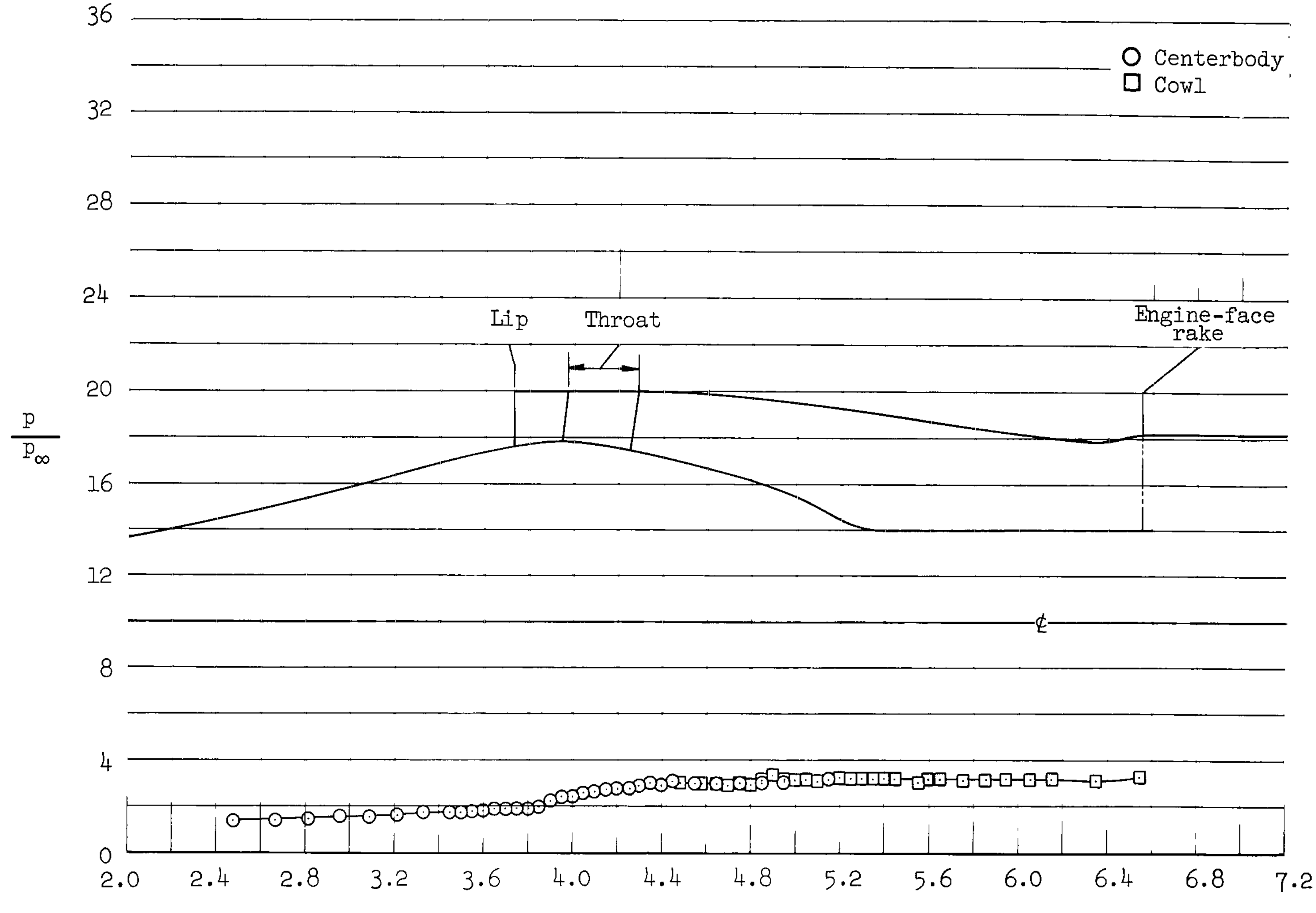

(a) $\bar{p}_{t_2}/p_{t_\infty} = 0.895$, $m_{bl}/m_\infty = 0.074$

Figure 27.- Static pressure distribution; bleed exit setting B, $(x/R)_{lip} = 3.728$; $M_\infty = 1.55$, $\alpha = 0°$.

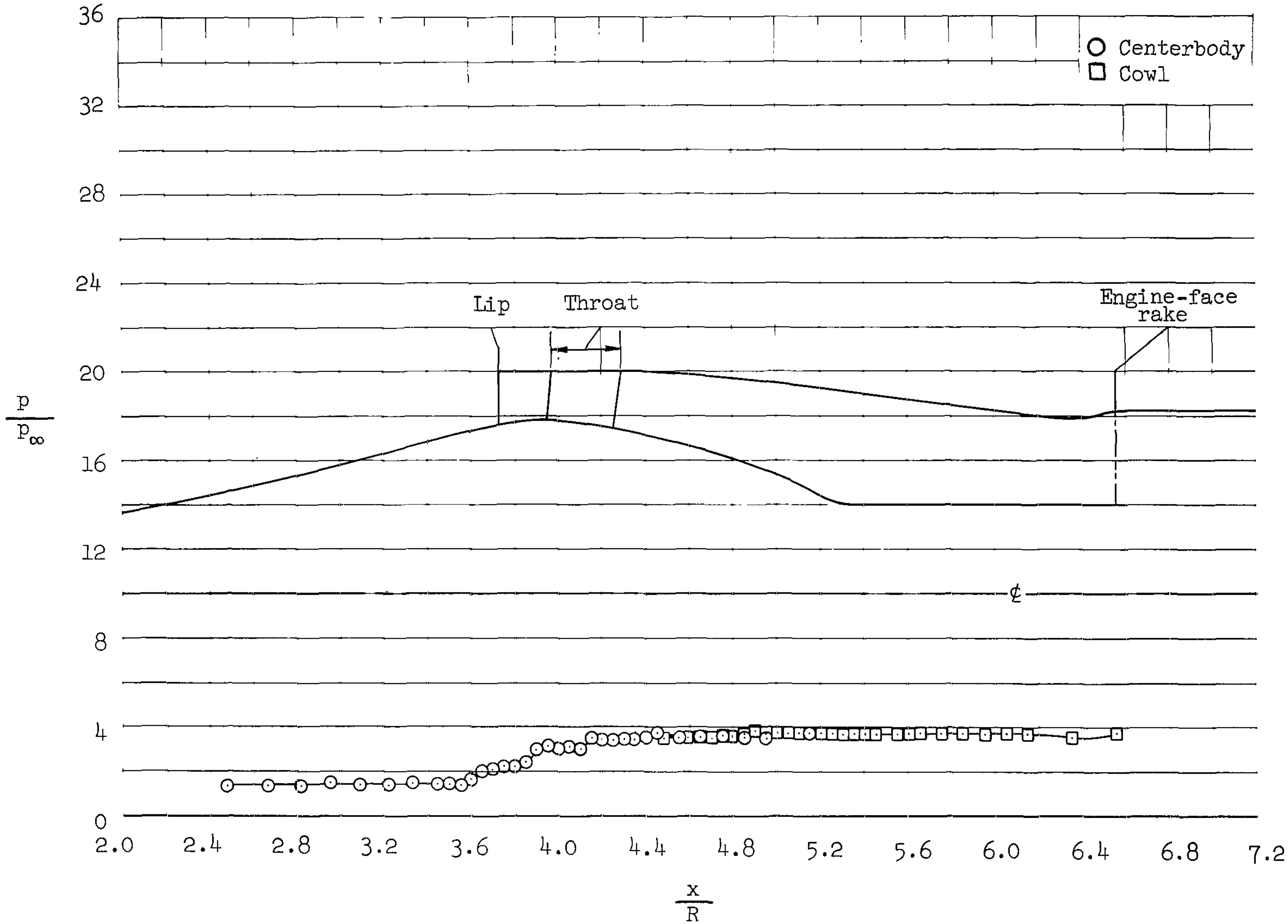

(b) $\bar{p}_{t_2}/p_{t_\infty} = 0.981$, $m_{bl}/m_\infty = 0.086$

Figure 27.- Continued.

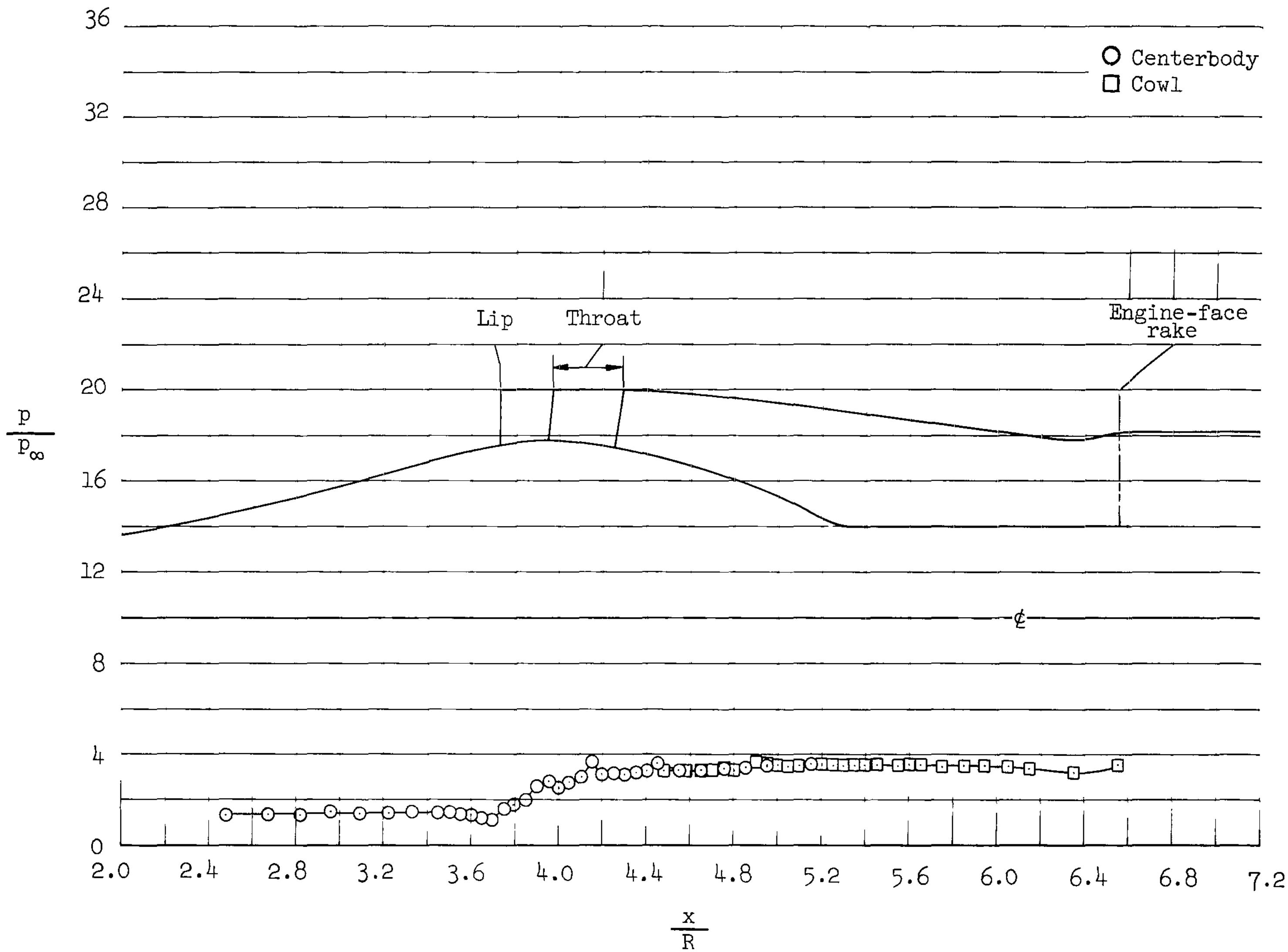

(c) $\bar{p}_{t_2}/p_{t_\infty} = 0.956$, $m_{bl}/m_\infty = 0.077$

Figure 27.- Concluded.

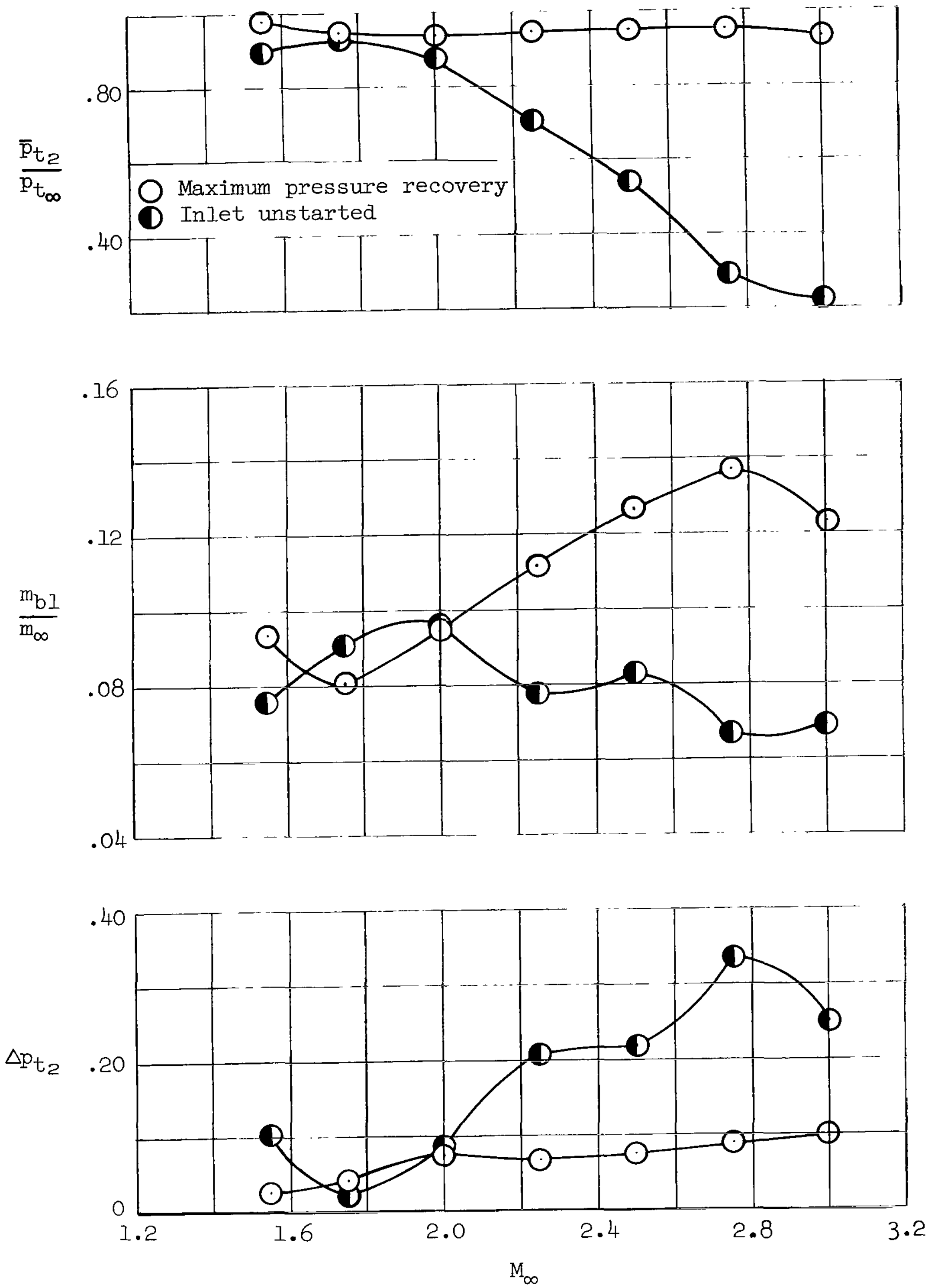

Figure 28.- Effect of unstarting the inlet on the main performance parameters; bleed exit setting A; $\alpha = 0^\circ$.

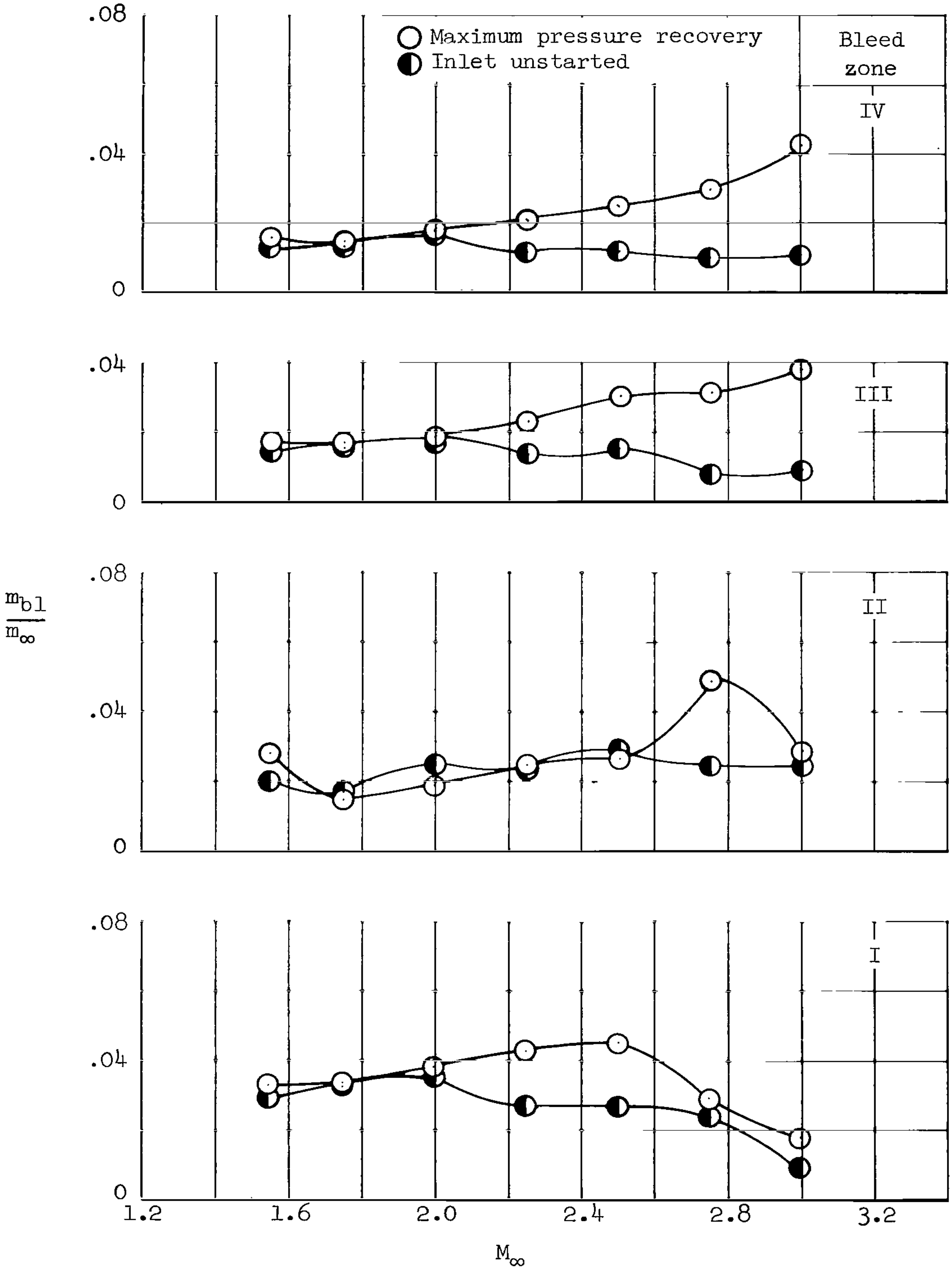

Figure 29.- Effect of unstarting the inlet on the individual bleed flows; bleed exit setting A; $\alpha = 0°$.

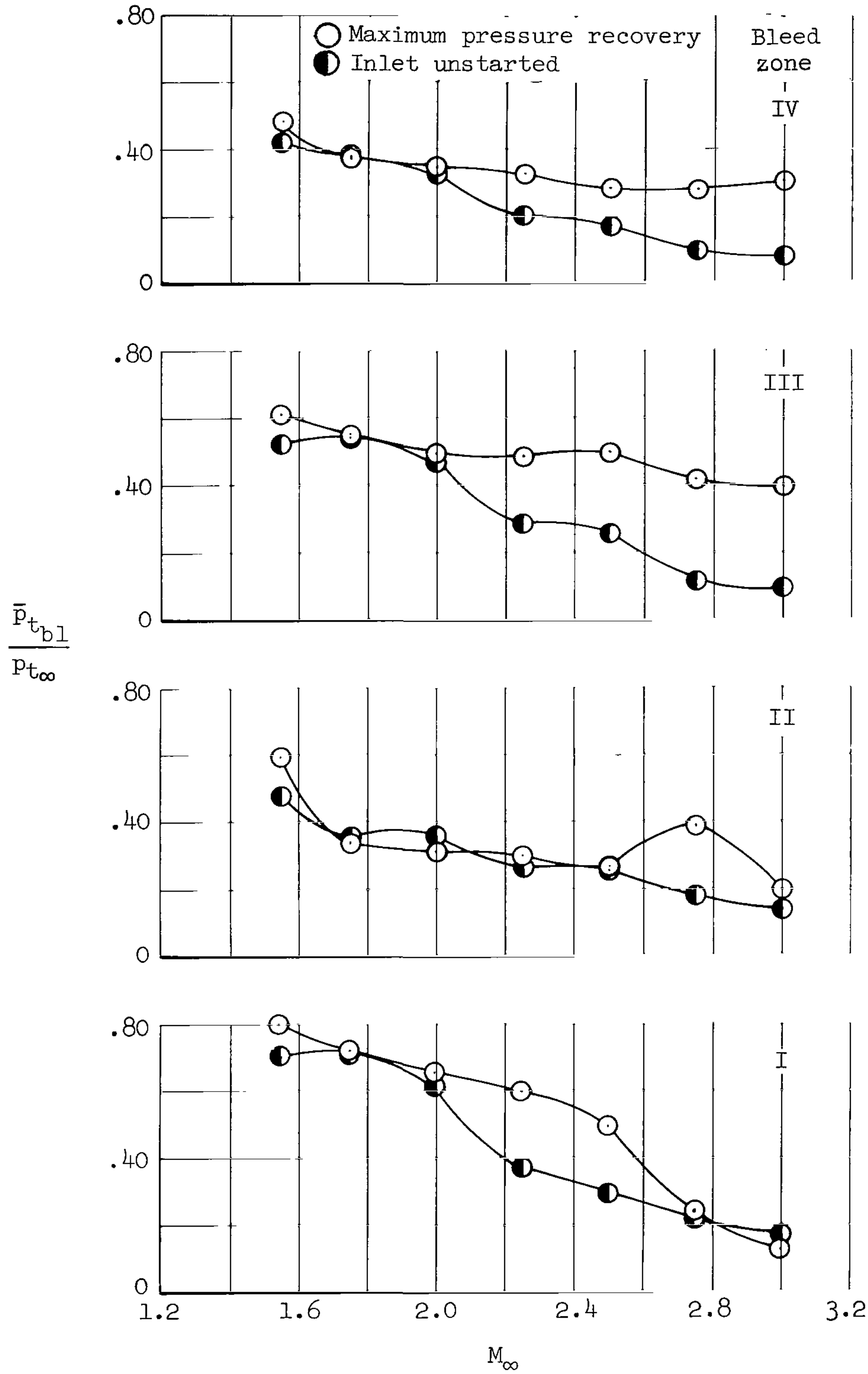

Figure 30.- Effect of unstarting the inlet on the individual bleed plenum chamber pressure recoveries; bleed exit setting A; $\alpha = 0°$.

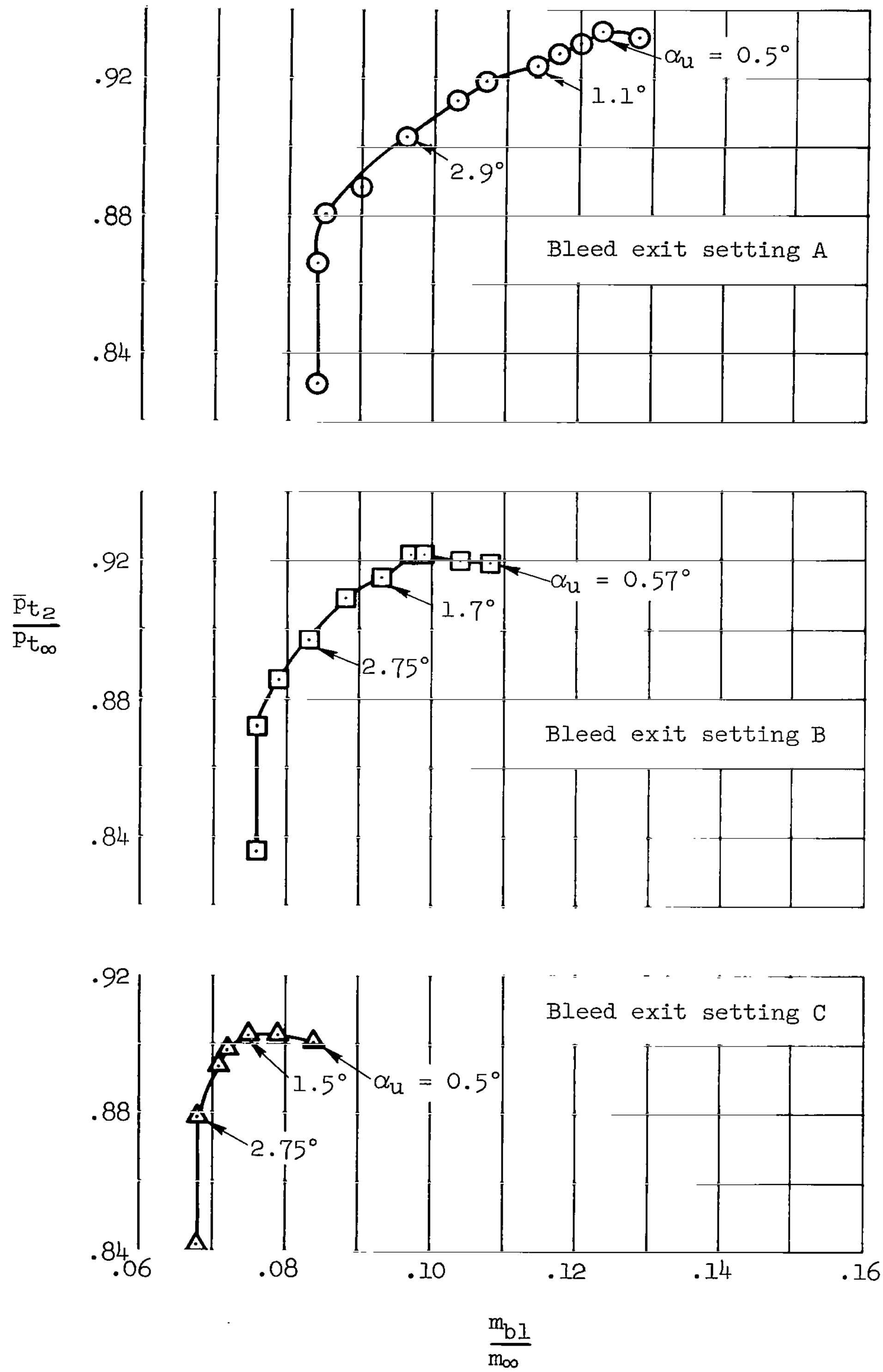

Figure 31.- Inlet tolerance to angle of attack; $M_\infty = 3.00$, $\alpha = 0°$; $(x/R)_{lip} = 2.548$.

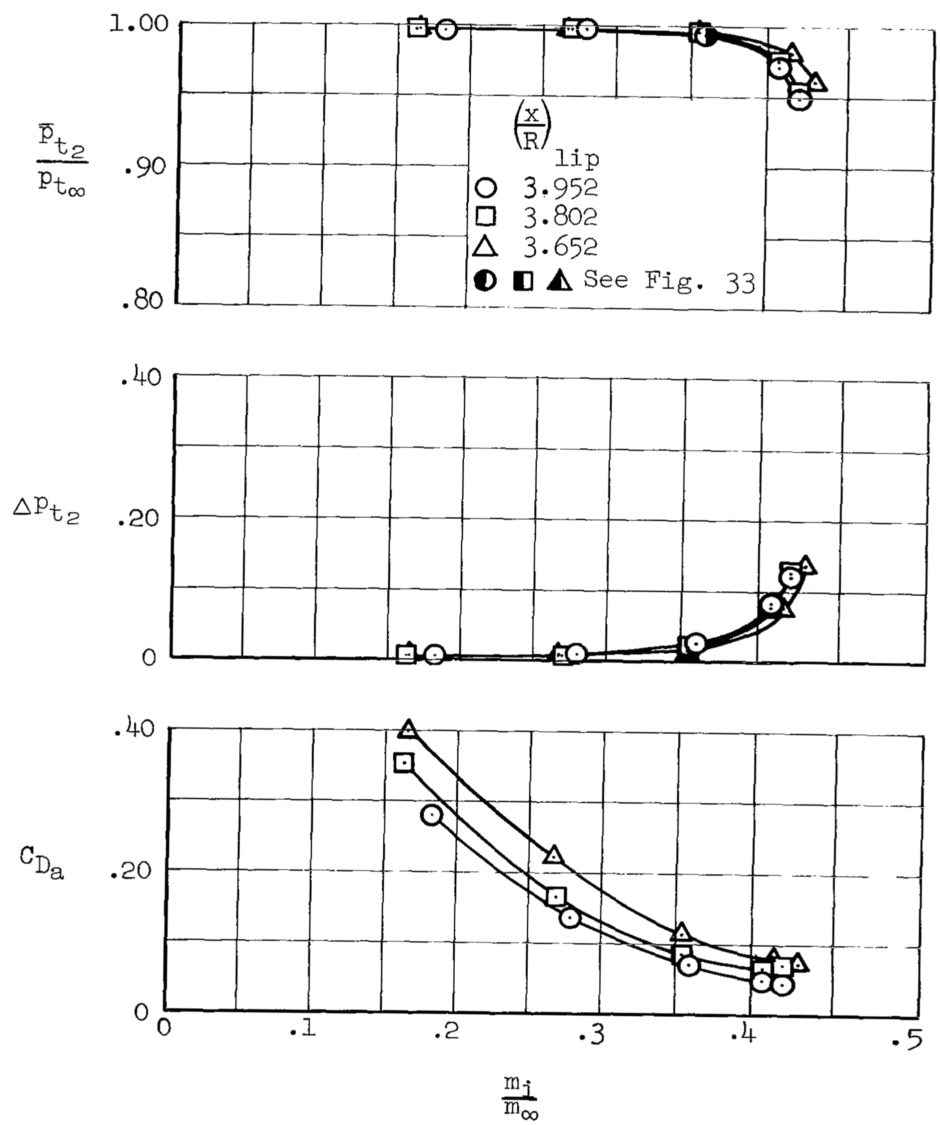

(a) $M_\infty = 0.60$

Figure 32.- Transonic performance; bleed exit setting B; $\alpha = 0°$.

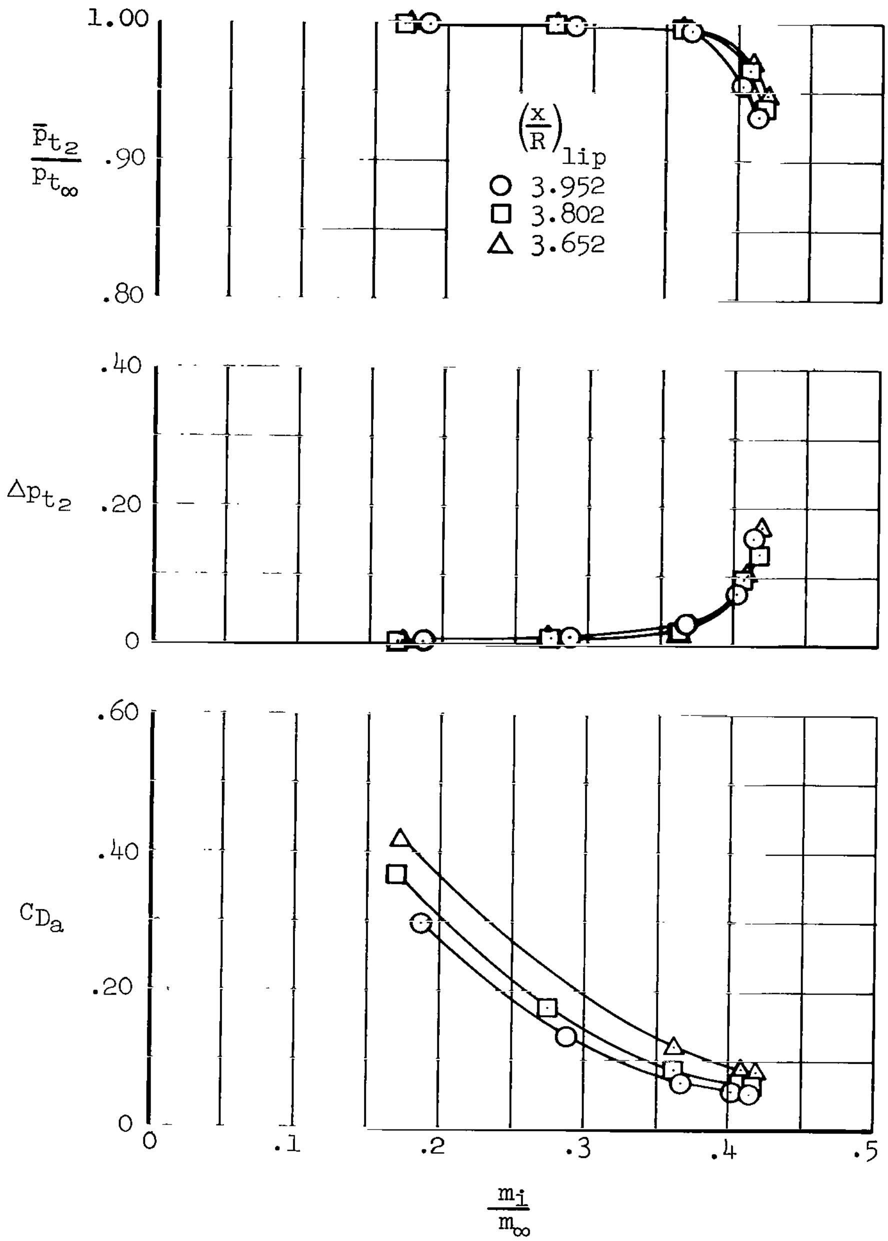

(b) $M_\infty = 0.70$

Figure 32.- Continued.

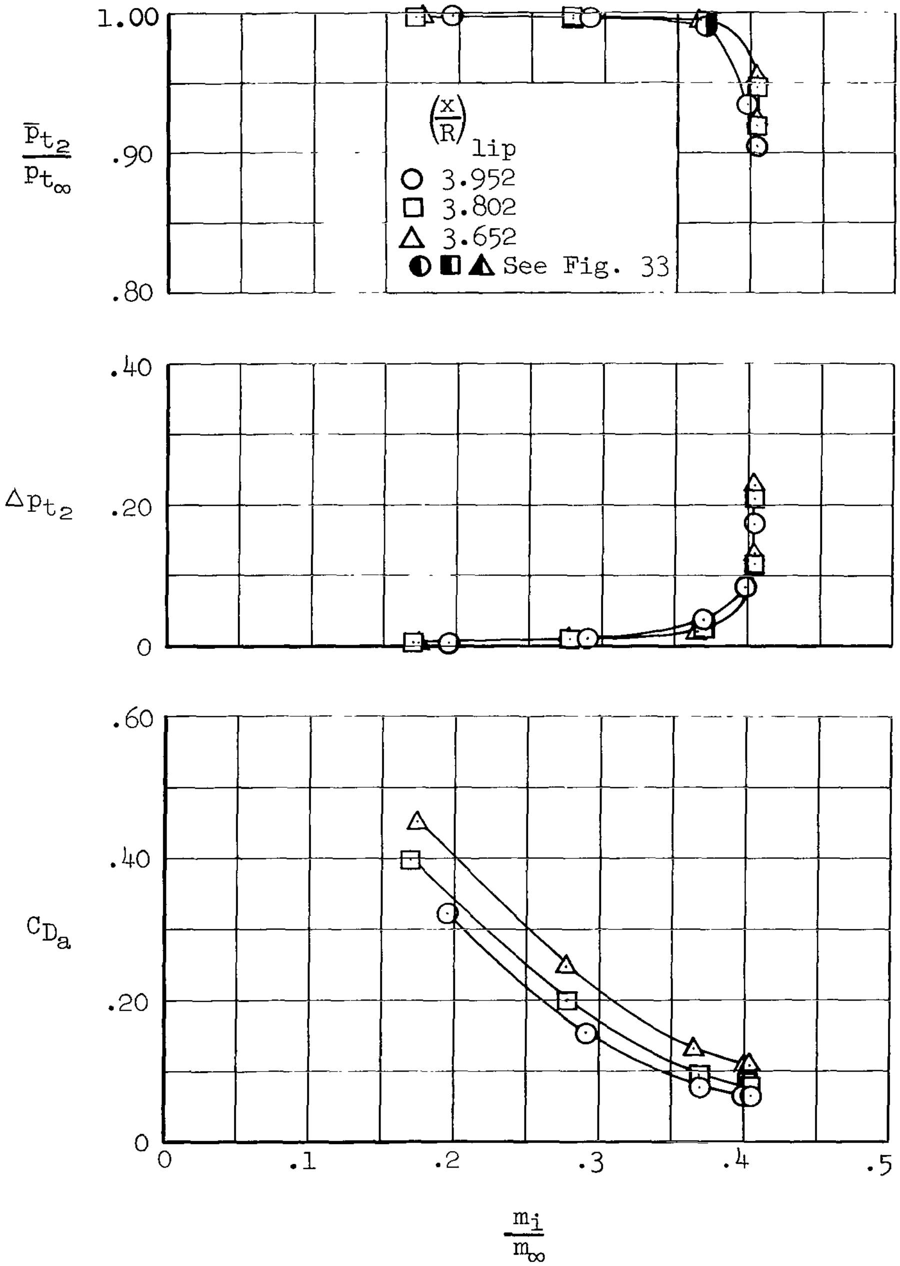

(c) $M_\infty = 0.80$

Figure 32.- Continued.

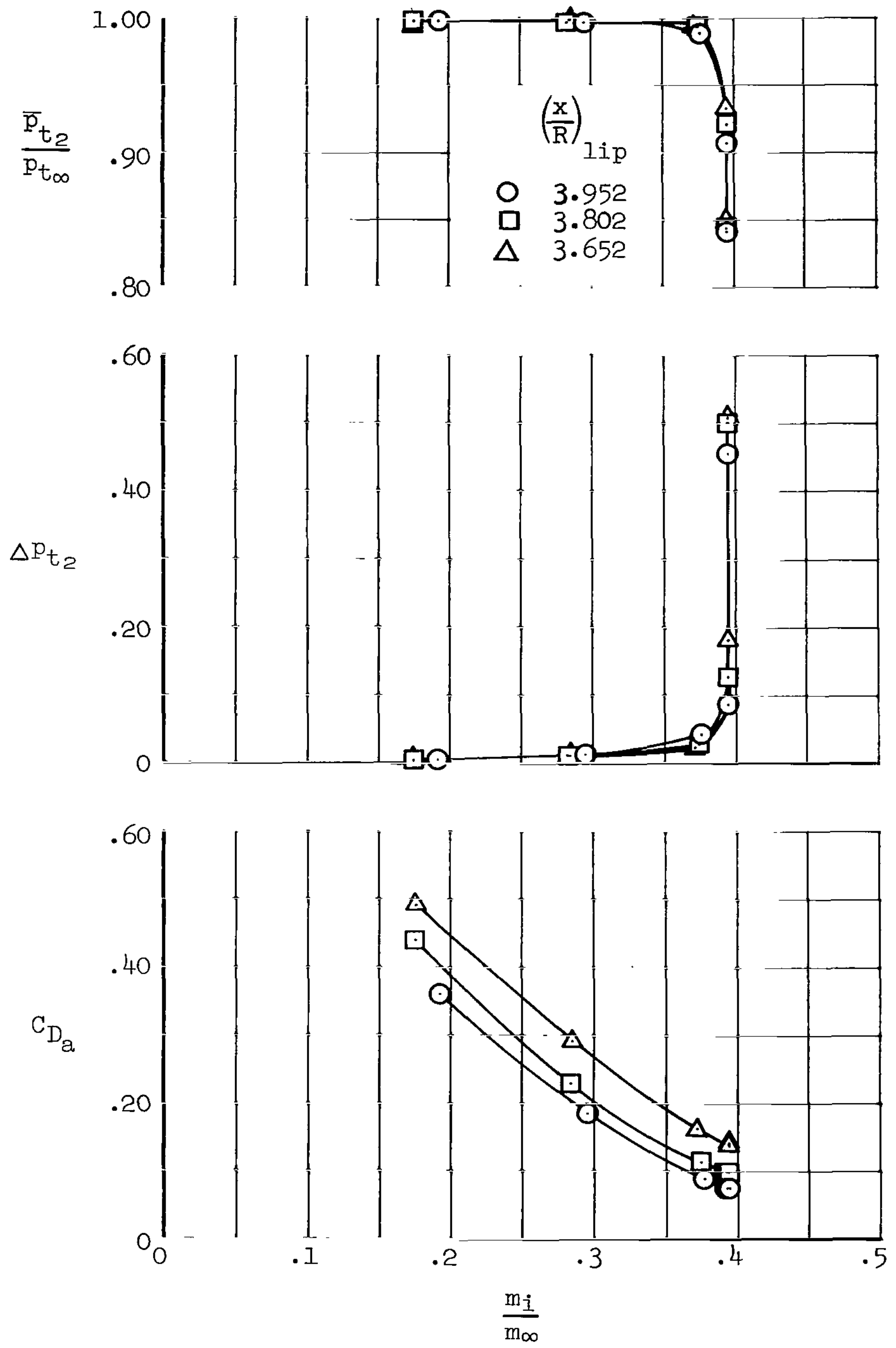

(d) $M_\infty = 0.90$

Figure 32.- Continued.

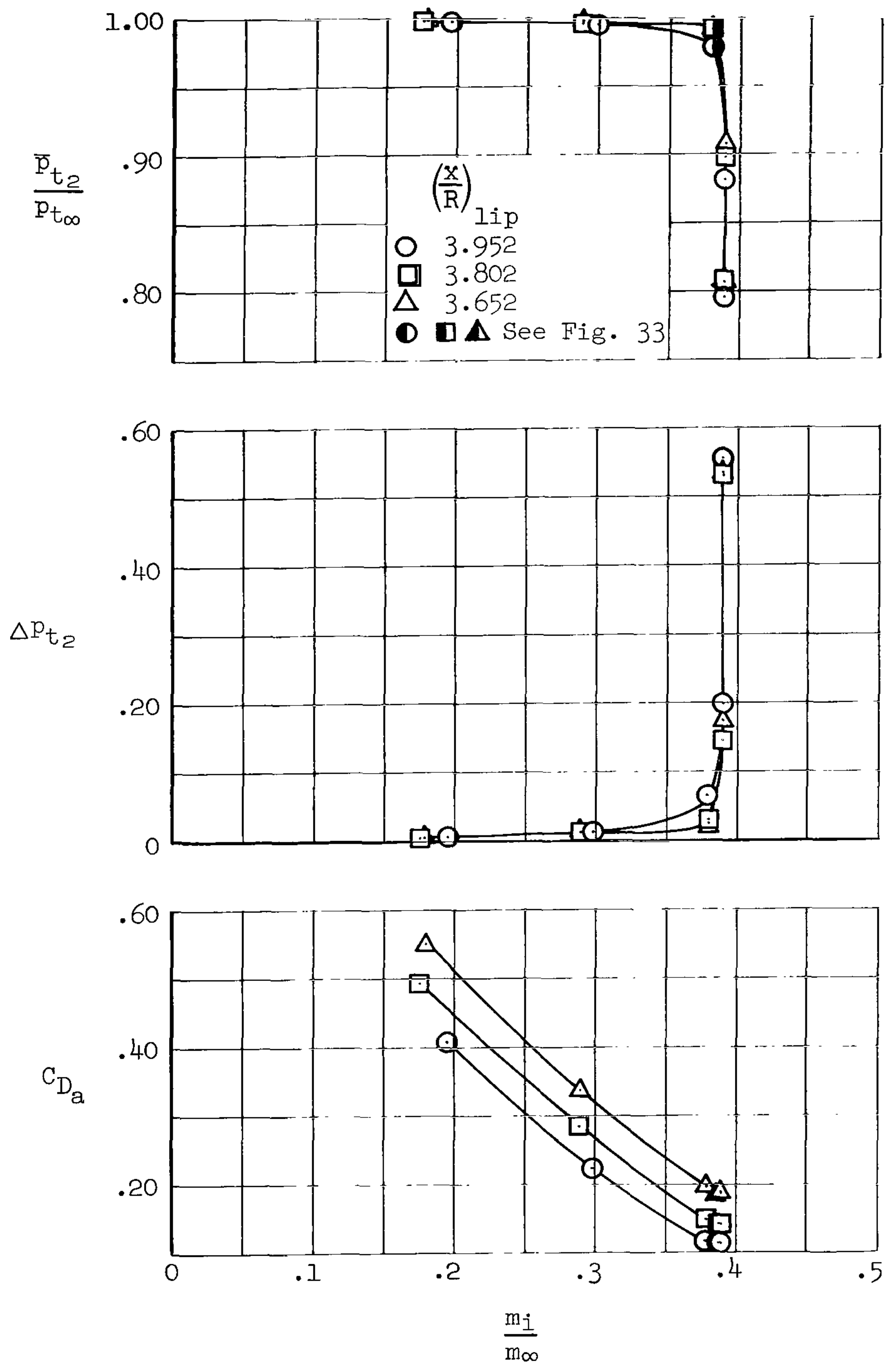

(e) $M_\infty = 1.00$

Figure 32.- Continued.

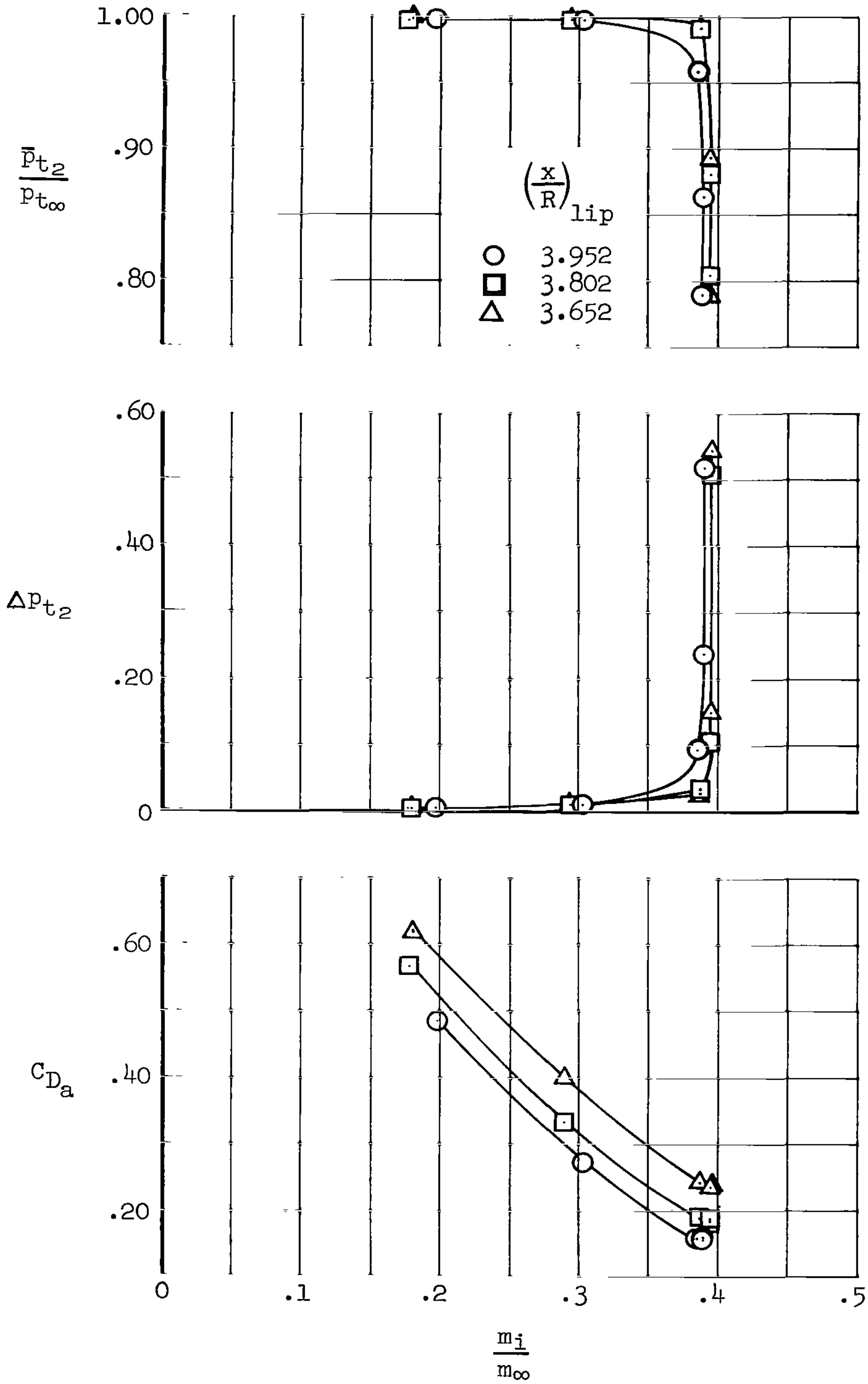

(f) $M_\infty = 1.10$

Figure 32.- Continued.

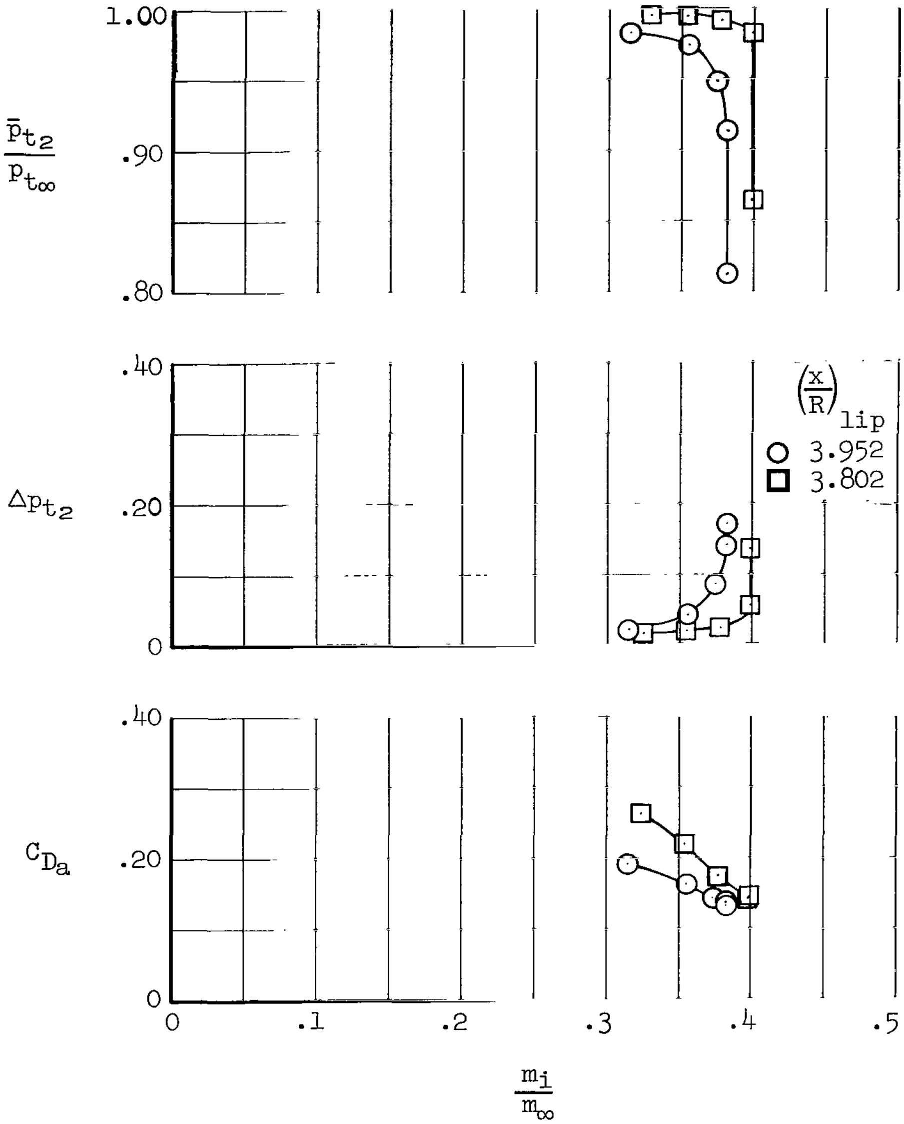

(g) $M_\infty = 1.20$

Figure 32.- Continued.

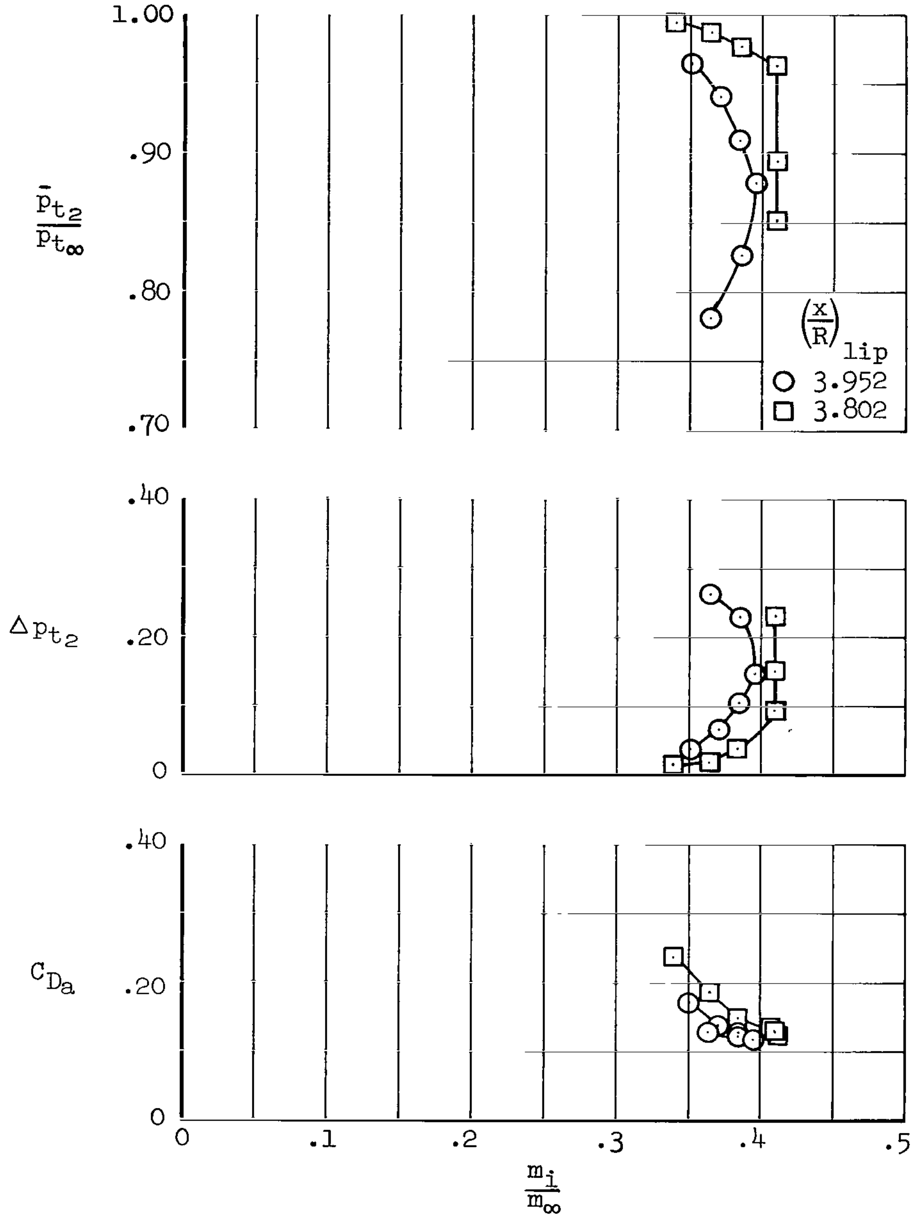

(h) $M_\infty = 1.30$

Figure 32.- Concluded.

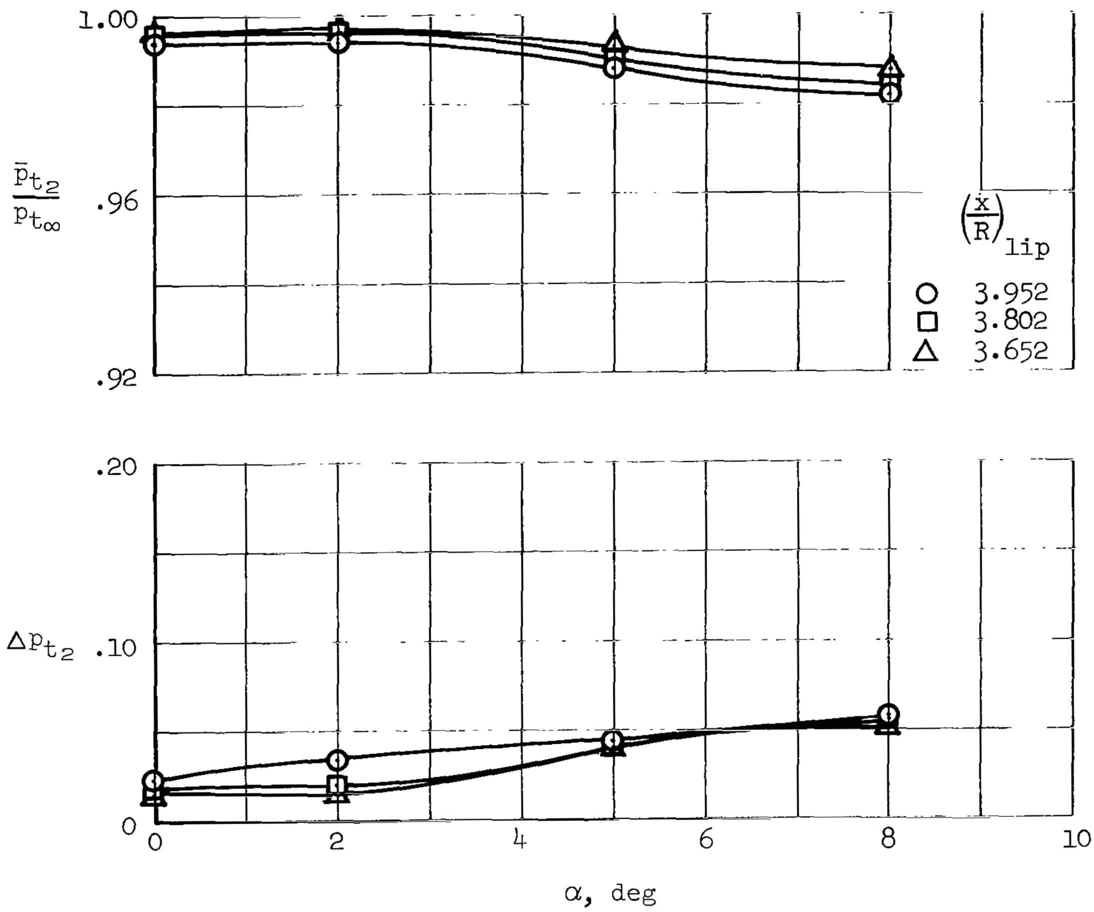

(a) $M_\infty = 0.6$

Figure 33.- Transonic performance at angle of attack.

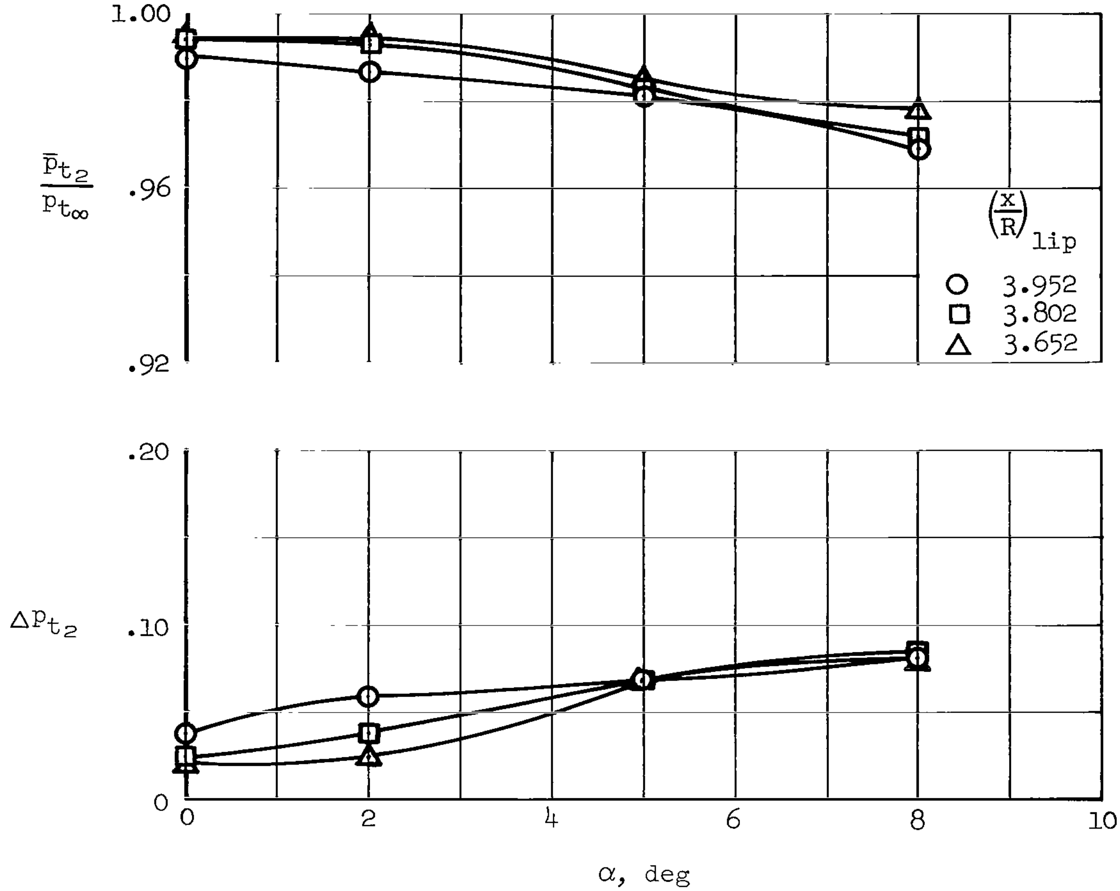

(b) $M_\infty = 0.8$

Figure 33.- Continued.

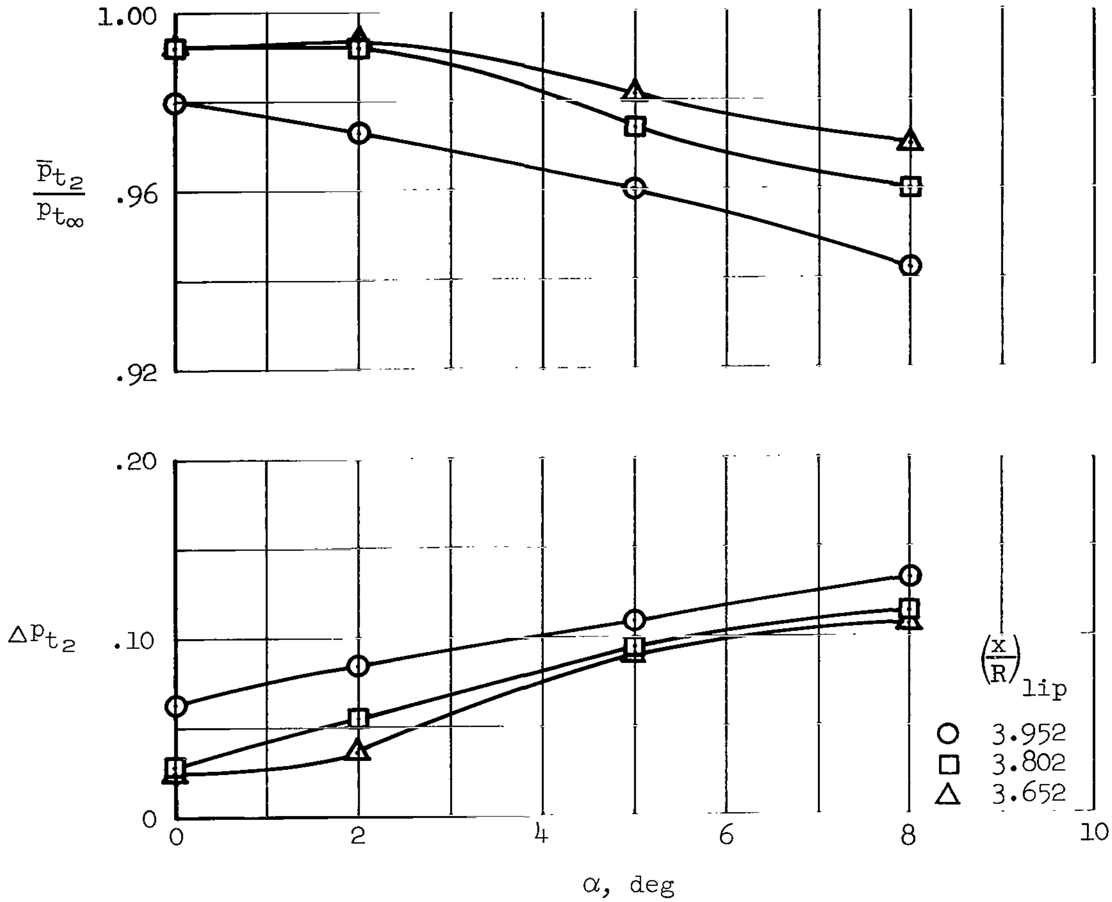

(c) $M_\infty = 1.0$

Figure 33.- Concluded.

NASA-Langley, 1968 —— 28 A-2837

NATIONAL AERONAUTICS AND SPACE ADMINISTRATION
WASHINGTON, D. C. 20546

OFFICIAL BUSINESS

FIRST CLASS MAIL

POSTAGE AND FEES PAID
NATIONAL AERONAUTICS AND
SPACE ADMINISTRATION

060 001 53 51 3US 68106 00903
AIR FORCE WEAPONS LABORATORY/AFWL/
KIRTLAND AIR FORCE BASE, NEW MEXICO 87117

ATT MISS MADELINE F. CANOVA, CHIEF TECHNICA
LIBRARY /WLIL/

POSTMASTER: If Undeliverable (Section 158 Postal Manual) Do Not Return

"The aeronautical and space activities of the United States shall be conducted so as to contribute . . . to the expansion of human knowledge of phenomena in the atmosphere and space. The Administration shall provide for the widest practicable and appropriate dissemination of information concerning its activities and the results thereof."

— NATIONAL AERONAUTICS AND SPACE ACT OF 1958

NASA SCIENTIFIC AND TECHNICAL PUBLICATIONS

TECHNICAL REPORTS: Scientific and technical information considered important, complete, and a lasting contribution to existing knowledge.

TECHNICAL NOTES: Information less broad in scope but nevertheless of importance as a contribution to existing knowledge.

TECHNICAL MEMORANDUMS: Information receiving limited distribution because of preliminary data, security classification, or other reasons.

CONTRACTOR REPORTS: Scientific and technical information generated under a NASA contract or grant and considered an important contribution to existing knowledge.

TECHNICAL TRANSLATIONS: Information published in a foreign language considered to merit NASA distribution in English.

SPECIAL PUBLICATIONS: Information derived from or of value to NASA activities. Publications include conference proceedings, monographs, data compilations, handbooks, sourcebooks, and special bibliographies.

TECHNOLOGY UTILIZATION PUBLICATIONS: Information on technology used by NASA that may be of particular interest in commercial and other non-aerospace applications. Publications include Tech Briefs, Technology Utilization Reports and Notes, and Technology Surveys.

Details on the availability of these publications may be obtained from:

SCIENTIFIC AND TECHNICAL INFORMATION DIVISION

NATIONAL AERONAUTICS AND SPACE ADMINISTRATION

Washington, D.C. 20546